



Antifungal plant extracts and phytochemicals,
mechanisms of action and microbial resistance

Adriana Cruz

UMinho | 2023



Universidade do Minho
Escola de Ciências

Adriana Ribeiro da Cruz

**Antifungal plant extracts and
phytochemicals, mechanisms of
action and microbial resistance**

outubro de 2023



Universidade do Minho
Escola de Ciências

Adriana Ribeiro da Cruz

**Antifungal plant extracts and
phytochemicals, mechanisms of action
and microbial resistance**

Master Thesis
Master's in Applied
Biochemistry

Work under the supervision of
Professor Doutor Rui Pedro Soares de Oliveira
**Professora Doutora Ana Cristina Gomes da
Cunha**

Despacho RT - 31 /2019 - Anexo 3

DIREITOS DE AUTOR E CONDIÇÕES DE UTILIZAÇÃO DO TRABALHO POR TERCEIROS

Este é um trabalho académico que pode ser utilizado por terceiros desde que respeitadas as regras e boas práticas internacionalmente aceites, no que concerne aos direitos de autor e direitos conexos.

Assim, o presente trabalho pode ser utilizado nos termos previstos na licença abaixo indicada.

Caso o utilizador necessite de permissão para poder fazer um uso do trabalho em condições não previstas no licenciamento indicado, deverá contactar o autor, através do RepositóriUM da Universidade do Minho.

Licença concedida aos utilizadores deste trabalho



Atribuição-NãoComercial-SemDerivações
CC BY-NC-ND

<https://creativecommons.org/licenses/by-nc-nd/4.0/>

ACKNOWLEDGEMENTS

A realização e concretização desta dissertação não teria sido possível sem o apoio e ajuda de algumas pessoas, pelo que não posso deixar de agradecer:

Ao professor Rui Oliveira e à professora Ana Cunha, os meus orientadores, por me terem aceitado neste projeto, por terem sido sempre incansáveis no que respeita à transmissão de conhecimento e por escutarem sempre as minhas ideias.

Aos meus colegas de laboratório, em especial, à Catarina Pereira, pelos momentos engraçados, gargalhadas e conversas, pelos almoços e viagens, mas sobretudo por me ajudar sempre que necessário. À Mariana Fernandes e à Raquel Coelho, pela disponibilidade, simpatia e entreajuda nos momentos mais complicados. À Ana Teixeira, pela amabilidade e ajuda prestada no início e fim deste projeto. À Eva Sánchez pela partilha de conhecimento e ajuda nas fases iniciais deste trabalho, mas também pela realização da análise química dos extratos estudados ao longo deste projeto.

A toda a equipa técnica do Departamento de Biologia, especialmente à Inês Pinheiro, ao Luís Correia e à Manuela Rodrigues, pela assistência incansável e amabilidade. A todos os investigadores do CBMA que de alguma forma me ajudaram e contribuíram para a realização deste trabalho.

À minha família, em especial aos meus pais, por me mostrarem que há sempre a possibilidade de, com esforço, chegar aos nossos objetivos, mas também por me apoiarem sempre de uma forma incondicional e pelo carinho e paciência demonstrados ao longo destes anos. Sem eles nada disto seria possível. Aos meus amigos, por estarem sempre presentes na minha vida, por nunca deixarem de me apoiar e por nunca cobrarem as minhas ausências.

STATEMENT OF INTEGRITY

I hereby declare having conducted this academic work with integrity. I confirm that I have not used plagiarism or any form of undue use of information or falsification of results along the process leading to its elaboration.

I further declare that I have fully acknowledged the Code of Ethical Conduct of the University of Minho.

Extratos de plantas e fitoquímicos antifúngicos, mecanismos de ação e resistência microbiana

RESUMO

Um dos maiores desafios do setor agrícola continua a ser o controle de doenças fúngicas, que afetam significativamente o rendimento das culturas e qualidade dos produtos. O uso contínuo de antifúngicos sintéticos levou ao desenvolvimento de resistências nos patógenos-alvo, tornando necessária a procura por alternativas naturais e sustentáveis. O objetivo deste trabalho foi descobrir antifúngicos que substituam os convencionais, que sejam biodegradáveis e não promovam resistências. Dos seis extratos aquosos e etanólicos de curcuma (CA e CE), noz-moscada (NMA e NME) e manjerição (OA e OE) testados, apenas CE e NME apresentaram toxicidade contra *Saccharomyces cerevisiae*, chegando a percentagens de viabilidade celular de 2,12% e 1,01%, respetivamente, ao fim de 120 min de exposição a 1000 µg/mL. Também vários fungos e oomicetes fitopatogénicos foram expostos à ação destes extratos, tendo-se obtido as seguintes inibições máximas do crescimento micelial com CE e NME para cada um deles: *Botrytis cinerea* 36,14% e 21,00%; *Colletotrichum acutatum* 23,23% e 10,74%; *Diplodia corticola* 34,32% e 27,73%; *Fusarium culmorum* 47,79% (só NME); *Phytophthora cactorum* 41,29% (só CE); e *Phytophthora cinnamomi* 65,88% e 25,23%, respetivamente. Os mecanismos de ação dos extratos foram estudados através de ensaios de viabilidade com mutantes de *S. cerevisiae* associados à via de síntese do ergosterol, à integridade da parede celular e ao processo de apoptose, tendo-se também estudado a viabilidade celular por microscopia de fluorescência. Os resultados sugerem que os extratos afetam a via biossintética do ergosterol, sendo os possíveis alvos a enzima esterol C-24 metiltransferase, o fecosterol e o episterol. Há também indícios de que CE causa a sobreativação da via de integridade da parede celular e que ambos os extratos provocam necrose. A toxicidade dos extratos foi testada na germinação de alface *in vitro* (250 e 500 µg/mL) e CE demonstrou não ser tóxico, ao contrário de NME. A capacidade de CE induzir resistência em células de *S. cerevisiae* foi estudada expondo as células a valores inferiores, iguais e superiores à concentração mínima inibitória (MIC) deste extrato (6,25, 12,50 e 50,00 µg/mL) e constatou-se que CE não induz resistência até concentrações iguais à MIC. A análise química revelou que CE é rico em (+)-β-turmerona, enquanto NME contém ácido mirístico em maior proporção. Em suma, este trabalho mostrou que os extratos CE e NME são promissores para serem utilizados como fungicidas naturais sem promoverem resistências nos organismos alvo.

Palavras-chave: atividade antifúngica, extratos de plantas, fitoquímicos, fungos filamentosos, resistência microbiana.

Antifungal plant extracts and phytochemicals, mechanisms of action and microbial resistance

ABSTRACT

One of the biggest challenges facing the agricultural sector continues to be the control of fungal diseases, which significantly affect crop yields and product quality. The continuous use of synthetic antifungals has led to the development of resistance in the target pathogens, making it necessary to look for natural and sustainable alternatives. The aim of this work was to find antifungals that replace conventional ones, are biodegradable and do not promote resistance. From the six aqueous and ethanolic extracts of turmeric (CA and CE), nutmeg (NMA and NME) and basil (OA and OE) tested, only CE and NME showed toxicity against *Saccharomyces cerevisiae*, reaching percentages of cell viability of 2.12% and 1.01%, respectively, after 120 min of exposure to 1000 µg/mL. Several phytopathogenic fungi and oomycetes were also exposed to the action of these extracts, and the following maximum inhibitions of mycelial growth were obtained with CE and NME for each of them: *Botrytis cinerea* 36.14% and 21.00%; *Colletotrichum acutatum* 23.23% and 10.74%; *Diplodia corticola* 34.32% and 27.73%; *Fusarium culmorum* 47.79% (NME only); *Phytophthora cactorum* 41.29% (CE only); and *Phytophthora cinnamomi* 65.88% and 25.23%, respectively. The extracts' mechanisms of action were studied through viability tests with *S. cerevisiae* mutants associated with the ergosterol synthesis pathway, cell wall integrity and the apoptosis process, and cell viability was also studied using fluorescence microscopy. Results suggest that the extracts affect the ergosterol biosynthetic pathway, being the possible targets sterol C-24 methyltransferase enzyme, fecosterol and episterol. There is also indications that CE causes overactivation of the cell wall integrity pathway and that both extracts cause necrosis. The toxicity of the extracts was tested on lettuce germination *in vitro* (250 and 500 µg/mL) and CE proved not to be toxic, unlike NME. The ability of CE to induce resistance in *S. cerevisiae* cells was studied by exposing the cells to values below, equal to and above the minimum inhibitory concentration (MIC) of this extract (6.25, 12.50 and 50.00 µg/mL) and it was found that CE does not induce resistance up to concentrations equal to the MIC. Chemical analysis revealed that CE is rich in (+)-β-turmerone, while NME contains a higher proportion of myristic acid. In short, this work has shown that CE and NME extracts are promising for use as natural fungicides without promoting resistance in target organisms.

Keywords: antifungal activity, filamentous fungi, microbial resistance, phytochemicals, plant extracts.

TABLE OF CONTENTS

ACKNOWLEDGEMENTS	iii
RESUMO	v
ABSTRACT	vi
ABBREVIATIONS.....	x
LIST OF FIGURES	xii
LIST OF TABLES.....	xv
1. INTRODUCTION.....	1
1.1. Current challenges in agriculture	1
1.1.1. Food production and losses	2
1.1.2. Phytopathogenic fungi and oomycetes and principal diseases.....	2
1.1.2.1. <i>Botrytis cinerea</i>	10
1.1.2.2. <i>Colletotrichum acutatum</i>	11
1.1.2.3. <i>Diplodia corticola</i>	12
1.1.2.4. <i>Fusarium culmorum</i>	14
1.1.2.5. <i>Phytophthora cactorum</i>	16
1.1.2.6. <i>Phytophthora cinnamomi</i>	18
1.1.3. Synthetic fungicides.....	21
1.1.3.1. Mechanisms of action	22
1.1.3.2. Microbial resistance associated with intensive use of synthetic fungicides.....	28
1.2. Natural fungicides	30
1.2.1. Biological control agents	31
1.2.2. Plant extracts and phytochemicals with antifungal and anti-oomycetal activities.....	32
1.2.2.1. <i>Curcuma longa</i> (turmeric)	37
1.2.2.2. <i>Myristica fragrans</i> (nutmeg).....	38
1.2.2.3. <i>Ocimum basilicum</i> (basil).....	39

1.3.	<i>Saccharomyces cerevisiae</i> as a fungal model.....	40
2.	BIOLOGICAL PROBLEM AND OBJECTIVES	41
3.	MATERIALS AND METHODS.....	42
3.1.	Preparation of plant extracts.....	42
3.2.	Microbial organisms, media and growth conditions	43
3.3.	Evaluation of the antifungal and anti-oomycetal activities of the extracts <i>in vitro</i>	44
3.3.1.	Viability assays with <i>Saccharomyces cerevisiae</i>	44
3.3.2.	Growth inhibition assays with filamentous fungi and oomycetes	45
3.4.	Assessment of cell viability with propidium iodide by fluorescence microscopy.....	46
3.5.	Phytotoxicity assays using the <i>in vitro</i> lettuce model	47
3.6.	Study of the resistance induction potential of extracts in comparison with itraconazole.....	48
3.6.1.	Determination of itraconazole Minimum Inhibitory Concentration (MIC).....	48
3.6.2.	Resistance induction.....	50
3.7.	Chemical characterization of the extracts	51
3.8.	Statistical analysis	51
4.	RESULTS AND DISCUSSION	53
4.1.	Antifungal activity of CE and NME extracts against <i>Saccharomyces cerevisiae</i>	53
4.2.	Growth inhibition potential of CE and NME extracts against various filamentous fungi and oomycetes.....	55
4.2.1.	Potential of CE extract.....	55
4.2.2.	Potential of NME extract.....	60
4.3.	Possible mechanisms of action of CE and NME extracts.....	65
4.4.	Assessment of viability with propidium iodide by fluorescence microscopy.....	76
4.5.	Susceptibility of lettuce seed germination and early growth of lettuce seedlings to the extracts CE and NME.....	79
4.6.	Resistance induction potencial of the extracts in comparison with itraconazol	82
4.7.	Chemical characterization of CE and NME extracts	84

4.7.1.	Compounds present in CE extract.....	84
4.7.2.	Compounds present in NME extract.....	86
5.	CONCLUSIONS AND FUTURE PERSPECTIVES.....	89
6.	BIBLIOGRAPHY.....	93
7.	ANNEXES	116

ABBREVIATIONS

ABC	ATP-Binding Cassette
ARAF	Azole-Resistant strains of <i>Aspergillus fumigatus</i>
ATR	Attenuated Total Reflectance
BCAs	Biological Control Agents
BF	Bright Field
CA	<i>Curcuma longa</i> Aqueous extract
CE	<i>Curcuma longa</i> Ethanolic extract
CFUs	Colony Forming Units
CWI	Cell Wall Integrity
DAMPs	Damage-Associated Molecular Patterns
dH₂O	Deionized water
DMI	Demethylation Inhibitors
DMSO	Dimethyl Sulfoxide
DTCs	Dithiocarbamates
ETI	Effector-Triggered Immunity
EtOH	Ethanol
FAO	Food and Agriculture Organization of the United Nations
FAOSTAT	Food and Agriculture Organization Statistical database of the United Nations
FHB	<i>Fusarium</i> Head Blight
FRR	<i>Fusarium</i> Root Rot
FTIR	Fourier-Transform Infrared
GC-MS	Gas Chromatography-Mass Spectrometry
IF	Infected Fruits
ITC	Itraconazol
LED	Light Emitting Diode
MAMPs	Microbe-Associated Molecular Patterns
MAP	Mitogen-Activated Protein
MAPK	Mitogen-Activated Protein Kinase
MAPKK	Mitogen-Activated Protein Kinase Kinase
MAPKKK	Mitogen-Activated Protein Kinase Kinase Kinase

MFS	Major Facilitator Superfamily
MIC	Minimum Inhibitory Concentration
MOA	Mechanisms of Action
MS	Murashige and Skoog medium
NIST11	National Institute of Standards and Technology
NMA	Nutmeg Aqueous extract
NME	Nutmeg Ethanolic extract
OA	<i>Ocimum basilicum</i> Aqueous extract
OD	Optical Density
OE	<i>Ocimum basilicum</i> Ethanolic extract
PAMPs	Pathogen-Associated Molecular Patterns
PBS	Phosphate Buffered Saline
PCD	Programmed Cell Death
PCWDEs	Plant Cell Wall Degrading Enzymes
PDA	Potato-Dextrose-Agar
PhCR	<i>Phytophthora</i> Crown Rot
PI	Propidium Iodide
PRRs	Pattern Recognition Receptor
PTI	PAMP-Triggered Immunity
QoI	Quinone oxidase Inhibitors
SBI	Sterol Biosynthesis Inhibitors
SD	Standard Deviation
SEM	Standard Error Mean
WT	Wild-Type
YM	Yeast Minimal media
YPDA	Yeast extract-Peptone-Dextrose-Agar
YPD	Yeast extract-Peptone-Dextrose
ZEN	Zearalenone

LIST OF FIGURES

Figure 1 – Colonization of plants by fungi with different lifestyles.....	6
Figure 2 – Images of <i>Botrytis cinerea</i>	11
Figure 3 – Infections and image of <i>Colletotrichum acutatum</i>	12
Figure 4 – Infections and image of <i>Diplodia corticola</i>	13
Figure 5 – Infections and image of <i>Fusarium culmorum</i>	14
Figure 6 – Infection and image of <i>Phytophthora cactorum</i>	17
Figure 7 – Infection and image of <i>Phytophthora cinnamomi</i>	19
Figure 8 – The chemical structure of dithiocarbamate and benzimidazole	23
Figure 9 – The chemical structure of amphotericin B and morpholine	24
Figure 10 – Biosynthetic pathway of ergosterol in <i>Saccharomyces cerevisiae</i>	26
Figure 11 – The chemical structures of imidazole and triazole.	27
Figure 12 – The chemical structure of a natural strobilurin.	27
Figure 13 – The chemical structure of flavonoids and coumarins.....	33
Figure 14 – The basic chemical structure of saponins, terpenes, terpenoids, and carvacrol.....	34
Figure 15 – The basic chemical structure of isoquinolines and indoles.....	36
Figure 16 – Schematic overview of pre-inoculum preparation and viability assay using <i>Saccharomyces cerevisiae</i>	45
Figure 17 – Schematic overview of a growth inhibition assay using filamentous fungi/oomycetes....	46
Figure 18 – Schematic overview of viability assessment using propidium iodide.....	47
Figure 19 – Schematic overview of the phytotoxicity assay using lettuce seeds.....	48
Figure 20 – Schematic overview of the determination of the MIC.	49
Figure 21 – Schematic overview of the protocol for inducing resistance in <i>S. cerevisiae</i> BY4741 yeast	50
Figure 22 – The viability of <i>Saccharomyces cerevisiae</i> BY4741 following exposure to ethanolic extracts of <i>Curcuma longa</i> , <i>Myristica fragrans</i> and <i>Ocimum basilicum</i>	54
Figure 23 – Mycelium diameter (mm) and mycelium growth inhibition (%) of <i>Botrytis cinerea</i> , <i>Colletotrichum acutatum</i> , <i>Diplodia corticola</i> and <i>Fusarium culmorum</i> when exposed to <i>Curcuma longa</i> ethanolic extract (CE).....	56
Figure 24 – Mycelium diameter (mm) and mycelium growth inhibition (%) of <i>Phytophthora cactorum</i> and <i>Phytophthora cinnamomi</i> when exposed to <i>Curcuma longa</i> ethanolic extract (CE).	58

Figure 25 – Photographic record of the filamentous fungus exposed to <i>Curcuma longa</i> ethanolic extract (CE)	59
Figure 26 – Mycelium diameter (mm) and mycelium growth inhibition (%) of <i>Botrytis cinerea</i> , <i>Colletotrichum acutatum</i> , <i>Diplodia corticola</i> and <i>Fusarium culmorum</i> when exposed to <i>Myristica fragrans</i> ethanolic extract (NME).....	61
Figure 27 – Mycelium diameter (mm) and mycelium growth inhibition (%) of <i>Phytophthora cactorum</i> and <i>Phytophthora cinnamomi</i> when exposed to <i>Myristica fragrans</i> ethanolic extract (NME)	63
Figure 28 – Photographic record of filamentous fungus exposed to <i>Myristica fragrans</i> ethanolic extract (NME)	64
Figure 29 – Mutant strains <i>erg6</i> , <i>erg2</i> , <i>erg5</i> , and <i>erg4</i> , exhibited higher resistance, while <i>erg3</i> mutant strain displayed higher sensitivity to ethanolic extracts of <i>Curcuma longa</i> (CE) and <i>Myristica fragrans</i> (NME) compared to their respective wild-type (WT) strains.....	70
Figure 30 – CWI signaling pathway	72
Figure 31 – Mutant strains <i>bck1</i> , and <i>mkk1/mkk2</i> , exhibited higher resistance to ethanolic extracts of <i>Curcuma longa</i> (CE) and <i>Myristica fragrans</i> (NME) compared to their respective wild-type (WT) strains	74
Figure 32 – Mutant strain <i>yca1</i> displayed higher sensitivity to ethanolic extracts of <i>Curcuma longa</i> (CE) and <i>Myristica fragrans</i> (NME) compared to its respective wild-type (WT) strain	76
Figure 33 – Plasma membrane integrity and viability of <i>Saccharomyces cerevisiae</i> cells exposed to <i>Curcuma longa</i> extract (CE) and <i>Myristica fragrans</i> extract (NME).....	78
Figure 34 – <i>Curcuma longa</i> extract (CE) does not exhibit toxicity towards lettuce seeds, but <i>Myristica fragrans</i> extract (NME) appears do be toxic, especially at a concentration of 500 µg/mL	81
Figure 35 – Chemical structures of phytochemicals identified in <i>Curcuma longa</i> (CE) extract by GC–MS.....	84
Figure 36 – Chemical structures of some of the phytochemicals found in <i>Myristica fragrans</i> (NME) extract.....	88
Figure 37 – The viability of <i>Saccharomyces cerevisiae</i> remains unaffected by the solvent extracts (80% ethanol; EtOH).....	116
Figure 38 – The mycelium growth of <i>Botrytis cinerea</i> , <i>Colletotrichum acutatum</i> , <i>Diplodia corticola</i> , <i>Fusarium culmorum</i> , <i>Phytophthora cactorum</i> and <i>Phytophthora cinnamomi</i> remains unaltered by the solvent extracts (80% ethanol; EtOH).....	117

Figure 39 – Mutant strains <i>erg6</i> , <i>erg2</i> , <i>erg5</i> , <i>erg4</i> , <i>bck1</i> , as well as <i>mkk1/mkk2</i> , exhibited higher resistance, while <i>erg3</i> and <i>yca1</i> mutant strains displayed higher sensitivity to ethanolic extracts of <i>Curcuma longa</i> (CE) and <i>Myristica fragrans</i> (NME) compared to their respective wild-type (WT) strains.....	118
Figure 40 – Infrared spectrum analysis of <i>Curcuma longa</i> (CE) extract.....	121
Figure 41 – GC-MS chromatogram of <i>Curcuma longa</i> (CE) extract.....	122
Figure 42 – ATR-FTIR spectrum of <i>Myristica fragrans</i> (NME) extract.....	124
Figure 43 – Chromatogram of <i>Myristica fragrans</i> (NME) extract.....	125

LIST OF TABLES

Table 1 – Top ten major phytopathogenic fungi according to plant mycologists and their lifestyle. Table adapted from Dean et al. (2012).....	3
Table 2 – Top 10 pathologic oomycetes that affect plants. Table adapted from Kamoun et al. (2015).9	9
Table 3 – Yeast strains used in this study	43
Table 4 – Phytopathogenic fungi and oomycetes used in this study	43
Table 5 – MIC values of cells exposed to three different concentrations of itraconazole (ITC).....	82
Table 6 – MIC values of cells exposed to three different concentrations of <i>Curcuma longa</i> (CE) extract.	83
Table 7 – Key infrared spectrum bands of <i>Curcuma longa</i> (CE) extract and their corresponding designations.	121
Table 8 – Chemical compounds detected in <i>Curcuma longa</i> (CE) extract by GC-MS.....	122
Table 9 – Pricipal bands in <i>Myristica fragrans</i> (NME) extract infrared spectrum and their designations.	124
Table 10 – Chemical compounds identified by GC–MS in <i>Myristica fragrans</i> (NME) extract.....	125

1. INTRODUCTION

1.1. Current challenges in agriculture

Throughout the recent history, the agricultural sector has faced numerous challenges in meeting the demand for products in the required quantity and quality. These challenges include decreasing crop yields caused by pests, diseases, climate changes, and abiotic stresses (Grassini et al., 2013). Furthermore, there is an urgent need for larger-scale production to meet the demands of a growing global population, projected to reach 10 billion by 2050 (FAOSTAT, 2022). It is estimated that food production will need to increase by 70% compared to current levels to sustain this population growth (Demestichas et al., 2020). The use of chemicals in agriculture, including efficient herbicides, fungicides, and other pesticides, is essential for protecting agricultural crops against pests and diseases (Brauer et al., 2019). However, continuous exposure to mixtures of bioactive synthetic compounds, both known and unknown, eventually becomes a significant environmental concern, leading to contamination of terrestrial and aquatic ecosystems and ultimately posing a major impact on environmental and human health. These unknown compounds are related to products that are formed through the incomplete degradation of primary bioactive compounds, exhibiting high variability over time. This degradation can occur during water treatment with abiotic processes, including chlorination, ozonation, or exposure to ultraviolet light, which are utilized in water treatment for disinfection or advanced oxidation. Some of the resulting transformation products exhibit higher toxicities compared to the original compound, and a significant concern is that only a few of these products have been identified so far (Celiz et al., 2009; Creusot et al., 2020).

Agriculture also contributes significantly to greenhouse gas (GHG) emissions through the manufacturing of fertilizers, which convert approximately 120 million tons of atmospheric N_2 into reactive forms each year. These reactive forms subsequently enter the environment, polluting water bodies and accumulating in soil, thereby contributing to various GHG released into the atmosphere. Biodiversity loss, agrochemical pollution, and soil degradation are additional problems associated with intensive agriculture (Amundson et al., 2015; Rockström et al., 2009). The excessive use of these chemicals gives rise to additional serious problems, such as the development of resistance in pathogens, rendering crops increasingly susceptible to these agents. This resistance to fungicides occurs due to the high genetic flexibility exhibited by pathogenic agents; additionally, their broad-spectrum lifecycles enable them to effectively invade new hosts (Khan et al., 2020). Another issue associated with agrochemicals is their potential impact on human health, especially in fostering resistance in pathogens, particularly fungi. The

emergence of resistance narrows down the available treatments for fungal infections in humans (Assres et al., 2021). Consequently, this poses significant risks to the health and well-being of both the planet Earth and humankind, emphasizing the importance of further study in this area. Considering the numerous challenges and risks associated with conventional agriculture, which have demonstrated the potential harm to living organisms and the environment, it becomes imperative to prioritize food security and the preservation of ecosystems. This can be achieved by adopting more sustainable farming systems, such as organic farming, integrated farming, and conservation agriculture (Reganold & Wachter, 2016).

1.1.1. Food production and losses

Currently, approximately 38% of our planet's land surface is dedicated to agriculture, making it a highly significant activity for various economic sectors worldwide, particularly the food sector (Jiménez-Reyes et al., 2019; Reganold & Wachter, 2016). The cultivation of cereals, fruits, and vegetables serves as a vital source of income globally. However, these crops are often exposed to environmental conditions, and also to more or less long transportation times after harvest, rendering them more susceptible to a wide range of pathogens, including bacteria, fungi, viruses, and nematodes. Consequently, these pathogens can cause substantial reductions in crop yield (Bajpai & Chul, 2012; Brauer et al., 2019; Jiménez-Reyes et al., 2019) and also food products waste. According to the Food and Agriculture Organization of the United Nations (FAO) and its statistical database (FAOSTAT), the world finds itself at a critical juncture, largely due to the COVID-19 pandemic. World hunger continues to increase, alongside rising levels of food insecurity and various forms of malnutrition. Factors such as conflict, climate variability, extreme weather events, and economic slowdowns further impede progress, particularly in countries marked by high levels of inequality (FAO, 2021). The ongoing invasion of Ukraine, the devastating impact of the war, and the resulting disruption in cereal exports from the region serve as stark reminders of how localized conflicts can have profound repercussions on a global scale.

1.1.2. Phytopathogenic fungi and oomycetes and principal diseases

Despite the extensive efforts made to enhance and improve agricultural techniques, particularly in the field of plant crop protection, a significant annual loss of 10 to 15% of the world's major crops still occurs due to diseases. This factor impedes the growth of agricultural production, posing a global limitation that affects numerous developed and developing countries and resulting in substantial direct

economic losses (Chatterjee et al., 2016; Khan et al., 2020; Teng et al., 1984). Among these diseases, 70-80% are attributed to fungi, which have a severe impact on crop growth, quality, and yield, resulting in significant economic and production losses (Li et al., 2017; Peng et al., 2021; Pusztahelyi et al., 2015). Furthermore, many of these fungi produce toxins that are harmful to plants, even at low concentrations, causing imbalances or inhibitions in normal physiological functions of plants (Peng et al., 2021; Soyer et al., 2015). These phytotoxins are primarily low molecular weight secondary metabolites generated by the metabolism of pathogens. Specific symptoms associated with these diseases can include wilting, growth inhibition, chlorosis, necrosis and leaf spots (Thynne et al., 2016; Yin et al., 2016). The mechanism of action (MOA) of phytotoxins involves interference in plant metabolism, resulting in significant impacts on plant development. These toxins primarily target cellular components such as the cell membrane, mitochondria, and chloroplasts, as well as other cellular targets, making the mechanism complex (Peng et al., 2021; Shang et al., 2016). Phytotoxins exert their effects through various MOA, including the inhibition of protein and nucleic acid synthesis, which leads to physiological disturbances, cell death, and, in some cases, even the demise of the entire plant (Zeilinger et al., 2016).

According to Dean et al. (2012), the top ten major phytopathogenic fungi responsible for causing severe diseases and resulting in significant economic and yield losses are *Magnaporthe oryzae*, *Botrytis cinerea* and various species of *Puccinia*, which occupy the first three positions (see Table 1).

Table 1 – Top ten major phytopathogenic fungi according to plant mycologists and their lifestyle. Table adapted from Dean et al. (2012).

Position	Phytopathogenic fungus	Lifestyle of the fungus	Researcher who described the fungus
1	<i>Magnaporthe oryzae</i>	Hemibiotrophic	Ralph Dean
2	<i>Botrytis cinerea</i>	Necrotrophic	Jan A. L. van Kan
3	<i>Puccinia</i> spp.	Biotrophic	Zacharias A. Pretorius
4	<i>Fusarium graminearum</i>	Necrotrophic	Kim Hammond-Kosack
5	<i>Fusarium oxysporum</i>	Hemibiotrophic or Necrotrophic	Antonio Di Pietro
6	<i>Blumeria graminis</i>	Obligate Biotrophic	Pietro Spanu
7	<i>Mycosphaerella graminicola</i>	Necrotrophic	Jason J. Rudd
8	<i>Colletotrichum</i> spp.	Hemibiotrophic	Marty Dickman
9	<i>Ustilago maydis</i>	Biotrophic	Regine Kahmann
10	<i>Melampsora lini</i>	Biotrophic	Jeff Ellis

When fungi colonize plants, they are detected by the plant immune system, which triggers host defenses. This immune response is initiated by specific molecular patterns found on the fungus, known as pathogen-associated molecular patterns (PAMPs) and microbe-associated molecular patterns (MAMPs). One example of a PAMP in fungi is chitin, a component of the fungal cell wall. Upon contact of fungal cells with plants, chitin fragments are released and recognized by plant chitinases. This recognition occurs through pattern recognition receptors (PRRs) located on the plant's cell membrane, leading to the activation of a defense mechanism called PAMP-triggered immunity (PTI) (Jones & Dangl, 2006; Presti et al., 2015). PRR signaling can also be activated by damage-associated molecular patterns (DAMPs) that originate from the host (Boller & Felix, 2009). PTI results in rapid responses, including the production of reactive oxygen intermediates, activation of ion channels, activation of defense-related protein kinase cascades, and changes in gene expression within the plant. These responses collectively lead to the production of antimicrobial compounds. These compounds include proteinases, chitinases, glucanases that damage fungal structures, enzyme inhibitors targeting molecules produced by the fungus, and other nonprotein antimicrobial molecules (Jones & Dangl, 2006; Presti et al., 2015; Manning et al., 2004). Also, PTI is effective in providing resistance against non-adapted fungi (known as non-host resistance) and can determine whether a plant is susceptible to fungal penetration (Uma et al., 2011).

For fungi to establish a compatible interaction and proliferate, they must either avoid triggering PTI or counteract/suppress it. This can be achieved by deactivating toxic metabolites or secreting fungal effectors. Fungal effectors can take the form of toxic secondary metabolites or proteins that harm the host plant (in necrotrophic and hemibiotrophic fungi during their necrotrophic stage). Alternatively, effectors can be secreted proteins that protect the fungus, suppress immune response of the host, or manipulate the physiology of host cells (Jonge et al., 2011; Okmen & Doehlemann, 2014; Zuccaro et al., 2014). Overall, fungal effectors specifically target components of plant defense, signaling, and metabolic pathways to facilitate the colonization of host plants (Presti et al., 2015). Effectors are typically expressed by fungi only after they come into contact with the plant. The expression of these effectors is finely regulated and tailored to different stages of infection, and it can be influenced by the specific cell type or organ being infected (Okmen & Doehlemann, 2014). Coevolutionary processes between plants and the fungi that colonize them have influenced the genomes of both organisms. There is evidence suggesting that effector genes are located in flexible genomic regions, which facilitates rapid evolution of these genes and influences the acquisition and loss of effector genes (Rep & Kistler, 2010). Additionally, recent host jumps have influenced the effector repertoire and promoted increased diversification (Dong et al., 2014; Sharma et al., 2014). While secreted effectors play a crucial role in suppressing PTI, they can also be

recognized by the plant's surveillance system, leading to a secondary defense mechanism known as effector-triggered immunity (ETI). The plant's surveillance system involves mechanisms and sensors that monitor the environment, detect threats, and trigger defense responses. These responses can be localized or systemic, impacting the entire plant. Integrated surveillance systems aid plants in adapting to changing conditions and challenges (Presti et al., 2015).

Fungi exhibit a wide range of lifestyles, employing various strategies to engage with their host plants. These strategies encompass necrotrophic, biotrophic, and hemibiotrophic approaches, each with distinct characteristics and interactions with the host. In addition, fungi also demonstrate significant variations in their ability to infect a wide range of plant species (Presti et al., 2015). The initial stages of infection, which involve fungal adhesion to the plant's surface, germ tube growth, and the development of infection structures like appressoria or hyphopodia, are similar among fungi that colonize plants. However, fungi differ in the specific surface cues they respond to. Pathogenic fungi form appressoria, while beneficial fungi form hyphopodia, in response to various plant cues, including topographical cues like stomatal pores, chemical cues like epicuticular waxes, or physical cues like hydrophobicity and thigmotropism in different systems (O'Connell & Panstruga, 2006; Rich et al., 2014; Tucker & Talbot, 2001). Pathogenic fungi with different lifestyles exhibit distinct types of appressoria. Hemibiotrophic fungi like *M. oryzae* and *Colletotrichum* spp. develop dome-shaped, melanized appressoria that generate turgor pressure, enabling the penetration of infection hyphae into the host through mechanical means (Tucker & Talbot, 2001). Most necrotrophic fungi form inconspicuous appressoria and penetrate the plant cuticle by secreting a large number of enzymes that degrade the plant cell wall (PCWDEs). Many pathogenic biotrophs combine turgor pressure with PCWDEs to breach the cell wall without harming host cell viability (O'Connell & Panstruga, 2006). In contrast, beneficial biotrophs heavily rely on host-derived enzymes that loosen the cell wall (Rich et al., 2014).

After breaching the host plant's initial defense mechanisms, colonization occurs, accompanied by the development of fungal growth structures. These structures can differ even in fungi that have the same lifestyle and mode of infection. Necrotrophic fungi such as *B. cinerea*, *Fusarium oxysporum* and *Mycosphaerella graminicola* generally grow subcuticularly and secrete toxic metabolites and proteins to kill epidermal cells. Due to this mode of action, their hyphae end up replacing a large area of the plant epidermis (see Figure 1A). Both beneficial and pathogenic biotrophic fungi and hemibiotrophs can form intracellular or intercellular hyphae, which expand inside the host. In the case of intercellular hyphae, they can insert feeding structures known as haustoria or arbuscules into host cells (O'Connell &

Panstruga, 2006) (see Figures 1B and C). In the case of hemibiotrophic fungi, such as *M. oryzae* and *Colletotrichum* spp. they initially form arched and invasive biotrophic hyphae that later transform into thin necrotrophic hyphae (O'Connell & Panstruga, 2006; Oliveira-Garcia & Deising, 2013) (see Figure 1D).

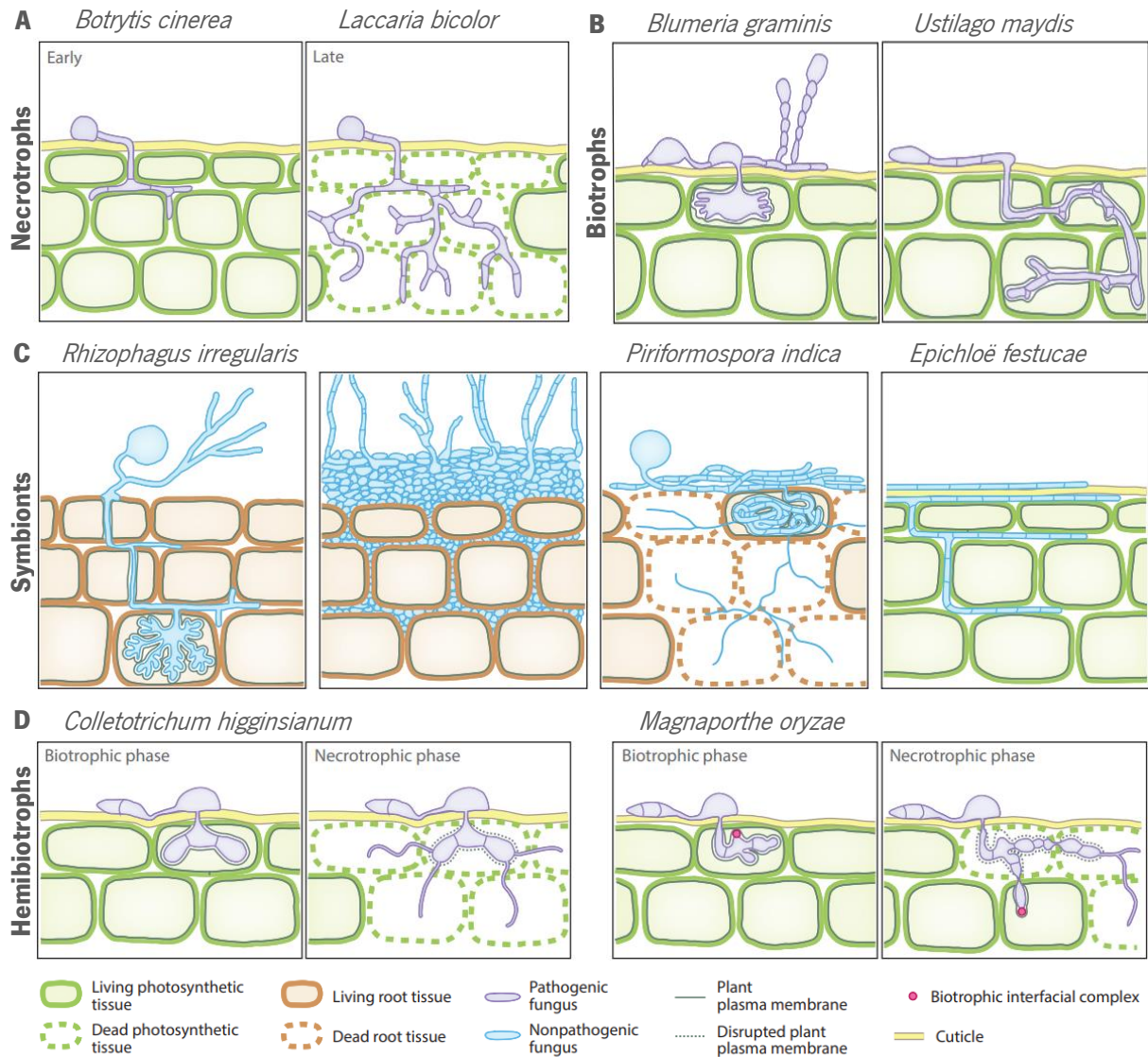


Figure 1 – Colonization of plants by fungi with different lifestyles. (A) Necrotrophic fungi, like *B. cinerea*, typically growth beneath the plant surface and cause the death of epidermal cells by releasing toxic metabolites and proteins. Over time, their hyphae replace substantial portions of the plant's epidermis. This process includes both the early and late developmental stages; **(B)** Obligate biotrophic pathogens, like *B. graminis*, form a haustorial mother cell that gives rise to a ballon-shaped feeding structure called haustorium. The biotrophic *U. maydis* initially grows inside plant cells but transitions to predominantly growing between cells in later stages, resulting in massive fungal proliferation and the formation of large plant tumors; **(C)** The obligate arbuscular mycorrhizal root symbiont *R. irregularis* colonizes specific cortical cells with highly branched feeding structures called arbuscules. The ectomycorrhizal fungus *L. bicolor* exclusively grows between cells, forming a mantle or sheath of hyphae that covers the root epidermis and generates the Hartig net between cortical cells. Endophytes, such as *P. indica* and *E. festuca*, can grow either inside or between plant cells; **(D)** Hemibiotrophic fungi, like *Colletotrichum* spp. and *M. oryzae*, initially develop bulged biotrophic invasive hyphae that later transition into thin necrotrophic hyphae. Both the biotrophic and necrotrophic phases are represented. Adapted from Presti et al. (2015).

Biotrophic fungi that grow intracellularly or insert structures such as haustoria or arbuscules into host plant cells exhibit a conserved characteristic. This characteristic involves the tight enclosure of the feeding structures by the plasma membrane of the plant cells (see Figure 1). This membrane is referred to as the extrahaustorial membrane in the case of haustoria-forming biotrophs and the periarbuscular membrane in the case of arbuscular mycorrhizal symbionts. It is continuous with the plant cell plasma membrane but differs in protein composition, featuring a unique group of transmembrane proteins (Koh et al., 2005; Micali et al., 2011; O'Connell & Panstruga, 2006; Rich et al., 2014). Further investigation is required to fully understand the molecular mechanisms underlying the formation of haustoria and arbuscules (Koh et al., 2005). However, it is clear that these structures play a crucial role in nutrient uptake and exchange, while also serving as the primary site for effector secretion (O'Connell & Panstruga, 2006). Additionally, in the case of intracellular hyphae of *Ustilago maydis* and biotrophic hyphae of *M. oryzae* and *Colletotrichum* spp., as occurs in haustoria, these hyphae are tightly entangled by the plasma membrane of the host cells, resulting in the formation of a tight biotrophic interface (see Figure 1). In *M. oryzae*, a membrane-rich structure known as the biotrophic interfacial complex forms specifically at the primary tips of invading hyphae. This structure, which was found recently to be of plant origin, normally appears outside the fungal plasma membrane and is thought to deliver a subset of effectors to host plant cells (Giraldo et al., 2013; Khang et al., 2010).

In addition to the aforementioned three fungal lifestyles, there exists a category known as saprotrophs. Saprotrophic fungi, also referred to as saprophytic fungi, are a group of fungi that obtain their energy and nutrients by decomposing non-living organic matter and do not colonize or engage in symbiotic associations with living hosts (Presti et al., 2015). They have various functional traits commonly linked to the processes of biogeochemical cycling in leaf litter and soil (Ceci et al., 2019), as exemplified by a study conducted by Persiani et al. (2008). Thus, these fungi play a vital role in ecosystems as decomposers, breaking down dead plant material, animal remains, and other organic substances. Saprotrophic fungi secrete enzymes that break down complex organic molecules into simpler forms, which they can then absorb and use as a source of energy and nutrients for their growth and reproduction. This process of decomposition helps recycle nutrients back into the environment, facilitating nutrient cycling and playing a crucial role in the overall functioning of ecosystems (Ceci et al., 2018, 2019). Also, it is possible for certain saprotrophic soil fungi to develop the capacity to metabolize pollutants as a result of exposure to contamination (Pinto et al., 2012).

Fungal diseases are not just caused by a single pathogen alone, some are rather caused by multiple pathogens, resulting from a synergistic interaction among them (Chatterjee et al., 2016). Over time, the co-evolution of plants and pathogenic fungi has given rise to highly specialized relationships, leading to complex interactions. Additionally, with the continuous emergence of pathogenic fungi, their relationships with plants have undergone changes (Peng et al., 2021; Quintanilha-Peixoto et al., 2019). As a result of these intricate interactions, these fungi have also contributed to the development of new techniques for sustainable agriculture (Marín-Menguiano et al., 2019).

In the other hand, oomycetes, also known as "water molds," are a group of fungus-like eukaryotic microorganisms within the Stramenopiles, that are filamentous, heterotrophic and can reproduce both sexually and asexually (Burki et al., 2020). According to Thines & Kamoun, (2010), over 60% of identified oomycete species are plant pathogens. Collectively, they pose a substantial menace to both global food security and natural ecosystems (McGowan & Fitzpatrick, 2020). The taxonomy of oomycetes has evolved over time and due to similarities in their filamentous growth, osmotrophic uptake of nutrients and similar ecological roles, they were originally classified as fungi (Richards et al., 2006). However, molecular and biochemical analyses as well as morphological features and phylogenetic studies revealed significant differences between fungi and oomycetes (Kamoun, 2009). The cell walls of oomycetes contain cellulose and beta-glucans, while fungal cell walls are primarily composed of chitin. Another distinction lies in the ploidy of their vegetative hyphae. Oomycetes have diploid hyphae, whereas true fungi have haploid or dikaryotic hyphae. In terms of reproduction, oomycetes employ oogamous reproduction, which involves the production of diploid oospores from zygotes following fertilization of haploid oospheres by haploid gametes. In contrast, true fungi generally undergo isogamous or heterogamous reproduction. Oomycetes further set themselves apart from fungi with their motile asexual spores, characterized by biflagellated zoospores, in contrast to fungi. Additionally, their hyphal structure differs, with oomycetes typically having aseptate and multinucleate hyphae, while true fungi have septate hyphae (Judelson & Blanco, 2005; Kamoun, 2009; McGowan & Fitzpatrick, 2020).

The classification of oomycetes is based on morphological and molecular characteristics, and the major orders of oomycetes include Peronosporales, Pythiales, Albuginales and Saprolegniales (McGowan & Fitzpatrick, 2020). They have the ability to utilize diverse modes of infection to colonize plants. Similar to fungal pathogens, they develop specialized infection structures, including appressoria and haustoria. The infection cycle of many oomycetes incorporates a biotrophic phase, during which the pathogen depends on living host cells. For instance, pathogens like *P. infestans* employ a two-step infection strategy,

characteristic of hemibiotrophs (Kamoun, 2009). Some of the key mechanisms involved in this process are sporangia dispersal, where oomycetes disperse through asexual sporangia that are produced from infected foliage and can be distributed to other plants, where they germinate directly; germination and penetration, where the germination of oomycete sporangia can occur directly, forming germ tubes that penetrate the plant's cuticle or stomata; mycelial growth and haustoria formation, where, once inside the plant, the oomycetes grow extensively between cells, forming a network of hyphae. They can also penetrate plant cells, forming long, curled haustoria, which facilitate nutrient uptake from the host; release of enzymes and toxins, where oomycetes secrete various enzymes and toxins that help them break down plant cell walls, suppress host defense responses, and obtain nutrients from the host; and disease development and spread, whereas oomycetes continue to grow and reproduce within the host plant, they cause various symptoms, such as leaf spots, wilting, and tissue decay. The spread of oomycete diseases can occur through the movement of infected plant material, soil water, or other means, depending on the specific pathogen (Fawke et al., 2015; He et al., 2020; Kamoun, 2009; McGowan & Fitzpatrick, 2020). This group of eukaryotic organisms include some of the most devastating plant pathogens, as evidenced in Table 2 compiled by Kamoun et al. (2015), which highlights the top ten oomycetes in molecular plant pathology. Overall, oomycetes are collectively responsible for a wide range of plant diseases, leading to significant economic and ecological impacts.

Table 2 – Top 10 pathogenic oomycetes that affect plants. Table adapted from Kamoun et al. (2015).

Position	Phytopathogenic oomycete	Lifestyle of the oomycete	Common disease name(s)
1	<i>Phytophthora infestans</i>	Hemibiotrophic	Late blight
2	<i>Hyaloperonospora arabidopsidis</i>	Biotrophic	Downy mildew
3	<i>Phytophthora ramorum</i>	Hemibiotrophic	Sudden oak death; Ramorum disease
4	<i>Phytophthora sojae</i>	Hemibiotrophic	Stem and root rot
5	<i>Phytophthora capsici</i>	Necrotrophic and Hemibiotrophic	Blight; stem and fruit rot; various others
6	<i>Plasmopara viticola</i>	Biotrophic	Downy mildew
7	<i>Phytophthora cinnamomi</i>	Necrotrophic and Hemibiotrophic	Root rot; dieback
8	<i>Phytophthora parasitica</i>	Necrotrophic and Hemibiotrophic	Root and stem rot; various others
9	<i>Pythium ultimum</i>	Necrotrophic	Damping off; root rot
10	<i>Albugo candida</i>	Biotrophic	White rust

In this study, the selection of phytopathogenic fungi and oomycetes was based not only on their significance but also on their reputation as highly destructive pathogens. The fungi investigated in this study included *B. cinerea*, *Colletotrichum acutatum*, *Diplodia corticola* and *Fusarium culmorum*, while the oomycetes investigated included *Phytophthora cactorum* and *Phytophthora cinnamomi*.

1.1.2.1. *Botrytis cinerea*

The fungus *B. cinerea* from the family Sclerotiniaceae and the causal agent of the disease known as gray mold, has the ability to infect over 1400 plant species, including solanaceous plants, and important crops such as cucurbits, tomatoes, grapes, strawberries and other vegetables (see Figure 2A) (Porquier et al., 2021). This fungus is particularly destructive on mature or senescent tissues, and contamination can occur from the seedling stage to the ripening stage. In addition, this fungus can remain dormant for a significant period of time until it starts decaying tissues when there are changes in the host's physiology and the environment becomes suitable (Williamson et al., 2007). As a result, crops, even if they appear healthy, remain susceptible to severe damage after harvest (Dean et al., 2012) and, despite the growing effectiveness of biocontrol measures in certain crops (Moser et al., 2008), the predominant method for controlling *B. cinerea* still relies on fungicide application (Dean et al., 2012).

B. cinerea is considered a typical necrotrophic pathogen, utilizing programmed cell death pathways in the host to facilitate infection (Van Baarlen et al., 2007). As shown by Shlezinger *et al.* (2011) extensive cell death in the pathogen occurs because plant defense molecules target the fungal programmed cell death (PCD) machinery. In contrast, the fungal anti-apoptotic machinery protects the fungus from host-induced PCD, enabling the formation of small infection zones that eventually develop into spreading lesions during the second stage of infection. When the anti-apoptotic machinery of *B. cinerea* weakens or strengthens, disease symptoms are reduced or enhanced, respectively. Conversely, a weakened plant defense system is associated with decreased fungal PCD and increased disease severity. Also, recent evidence has revealed that the expression of retrotransposons in *B. cinerea* results in the suppression of plant defense-related genes during infection. This raises the hypothesis that retrotransposons could potentially function as fungal pathogenicity factors (Porquier et al., 2021).

Moreover, the short life cycle of *B. cinerea*, coupled with its rapid genetic variation, further complicates the management of gray mold in agricultural production, being this fungus considered as a high-risk pathogen for fungicide resistance (Liu et al., 2021). In addition, hosts can be infected by various

forms of the fungus, including mycelia, conidia, and sclerotia (see Figure 2B) (Breeze, 2019; Liu et al., 2017).

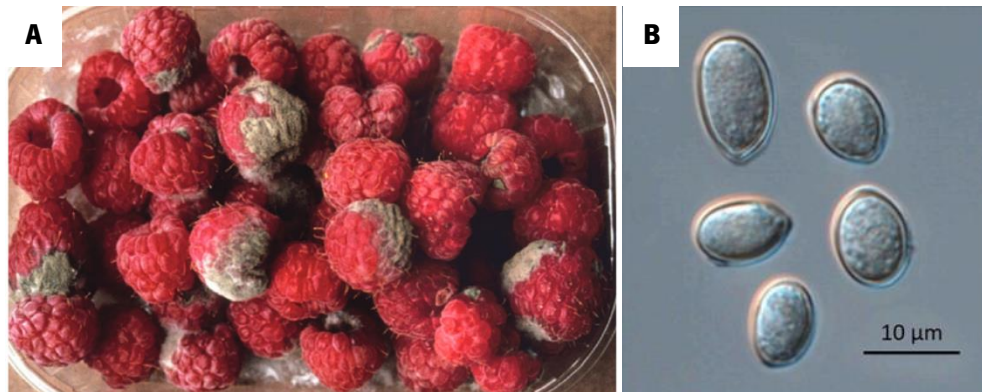


Figure 2 – Images of *Botrytis cinerea*. (A) *B. cinerea* affecting raspberry fruits; (B) Conidia of *B. cinerea*. Adapted from Williamson et al. (2007) and Pei et al. (2019).

As a curiosity, *B. cinerea* stands out as a remarkable pathogen due to its occasional beneficial effects. In certain climatic conditions, *B. cinerea* can induce noble rot in grape berries, which is desirable for the production of sweet wines. However, despite these isolated benefits in the wine industry, the overall impact of *B. cinerea* remains negative (Dean et al., 2012).

1.1.2.2. *Colletotrichum acutatum*

Colletotrichum acutatum from the family Glomerellaceae is a phytopathogenic fungus widely studied and recognized as one of the most important species within the genus. This fungus is considered a hemibiotrophic and is responsible for causing serious diseases, such as anthracnose, which affect a wide range of plants, both woody and herbaceous. It is particularly notorious for its impact on high-value agricultural crops worldwide, including strawberries, which are commonly affected by this holonecrotic disease that affects all organs of the plant (Cannon et al., 2012; Tomas-Grau et al., 2019).

This fungus was initially discovered in Australia by Simmonds, (1965) on infected tissues of *Carica papaya*, *Capsicum frutescens* and *Delphinium ajacis*, commonly known as papaya, pepper, and delphinium flowers, respectively. Over time, *C. acutatum* has been found to infect not only these aforementioned species but also other economically important ones. It has been reported to affect citrus (Peres et al., 2008), apple (Lee et al., 2007), olive (Talhinhas et al., 2011), cranberry (Polashock et al., 2009), and blueberry (Wharton & Schilder, 2007). It is considered one of the most destructive fungi affecting these fruits and causing severe diseases that significantly impact commercial fruit production (see Figures 3A and B). Additionally, *C. acutatum* has been associated with other diseases, including

terminal crook disease in pine (Dingley & Gilmour, 1972) and leatherleaf fern anthracnose (Schiller et al., 2006). Moreover, there have been reports of infection by this fungus in a sea turtle (Manire et al., 2002) and a cochineal insect (Marcelino et al., 2008).



Figure 3 – Infections and image of *Colletotrichum acutatum*. (A) Ripe rot of blueberry and (B) bitter rot of apple caused by *C. acutatum*, (C) Conidia of *C. acutatum*. Adapted from Peres et al. (2005) and Damm et al. (2012).

Colletotrichum acutatum is primarily known for its distinctive conidia shape with pointed ends (Simmonds, 1965) (see Figure 3C). However, variations in conidial forms, particularly cylindrical ones with a single pointed end, can also be observed, especially in strains that have undergone multiple subcultures. It is worth noting that these conidial forms can be found in species outside the *C. acutatum* species complex as well. In the host, conidia are formed on acervuli, while in culture, they are often produced on the aerial mycelium (Johnston & Jones, 1997). Additionally, *C. acutatum* develops simple pigmented appressoria, typically without many or any bristles (Damm et al., 2012; Simmonds, 1965).

Extensive research is required to explore the mechanisms of pathogenicity and population-level evolution in *C. acutatum*. However, it is evident that numerous *Colletotrichum* species demonstrate exceptional proficiency in overcoming multiple host barriers as shown in the aforementioned topic. Thus, there is strong evidence to suggest that the *C. acutatum* species complex is undergoing rapid evolution (Damm et al., 2012).

1.1.2.3. *Diplodia corticola*

Diplodia corticola from the family Botryosphaeriaceae is an ascomycete fungus that causes several diseases in woody plants such as *Quercus afares*, *Quercus canariensis*, *Quercus coccifera* and *Quercus ilex*, commonly known as African Oak, Algerian Oak, Hangman's Oak and Holm Oak, respectively. One of the diseases most commonly associated with this fungus is Botryosphaeria canker

(see Figures 4A and B), which unfortunately has been spreading in Mediterranean landscapes, particularly affecting the cork oak (*Quercus suber*) (Moricca et al., 2016). Over the past few decades, this pathogen has contributed to the decline of cork oaks in the Iberian Peninsula and other Mediterranean regions, such as Sardinia in Italy (Phillips et al., 2013). However, *D. corticola* has also been found infecting other hosts outside the Mediterranean area, including some American oaks (*Quercus agrifolia*, *Quercus chrysolepis*, *Quercus rubra* and *Quercus virginiana*) (Dreaden et al., 2011), grapevines (*Vitis vinifera*) in California, Italy, Spain and Texas (Carlucci & Frisullo, 2009; Úrbez-Torres et al., 2009, 2010; Varela et al., 2011) and eucalyptus trees, mainly *Eucalyptus globulus* (Barradas et al., 2016).

This phytopathogenic fungus can cause various symptoms in infected plants, including seedling mortality, severe necrosis, wilting, and dieback. Furthermore, it significantly reduces the regeneration of bark after stripping in mature cork oaks, leading to a drastic decline in cork extraction. This has profound economic, ecological and social implications, threatening the traditional and sustainable use of forests in the medium term (Muñoz-Adalia & Colinas, 2021; Serrano et al., 2015). Despite the importance of this disease, the infection process and underlying factors still require further research for a comprehensive understanding. Recent studies suggest that *D. corticola* is a hemibiotrophic fungus, displaying a transition from biotrophic to necrotrophic interaction following episodes of plant stress. This transition is supported by the colonization of living plant tissues by the pathogen, accompanied by the secretion of proteins such as kerato-platanin and necrosis-inducing factors, which are characteristic of hemibiotrophic fungi (Dou & Zhou, 2012; Fernandes, 2015; Horbach et al., 2011). In addition to colonizing the stems of host plants, there are indications that *D. corticola* can also infect the roots of *Q. agrifolia* (Linaldeddu et al., 2014; Lynch et al., 2013), and penetrate the leaves of *Q. suber* and *Quercus cerris* (Paoletti et al., 2007). Further research is needed to elucidate the infection mechanisms and contributing factors associated with this fungus.

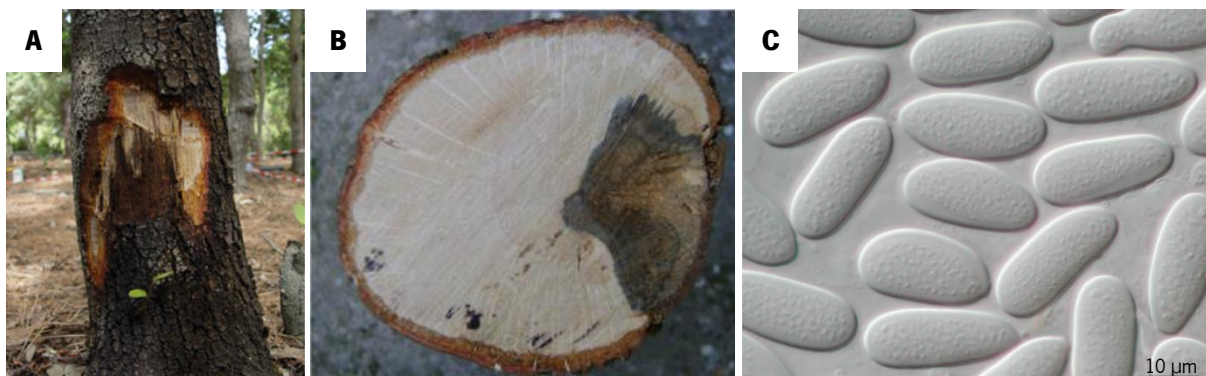


Figure 4 – Infections and image of *Diplodia corticola*. Symptoms observed on holm oak trees include (A) necrotic xylem tissues at the collar region and (B) cross section of a branch canker that reveals a distinct wedge-shaped necrotic sector; (C) Conidia of *D. corticola*. Adapted from Linaldeddu et al. (2014) and Phillips et al. (2013).

The conidia of *D. corticola* are typically larger than those found in any other *Diplodia* species (see Figure 4C) (Phillips et al., 2013). It is believed that the dispersal of conidia in this species primarily occurs through wind (Bérubé et al., 2018) and raindrops, similar to other species within the Botryosphaeriaceae family (Kuntzmann et al., 2009; Úrbez-Torres et al., 2010). Additionally, some researchers hypothesize that *D. corticola* may exist as a latent pathogen in oaks (Muñoz-Adalia et al., 2022). Furthermore, *D. corticola* is known to produce secondary metabolites that exhibit potential biological activities, including antimicrobial, insecticidal, herbicidal and anticancer properties. These metabolites hold promise for applications in agriculture and medicine. However, ongoing research is being conducted in this area (Cimmino et al., 2016; Lecce et al., 2021; Masi et al., 2016; Salvatore et al., 2022).

1.1.2.4. *Fusarium culmorum*

Fusarium culmorum from the family Nectriaceae is a phytopathogenic ascomycete present in soil, with a significant impact on a wide variety of small-grain cereals worldwide (Birr et al., 2020; Scherm et al., 2013). These cereals include wheat (Birr et al., 2020; O'Donnell et al., 2013; Scherm et al., 2013), maize (Pfordt et al., 2020), barley, oats, triticale and rye (Nielsen et al., 2011; Sundheim et al., 2013). The pathogen has also been found to infect *Arabidopsis* floral tissues (see Figure 5B) (Cuzick et al., 2009), although its significance in this context needs further investigation. Furthermore, *F. culmorum* exhibits a highly competitive saprophytic capacity and is responsible for causing *Fusarium* stem and root rot (FRR) and *Fusarium* head blight (FHB) in wheat (see Figure 5A) (Scherm et al., 2013). Although this fungus is more commonly found in temperate or colder regions of Europe and Canada (Pasquali et al., 2016), in the last few decades, this pathogen has been increasingly reported in Italy, Spain, Turkey, Tunisia (Kammoun et al., 2010; Yörük & Albayrak, 2012), Australia and New Zealand (Bentley et al., 2006).



Figure 5 – Infections and image of *Fusarium culmorum*. (A) A wheat head displaying symptoms of *Fusarium* head blight (FHB). (B) *Arabidopsis* flowers infected with *F. culmorum*; (C) Macroconidia of *F. culmorum*. Adapted from Pancaldi et al. (2010) and Cuzick et al. (2009).

Fusarium culmorum is also known to particularly infect freshly harvested grain that has not been properly dried or correctly stored post-harvest (Aldred & Magan, 2004; Eifler et al., 2011; Lowe et al., 2012). This pathogen is of significant concern in wheat production, as it induces FHB, leading to substantial losses in yield, grain quality and safety. The disease initiates with anthesis infection, spreading to infect the wheat heads, colonizing the ear and contaminating the grain with a large amount of secondary metabolites produced by the fungus – mycotoxins, that pose a considerable threat to human and animal health (Nešić et al., 2021), exhibiting a marked cytotoxic effect in eukaryotic organisms (Senter et al., 1991).

These mycotoxins are divided into two main groups: type-B trichothecenes and estrogenic zearalenone (ZEN) (Bentley et al., 2006; Kammoun et al., 2010; Nešić et al., 2021; Pasquali et al., 2016; Scherm et al., 2013; Yörük & Albayrak, 2012). Trichothecenes, considered the most bioactive compounds produced by this fungus, inhibit the synthesis of eukaryotic proteins and cause oxidative damage in cells, which leads to disruption of nucleic acid synthesis and ultimately to apoptosis (Abbas et al., 2013; Senter et al., 1991; Suzuki & Iwahashi, 2014; Wagacha & Muthomi, 2007). These mycotoxins can also induce toxicosis in humans and animals when ingested through contaminated food (Sudakin, 2003), and play an important role as virulence factors (Bai et al., 2002). On the other hand, ZEN's chemical structure resembles that of natural estrogens, enabling it to bind to estrogen receptors. This means that ZEN can cause endocrine disruption in reproductive functions in farm animals and may lead to hyperestrogen syndromes in humans (Gromadzka et al., 2008; Ropejko & Twarużek, 2021; Zinedine et al., 2007). Additionally, this mycotoxin has been shown to exhibit hepatotoxic, hematotoxic, immunotoxic and genotoxic effects. However, the precise mechanisms responsible for ZEN toxicity remain to be fully discovered (Gromadzka et al., 2008; Zinedine et al., 2007).

An impressive feature of this phytopathogenic fungus is its ability to remain viable in the form of mycelium in crop residues left on the soil surface. Under these conditions, it can survive between 2 and 4 years, through the formation of chlamydospores (see Figure 5C) (Bateman et al., 1998; Cook, 1980). Typically, when the seed germinates, the fungus infects the host plant through the lesions that are created when the primary root emerges, gradually progressing the infection towards the stem. However, on some occasions, the infection occurs through the stomata at the point of insertion of the basal sheath of the leaf, towards the stem. The colonization process primarily follows an intercellular apoplastic pathway, meaning it occurs between cells in the epidermis and cortex. Subsequently, the fungus advances intracellularly in the symplast, penetrating the cells to complete tissue colonization (Beccari et al., 2011;

Covarelli et al., 2012; Pettitt & Parry, 2001). Later, *F. culmorum* can grow along the stem, but its growth is limited to the first basal internodes. The appearance of basal browning symptoms may precede the detection of the fungus in these areas, as they are the plant's response to the infection (Beccari et al., 2011; Covarelli et al., 2012).

In the case of *Arabidopsis* flowers (see Figure 5B), *F. culmorum* spores germinate, giving rise to colonizing hyphae that grow through living tissue, facilitating the development of mycelium on the surface of the floral tissue. Subsequently, the fungus penetrates and colonizes the tissues, leading to the formation of a necrotic zone, starting with the petals and sepals, followed by constriction of the pedicel and upper stem tissues. Mycotoxin production occurs in the infected floral tissues (Cuzick et al., 2009). Consequently, this fungus is primarily considered necrotrophic, although it can exhibit hemibiotrophic behavior in specific situations.

Several studies have demonstrated that the infection caused by *F. culmorum* is strongly influenced by various factors, including temperature, humidity, carbon and nitrogen availability. Additionally, the fungus's ability to produce mycotoxins can confer greater aggressiveness, potentially affecting or inhibiting the host plant's defense response. Agronomic practices, such as the use of nitrogen fertilizers, seeding in uncultivated soil and soil tillage, have been identified as contributing factors in crop susceptibility to the fungus (Pancaldi et al., 2010; Scherm et al., 2013). However, among these factors, temperature and water availability have been found to significantly impact its growth (Scherm et al., 2013). Furthermore, microscopic studies have revealed that *F. culmorum* can cause disease only in tissues where plant cells are capable of initiating a cell death response and an oxidative burst (Cuzick et al., 2009). Due to the aforementioned risks, it becomes imperative to develop methods for combating the diseases caused by *F. culmorum*, but also prevent the entry of mycotoxins into the food chain (Błaszczuk et al., 2023).

1.1.2.5. *Phytophthora cactorum*

The pathogen *Phytophthora cactorum* from the family Peronosporaceae is a highly destructive hemibiotrophic oomycete known to affect a wide range of plants worldwide (Li et al., 2011). It has been reported to affect more than 200 plant species (Sharma et al., 2022), and it can cause various diseases such as root, crown and collar rot, fruit rot, cankers, leaf burn, wilt and seedling burn in host plants. Additionally, it can lead to foliar and fruit infections in herbaceous and woody species (Erwin & Ribeiro,

1996). Among the diseases caused by *P. cactorum*, one of the most economically significant is *Phytophthora* crown rot (PhCR) (see Figure 6A), which affects strawberries globally. This disease is one of the most important soil-borne diseases and alone can cause production losses of up to 40% (Stensvand et al., 1999). Unfortunately, conventional methods like soil fumigation before planting are ineffective against this disease, mainly because the primary source of inoculum is often present in infected nurseries (Baggio et al., 2021). Therefore, the impact of this oomycete extends beyond strawberries, affecting economically relevant crops like tomato, alfalfa and other fruits (Cai et al., 2021; Chen et al., 2018).

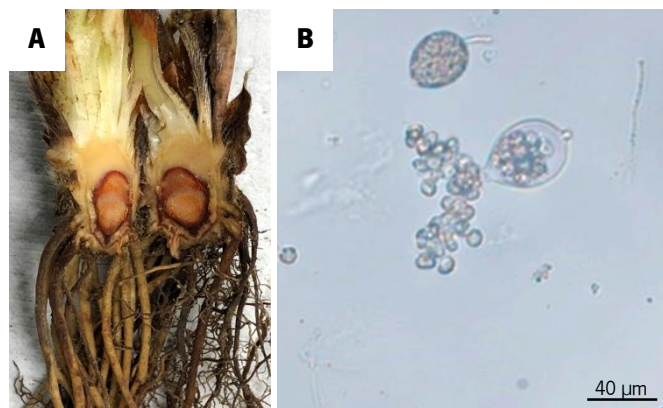


Figure 6 – Infection and image of *Phytophthora cactorum*. (A) Crown rot symptoms caused by *P. cactorum* in strawberry plants; (B) Sporangia releasing zoospores. Adapted from Sharma et al. (2022) and Tao et al. (2023).

Although *P. cactorum* is now widespread throughout the world, it is predominantly found in temperate zones, affecting strawberry crops with PhCR in various regions such as the United States, Europe and parts of Asia and Africa. Typically, this disease first manifests on the young leaves of the plant, causing them to exhibit a bluish-green coloration. Over time, these leaves wilt, and as the disease progresses, crown collapse occurs, leading to the entire plant wilting and dying within a few days (Peres & Baggio, 2019). During the removal of the diseased plant from the ground, the upper end of the crown often breaks due to the crown collapse. Additionally, other characteristic symptoms of this disease include dark reddish-brown discoloration at the top or bottom of the crowns and disintegration of the vascular tissue (see Figure 6A) (Maas, 1998).

One of the distinguishing characteristics of *P. cactorum* from other species is its production of caducous sporangia with short pedicels and paragynous antheridia (Erwin & Ribeiro, 1996). Additionally, it is a homothallic species, capable of producing oospores in diverse natural environments (Sharma et al., 2022). However, the infection process and the development of the diseases themselves are influenced by certain factors, particularly warm weather and abundant moisture. In environments lacking optima or sub-optima for these factors, infections can remain latent (Maas, 1998). Moreover, plants experiencing

stress are more susceptible to diseases caused by this oomycete, as observed in frigo plants transplanted during warm weather (Pettitt & Pegg, 2008). The ability of *P. cactorum* to produce caducous sporangia and oospores, along with its dependency on certain environmental conditions, plays a crucial role in its pathogenicity and the diseases it causes.

As with most *Phytophthora* species, the infection mechanism of *P. cactorum* relies on its motile zoospores. The process begins with sexual reproduction between the antheridia and oogonia, resulting in the production of oospores that can survive in the soil or on plant debris (Srivastava et al., 2020). Under favorable conditions, these oospores germinate and give rise to sporangia, which contain zoospores inside. The germinated sporangia and flagellated zoospores have the ability to infect plants, often entering through wounds that may occur during the transplanting process. These mononuclear zoospores possess double flagella and are released from the sporangia (see Figure 6B). In water, they navigate towards the roots of the host plants. Upon establishing a connection with the host, the zoospores discard their flagella and synthesize a cell wall, resulting in the formation of a cyst. Subsequently, the cyst germinates and penetrates the host tissue through natural openings, such as stomata, or by penetrating epidermal cells with the aid of a swollen tube-like structure similar to an appressorium (Hohl & Stössel, 1976; Sharma et al., 2022; Tao et al., 2023). Understanding the infection mechanism of *P. cactorum* through its motile zoospores is crucial for developing effective strategies to manage and control its impact on plant health.

1.1.2.6. *Phytophthora cinnamomi*

Phytophthora cinnamomi from the family Pythiaceae, like *P. cactorum*, is a soil-borne pathogenic oomycete that causes root rot diseases in a wide variety of plants (Hardham & Blackman, 2018), affecting biodiversity as well as natural ecosystems, nurseries and horticultural crops worldwide. Considering the negative economic and ecological impact of this pathogen, it is considered one of the ten most destructive and devastating oomycetes known (Kamoun et al., 2015). Although *P. cinnamomi* has been observed on trees in forest plantations and natural ecosystems, it significantly threatens economically important host plants, including ornamental crops, avocado, durian, chestnut, macadamia, peach, pineapple and lentisk (see Figure 7A), which are highly susceptible to diseases caused by this oomycete. To date, more than 5000 plant species have been reported infected by *P. cinnamomi* (Hardham & Blackman, 2018), and it poses a significant threat to many native species, mainly in temperate regions (Dell et al., 2004).

In the horticultural industry, avocado trees, as already mentioned, are heavily affected by this agent, leading to declines in quality and yield, which causes significant economic losses (Belisle et al., 2019). Similarly, chestnut trees (*Castanea sativa*) are also highly susceptible to chestnut ink disease caused by infection with *P. cinnamomi*. This represents a major economic problem in Europe, including Portugal, impacting wood and nut production as well as soil stability (Lourenço et al., 2019). In natural ecosystems, the impact of *P. cinnamomi* is particularly pronounced on chestnut stands in the United States of America and Europe, native oak species in Mexico and throughout the Iberian Peninsula, and the natural vegetation of Western Australia. In Western Australia alone, nearly 40% of almost 6000 plant species have been found to be susceptible to *P. cinnamomi*, highlighting its wide-ranging impact (Shearer et al., 1994). Furthermore, *P. cinnamomi* poses a threat to other tree species in natural ecosystems. Holm oak (*Q. ilex*) and cork oak (*Q. suber*) are also highly susceptible to infection (Hardham & Blackman, 2018). The detrimental effects on these tree species can have cascading impacts on the biodiversity and ecological balance of their respective ecosystems.

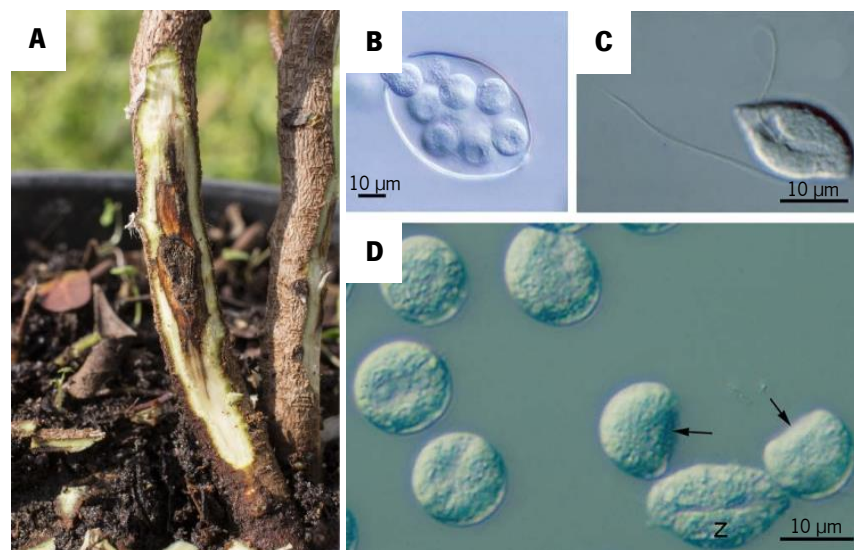


Figure 7 – Infection and image of *Phytophthora cinnamomi*. (A) Symptoms observed on lentisk seedling 20 days after inoculation with *P. cinnamomi*; (B) Zoospore release from a sporangium; (C) A biflagellate zoospore; (D) A zoospore (z) and six young cysts. Adapted from Bregant et al. (2021), Hee et al. (2013) and Hardham & Blackman, (2018).

A striking feature of *P. cinnamomi* is that host plants remain apparently healthy, without symptoms, until the late stages of infection. This characteristic makes control strategies for this oomycete very limited due to the difficulty in early diagnosis. The most favorable condition for this pathogen to produce and increase the dispersion of its zoospores is high soil moisture (Brown et al., 2019). Therefore, irrigation and drainage techniques are employed to prevent the spread of *P. cinnamomi*. However, these techniques are only useful and efficient when the soil is not contaminated with zoospores. When the soil

is contaminated, fumigation (involves the application of specific chemicals or treatments) is utilized to clean the soil and extinguish this pathogen (Hardham & Blackman, 2018). In addition to fumigation, other control strategies include seed and cultivar treatments on zoospore-free soils and crop rotation. However, the latter is not widely used due to the restrictions that plantation land presents and the fact that zoospores of *P. cinnamomi* can survive for long periods of time (You et al., 2020). These resilient zoospores contribute to the challenges faced in managing the spread of this pathogen.

As in other species of the genus *Phytophthora*, the infection process of *P. cinnamomi* starts through the active movements of its zoospores, which have two flagella adorned with tubular hairs (see Figure 7C) (Beakes et al., 2012; Cahill et al., 1996). After these zoospores have been expelled by the sporangium (see Figure 7B), they swim towards the elongation zone of host roots, connecting to grooves above the epidermal anticlinal walls (Hardham, 2005). Additionally, they have the ability to self-aggregate at specific locations on the host root surface when in high densities, possibly influencing the infection process (Savory et al., 2014). After cysts are formed (see Figure 7D), similar to the process previously described for *P. cactorum*, penetration and colonization of the plant occur due to the action of degradation enzymes produced by the oomycete (Hardham & Blackman, 2018). Once inside, *P. cinnamomi* hyphae expand intracellularly or intercellularly from the root to the central vascular bundle. This growth leads to obstruction of the xylem pathway and deposition of material by the plant, resulting in a blockage of water movement. Consequently, this interference disrupts the absorption and transport of water to the shoot, leading to water stress, wilting and chlorosis in the foliage (Ruiz Gómez et al., 2015). Infected roots begin to rot, which can lead to rapid plant death in severe cases (Hardham & Blackman, 2018). However, if plants manage to survive the infection, they may not show symptoms of the disease for many years, contributing to the long-term survival of the pathogen within the plant.

Previously, *P. cinnamomi* was considered an oomycete with a necrotrophic lifestyle. However, more recent studies have provided insights into its infection mechanisms. Research on its putative haustoria in cortical and vascular tissues of infected plants has shown that *P. cinnamomi* can also develop as a hemibiotrophic oomycete (Crone et al., 2013; Redondo et al., 2015). Additionally, it exhibits saprophytic growth on dead organic matter or behaves as a parasite on susceptible plants. Usually, this oomycete primarily infects fine roots, but it can also invade woody stems through natural wounds or breaks in the epidermal layer (O'Gara et al., 2014).

Unfortunately, due to global warming and climate change, infections caused by *P. cinnamomi* are expected to increase, posing serious threats to biodiversity and endemic plant species (Burgess et

al., 2017; Malcolm et al., 2006). The pathogen's ability to infect a wide range of plant species, combined with changing climatic conditions, could lead to a higher extinction rate of endemic plants that are already restricted to specific regions. The Mediterranean basin and southwestern Western Australia are particularly vulnerable to the impact of *P. cinnamomi*. These regions may experience more frequent and severe outbreaks due to factors such as higher temperatures and altered rainfall patterns, creating favorable conditions for the pathogen's growth and spread. Researchers' simulations indicate that periods of drought followed by waterlogging will exacerbate disease development and potentially lead to increased mortality rates in affected plants (Corcobado et al., 2014). To address this pressing issue, conservation efforts are crucial. Implementing measures to protect susceptible plant populations, promoting habitat restoration and exploring disease-resistant plant varieties can help mitigate the impact of increased *P. cinnamomi* infections on vulnerable ecosystems. In summary, the combination of global warming and the pathogen's adaptability poses significant challenges for plant conservation, requiring proactive strategies to safeguard endemic plant species and preserve ecological balance in at-risk regions.

1.1.3. Synthetic fungicides

In recent times, farmers are increasingly adopting good agricultural practices, aiming to minimize their reliance on agrochemicals while maintaining crop productivity. These practices include optimizing resource use, implementing integrated pest management techniques and adopting sustainable cultivation methods. However, despite these efforts, the application of agrochemicals remains an inevitability in some cases due to the lack of viable alternatives (Soares et al., 2016). According to their function, agrochemicals can be divided into insecticides, fungicides, herbicides, fumigants, nematocides, molluscicides and acaricides (Carraro, 1997). Fungicides, specifically, play a crucial role in safeguarding crops against fungal diseases in agriculture. Depending on their composition, fungicides can target different aspects of fungal cell activity. They may act on cell division, on the synthesis of nucleic acids, amino acids, proteins and lipids, as well as on the cell membrane and on melanin of the cell wall. Additionally, fungicides can inhibit respiration and the biosynthesis of sterols in fungi (Baćmaga et al., 2018; Ijaz et al., 2015; Petit et al., 2012). However, the use of fungicides can have unintended consequences. Notably, they may impact not only the target fungi but also non-target fungi, leading to potential ecological issues. For instance, the reduction of soil fungal biodiversity can disrupt important ecological processes and may have long-term effects on soil health and nutrient cycling (Yumnam et al., 2014).

Agrochemicals, which encompass a range of compounds used in phytosanitary treatments to prevent and control microorganisms, pests, diseases and weeds, have become essential tools in modern agriculture (Soares et al., 2016). As global agricultural production continues to grow to meet the demands of a growing population, the usage of agrochemicals has witnessed a notable surge. Unfortunately, this increased reliance on agrochemicals has led to a concerning rise in environmental pollution. Water sources, soil quality, air and vegetation have all been impacted by the accumulation of these chemicals, causing disruptions in ecosystems and posing a threat to biodiversity, including beneficial fauna and flora populations (Aktar et al., 2009). Furthermore, there are potential implications on human health, warranting further investigation and precautionary measures (Forget, 1993).

Recognizing the gravity of these environmental issues, researchers, policymakers and agricultural communities worldwide are actively collaborating to find innovative solutions. Ongoing efforts focus on developing eco-friendly alternatives, promoting sustainable farming practices and raising awareness about the responsible use of agrochemicals (Aktar et al., 2009). Therefore, the growing awareness of the environmental consequences linked to agrochemical usage has prompted significant changes in attitudes towards their application. By fostering a holistic approach to agricultural practices and supporting research on sustainable alternatives, we can strive towards a more environmentally friendly and resilient agricultural system.

1.1.3.1. Mechanisms of action

In the 17th century agrochemicals were primarily derived from mixtures of natural compounds, and it wasn't until the 20th century that significant advancements were made in the discovery of antifungal compounds for agricultural use. Fungicides gained prominence as effective tools to combat plant diseases and various classes of fungicides emerged, including dithiocarbamates (DTCs), benzimidazoles, azole derivatives and strobilurins (Berger et al., 2017; Hof, 2001).

During the 1940s, chemically synthesized compounds began to outperform the previously used substances, such as dithiocarbamates and benzimidazoles (Berger et al., 2017). DTCs, derived from dithiocarbamic acid, possess the unique ability to form stable metal complexes due to the presence of two sulfur atoms with free electron pairs, making them effective metal chelators (Figure 8) (Adeyemi & Onwudiwe, 2020). Besides their chelating characteristics, they also inhibit ergosterol synthesis without cytochrome deactivation, making them valuable for their antifungal and antioxidant effects, effectively

eliminating plant diseases. Recent studies have also explored their potential use in eliminating metal residues accumulated in agricultural soils (Ajiboye et al., 2022).

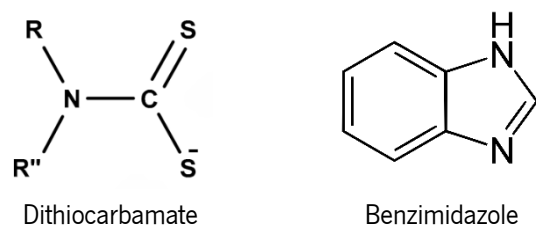


Figure 8 – The chemical structure of dithiocarbamate and benzimidazole. Dithiocarbamate has two sulfur atoms with free electron pairs. Benzimidazole, a heterocyclic aromatic organic compound, has two fused rings of benzene and imidazole. Adapted from Adeyemi & Onwudiwe, (2020) and PubChem.

Benzimidazoles, another class of fungicides, have garnered considerable interest among researchers due to their wide array of biological activities and potential applications. These activities span various fields, including anticancer, antiviral, antibacterial, antifungal, anthelmintic, anti-inflammatory, antihistamine, proton pump inhibitor, antioxidant, antihypertensive and anticoagulant properties. The presence of the benzimidazole ring in their chemical structure (Figure 8) is a crucial heterocyclic pharmacophore, playing a pivotal role in drug discovery (Tunçbilek et al., 2009). Initially, it was believed that the MOA of benzimidazoles solely involved inhibiting DNA and RNA synthesis. However, subsequent research revealed that while DNA synthesis inhibition was a secondary effect, the primary target was the blocking of nuclear division. This blockage led to the inhibition of both DNA and RNA synthesis (Davidse, 1973). In fungal cells, benzimidazoles share similarities with colchicine, a secondary metabolite produced by plant cells, which disrupts mitosis and meiosis in both animal and plant cells by inactivating the spindle. Biochemical studies have further shown that benzimidazoles interfere with the normal functioning of microtubules by binding to tubulin (Davidse & Flach, 1977; Zhou et al., 2016). This ability to disrupt microtubules and block cell division is what makes benzimidazoles effective in controlling diseases in crop plants and affecting DNA and RNA synthesis.

In the 1950s, polyene fungicides emerged, with one of the most well-known and significant fungicides being amphotericin B (Figure 9). Initially developed as an antifungal medication, amphotericin B was later adapted for agricultural purposes to combat fungal infections in crops. Its MOA involves direct interaction with the fungal cell membrane, specifically extracting ergosterol, a crucial component of the membrane (Prasad et al., 2019). Polyene fungicides, including amphotericin B, are amphipathic in nature, featuring both hydrophobic and hydrophilic sides. This amphipathicity allows them to bind to the ergosterol present in the fungal cell membrane. Upon intercalation into the membrane, they create channels that promote the efflux of potassium ions, thereby disrupting the proton gradient and

compromising the integrity of the fungal cell (Shapiro et al., 2011). However, despite its effectiveness as a fungicide, the greatest limitation of amphotericin B lies in its toxicity, particularly its potential to cause renal dysfunction. This toxicity arises from the similarity between ergosterol, which is targeted by the fungicide, and the cholesterol present in the cell membranes of animal and human cells (Shapiro et al., 2011). Careful consideration of its application and dosage is necessary to mitigate potential adverse effects while benefiting from its antifungal properties.

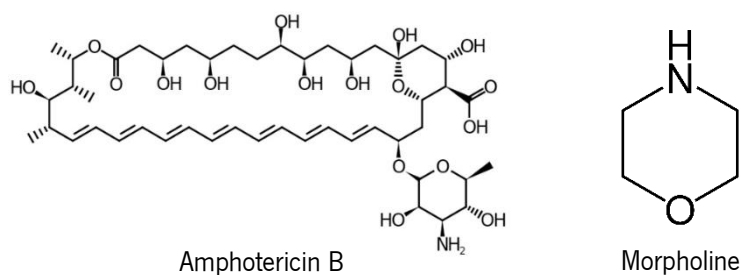


Figure 9 – The chemical structure of amphotericin B and morpholine. Amphotericin B is amphipathic, allowing it to form a transmembrane channel that affects the permeability of the membrane. Morpholine, a saturated hexagonal organic heterocyclic compound, has an oxygen and a nitrogen in opposite positions. Adapted from PubChem.

In the 1960s, morpholines emerged as a class of fungicides and have since been widely used to control various plant diseases (Figure 9). Their MOA involves affecting the ergosterol biosynthetic pathway, which is crucial for the growth and survival of fungi (Prasad et al., 2019). The MOA of morpholines centers around two key enzymes in the ergosterol biosynthetic pathway: sterol C14 reductase (Erg24) and sterol G8 isomerase (Erg2), encoded by the *ERG24* and *ERG2* genes, respectively (Figure 10). By targeting these enzymes, morpholines disrupt the synthesis of ergosterol, which is vital for the integrity of the fungal cell membrane (Jachak et al., 2015). It is important to note that due to its rapid metabolism when in the host, morpholines become less effective against invasive fungal infections in medicine. As a result, only one drug from this class of fungicides is currently used in medical treatments. However, in agriculture, morpholine fungicides are widely employed. Some common examples include aldimorph, fenpropimorph, fenpropidin, tridemorph and dodemorph, which have proven effective in managing fungal diseases in crops (Herrick & Hashmi, 2023; Jachak et al., 2015).

Despite the specificity of the molecular target in fungi, morpholine fungicides can have unintended effects on non-target organisms, harming beneficial insects, birds and wildlife, disrupting natural ecosystems and biodiversity. They can persist in the environment, accumulating in soil, water bodies and ecological niches, leading to environmental contamination and adverse effects on non-target organisms. Some morpholine fungicides are toxic to humans and animals, posing health risks to farmworkers, consumers and animals. Their limited MOA targeting the ergosterol biosynthetic pathway

can lead to resistance in fungal populations, reducing long-term effectiveness. Regulatory restrictions in certain regions may limit farmers' choices in disease management. Furthermore, during application, drift may occur, unintentionally exposing neighboring crops, plants or water sources, resulting in phytotoxicity and environmental contamination (Herrick & Hashmi, 2023).

In 1970, the introduction of azole derivatives marked a significant milestone in the realm of antifungals. Azole derivatives are unsaturated aromatic molecules containing at least one nitrogen atom, and their applications extend beyond human and animal fungal infections to include agriculture and even personal care products (Berger et al., 2017; Hof, 2001). In agriculture, azole derivatives have become the most widely used antifungals due to their remarkable efficacy and versatility. These compounds are often applied both pre-harvest and post-harvest to prevent the degeneration of crop products caused by fungi. Azole-derived antifungals fall into the category of Sterol Biosynthesis Inhibitors (SBI) (Azevedo et al., 2015). Their MOA revolves around inhibiting the ergosterol biosynthetic pathway (Price et al., 2015).

The biosynthesis of ergosterol involves a series of enzymatic reactions that transform precursor molecules into ergosterol, the end product. This biosynthetic pathway is a crucial process for the proper functioning of all fungi, as ergosterol is a sterol molecule that plays a vital role in the structure and function of fungal cell membranes. Ergosterol plays a key role in maintaining integrity, permeability and fluidity of the fungal cell membrane, which is essential for various cellular processes, including nutrient uptake, waste elimination and signal transduction. It serves a function similar to cholesterol in animal cell membranes. Moreover, the ergosterol biosynthetic pathway is regulated by the enzyme lanosterol 14 α -desmethylase (Erg11), which is encoded by the *ERG11* gene (see Figure 10). When an azole-derived fungicide is applied, some of them bind to this enzyme, forming a catalytically inactive complex. Consequently, the loss of activity of lanosterol 14 α -desmethylase leads to an inhibition of ergosterol synthesis and a toxic buildup of demethylated lanosterol within the fungal cell (Price et al., 2015). The accumulation of demethylated lanosterol disrupts cellular transport and impairs the integrity of the fungal cell membrane, ultimately leading to its demise (Berger et al., 2017). This MOA makes azole derivatives highly effective in controlling fungal infections in agriculture and protecting harvested crops from spoilage.

Furthermore, it's worth noting that there are other fungicides that specifically target enzymes involved in the final stages of ergosterol biosynthesis (Jordá & Puig, 2020). This final pathway occurs in the endoplasmic reticulum (ER), but ergosterol is mostly transported to the plasma membrane. Interestingly, among the Erg enzymes, the only ones not conserved in mammals are sterol C-24 methyltransferase (Erg6), Erg2, sterol C-22 desaturase (Erg5) and sterol C-24 reductase (Erg4).

Demonstrating the importance of these enzymes, the deletion or overexpression of *ERG6* results in the most compromised phenotypes, highlighting its potential as a promising target for the development of new antifungal agents (Bhattacharya et al., 2018; Kodedová & Sychrová, 2015). It is worth noting that Erg6 predominantly localizes to lipid particles (LPs) (Leber et al., 1998), although it can also be detected in the ER, cytoplasm and mitochondria. On the other hand, Erg2, sterol C-5 desaturase (Erg3), Erg5 and Erg4 primarily reside in the ER, serving as essential components in the ER-mediated distribution of ergosterol to its final membranous destinations (Kristan & Rižner, 2012; Zweytick et al., 2000).

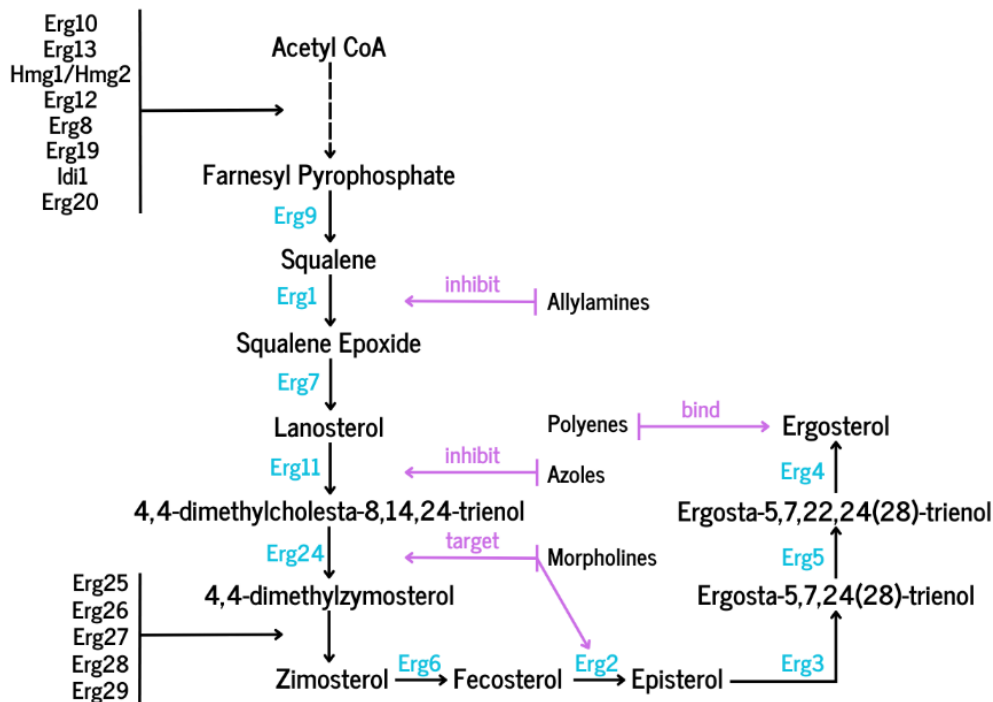


Figure 10 – Biosynthetic pathway of ergosterol in *Saccharomyces cerevisiae*. The ergosterol biosynthetic pathway can be divided in three modules: the mevalonate pathway (from acetyl CoA to mevalonate), which occurs in the vacuole and mitochondria; the farnesyl pyrophosphate (farnesyl-PP) biosynthesis (from mevalonate to farnesyl-PP), which is carried out in the vacuole; and the late pathway, culminating in ergosterol biosynthesis (from farnesyl-PP to ergosterol), primarily taking place in the endoplasmic reticulum (ER). Additionally, farnesyl-PP is utilized in the synthesis of ubiquinone, dolichol, heme and prenylated proteins. The words in blue represent the enzymes that are encoded by those respective genes. So, Erg10 is acetyl-CoA C-acetyltransferase; Erg13 is HMG-CoA synthase; Hmg1/2 is HMG-CoA reductase; Erg12 is mevalonate kinase; Erg8 is phosphomevalonate kinase; Mvd1/Erg19 is mevalonate pyrophosphate decarboxylase; Idi1 is Isopentenyl diphosphate Isomerase; Erg20 is farnesyl pyrophosphate synthetase; Erg9 is squalene synthase; Erg1 is squalene epoxidase; Erg7 is lanosterol synthase; Erg11 (Cyp51) is lanosterol C-14 demethylase; Erg24 is sterol C-14 reductase; Erg25 is sterol C-4 methylxydase; Erg26 is sterol C-3 dehydrogenase (C4-decarboxylase); Erg27 is sterol C-3 ketoreductase; Erg6 is sterol C-24 methyltransferase; Erg2 is sterol C-8 isomerase; Erg3 is sterol C-5 desaturase; Erg5 is sterol C-22 desaturase; and Erg4 is sterol C-24 reductase. The words in lilac represent the inhibitors, and these are statins that target Hmg1/2; allylamines that inhibit Erg1; azoles that inhibit Erg11; morpholines that target Erg2 and, mainly, Erg24; and lastly, polyenes that bind ergosterol. Adapted from Jordá & Puig, (2020).

Among azole derivatives, triazole and imidazole stand out as the most widely used compounds in agriculture (Figure 11). Their systemic nature allows for efficient absorption by plants, enabling both curative and preventive actions against fungal diseases. Remarkably, these compounds account for

approximately one third of all fungicides, with nearly 99% falling under the category of Demethylation Inhibitors (DMI). One of the most striking features of triazole and imidazole fungicides is their high stability, granting them the ability to persist actively in soil, water and certain ecological niches for several months (Hof, 2001). While this stability contributes to their long-lasting effectiveness in protecting crops, it also raises concerns about potential environmental implications. The accumulation of these compounds in the environment over extended periods warrants careful consideration to ensure responsible and sustainable agricultural practices (Aktar et al., 2009).

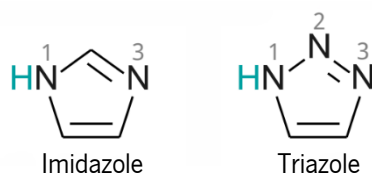


Figure 11 – The chemical structures of imidazole and triazole. Imidazole and triazole are heterocyclic compounds. Both of them feature a five-membered ring structure; however, imidazole consists of three carbon atoms and two nitrogen atoms, while triazole consists of two carbon atoms and three nitrogen atoms. Adapted from Gustincic & Kokalj, (2018).

The strobilurins (Figure 12) emerged in the 1980s as a group of mesostimeric chemical compounds, originally extracted from the fungus *Strobilurus tenacellus*. They are classified as Quinone oxidase Inhibitors (Qol) and have become vital fungicides in agriculture due to their unique MOA. Strobilurins work by inhibiting mitochondrial respiration through the blockage of the electron transfer chain in complex III. Specifically, they bind to the ubihydroquinone-cytochrome-c oxyreductase, effectively obstructing the binding of oxygen and, in turn, preventing cellular respiration. As a consequence, ATP formation, a key component for fungal growth, is disrupted, thus halting the development of fungi (Parreira et al., 2010). Initially extracted from *S. tenacellus*, strobilurins have since been produced synthetically, making them more readily available and widely used in agriculture. Their effectiveness as Qol fungicides has made them an essential tool in protecting crops from fungal diseases and contributing to higher agricultural yields (Nofiani et al., 2018).

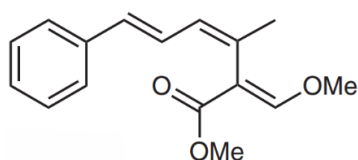


Figure 12 – The chemical structure of a natural strobilurin. Strobilurin is a methacrylic acid derivative, either benzene-based or pyrimidine-based, that obstruct the quinone oxidase site of cytochrome B. Adapted from Nofiani et al. (2018).

Thus, the presence ofazole antifungal residues has far-reaching consequences, not only affecting the environment but also posing significant risks to non-target organisms. These compounds exhibit extreme toxicity, impacting the survival, development, growth, reproduction and behavior of various

organisms (Creusot et al., 2020). High concentrations of azole antifungals have been linked to endocrine dysregulation, altered gene expression, decreased growth and impaired larval development. Furthermore, they may increase the sensitivity of affected organisms to other chemicals (Lieberman & Curtis, 2018). Studies have shown that azole antifungals can also cause reduced growth in fish, although the precise mechanism behind this effect remains unknown (Stadnicka-Michalak et al., 2015).

Another concerning consequence of the extensive use of antifungals, particularly azoles, is the development of antifungal resistance. This resistance not only affects the targeted fungi but can also extend to other fungi present in the environment (Hof, 2001; Sharma, 2021). The emergence of antifungal-resistant strains poses a serious threat to food resources and human health, compromising the effectiveness of antifungal treatments in both agricultural and medical settings (Creusot et al., 2020). Given the widespread usage and potential ecological impacts of azole antifungals, it is crucial to adopt responsible and sustainable practices to minimize the risks associated with their presence in the environment and preserve both ecosystem integrity and human well-being.

1.1.3.2. Microbial resistance associated with intensive use of synthetic fungicides

Several methods have been employed to control phytopathogenic fungi in agriculture. However, the widespread and excessive use of synthetic chemical fungicides has led to significant challenges, foremost among them being the emergence of antifungal resistance (Khan et al., 2020). Antifungal resistance refers to the development of non-susceptibility in a fungal microorganism to the action of a specific compound with antifungal activity, as compared to other susceptible members of the same species. This resistance can manifest in two distinct ways: intrinsic or primary resistance, which is genetically inherited, and acquired or secondary resistance, which results from continuous exposure to an antimicrobial agent over an extended period (Assress et al., 2021). Of particular concern is the prevalence of resistance to azoles, a class of antifungals commonly used in agriculture. This widespread resistance has rendered many fungal strains and species non-responsive to currently available antifungal agents, leaving crops vulnerable and unprotected (Prasad et al., 2019). The emergence of antifungal resistance poses grave implications for agriculture, as it jeopardizes the effectiveness of fungicides in protecting crops from devastating fungal diseases. Addressing this issue is critical for ensuring sustainable crop protection and safeguarding global food security.

Furthermore, the widespread use of azoles, not only in agriculture but also in medicine and material preservation, has given rise to an environmental stressor capable of inducing resistance to azoles in other organisms present in the environment (Assres et al., 2021; Azevedo et al., 2015). As a notable example, *Aspergillus fumigatus*, a fungal pathogen distributed in soil, water and air, poses a significant threat to human health. *A. fumigatus* can cause aspergillosis, a disease that affects the lungs and can also lead to infections in other parts of the body. In immunocompromised patients, aspergillosis can be fatal, with an estimated global incidence of approximately 4 to 5 million cases of allergic bronchopulmonary aspergillosis (Denning et al., 2013), and an annual incidence of up to 10% of invasive aspergillosis, with a mortality rate of up to 90% in high-risk groups (Kosmidis & Denning, 2015). This species has shown resistance to various antifungal drugs, with azole-resistant strains of *A. fumigatus* (ARAF) being widely observed, particularly in European countries. The extensive use of azole derivatives in these regions, including countries like Portugal, is likely associated with the prevalence of ARAF in the environment (Assres et al., 2021). The emergence of azole-resistant *A. fumigatus* strains globally presents a major challenge as infections caused by these resistant strains cannot be effectively treated with azolic compounds, which are commonly used in treatments (Berger et al., 2017). This alarming trend calls for urgent attention and effective strategies to manage the spread of azole resistance in *A. fumigatus* to protect public health and address this major concern.

Azole resistance is also a well-documented phenomenon among *Candida* spp., and it can occur through several key pathways. These mechanisms include the upregulation of drug transporters, overexpression or alteration of the drug targets and cellular changes induced by stress responses. These mechanisms may manifest independently or concurrently within a single isolate, potentially leading to additive effects or cross-resistance among azole drugs. The induction of efflux pumps, which reduce intracellular drug concentrations, is the most prevalent mechanism of drug resistance. These drug pumps are encoded by genes belonging to the ATP-binding cassette (ABC) superfamily or the major facilitator superfamily (MFS). In addition to efflux pump-related resistance, the target of the antifungal can be changed by mutations, leading to a lower affinity for the antifungal compounds. For instance, numerous point mutations have been identified in the *ERG11* gene in response to fluconazole. Some of these aminoacid substitutions induce structural changes in the active site of the demethylase resulting in reduced target affinity and, consequently, azole resistance (Bhattacharya et al., 2020; Lee et al., 2023; Paul et al., 2022; Pristov & Ghannoum, 2019; Whaley et al., 2017). Overexpression of *ERG11*, due to mutations in the transcription factor UPC2 of *C. albicans*, can also confer resistance to azoles. Furthermore, azole resistance may be linked to the loss of function of the sterol $\Delta 5,6$ -desaturase gene

(*ERG3*) (Bhattacharya et al., 2020; Lee et al., 2023). Additionally, the formation of biofilm is another mechanism that impacts the efficacy of azoles and other systemic antifungal drug classes. Biofilm formation can either resist drug action directly or promote microbial resistance through mechanisms like drug pumps (Bhattacharya et al., 2020; Lee et al., 2023; Pristov & Ghannoum, 2019).

At this moment, the rapid evolution of pathogens continues to pose significant challenges, leading to an increasing emergence of resistances and rendering plants susceptible to diseases. Consequently, epidemics still occur, causing substantial yield losses. To address this pressing issue, there is a compelling need to explore and enhance alternative disease management techniques that are both consumer and environmentally friendly. Promising alternatives include the use of biological control agents and their secondary metabolites, as well as plant extracts and phytochemicals with antifungal activity (Callaway, 2016; Khan et al., 2020). These techniques offer the potential to reduce the reliance on synthetic chemical fungicides while providing effective disease control measures. Moreover, they may offer advantages in terms of sustainable and eco-friendly agricultural practices, preserving beneficial organisms, and minimizing the risk of antifungal resistance development. Continuing to improve and discover new methods of disease management that prioritize environmental sustainability and consumer safety is of utmost importance to ensure long-term crop health, productivity, and global food security (Robbins et al., 2017).

1.2. Natural fungicides

Considering the challenges associated with chemical control and the emergence of fungal resistance, researchers have increasingly turned their attention to antifungals of natural origin, since chemical control continues to be essential for good crop yields. The awareness of these challenges has prompted the exploration of alternative methods that prioritize effectiveness, safety, and environmental and social sustainability (Brauer et al., 2019). As a result, innovative approaches, including nanotechnology, have surfaced, aiming to realize precision agriculture while effectively managing fungi, pests and boosting agricultural productivity. Simultaneously, there is growing interest in investigating new biological control agents, plant extracts and phytochemicals that demonstrate promising antifungal activity against specific fungal pathogens.

1.2.1. Biological control agents

Each year, agricultural crop yield losses are largely caused by diseases from phytopathogenic fungi (Li et al., 2017). Unfortunately, some of these fungi have developed resistance to synthetic antifungals, while the banning of several agrochemicals due to pollution and toxicity further aggravates the problem (Brauer et al., 2019; Sharma, 2021). To address this issue, alternative methods are urgently needed to protect crops. One promising approach is plant health control using biological agents, which has shown improved agricultural productivity and disease and pest elimination in various studies. Biological control agents (BCAs) encompass microorganisms, like bacteria or fungi that specifically target pests or pathogens harming plants without harming the environment (Backman & Sikora, 2008; Sharma, 2021). These agents may be natural enemies of phytopathogens or pests or even non-pathogenic microorganisms (Schouten et al., 2004). BCAs employ diverse mechanisms to control fungal diseases, including growth inhibition, infection prevention and predation. Overall, they offer a promising mean to control and eradicate diseases and pathogen populations (Sharma, 2021).

Some examples of biological control agents that are already being used in agriculture today are endophytic fungi, such as *Trichoderma* spp. or *Xylaria* sp. Endophytic fungi are found inside the living tissues of all plants in endosymbiosis, growing without causing damage or disease, and establishing important interactions with the host plant. Some of these interactions involve the production of enzymes or secondary metabolites that directly inhibit the action of microbial pathogens, surrounding growing plants and animals, improving their defenses and protecting them. Moreover, they also have the ability to convert natural plant compounds into antifungal compounds in order to combat pathogens (Deshmukh et al., 2018). Thus, these fungi provide several benefits to their hosts when used as fungicides, such as aiding growth, survival, increasing tolerance to extreme temperatures and drought and even removing contaminants from the soil (Kauppinen et al., 2016). Species of the genus *Trichoderma* such as *T. hamatum*, *T. harzianum*, *T. polysporum* and *T. viride* are soil-associated, have minimal nutritional requirements, grow rapidly, possess diverse mechanisms of action, adapt easily to various environmental conditions and exhibit tolerance to certain fungicides (Card et al., 2016). They are important BCAs with antifungal activity, being the most potent currently also due to the diverse set of antimicrobial secondary metabolites they produce (Brauer et al., 2019; Khan et al., 2020). Consequently, these species are used to suppress soil fungal pathogens, but also some foliar pathogens, in which different groups of secondary metabolites such as terpenes, pyrones, gliotoxin, gliovirin and peptaibols may be involved (Vinale et al., 2014). Therefore, these compounds can not only be used in agriculture, but can also be used in industry

and medicine, presenting a great relevance for humans (Khan et al., 2020). On the other hand, species of the genus *Xylaria* are fast-growing endophytic fungi that can be isolated from various plant types, including vascular plants such as conifers, monocotyledons, dicotyledons, ferns and lycopsids, as well as non-vascular plants like liverworts. These fungi serve as another example of BCAs exhibiting antifungal activity against *Candida albicans*, *Aspergillus niger* and *Fusarium avenaceum* (Deshmukh et al., 2018). Moreover, their bioactive secondary metabolites also showcase essential pharmacological properties, such as antimicrobial, antioxidant and anti-inflammatory (Macías-Rubalcava & Sánchez-Fernández, 2016). As evident, a wide diversity of BCAs is already available for use, however, more research is still required to better understand the complex interactions between plants, people and the environment (Sharma, 2021).

1.2.2. Plant extracts and phytochemicals with antifungal and anti-oomycetal activities

Over the past few years, several studies have been conducted to develop alternatives to synthetic fungicides. One of these alternatives is the use of plant extracts. Plants are known for their biological properties and incomparable chemical diversity, enabling them to synthesize metabolites with protective functions against abiotic and biotic stresses. This makes them a source of potentially promising compounds for creating new agrochemicals and for eliminating phytopathogens and pests in an environmentally non-harmful way (D'Addabbo et al., 2020; Han et al., 2018). In this way, new antifungal bioactive compounds can be extracted, including phytochemicals. Phytochemicals are secondary metabolites produced by plants that typically exhibit numerous biological activities, such as protecting plants from diseases or pests. Some examples of these compounds are phenolic compounds, flavonoids, coumarins, saponins, terpenes and alkaloids (Arif et al., 2009; Madhumitha & Saral, 2011; Sakka Rouis-Soussi et al., 2014; Singh et al., 2021).

Phenolic compounds, the most abundant phytochemicals in plants, contain at least one aromatic ring attached to one or more hydroxyl groups in their chemical structure (Farias et al., 2021). These compounds exhibit a diverse range of structures, with some being simple low molecular weight compounds, such as phenylpropanoids, coumarins (Figure 13) and benzoic acid derivatives, while others possess more complex structures like flavonoids (Figure 13), tannins and stilbenes (Kennedy & Wightman, 2011). One of the most prominent biological activities of phenolic compounds is their

antioxidant activity. Additionally, they also display antibacterial and antifungal properties, making them suitable for use as biopesticides (Ferguson, 2001).

Flavonoids, a highly diverse subgroup of phenolic compounds, can be further subdivided into classes such as anthocyanidins, flavones, flavonols, isoflavonoids and biflavonoids (Ferguson, 2001). These phytochemicals play crucial roles in protecting cells from damage caused by ultraviolet radiation, attracting pollinators through their influence on flower color, and participating in symbiotic nitrogen fixation (Ferreyra et al., 2012). Moreover, they exhibit various other biological activities, including antifungal, anti-inflammatory, antioxidant and antidepressant (Hsu et al., 2021). As said, flavonoids have a wide range of biological activities, but have been increasingly prominent due to their strong antifungal activity. These metabolites have shown promise as they are efficient against various phytopathogenic organisms such as *F. oxysporum* and *B. cinerea*. Flavonoids have the ability to inhibit fungal growth through various mechanisms such as plasma membrane disruption, induction of mitochondrial dysfunction, inhibition of cell wall formation, cell division, RNA/DNA or protein synthesis and inhibition of the efflux-mediated pumping system (Al Aboody & Mickymaray, 2020).

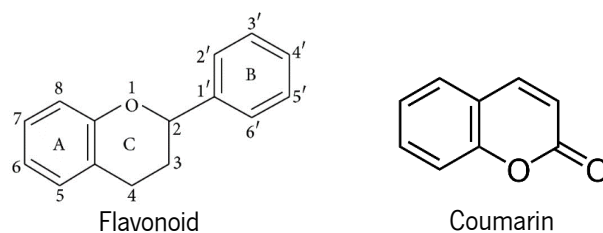


Figure 13 – The chemical structure of flavonoids and coumarins. Flavonoids contain two benzene rings, A and B, connected by a heterocycle pyrene ring, C, that contains oxygen. Coumarins are chromenones that have the keto group located at the 2-position. Adapted from PubChem.

Coumarins, another important group of phenolic compounds derived from benzopyrazole, are found in plants in both free and glycoside form. They exhibit diverse activities, such as antimicrobial, antiviral, antifungal, antioxidant, antiasthmatic, anticoagulant and anti-inflammatory. However, it's important to note that they can also exhibit phototoxic and carcinogenic effects (Wu et al., 2013; Xin-Mei et al., 2013). In terms of antifungal activity, molecular docking studies have shown that coumarins have a high affinity and binding capacity to the active site of lanosterol 14 α -desmethylase. This suggests that coumarins can inhibit the activity of this enzyme by occupying the place that should be occupied by its substrate, thus inhibiting the biosynthesis of ergosterol (Annunziata et al., 2020). Moreover, previous research has evaluated the antifungal and antibiofilm activity of coumarins against *C. albicans*, revealing that these metabolites not only suppress biofilm formation but also affect the structure of mature biofilms, adhesion, cell surface hydrophobicity and filamentous growth (Xu et al., 2019). These mechanisms

collectively contribute to cell death of fungal cells (Annunziata et al., 2020). Additionally, coumarins have demonstrated antifungal activity against *Colletotrichum musae*, which is known to attack subtropical fruit crops, like mango and banana. In viability assays, coumarins reduced the mycelial growth of this fungus (Sousa et al., 2018).

Saponins are commonly found in roots, leaves and fruits of higher plants, such as peas and soybeans, and exhibit various biological activities, including antifungal, antimicrobial, anti-inflammatory, antiviral and antioxidant, all of which contribute to the plant's defense system against pathogens (Porsche et al., 2018). Their chemical structure consists of a hydrophobic triterpene or steroidal aglycone, with one or more hydrophilic sugar chains attached (Figure 14) (Tava & Avato, 2006). In terms of antifungal activity, saponins have demonstrated the ability to inhibit the growth of various species, such as *A. fumigatus*, *Venturia inaequalis* and *B. cinerea* (Li et al., 1999; Porsche et al., 2018). However, it is important to note that their antifungal activity can vary among strains due to differences in the amount of sterol in the plasma membrane (Sparg et al., 2004). Moreover, saponins can induce the formation of transmembrane pores, potentially leading to loss of membrane permeability and cell death. The extent of this ability depends on the specific type of saponin and the lipid composition of the membrane; pore formation increases when the amount of ergosterol in the membrane is higher (Efimova & Ostroumova, 2021). Additionally, saponins can regulate fluxes through ion channels, particularly through cation-selective gramicidin A pores, by altering the transmembrane electric potential. They also influence the dipolar potential by altering the membrane hydration layer (Efimova & Ostroumova, 2021).

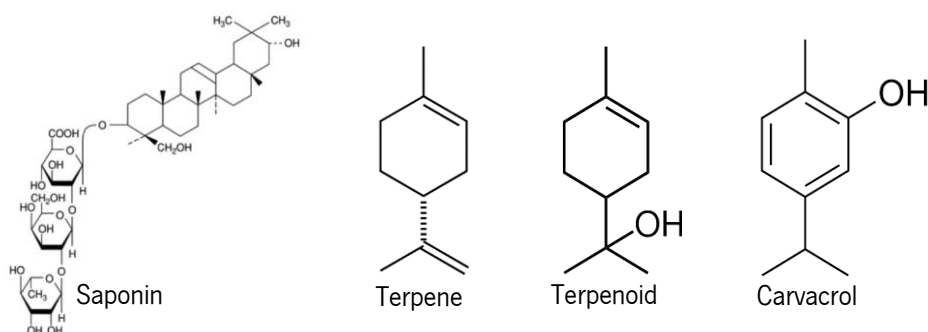


Figure 14 – The basic chemical structure of saponins, terpenes, terpenoids, and carvacrol. Saponins have a hydrophobic triterpene, with one or more hydrophilic sugar chains attached. Terpenes are considered fusions of two or more isoprenes unities (C₅H₈). Terpenoids derive from terpenes and the difference consists on their oxygenated, hydrogenated and dehydrogenated derivatives. Carvacrol is a phenolic monoterpene. Adapted from PubChem.

Terpenes are a diverse group of unsaturated and fat-soluble hydrocarbons mainly produced by plants (Figure 14) (Davis & Croteau, 2000). Terpenoids, which are derived from terpenes, play a significant role in plant defense and are also involved in attracting pollinators. Moreover, they exhibit a wide range of biological activities, including antimicrobial, antiviral, antibacterial and anti-inflammatory

(Mahato & Sen, 1997; Tian et al., 2012). The antifungal activity of terpenoids has been extensively studied, and it has been found to depend on their specific structure and composition, particularly the presence of a free hydroxyl group and an aromatic ring (see Figure 14) (Rao et al., 2010). For example, carvacrol (Figure 14), a terpenoid, has been shown to dissipate pH and K^+ gradients due to its delocalized electron system, facilitating the dissociation of H^+ from the hydroxyl group. Consequently, carvacrol can transport H^+ and monovalent cations, such as K^+ , across cell membranes, disrupting H^+ homeostasis (Ultee et al., 2002). However, the transient Ca^{2+} bursts associated with the interaction with carvacrol, leading to the disruption of Ca^{2+} homeostasis and increased membrane fluidity, remain less understood. It has been hypothesized that these effects cause ion channels to open, resulting in a rapid loss of sensitivity and membrane integrity (Rao et al., 2010; Ultee et al., 2002). As a consequence, carvacrol induces a loss of metabolic activity, depolarization of cell membranes, increased membrane permeability and subsequent cell death. Furthermore, it is believed that terpenoid interaction with the cell membrane activates specific signaling pathways downstream (Rao et al., 2010). These combined mechanisms contribute to the antifungal properties of terpenoids and highlight their potential as effective natural agents for combating fungal infections.

Alkaloids are a diverse group of chemical compounds of natural origin, typically characterized by the presence of nitrogen atoms in their structure. Some alkaloids may also contain sulfur and, more rarely, elements such as bromine, phosphorus or chlorine (Knunyants & Zefirov, 1988). These phytochemicals are produced by a variety of organisms, including plants, animals, fungi and bacteria. Their significance lies in their wide range of biological activities, encompassing anticancer, antimalarial, anesthetic and stimulant properties (Ziegler & Facchini, 2008). Among their notable properties, alkaloids are renowned for their antibacterial and analgesic effects, making them frequently utilized in headache and fever medications (Singh et al., 2021). Moreover, these compounds possess the ability to bind to neurological receptors and interfere with neurotransmitter metabolism (Wink, 2003). Alkaloids can be classified into several groups based on their chemical structure, including tropane, pyrrolizidine, piperidine, quinolines, isoquinoline, indole, steroidal, imidazole, purine and pyrrolidine. Among these groups, only the isoquinoline and indole alkaloids have demonstrated antifungal activity. Isoquinoline alkaloids, derived mainly from higher plants, form a vast and diverse group of compounds. Characterized by their isoquinoline core (Figure 15), they exhibit a wide range of biological activities, such as antiviral, antifungal, anticancer, antioxidant, antispasmodic and enzyme inhibition. Several isoquinoline alkaloids find applications in medicine, with morphine and codeine being the most extensively studied and utilized.

Typically derived from tyrosine or phenylalanine, isoquinoline alkaloids hold significant importance in various therapeutic contexts (Dey et al., 2020).

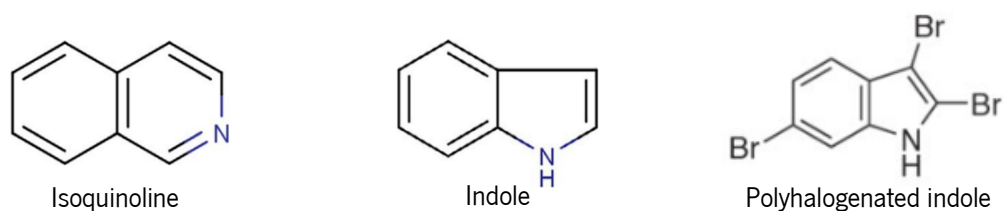


Figure 15 – The basic chemical structure of isoquinolines and indoles. Isoquinolines are benzopyridines, which are composed of a benzene ring fused to a pyridine ring. Indoles have a bicyclic structure, which consists of a benzene ring coupled to a pyrrole ring. Adapted from PubChem and Gribble, (2012).

Indole alkaloids (Figure 15), derived from diverse sources such as terrestrial, fungal and marine, feature polyhalogenation as a common characteristic. As the largest group of alkaloids derived from tryptophan, indole alkaloids exhibit a broad spectrum of biological activities. Relevant metabolites within this group include reserpine, vinblastine and vincristine, which demonstrate antihypertensive and antitumor properties (El-Sayed & Verpoorte, 2007; Sagi et al., 2016). Additionally, other indole alkaloids display various biological activities, such as antimicrobial, antifungal, central nervous system stimulant and antiviral. Remarkably, marine-derived indole alkaloids have shown considerable promise, with demonstrated activities such as antiparasitic, cytotoxic, serotonergic, antagonistic, anti-inflammatory and antiviral (Gul & Hamann, 2005). These diverse phytochemicals represent an active group of molecules with significant therapeutic and pharmacological potential.

From the above, it is clear that there are several plants species that have in their constitution phytochemicals with antifungal activity. Among many other plant species, some examples of these species are: *Phytolacca dioica* and *Sapindus mukorossi* that have saponins (Liberto et al., 2010; Porsche et al., 2018), *Medicago* sp. that has alkaloids, coumarins, flavonoids and saponins (D'Addabbo et al., 2020), *Allium* sp. which has phenolic compounds and flavonoids (Sakka Rouis-Soussi et al., 2014) and *Crossandra infundibuliformis* which has alkaloids, saponins and terpenoids (Madhumitha & Saral, 2011). Natural metabolites offer several advantages as antifungal agents, including biodegradability and a diverse range of MOA, which reduces their persistence and accumulation in the environment, while also lowering the likelihood of new antifungal resistant strains to emerge. However, it is essential to acknowledge some disadvantages of these compounds, such as their rapid degradation and relatively lower efficiency compared to synthetic fungicides (Scognamiglio et al., 2019). Despite these limitations, the environmental benefits of natural metabolites cannot be ignored. Their biodegradability and reduced environmental persistence make them more environmentally friendly than synthetic alternatives. Moreover, the array of

mechanisms they employ in combating fungi makes them less prone to induce resistance. Given these advantages, it becomes imperative to conduct further research on the MOA of these phytochemicals. Expanding our knowledge in this area will facilitate the development and application of natural antifungal drugs effectively.

1.2.2.1. *Curcuma longa* (turmeric)

Curcuma longa, a member of the Zingiberaceae family, is an herbaceous plant species extensively used in traditional Chinese medicine, more commonly known as turmeric. In recent times, researchers have shown increasing interest in this plant due to its production of complex compounds with diverse biological activities. These activities include insecticidal (Amalraj et al., 2017), antimicrobial (Chen et al., 2008), antifungal (Avanço et al., 2017; Y. Hu et al., 2017), antimalarial (Martinez-Correa et al., 2017), antiviral (Dao et al., 2012), and antioxidant (Avanço et al., 2017). The compounds derived from *C. longa* find applications not only as spices, flavorings and condiments in the food industry, but also as potential pharmacological agents in the cosmetic and pharmaceutical sectors (Chen et al., 2008). Additionally, researchers have been captivated by the toxicity of *C. longa* towards phytopathogenic fungi, leading to inhibition of mycelial growth (Ferreira et al., 2013). Several studies have examined the antifungal activity of *C. longa* extracts, particularly ethanol and hexane extracts, against various fungi, including *B. cinerea*, *Chaetomium olivaceum*, *F. graminearum*, *Mycogone pernicioso*, *Penicillium pallidum*, *Phoma wasabiae*, *Sclerotinia sclerotiorum*, *Verticillium dahliae*, *Plasmodiophora brassicae* and *Magnaporthe grisea* (Chen et al., 2018).

Extensive investigation and literature has identified chemical compounds present in *C. longa*, such as curcumenol, curdione, curcumin, isocurcumenol, curcumol, stigmaterol, zingiberene and curcumene (Hamdi et al., 2010; Lakshmi et al., 2011; Li et al., 2011). In their study, Chen *et al.* (2018) demonstrated that the ethanol extract of *C. longa* effectively disrupts the synthesis of critical proteins and enzymes, potentially impeding fungal growth. Additionally, their research indicated that *C. longa* has the capacity to inhibit the synthesis of ergosterol, thereby compromising the integrity of fungal cell membranes, and possibly affecting the respiratory chain. Despite these insights, the specific targets of the individual chemical compounds of *C. longa* remain unidentified. Therefore, conducting further research is essential to better understand how these extracts exert antifungal effects, identify the primary targets and pinpoint the key active compounds (Chen et al., 2018). Some studies have also explored the potential of combining *C. longa* extracts with other natural extracts as a potential antifungal agent.

However, more extensive investigations are required to validate this claim and unravel the mechanisms underlying this combined activity (Lee et al., 2007).

1.2.2.2. *Myristica fragrans* (nutmeg)

Myristica fragrans, commonly known as nutmeg, belongs to the Myristicaceae family and is a tropical evergreen tree native to the Maluku Islands of Indonesia. However, it is now extensively cultivated in several countries. Nutmeg is derived from the dried kernel of the ripe seed and has a rich history of use in traditional Indian medicine to alleviate various symptoms, including anxiety, nausea, diarrhea, cholera, stomach cramps, chronic vomiting, hemorrhoids, headaches, psychosis, fever, rheumatism and paralysis (Arumugam et al., 2019). The widespread culinary and medicinal applications of *M. fragrans* have drawn the attention of researchers in the last few decades (Ha et al., 2020). *Myristica fragrans* contains a myriad of phytochemicals, including lignans, neolignans, diphenylalkanes, phenylpropanoids, terpenoids, alkanes, fatty acids, fatty acid esters, as well as minor constituents such as steroids, saponins, triterpenoids and flavonoids. In total, about 250 compounds have been identified in this plant species. These compounds exhibit a wide range of biological activities, making nutmeg a subject of interest in research fields. Notably, it demonstrates anti-inflammatory, antioxidant, antibacterial, antifungal, anti-obesity, antidiabetic, anticancer, analgesic, chemopreventive, hepatoprotective, neuropharmacological, cardioprotective and other pharmacological effects (Ahmad et al., 2008; Ha et al., 2020; Jin et al., 2005).

Despite the mentioned benefits, it is essential to exercise caution with nutmeg consumption, as compounds such as myristicin and elemicin present in the seeds can lead to toxic effects when ingested in large quantities (Ehrenpreis et al., 2014). These toxic effects may affect the nervous system, leading to symptoms such as drowsiness, paresthesia, delirium, numbness and detachment from reality. Additionally, gastrointestinal symptoms such as vomiting and ileus, as well as cardiovascular symptoms like hypotension and tachycardia, have been reported in relation to nutmeg consumption (Sangalli et al., 2000). Despite these considerations, studies have explored the potential benefits of nutmeg extracts in certain applications. For instance, after removing substances like safrole and myristicin, the extract has shown promise, for example, as a potential nutraceutical candidate for the treatment of atopic dermatitis (Chung et al., 2012). In various studies, metabolites from *M. fragrans* have demonstrated inhibitory effects against pathogens such as *C. acutatum*, *Colletotrichum fragariae*, *Colletotrichum gloeosporioides* (Radwan et al., 2014), and *A. fumigatus*, *A. niger*, and *Aspergillus flavus* (Gupta et al., 2013). While these findings are promising, further research is warranted to explore the full potential of this plant in diverse

scientific areas. To date, most existing studies have focused on the essential oils of *M. fragrans* and so there is a need for more investigations on its various extracts to unlock additional possibilities for its applications.

1.2.2.3. *Ocimum basilicum* (basil)

Ocimum basilicum, commonly known as basil, belongs to the Lamiaceae family and is considered an ethnomedicinal plant, commonly grown in Asia, South America and Africa. It has been used for culinary purposes as a spice for many hundreds of years, as well as in traditional medicines to treat various nervous disorders such as headache, nerve pain, epilepsy, depression, migraine, dementia and other neurodegenerative diseases, as well as infections (Bora et al., 2011; Seyed et al., 2021). *Ocimum basilicum* extracts are typically made from its leaves or seeds (Farzana et al., 2022), which contain a variety of bioactive compounds, including phenols, flavonoids, terpenes, ellagitannins, steroids and anthocyanins (Jayasinghe et al., 2003; Shahrajabian et al., 2020; Siddiqui et al., 2007).

In addition to its culinary and medicinal uses, multiple studies indicate that *O. basilicum* exhibits a wide range of biological activities, such as neuroprotective, hepatoprotective, antihypertensive, cardioprotective, anti-ulcer, anti-diabetic, anti-inflammatory, antidepressant, anxiolytic, antitumor and chemoprotective. Moreover, it demonstrates antimicrobial, antinematodal and antioxidant activities, while also exhibiting dermatological and cosmetic properties (Sestili et al., 2018; Singh et al., 2022). Due to this impressive array of biological activities, the interest in this plant has been steadily growing in the scientific community. Regarding its antifungal activity, research has demonstrated that *O. basilicum* extracts effectively inhibit the growth of mycelia of phytopathogens such as *Macrophomina phaseolina*, *Rhizoctonia solani* and *F. oxysporum* (Farzana et al., 2022). Additionally, the essential oils of this plant have been found to inhibit the growth of *Alternaria brassicicola*, *A. flavus*, *Bipolaris oryzae*, *Fusarium moniliforme*, *Fusarium proliferatum*, *Pyricularia arisea* and *R. solani* (Piyo et al., 2009). However, it is necessary to do more research on this plant to understand its MOA and explore its potential applications, as *O. basilicum* holds great promise for future therapeutic research. Therefore, further studies are essential in uncovering the plant's medicinal properties and expanding its potential uses.

1.3. *Saccharomyces cerevisiae* as a fungal model

Saccharomyces cerevisiae is a single-celled eukaryotic organism, commonly known as baker's yeast or brewer's yeast, belonging to the kingdom Fungi and family Saccharomycetaceae. Like other eukaryotic organisms, *S. cerevisiae* contains membrane-bound organelles such as the nucleus, endomembrane system and mitochondria. Furthermore, yeast cells have the remarkable ability to rapidly divide, with a generation time as short as 120 minutes. This rapid division is facilitated by the budding process, where the smallest daughter cells separate from the mother cell, giving rise to the term "budding yeast". Due to their microscopic size and simplicity in growth requirements, these cells are easy to cultivate in the laboratory and are cost-effective for research purposes (Duina et al., 2014). In laboratory settings, *S. cerevisiae* forms colonies within a few days on agar plates. In nature, it is abundant in vineyards, specifically in fruits, but it can also be present in oaks and other natural habitats (Greig & Leu, 2009).

The use of yeast by humans dates back approximately 7,400 to 7,000 years (to Neolithic times), to the fermentation of grapes for wine production. This historical practice is supported by the discovery of tartaric acid calcium salt and *Pistacia* (terebinth) tree resin in ancient pottery, providing strong evidence for the remarkable early achievement in human history (McGovern et al., 1996). Nowadays, various strains of *S. cerevisiae* are extensively used in the food industry for baking, brewing, fermentation and wine production (Mortimer, 2000). However, yeast's value extends beyond the culinary world and into scientific research due to its genetic versatility. Geneticists can easily manipulate yeast genes, whether on plasmids or within chromosomes, allowing them to study phenotypes with relative ease (Duina et al., 2014). Moreover, yeast can be utilized in the production of ethanol and various other chemicals, earning its reputation as a cell factory platform (Nielsen, 2015).

One impressive aspect of yeast biology is the high conservation of many cellular processes between yeast and human cells, such as autophagy, translocation, protein secretion, among other processes. Furthermore, of the 414 essential genes found in yeast, 47% have a 1:1 human orthologs, suggesting a significant degree of gene conservation (Kachroo et al., 2015). Also, the preservation of several key signal transduction processes suggests the existence of conserved protein-protein interactions, regulatory hierarchies and signal cross-communication between yeast and human cells (Nielsen, 2019). These characteristics, combined with its genetic flexibility and straightforward regulation, make *S. cerevisiae* an exceptionally valuable and widely used eukaryotic model organism in scientific research (Duina et al., 2014; Nielsen, 2019).

2. BIOLOGICAL PROBLEM AND OBJECTIVES

Due to the overuse and misuse of conventional antifungals, an increasing number of phytopathogenic fungi are developing resistance to these products. This resistance poses serious problems in agriculture, leaving crops unprotected, and medicine, where immunosuppressed individuals face life-threatening infections with resistant fungal species, for which effective treatments are lacking. Additionally, synthetic fungicides contribute to other significant issues, as previously mentioned, including soil and water contamination, genetic alterations in non-target organisms, disruptions to the endocrine systems of aquatic animals, among others. Consequently, there is a growing demand for natural and environmentally friendly fungicides to address these challenges.

As mentioned earlier, natural extracts offer several advantageous characteristics, including biodegradability, diverse biological activities and multiple MOA, thereby reducing the likelihood of pathogens developing resistance. Consequently, these extracts have gained significant relevance in recent times and are increasingly utilized as biopesticides.

The primary objective of this study was to develop natural antifungals that can effectively replace conventional fungicides without their associated problems. To achieve this goal, we aim to enhance our understanding of the MOA responsible for the antifungal activity of plant extracts, investigate the mechanisms underlying the development of pathogen resistance and assess the efficacy of these plant extracts in inhibiting fungal growth and protecting agricultural crops against these pathogens. To accomplish these tasks, we propose:

1. To evaluate the *in vitro* antifungal activity of the chosen plant extracts through viability tests with *S. cerevisiae* as an experimental fungal model;
2. To evaluate whether the most active extracts can inhibit the growth of phytopathogenic fungi known to devastate relevant crops and to have resistance to synthetic fungicides, through *in vitro* viability assays;
3. To investigate possible mechanisms of action involved in the antifungal activity of the extract through viability assays with mutants;
4. To test their potential phytotoxic effect in germination and early growth bioassays *in vitro*;
5. Evaluate if the extracts with more active antifungal activity have the ability to induce resistance in phytopathogenic fungi, as with conventional fungicides.

3. MATERIALS AND METHODS

3.1. Preparation of plant extracts

Selected plants (turmeric, nutmeg and basil) were acquired already powdered in an organic products store, where turmeric was obtained from the ground rhizome (commercial brand: Vertente dos sabores), nutmeg from the ground fruit (commercial brand: Naturesana Artemis Bio) and basil from its leaves (commercial brand: Vertente dos sabores). Then, to obtain extracts rich in phytochemicals, two extractions were performed: aqueous and ethanolic. The goal was to extract polar and non-polar constituents and determine which type of constituents exhibited higher antimicrobial activity. Water was chosen for extracting polar phytochemicals due to its intrinsic non-toxic nature to organisms, while ethanol was selected for non-polar constituents because of its lower toxicity compared to methanol or other organic solvents concerning humans and animals. Specifically, 80% ethanol was chosen to minimize its toxic effects on plants. In similar works and studies, this solvent is typically the most commonly used.

To prepare the aqueous extracts, 5 g of the powdered plant material was extracted with 30 mL of deionized water, in a water bath at 60 °C, for 30 minutes, and protected from sunlight. Then gravity filtration was performed, followed by centrifugation for 10 minutes, at 5000 rpm. After centrifugation, the supernatant was collected and stored at -80 °C. Finally, after a 4-day lyophilization at -80 °C and 0.14 mbar, the aqueous extracts were dissolved in deionized water to make stock solutions at concentrations of 50 and 200 mg/mL and stored in the dark at -20 °C until use.

To prepare the ethanolic extracts, the powdered plant material was extracted with an 80% (v/v) ethanolic solution using the same mass:volume and procedure as above described. Next, gravity filtration was performed, followed by centrifugation for 10 min at 5000 rpm. After centrifugation, the supernatant was collected and the solvent was evaporated using rotavapor (BUCHI Rotavapor® R-100). After evaporation, the extract was suspended in deionized water and deep frozen. Finally, after freeze-drying for 7 days at -80 °C and 0.14 mbar, stock solutions at 50 and 200 mg/mL were made using 80% ethanol as solvent and stored at -20 °C, in the dark, to be used in future assays. The extraction yield was calculated for both types of extracts using the following equation:

$$\text{Yield (\%)} = \frac{\text{Dry extract obtained (g)}}{\text{Dry sample (g)}} * 100$$

3.2. Microbial organisms, media and growth conditions

The *S. cerevisiae* yeast strains used in this work are listed and described in Table 3, while the filamentous phytopathogenic fungi and oomycetes used are listed and described in Table 4. For *S. cerevisiae* strains, the stock culture was prepared weekly in YPDA medium (1% w/v yeast extract BD Bacto™, 2% w/v peptone, 2% w/v dextrose, and 2% w/v agar). The preparation involved a 48-hour incubation at 30 °C, followed by storage at 4 °C. The stock cultures of the fungi and oomycetes were prepared on Potato-Dextrose-Agar medium (PDA; BioLife®). This involved placing an 8-mm disc of mycelium in the center of plates with PDA medium, and then incubated in the dark, at 25 °C. Once the culture reached its complete growth, the plates containing the fungus were stored at 4 °C.

Table 3 – Yeast strains used in this study

Yeast strains	Genotype
BY4741	BY4741; Mata; <i>his3Δ1</i> ; <i>leu2Δ0</i> ; <i>met15Δ0</i> ; <i>ura3Δ0</i>
<i>bck1</i>	BY4741; Mata; <i>his3Δ1</i> ; <i>leu2Δ0</i> ; <i>met15Δ0</i> ; <i>ura3Δ0</i> ; <i>YJL095w::kanMX4</i>
<i>mkk1/ mkk2</i>	BY4741; Mata; <i>his31</i> ; <i>leu20</i> ; <i>met150</i> ; <i>ura30</i> ; <i>mkk2::kanMX4</i> ; <i>mkk1::LEU2</i>
<i>erg2</i>	BY4741; Mata; <i>his3Δ1</i> ; <i>leu2Δ0</i> ; <i>met15Δ0</i> ; <i>ura3Δ0</i> ; <i>erg2Δ::kanMX4</i>
<i>erg3</i>	BY4741; Mata; <i>his3Δ1</i> ; <i>leu2Δ0</i> ; <i>met15Δ0</i> ; <i>ura3Δ0</i> ; <i>erg3Δ::kanMX4</i>
<i>erg4</i>	BY4741; Mata; <i>his3Δ1</i> ; <i>leu2Δ0</i> ; <i>met15Δ0</i> ; <i>ura3Δ0</i> ; <i>erg4Δ::kanMX4</i>
<i>erg5</i>	BY4741; Mata; <i>his3Δ1</i> ; <i>leu2Δ0</i> ; <i>met15Δ0</i> ; <i>ura3Δ0</i> ; <i>erg5Δ::kanMX4</i>
<i>erg6</i>	BY4741; Mata; <i>his3Δ1</i> ; <i>leu2Δ0</i> ; <i>met15Δ0</i> ; <i>ura3Δ0</i> ; <i>erg6Δ::loxP-kanMX-loxP</i>
W303-1A	BY4741; Mata; <i>ade2-1</i> ; <i>ura3-1</i> ; <i>leu2-3,112</i> ; <i>trp1-1</i> ; <i>his3-11,15</i> ; <i>can1-100</i>
<i>yca1</i>	W303-1A; Mata; <i>ade2-1</i> ; <i>ura3-1</i> ; <i>leu2-3,112</i> ; <i>trp1-1</i> ; <i>his3-11,15</i> ; <i>can1-100</i> ; <i>yca1::kanMX4</i>

Table 4 – Phytopathogenic fungi and oomycetes used in this study

Wild-type isolate	Provider
<i>Botrytis cinerea</i>	Rui Oliveira (Centre of Molecular and Environmental Biology (CBMA), University of Minho)
<i>Colletotrichum acutatum</i>	Rui Oliveira (Centre of Molecular and Environmental Biology (CBMA), University of Minho)
<i>Diplodia corticola</i>	Rui Oliveira (Centre of Molecular and Environmental Biology (CBMA), University of Minho)
<i>Phytophthora cinnamomi</i>	Eva Sánchez-Hernández (Department of Agricultural and Forestry Engineering, ETSIIAA, University of Valladolid)
<i>Phytophthora cactorum</i>	Eva Sánchez-Hernández (Department of Agricultural and Forestry Engineering, ETSIIAA, University of Valladolid)
<i>Fusarium culmorum</i>	Eva Sánchez-Hernández (Department of Agricultural and Forestry Engineering, ETSIIAA, University of Valladolid)

3.3. Evaluation of the antifungal and anti-oomycetal activities of the extracts *in vitro*

3.3.1. Viability assays with *Saccharomyces cerevisiae*

To perform this assay, a pre-inoculum was prepared from an isolated colony from the stock culture of the *S. cerevisiae* BY4741 strain and subsequently suspended in 5 mL of liquid YPD medium. Then the pre-inoculum was incubated overnight at 30 °C, under agitation (200 rpm). In the morning, cell proliferation was monitored by reading the optical density at 600 nm (OD_{600}), and cultures were diluted with fresh YPD to an OD_{600} of 0.1 and incubated for 4 h to reach an OD_{600} between 0.4 and 0.6 (exponential growth phase of the culture). Subsequently, the culture was divided into 4 aliquots: the negative control, which was prepared with the cell suspension (980 μ L) and solvent (20 μ L, which is equal to the volume of the highest extract concentration, resulting in a final solvent concentration of 1.6%) and the 3 treatments, in which the suspension was mixed with the extract to final concentrations of 250, 500 or 1000 μ g/mL. The suspensions were then incubated at 30 °C and after 0 (no extract), 30, 60, 90 and 120 min, 100 μ L of the different aliquots were sampled and serially diluted in 900 μ L of sterile deionized water (dilutions of: 10^{-1} , 10^{-2} , 10^{-3} and 10^{-4}). Then, for each treatment, three 40- μ L drops of the 10^{-4} dilution were placed on plates with YPDA (Figure 16). Finally, after an incubation of 48 h at 30 °C, the number of colony-forming units (CFUs) was counted on each plate and the percentage cell viability of the CFUs was calculated, assuming 100% viability for colonies counted at time 0 for each treatment, using the equation:

$$\text{Viability (\%)} = \frac{x_t}{x_0} \times 100$$

Where x_t are the CFUs of each replicate at each time t and the \bar{x}_0 is the mean value of CFUs at time zero. The mean value of viability will be estimated from the values obtained for each replicate.

To determine the MOA of the extracts, the same procedure was done, except that mutant yeasts were used instead of yeast from the BY4741 strain. The mutant yeasts that were used in this study were: *bck1* and *mkk1/mkk2* affected in cell wall remodeling, *yca1* affected in apoptosis and W303-1A (which is the parental strain of *yca1*), *erg2*, *erg3*, *erg4*, *erg5* and *erg6* affected in ergosterol synthesis. With these mutants it was thus possible to start to have indications about the cellular targeting of the extracts.

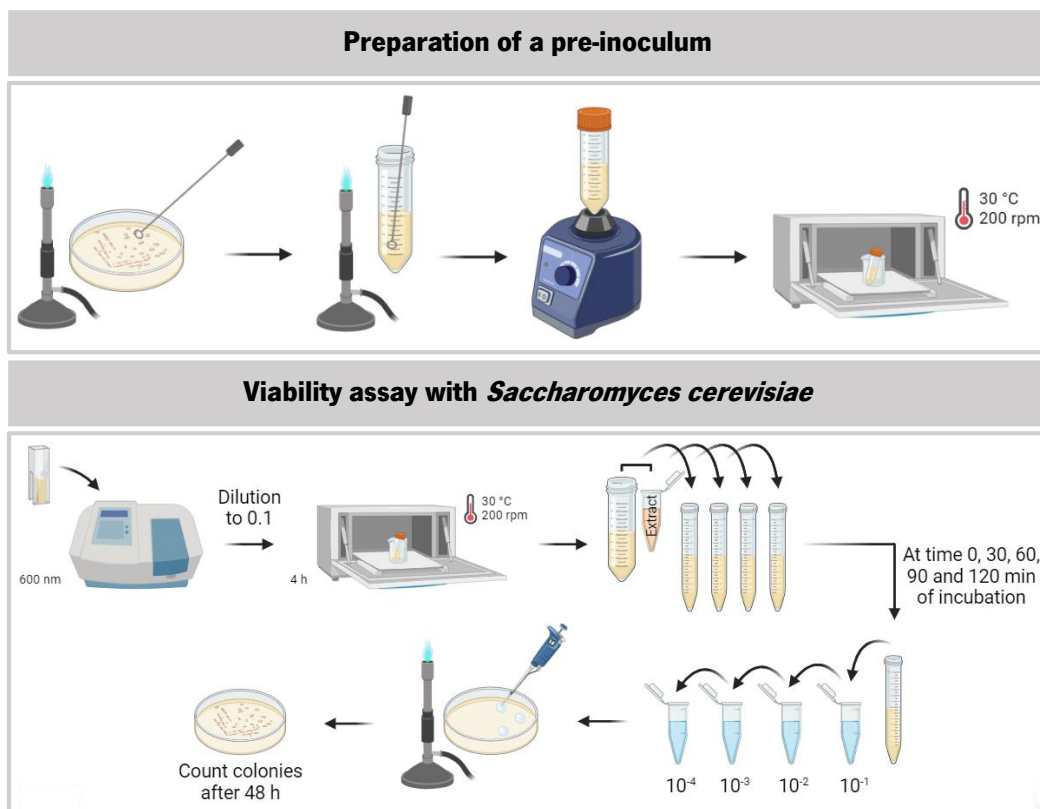


Figure 16 – Schematic overview of pre-inoculum preparation and viability assay using *Saccharomyces cerevisiae*. In the pre-inoculum preparation an isolated colony of the *S. cerevisiae* BY4741 strain was suspended in liquid YPD medium and incubated overnight at 30 °C and 200 rpm. For the viability assay, cell proliferation was monitored and diluted to an OD₆₀₀ of 0.1, and incubated again for 4h to reach an OD₆₀₀ between 0.4 and 0.6. Subsequently, the culture was divided into 4 aliquots and after 0, 30, 60, 90 and 120 min of incubation, 100 µL of each aliquot were sampled and serially diluted to 10⁻⁴. Then, for each treatment, three 40 µL drops of the last dilution were placed on plates with YPDA and incubated.

3.3.2. Growth inhibition assays with filamentous fungi and oomycetes

In this assay, the evaluation of the antifungal activity was performed through viability assays determining the inhibition of the mycelial growth of the phytopathogenic fungi and oomycetes by the extracts that had more antifungal activity in the previous assay. In 15 mL of molten PDA culture medium, the extract as well as deionized water or ethanol 80% was incorporated to test these different concentrations: 250, 500 and 1000 µg/mL. For the negative control, only the solvent (deionized water or ethanol at a volume of 75 µL, which is equal to the volume of the highest extract concentration, resulting in a final solvent concentration of 0.4%) was incorporated into PDA medium. Next, each mixture was poured into a plate and after solidification, an 8-mm diameter mycelium disk of each fungus/oomycete was placed in the center of the Petri plates. Then, the plates were incubated in the dark at 25 °C (Figure 17). Subsequently, the radial mycelial growth was determined by measuring two perpendicular diameters of the colony every three days in all plates. The assay ended when the growth

of the negative control reached the total area of the Petri dish. Finally, the antifungal activity of each treatment was calculated as a percentage of inhibition using the following formula:

$$\text{Inhibition (\%)} = \frac{dc - dt}{dc} \times 100$$

Where dc is the mean diameter of the fungal/oomycete colony in the negative control and dt is the diameter of the fungal colony in each replicate of the corresponding treatment. The average value of the inhibition (%) that occurred was estimated from the values obtained for each replicate.

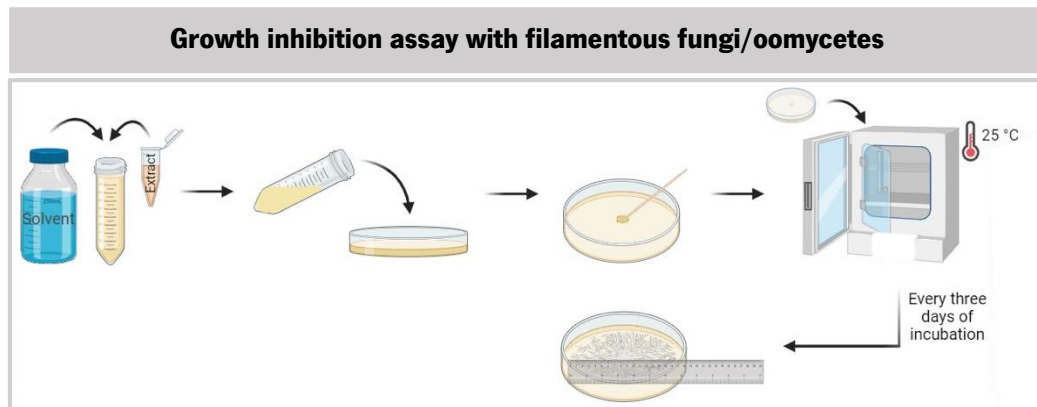


Figure 17 – Schematic overview of a growth inhibition assay using filamentous fungi/oomycetes. For the growth inhibition assay, with the molten PDA culture medium, the extract as well as the solvent was incorporated into the medium. Next, the mixture was poured into a plate and after solidification, an 8-mm diameter mycelium disk of the fungus was placed in the center of the Petri plates and incubated in the dark at 25 °C. Subsequently, the radial mycelial growth of the fungi was determined by measuring two perpendicular diameters of the colony every three days of incubation.

3.4. Assessment of cell viability with propidium iodide by fluorescence microscopy

Initially, a pre-inoculum of *S. cerevisiae* BY4741 was prepared from a colony isolated from a stock culture. The colony was resuspended in liquid YPD medium and incubated overnight at 30 °C under orbital agitation (200 rpm). The next morning, cell proliferation was measured at OD_{600} , and the culture was diluted with fresh YPD medium to an OD_{600} of 0.2. The diluted culture was then incubated for 4 h under the same conditions to reach an OD_{600} of 0.8, after which the cell suspension was divided into two falcon tubes (980 μ L). In one falcon tube, cells were exposed to temperatures between 90 and 100 °C, for 10 min, to induce cell death for testing the effectiveness of propidium iodide (PI). Following this process, a 19- μ L aliquot was collected in a sterile eppendorf tube. In the other falcon tube, before adding the extract at 500 μ g/mL, a 19- μ L aliquot was taken as the time 0 (no extract) control. These two aliquots were then centrifuged at 7100 $\times g$ for 6 min, the supernatant was discarded and the cells were resuspended in 19 μ L of filtered 1x PBS. Subsequently, 1 μ L of PI (5 μ g/mL) was added, and the mixture was incubated for 20 minutes, in the dark, at room temperature. At 120 minutes, another 19- μ L aliquot

was collected from the condition with extract added, and processed as described above for the other two aliquots. Finally, a 7.5- μ L drop of the cell suspension was placed on a slide, and the PI-labeled cells were observed under a fluorescence microscope (DM5000B+CTR5000+ebq100, Leica) (see Figure 18). The number of labeled cells was calculated by counting 200 to 300 cells per replicate in each condition, and the following formula was used:

$$\text{Stained cells (\%)} = \frac{\text{Stained cells}}{\text{Total cells}} \times 100$$

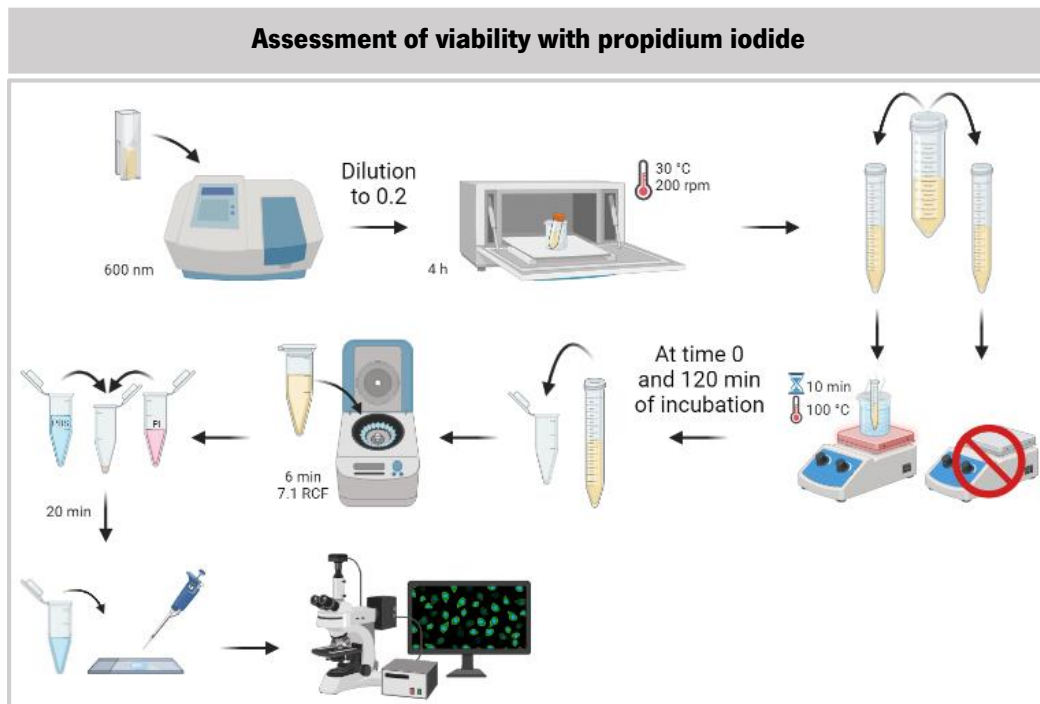


Figure 18 – Schematic overview of viability assessment using propidium iodide. After the preparation of a pre-inoculum, cell proliferation was measured at OD₆₀₀, diluted to 0.2 and incubated for 4 hours at 30 °C and 200 rpm. Then, the cell suspension was divided into two falcon tubes. In one of them, cells were exposed to a temperature of 100 °C for 10 minutes. Following this process, a 19 μ L aliquot from each falcon tube was collected to two eppendorf tubes and centrifuged at 7100 \times g for 6 min. Then, the cells were resuspended in 19 μ L of filtered 1x PBS and 1 μ L of PI at a concentration of 5 μ g/mL was added and incubated for 20 minutes in the dark at room temperature. At 120 minutes, another 19 μ L aliquot was collected from the extract condition, and the same procedure was repeated. Finally, a 7.5 μ L drop of the cell suspension was placed on a slide, and the PI-labeled cells were observed under a fluorescence microscope.

3.5. Phytotoxicity assays using the *in vitro* lettuce model

Seeds of lettuce (*Lactuca sativa*) variety Maravilha das 4 Estações (Casa César Santos, Lot C22373) were placed in a falcon tube, disinfected in 5% bleach for 20 minutes with periodic manual agitation and then rinsed three times with sterile deionized water in a UV-sterilized flow chamber. Twenty seeds were placed into Petri dishes containing 15 mL of MS medium (2% sucrose, 0.8% agar) at a pH of 5.7, preparing four dishes-replicates per experimental condition: a solvent control, prepared by incorporating only 80% ethanol (37.50 μ L, equal to the volume of the highest extract concentration,

resulting in a final concentration of 0.2%) into the 15 mL of MS medium and two concentrations of each extract, 250 and 500 $\mu\text{g}/\text{mL}$ (18.75 μL and 37.50 μL of extract, respectively). As in antifungal assays, solvent and the extract volumes were incorporated in molten medium and vigorously agitated before plating. The plates containing the seeds were then sealed with parafilm and placed in a plant growth room (24 °C, 16-h photoperiod, 50-70 $\mu\text{mol m}^{-2} \text{s}^{-1}$). After 7 days, a photographic record was made and a destructive analysis was performed to assess percentage of germination, cotyledon expansion, presence of the epicotyl apex, number of leaves, and measurement of root length of the seedlings (see Figure 19).

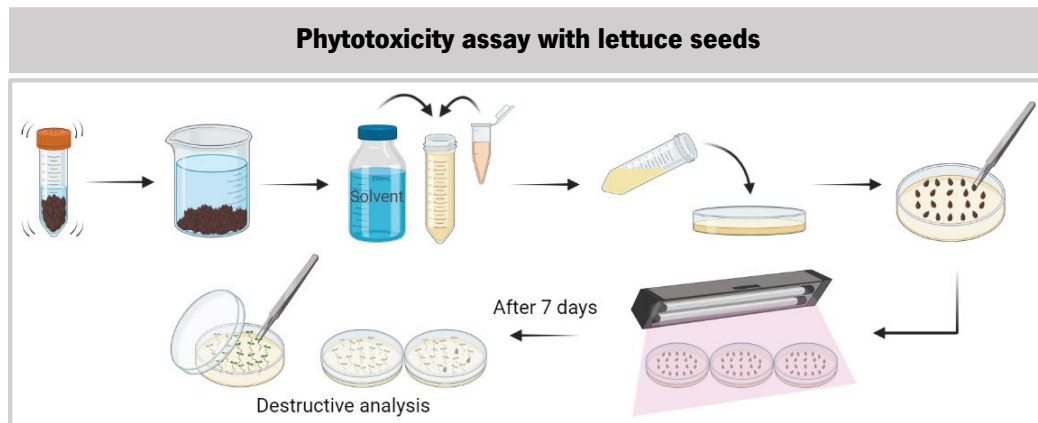


Figure 19 – Schematic overview of the phytotoxicity assay using lettuce seeds. The seeds were washed in 5% bleach for 20 minutes with gentle manual agitation. Subsequently, they were rinsed three times with sterile deionized water. The solvent and the extract were incorporated in the MS medium before solidification, and poured into Petri dishes. Once the seeds were dry, they were carefully placed into the Petri dishes and were then placed in a plant growth room, at 24 °C, 16-h photoperiod, 50-70 $\mu\text{mol m}^{-2} \text{s}^{-1}$ for 7 days. At the end of the trial, a destructive analysis was performed.

3.6. Study of the resistance induction potential of extracts in comparison with itraconazole

3.6.1. Determination of itraconazole Minimum Inhibitory Concentration (MIC)

To determine the minimum inhibitory concentration (MIC) of itraconazole (ITC) and of the extracts, stock solutions of the antifungal were prepared at a concentration of 1600 $\mu\text{g}/\text{mL}$ in DMSO for ITC and of 10 mg/mL for the extracts. From these stock solutions, the antifungal agent was diluted to create a range of concentrations from 0.0313 to 16 $\mu\text{g}/\text{mL}$ for ITC and 1.5625 to 100 $\mu\text{g}/\text{mL}$ for the extract. The antifungal agents were then diluted with liquid YM medium [0.67% (p/v) of yeast nitrogen base without aminoacids, 2% (p/v) glucose, 50 $\mu\text{g}/\text{mL}$ histidine, 100 $\mu\text{g}/\text{mL}$ leucine, 100 $\mu\text{g}/\text{mL}$ methionine, 100 $\mu\text{g}/\text{mL}$ uracil] in two stages, initially at a dilution of 1:10 and then 1:5. The same dilution procedure was applied to the solvent control, which, in the case of ITC is DMSO and in the case of the extracts is 80% ethanol. For the preparation of the *S. cerevisiae* BY4741 yeast inoculum, the yeast was first repitched onto a solid YM medium plate and allowed to grow for 48 hours at 30 °C. On the day of the experiment, 3 mL of sterile deionized water was mixed with 5 colonies of approximately 1 mm in

diameter. After vortexing for 15 seconds, the OD₆₆₀ was adjusted to 0.4 using sterile dH₂O. This inoculum was then further diluted 1:50 and 1:20 with liquid YM medium to achieve a final concentration of 5x10³ CFU/mL (see Figure 20A and B).

The broth microdilution was conducted in sterile 96-well plates with a U-shaped bottom. Antifungal concentrations were distributed across rows 1 to 10, where row 1 represented a concentration of 16 or 100 µg/mL, and row 10 represented 0.0313 or 1.5625 µg/mL. Rows 11 and 12 served as controls, with row 11 containing cells suspended in liquid YM medium with 1% DMSO or 0.48% of ethanol, and row 12 containing cells suspended in liquid YM medium only. The microplate contained the desired antifungal concentrations (0.0313 to 16 or 1.5625 to 100 µg/mL) and an inoculum at a final concentration of 2.5x10³ CFU/mL. The plate was then sealed with parafilm and incubated at 30 °C, without shaking (see Figure 20C). After 48 hours, the presence or absence of growth was observed in each well of the microplate, and the growth in each well was compared with the well containing the solvent control (without antifungal). A turbidity scale was established for comparison, with a score of 0 indicating optical clarity, 1 indicating slight turbidity, 2 indicating a prominent decrease (≈50%) in turbidity, 3 indicating a slight reduction in turbidity, and 4 indicating no reduction in turbidity. For azoles, the MIC is defined as the lowest concentration at which a score of 2 is observed, while for the extracts, it is defined as the lowest concentration at which a score of 0 is observed.

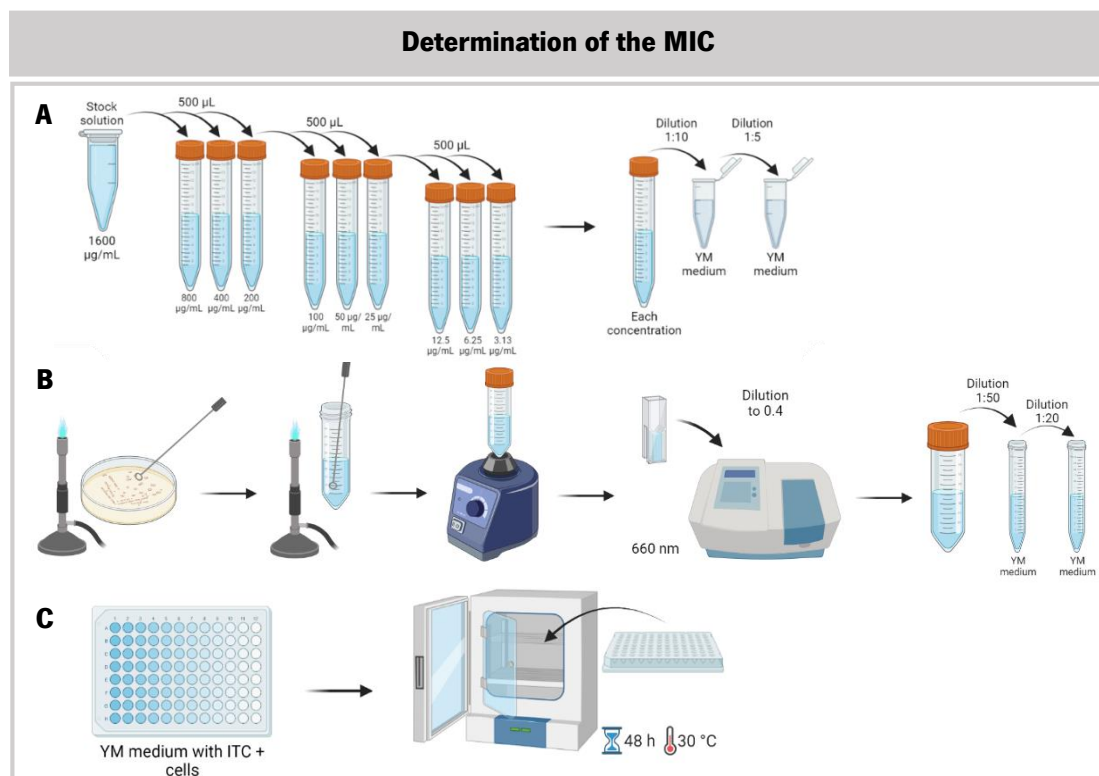


Figure 20 – Schematic overview of the determination of the MIC. (A) Dilution of the antifungal agent; **(B)** Preparation of the inoculum; **(C)** Preparation of the well plate and incubation.

3.6.2. Resistance induction

To induce resistance in the yeast *S. cerevisiae* BY4741, 3 mL of liquid YM medium was mixed with a colony isolated from this yeast and incubated overnight, at 30 °C and 200 rpm. The following day, the OD₆₆₀ was adjusted to 0.4 to achieve a culture concentration of approximately 10⁶ cells/mL. Subsequently, 1 mL of this culture (at 10⁶ cells/mL) was transferred to 10 mL of liquid YM medium containing 0.125, 0.25 or 1.0 µg/mL of ITC, or 6.25, 12.5 or 50 µg/mL of the extract. These three suspensions were incubated overnight at 30 °C and 200 rpm. Upon reaching a cell density of approximately 10⁸ cells/mL in the cultures, 1 mL of cells (at 10⁶ cells/mL) from each condition was transferred to 10 mL of fresh liquid YM medium, maintaining the respective ITC concentrations for each condition. At each passage (on days 1, 2, 3, and 4) of antifungal exposure, a 1-mL aliquot of the cell suspension in liquid YM medium with ITC was mixed with 0.5 mL of 50% glycerol and frozen at -80 °C (see Figure 21). Subsequently, antifungal susceptibility tests (as described in the previous section) were performed using these cells exposed to varying ITC concentrations to assess if the MIC had increased. The cells were classified based on their MIC values: as susceptible to ITC if their MIC was 0.125 µg/mL, as susceptible and dose-dependent to ITC if MICs ranged between 0.25 and 0.5 µg/mL, and as resistant to ITC if MICs were greater than or equal to 1.0 µg/mL. In the case of the extract, the cells were considered resistant to the extract if MICs were greater than the initial MIC value (before the procedure).

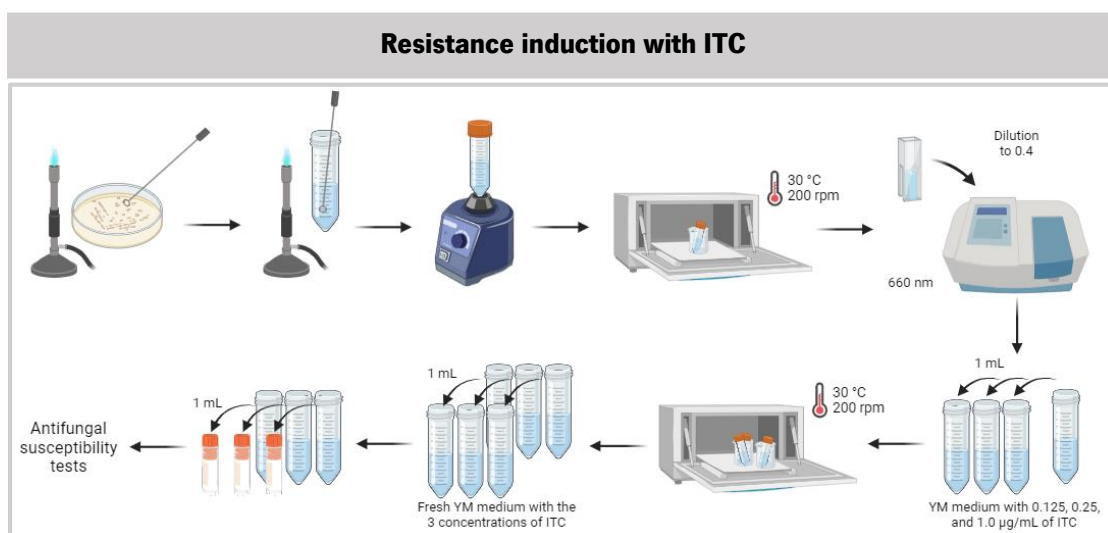


Figure 21 – Schematic overview of the protocol for inducing resistance in *S. cerevisiae* BY4741 yeast. For this assay liquid YM medium was inoculated and incubated overnight at 30 °C and 200 rpm. The following day, the OD₆₆₀ was adjusted to 0.4. Subsequently, 1 mL at 10⁶ cells/mL of this culture was transferred to 10 mL of liquid YM medium containing 0.125, 0.250, and 1.0 µg/mL of ITC, respectively, and were incubated overnight at 30 °C and 200 rpm. The next day, 1 mL of cells at 10⁶ cells/mL from each condition was transferred to 10 mL of fresh liquid YM medium. At each passage (on days 1, 2, 3, and 4) of antifungal exposure, a 1 mL aliquot of the cell suspension was mixed with 0.5 mL of 50% glycerol and frozen at -80 °C. Subsequently, antifungal susceptibility tests were performed.

3.7. Chemical characterization of the extracts

The liquid extract was initially filtered through Whatman No. 1 paper and subsequently freeze-dried, resulting in a solid extract. The infrared vibrational spectrum of the solid extract was measured using a Nicolet iS50 Fourier-transform infrared (FTIR) spectrometer with an attenuated total reflectance (ATR) system (Thermo Scientific; Waltham, MA, USA). The spectrum was recorded over a range of 400–4000 cm^{-1} , with a resolution of 1 cm^{-1} , and was generated by combining 64 scans. For gas chromatography–mass spectrometry (GC–MS) analysis, conducted at the Research Support Services of Universidad de Alicante, the freeze-dried extract was dissolved in HPLC-grade methanol (5 mg mL^{-1} solution) and the solution was subsequently filtered. The analysis was carried out using an Agilent Technologies (Santa Clara, CA, USA) 7890A gas chromatograph coupled to a 5975C quadrupole mass spectrometer. The chromatography conditions were as follows: injection volume = 1 μL ; injector temperature = 280 $^{\circ}\text{C}$ (in splitless mode); initial oven temperature = 60 $^{\circ}\text{C}$ for 2 minutes, followed by a temperature ramp of 10 $^{\circ}\text{C min}^{-1}$ to a final temperature of 300 $^{\circ}\text{C}$ for 15 minutes. Compound separation was achieved using an Agilent Technologies HP-5MS UI column with dimensions of 30 m in length, 0.250 mm in diameter and a film thickness of 0.25 μm . The mass spectrometer conditions included: electron impact source temperature = 230 $^{\circ}\text{C}$; quadrupole temperature = 150 $^{\circ}\text{C}$; and ionization energy = 70 eV. Identification of components relied on comparing their mass spectra and retention times with authentic compounds and utilizing the National Institute of Standards and Technology (NIST11) database.

3.8. Statistical analysis

Statistical analysis and graphical representation were performed using GraphPad Prism version 8.4.2 for Windows (GraphPad Software, San Diego, California, USA). For the viability assay with *S. cerevisiae*, growth inhibition assay with filamentous fungi and oomycetes and the assessment of cell viability with PI through fluorescence microscopy, three independent trials were conducted. In the phytotoxicity assay using the *in vitro* lettuce model, a single trial was performed with four replicates per condition. The determination of ITC and CE extract MIC involved a single assay with three technical replicates and the resistance induction assay with ITC and CE extract consisted of a single assay with two technical replicates. All results are presented as the mean \pm standard deviation (SD), except for the viability assessment with PI through fluorescence microscopy, where the mean \pm standard error of the mean (SEM) was employed. In all assays, treatments were compared with the negative control, and

additionally, in the viability assays with *S. cerevisiae* mutants, three comparisons were made: WT untreated *vs.* mutant untreated, mutant untreated *vs.* mutant treated and WT treated *vs.* mutant treated at all concentrations tested. For statistical analysis, the normality test was applied, the homogeneity of variances between groups verified with Bartlett test, before one-way ANOVA was applied and Dunnett's test for multiple comparisons between treatment groups and the control. For the analysis of the results obtained with viability assays with *S. cerevisiae* and mutant strains, a *t*-test was also applied at the last time point. The level of significance (*p* value) of each test is denoted in the figures as follows: ns ($p > 0.05$) – non-significant, * ($0.01 < p \leq 0.05$) – significant, ** ($0.001 < p \leq 0.01$) – very significant, *** ($0.0001 < p \leq 0.001$) – highly significant, and **** ($p \leq 0.0001$) – very highly significant.

4. RESULTS AND DISCUSSION

4.1. Antifungal activity of CE and NME extracts against *Saccharomyces cerevisiae*

As previously referred, plant extracts from *C. longa*, *M. fragrans* and *O. basilicum* are extremely rich in a wide range of compounds with various biological activities, including antifungal. These extracts have been reported in the literature for their antifungal activity against various pathogenic fungi in both plants and humans, indicating potential applications in agriculture and medicine. To study the potential of these plants, *C. longa* aqueous (CA) and ethanolic (CE), Nutmeg aqueous (NMA) and ethanolic (NME), and *O. basilicum* aqueous (OA) and ethanolic (OE) extracts were prepared through extractions with water for the aqueous extracts and 80% ethanol for the ethanolic extracts. The viability of these extracts was assessed on the yeast *S. cerevisiae* BY4741, following the procedure described in section 3.3.1. Both 80% ethanol and water were used as extraction solvents and also as solvents for the stock solutions to ensure that all extracted compounds were dissolved. Furthermore, a comparison test was conducted, treating *S. cerevisiae* yeasts with 0.8% and 1.6% of ethanol and comparing the results with a treatment using liquid YPD medium, which showed no significant differences (see Annex 1).

Aqueous extracts CA (Figure 22A), NMA (Figure 22C), OA (Figure 22E), and ethanolic extract OE (Figure 22F) exhibited no antifungal activity, as viability remained consistent across all tested concentrations after 120 minutes, similar to the control and, although the concentration of 1000 µg/mL of the CA extract was more affected than the control, it was not significant. However, CE (Figure 22B) and NME (Figure 22D) extracts displayed robust antifungal activity at all concentrations. For the CE extract, concentrations of 250, 500, and 1000 µg/mL resulted in viability reductions to approximately 50% ($p < 0.0001$), 20% ($p < 0.0001$) and 5% ($p < 0.0001$), respectively, at timepoint 30 min, further declining to 35%, 15% and 2% ($p < 0.0001$) after 120 minutes. In the NME extract, concentrations of 250, 500, and 1000 µg/mL led to viability drops of around 15% ($p < 0.0001$), 5% ($p < 0.0001$) and 1% ($p < 0.0001$), also at timepoint 30 min, maintaining these levels over time. These results suggest both CE and NME extracts are toxic to *S. cerevisiae*, both exhibiting dose-dependent and relatively constant effects. Thus, the study confirms the antifungal activity of CE and NME extracts against yeast, in contrast to CA, NMA, OA, and OE extracts. Previous research by Chen et al. (2018) and Radwan et al. (2014) had already demonstrated the toxic effect of *C. longa* ethanolic extract and *M. fragrans* methanolic extract on *S. cerevisiae*, which is consistent with our findings in the case of *C. longa*. Furthermore, the ethanolic extract of *C. longa* has also exhibited activity against various yeast such as *Candida* spp. and *Cryptococcus neoformans* (Ungphaiboon et al., 2005), attributed to some of its constituents (Chen et al., 2018).

Although nutmeg extract via supercritical fluid extraction with CO₂ has shown activity against *C. albicans* (Iyer et al., 2017), the chemical characterization and the knowledge of the MOA remains limited. Considering the inhibitory effect on *S. cerevisiae* (used as a fungal model), there is potential for these two extracts to inhibit filamentous fungi, including phytopathogenic fungi, then they were chosen to continue the evaluation of antifungal/anti-oomycete activities against the selected phytopathogens.

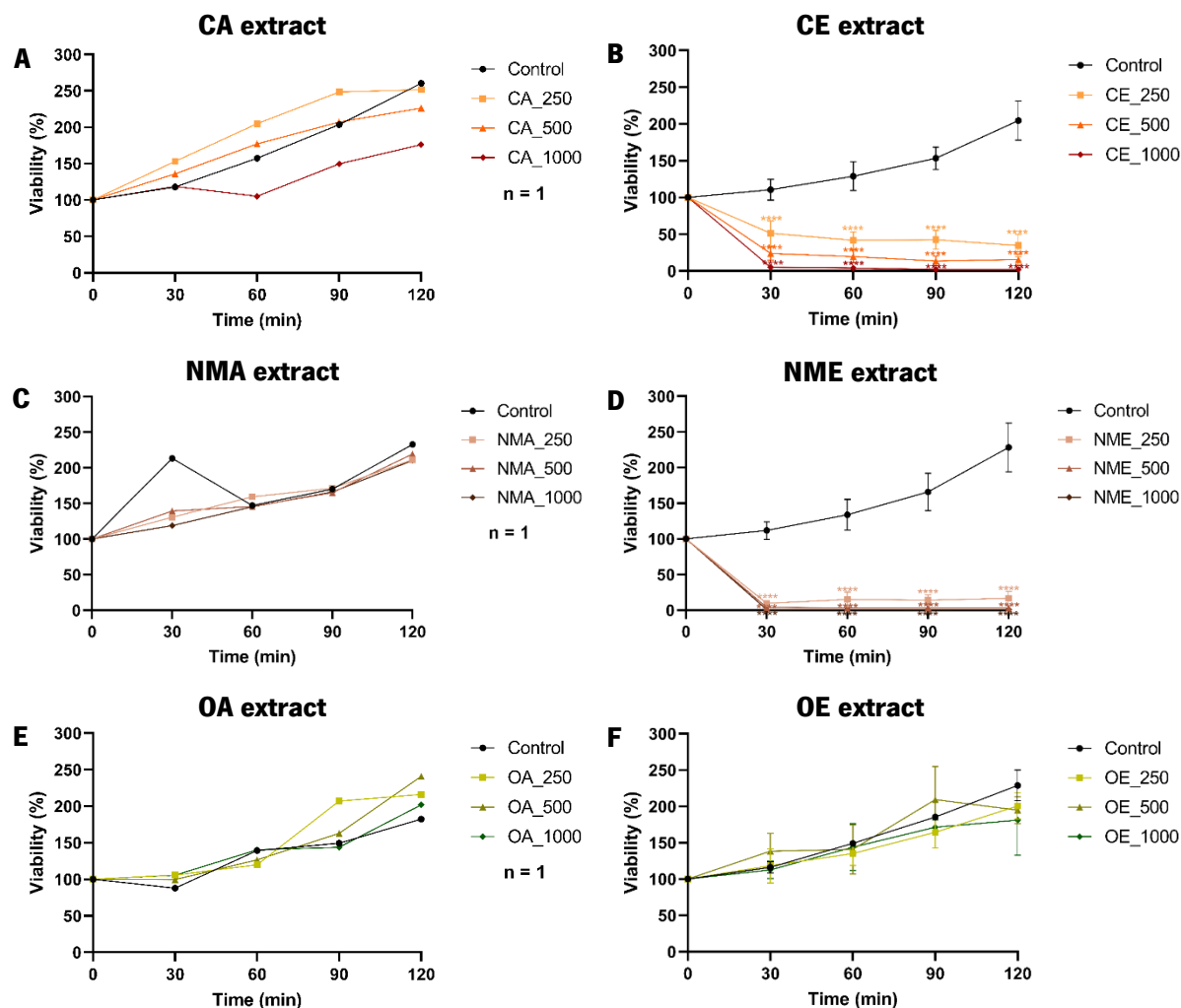


Figure 22 – The viability of *Saccharomyces cerevisiae* BY4741 following exposure to ethanolic extracts of *Curcuma longa*, *Myristica fragrans* and *Ocimum basilicum*. Cells from exponentially growing cultures were incubated at 30 °C with 250, 500 or 1000 µg/mL extract, aliquots were harvested at 0, 30, 60, 90, and 120 min, serially diluted until 10⁻⁶, and the latter dilution was spread in YPDA plates and incubated for 48 h at 30 °C. Controls were prepared with the extract solvent (80% ethanol). (A) *C. longa* aqueous extract; (B) *C. longa* ethanolic extract; (C) *M. fragrans* aqueous extract; (D) *M. fragrans* ethanolic extract; (E) *O. basilicum* aqueous extract; and (F) *O. basilicum* ethanolic extract. Cell viability percentages were determined by dividing the mean CFU value at each time point by the mean value at 0 min. The data represent the average from three independent experiments, presented as mean ± SD, except for the aqueous extracts, where the data represents a single independent experiment. Statistical analysis was conducted by one-way ANOVA, followed by the Dunnett test for multiple comparisons. Each treatment was compared to the corresponding control at each time point and the statistical significance (p value) is indicated.

4.2. Growth inhibition potential of CE and NME extracts against various filamentous fungi and oomycetes

4.2.1. Potential of CE extract

To assess the potential antifungal and anti-oomycetal activities of CE extract against phytopathogenic filamentous fungi and oomycetes, the following species were selected: *B. cinerea*, *C. acutatum*, *D. corticola*, *F. culmorum*, *P. cactorum* and *P. cinnamomi*. These microorganisms were exposed to various extract concentrations to examine the mycelium growth, as outlined in section 3.3.2. Results are represented in Figure 23, 24 and 25. It is important to state here, that in these assays with filamentous fungi and oomycetes, the solvent control contained 0.4% of ethanol, in contrast to the previous viability assay with *S. cerevisiae*, where the solvent concentration was 1.6% of ethanol. This concentration was chosen because the filamentous fungi/oomycetes under study have been shown to be more susceptible to the toxic effects of ethanol compared to *S. cerevisiae*. Importantly, it is worth noting that the solvent used for the extract, 80% ethanol, at the volume used, did not significantly impact the diameter of the fungi/oomycetes when compared with a negative control without solvent (see Annex 2).

The diameters of *B. cinerea* decreased significantly after 6 days of incubation in the presence of CE extract at 250 µg/mL ($p < 0.01$), 500 µg/mL ($p < 0.001$) and 1000 µg/mL ($p < 0.0001$) compared to the solvent control (Figure 23A), showing inhibitions of 12.49%, 21.99% and 36.14%, respectively (Figure 23C). This inhibitory effect remained constant over time at all concentrations, suggesting that CE is toxic to *B. cinerea* at these tested concentrations. The photographic record reveals that the mycelium of *B. cinerea* maintained the same color and appearance as the solvent control (Figure 25A). However, a subtle, less dense layer of mycelium can be observed surrounding the denser layers. This indicates that the CE extract indeed weakens and inhibits the mycelium's growth, and a dose-response trend is evident.

For *C. acutatum*, after 20 days of incubation with CE extract at 500 µg/mL ($p < 0.01$) and 1000 µg/mL ($p < 0.001$), the diameters also significantly decreased compared to the solvent control (Figure 23B), resulting in inhibitions of 17.23% and 23.23%, respectively (Figure 23D). Somewhat differently from *B. cinerea*, a peak of inhibition was observed on day 13, reaching 25.22% and 34.88% at concentrations of 500 and 1000 µg/mL, respectively, decreasing afterwards to 17.23% and 23.23% at the end of the experiment. These findings indicate that CE is toxic to *C. acutatum* at these two concentrations. The photographic record reveals that the mycelium of *C. acutatum* appears slightly lighter in color at all three tested concentrations compared to the solvent control (Figure 25B). Moreover, a clear dose-response effect is evident, demonstrating that the CE extract significantly inhibits the growth of the mycelium.

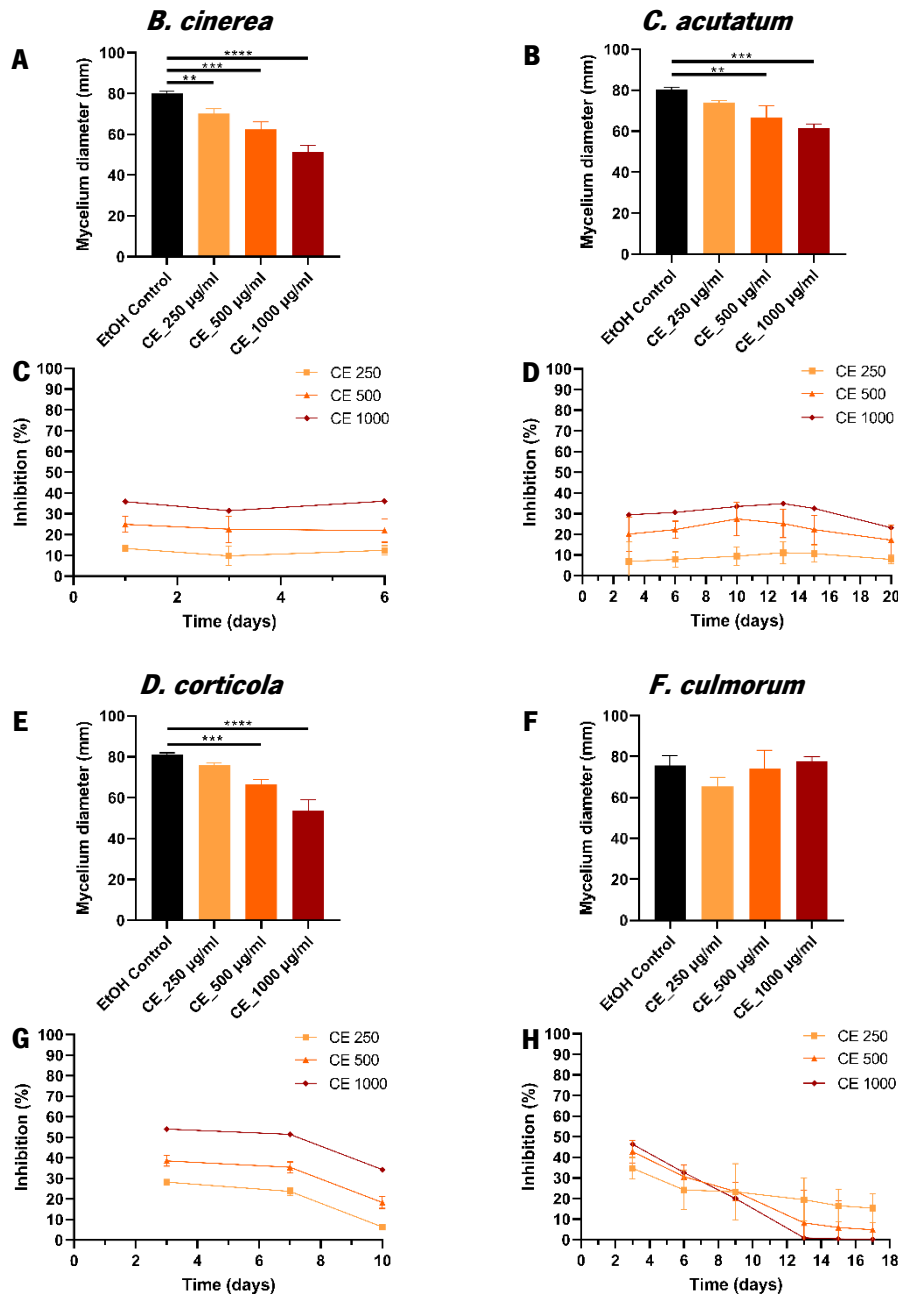


Figura 23 – Mycelium diameter (mm) and mycelium growth inhibition (%) of *Botrytis cinerea*, *Colletotrichum acutatum*, *Diplodia corticola* and *Fusarium culmorum* when exposed to *Curcuma longa* ethanolic extract (CE). The CE extract was incorporated into molten PDA medium at varying concentrations (250, 500, or 1000 µg/mL), alongside controls where 80% ethanol was matched in volume to the highest extract concentration. A mycelium disc was placed at the center of each plate and incubated in darkness at 25°C until the fungus reached the Petri dish's edge. Diameter graphs represent the mycelium diameter measured on the final assay day for each fungus (**A-B** and **E-F**). Additionally, graphs depicting growth inhibition over the assay period are shown (**C-D** and **G-H**) for the fungi *B. cinerea* (**A and C**), *C. acutatum* (**B and D**), *D. corticola* (**E and G**) and *F. culmorum* (**F and H**). Data for diameter and inhibition of mycelium growth present the mean of three independent experiments ± SD. One-way ANOVA was conducted, followed by the Dunnett test for multiple comparisons: *0.01 < p ≤ 0.05, **0.001 < p ≤ 0.01, ***0.0001 < p ≤ 0.001 and ****p ≤ 0.0001, depicted the significance level of the differences to the respective controls.

In the case of *D. corticola*, the diameters significantly decreased after 10 days of incubation with CE extract at 500 µg/mL ($p < 0.001$) and 1000 µg/mL ($p < 0.0001$) compared to the solvent control (Figure 23E), with inhibitions of 18.28% and 34.32%, respectively (Figure 23G). The inhibition remained consistent around 37.00% and 52.74% for concentrations of 500 and 1000 µg/mL, respectively, on days 3 and 7, but similarly to *C. acutatum* decreased afterwards to 18.28% and 34.32% at the end of the experiment. This further confirms that CE is toxic to *D. corticola*. The photographic record reveals that the mycelium of *D. corticola* exhibits a slightly lighter color with a central grey tinge compared to the uniform grey of the solvent control. Additionally, the mycelium's appearance at the three concentrations tested is less distinct than in the solvent control, with less clearly defined layers (Figure 25C). Moreover, a noticeable dose-response effect is observed, confirming that the CE extract inhibits mycelium growth.

For *F. culmorum*, the diameters did not decrease after 17 days of incubation with CE extract at 250, 500 and 1000 µg/mL compared to the solvent control (Figure 23F). On day 3, inhibitions of 34.68%, 42.77%, and 46.38% were observed for the respective concentrations. However, inhibition dramatically decreased in the subsequent days, especially for the concentrations of 500 and 1000 µg/mL, reaching only 4.85% and 0.23% inhibition on day 17, respectively. The concentration of 250 µg/mL showed a relatively constant inhibitory effect, reaching 15.36% on day 17, but this was not statistically significant when compared to the solvent control (Figure 23H). These results suggest that CE is not toxic to *F. culmorum*, indicating a possible adaptation over time, particularly at higher concentrations. The photographic record indicates, however, that the mycelium of *F. culmorum* exhibits a yellow color at the three tested concentrations, in contrast to the pink color seen in the solvent control, suggesting qualitative alterations, possibly metabolic. Although at the concentration of 250 µg/mL the mycelium appears smaller compared to the solvent control, this decrease is modest, and no clear dose-response effect is observed (Figure 25D). This suggests that the CE extract has limited inhibitory effects on mycelium growth.

For *P. cactorum*, the diameters decreased significantly after 24 days of incubation with CE extract at 500 µg/mL ($p < 0.05$) and 1000 µg/mL ($p < 0.0001$) compared to the solvent control (Figure 24A), resulting in inhibitions of 18.67% and 41.29%, respectively (Figure 24C). The inhibitory effect remained relatively constant over time, especially at the concentration of 1000 µg/mL. This indicates that CE is toxic to *P. cactorum* at these tested concentrations. The photographic record reveals that the mycelium of *P. cactorum*, across all concentrations, maintains the same color and appearance as the solvent control. Furthermore, a distinct dose-response effect is evident, with the concentration of 1000 µg/mL

displaying the smallest mycelium size. This observation confirms that the CE extract effectively inhibits the growth of the mycelium of this oomycete (Figure 25E).

Finally, in the case of *P. cinnamomi*, the diameters significantly decreased after 6 days of incubation with CE extract at 250 µg/mL ($p < 0.0001$), 500 µg/mL ($p < 0.0001$) and 1000 µg/mL ($p < 0.0001$) compared to the solvent control (Figure 24B), resulting in inhibitions of 57.58%, 61.17%, and 65.88%, respectively (Figure 24D). The inhibitory effect remained constant over time at all concentrations, without a clear dose-response effect. This suggests that CE is toxic to *P. cinnamomi* at these tested concentrations. The photographic record reveals that the mycelium of *P. cinnamomi*, at all concentrations, maintains the same color and appearance as the solvent control. Although a clear dose-response effect is not readily apparent, the noticeable reduction in mycelium growth indicates that the CE extract significantly inhibits mycelium growth (Figure 25F).

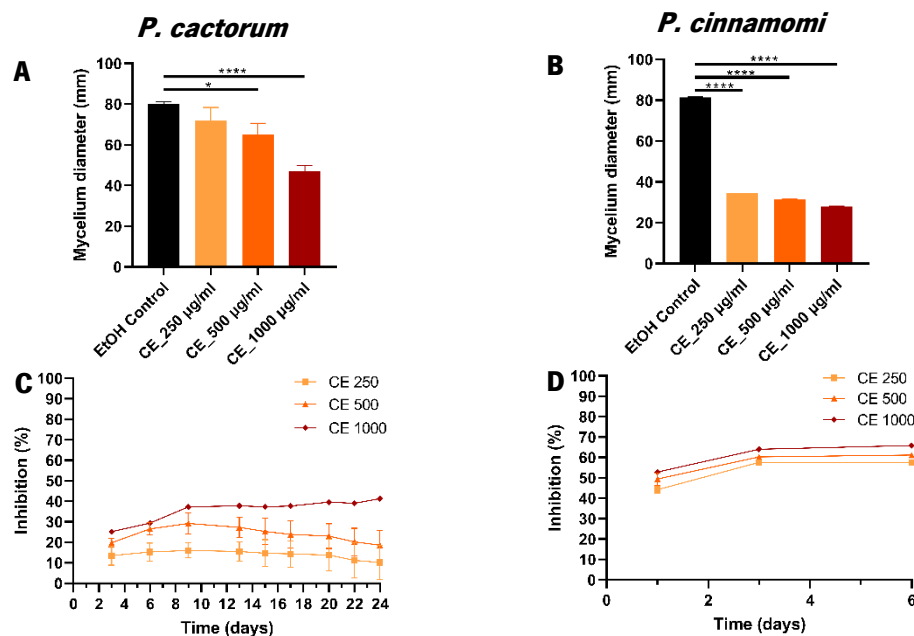


Figure 24 – Mycelium diameter (mm) and mycelium growth inhibition (%) of *Phytophthora cactorum* and *Phytophthora cinnamomi* when exposed to *Curcuma longa* ethanolic extract (CE). The CE extract was incorporated into molten PDA medium at varying concentrations (250, 500, or 1000 µg/mL), alongside controls where 80% ethanol was matched in volume to the highest extract concentration. A mycelium disc was placed at the center of each plate and incubated in darkness at 25°C until the oomycetes reached the Petri dish's edge. Diameter graphs represent the mycelium diameter measured on the final assay day for each oomycete (A-B). Additionally, graphs depicting growth inhibition over the assay period are shown (C-D) for the oomycetes *P. cactorum* (A and C) and *P. cinnamomi* (B and D). Data for diameter and inhibition of mycelium growth present the mean of three independent experiments ± SD. One-way ANOVA was conducted, followed by the Dunnett test for multiple comparisons: *0.01 < p ≤ 0.05, **0.001 < p ≤ 0.01, ***0.0001 < p ≤ 0.001 and **** p ≤ 0.0001, depicted the significance level of the differences to the respective controls.

Based on the assay results, the CE extract demonstrates notable antifungal and anti-oomycetal activity and toxicity against all tested phytopathogenic fungi and oomycetes (*B. cinerea*, *C. acutatum*, *D.*

corticola, *P. cactorum* and *P. cinnamomi*), with the exception of *F. culmorum*, which appears to adapt to the extract over time. Nonetheless, further research is warranted to comprehensively understand the observed phenomenon in relation to *F. culmorum*. Chen et al. (2018) highlighted that the antifungal activity of ethanolic and hexane extracts of *C. longa* is attributed to some of its compounds, that effectively inhibit mycelium growth in phytopathogenic fungi by reducing ergosterol content in their cell membranes, contributing to a broad-spectrum antifungal effect. Although the specifics of this mechanism remain elusive, these extracts have exhibited antifungal activity against approximately 20 phytopathogenic fungi according to Chen et al. (2018). However, it is clear that this extract has another MOA, as *F. culmorum* contains ergosterol in its membrane while oomycetes do not. Despite this, the CE extract did not inhibit *F. culmorum*, but displayed higher activity against the tested oomycetes, so this results suggest that CE extract acts in another way. Additionally, this assay holds significance due to its examination of certain fungi and oomycetes that have not been previously tested with this extract, namely *C. acutatum*, *D. corticola*, *P. cactorum* and *P. cinnamomi*.

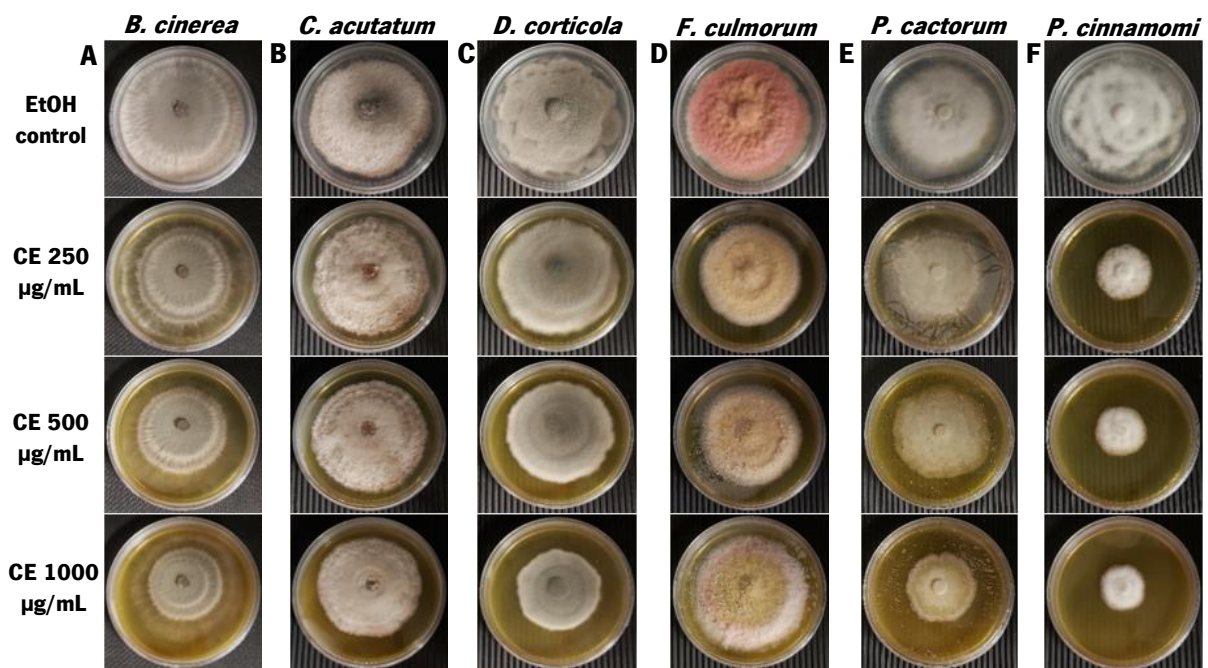


Figure 25 – Photographic record of the filamentous fungus exposed to *Curcuma longa* ethanolic extract (CE). *B. cinerea* (A), *C. acutatum* (B), *D. corticola* (C), *F. culmorum* (D), *P. cactorum* (E) and *P. cinnamomi* (F) were exposed to 250, 500 or 1000 µg/mL of CE extract and incubated in darkness at 25°C until the fungus reached the Petri dish's edge. The images of the mycelium are representative of three experiments at the last day of the assay for each fungus.

4.2.2. Potential of NME extract

The evaluation of the potential antifungal and anti-oomycetal activities of the NME extract also involved the same phytopathogenic filamentous fungi and oomycetes, as above: *B. cinerea*, *C. acutatum*, *D. corticola*, *F. culmorum*, *P. cactorum* and *P. cinnamomi*. These species were subjected to various concentrations to assess their mycelium growth, as detailed in section 3.3.2, and Figure 26, 27 and 28 depicts the overall results.

The diameters of *B. cinerea* decreased after 7 days of incubation in the presence of the NME extract at concentrations of 500 µg/mL ($p < 0.05$) and 1000 µg/mL ($p < 0.05$), compared to the solvent control (Figure 26A). This observation indicates inhibitions of 17.13% and 21.00%, respectively (Figure 26C), thus highlighting a clear dose-response trend. The inhibitory effect slightly decreased up to day 4 and remained constant from day 4 to day 7 at all concentrations, suggesting that the NME is toxic to *B. cinerea* at these two concentrations. Photographic records reveal that the mycelium of *B. cinerea* maintained the same color and appearance as the solvent control (Figure 28A). Furthermore, it is evident that the fungus in the presence of concentrations of 500 and 1000 µg/mL was inhibited compared to the solvent control. This substantiates that the NME extract, as the CE, effectively inhibits the mycelium growth of this species.

For *C. acutatum*, following a 20-day incubation period with NME extract at 1000 µg/mL ($p < 0.001$), there was a slight reduction in diameters when compared to the solvent control (Figure 26B). This reduction corresponded to a growth inhibition of 10.74% (Figure 26D). However, it is noteworthy that the growth inhibition percentage remained consistently at 25.45% up to day 9, at 1000 µg/mL. This observation suggests that the NME extract demonstrates toxicity towards *C. acutatum* at this concentration. Visual evidence, in the form of photographic records, highlights that the mycelium of *C. acutatum* exhibited a lighter coloration across all three tested concentrations, with particular prominence at the 1000 µg/mL concentration, in comparison to the solvent control (see Figure 28B). Furthermore, the data exhibits a dose-response pattern, affirming the inhibitory impact of the NME extract on mycelium growth.

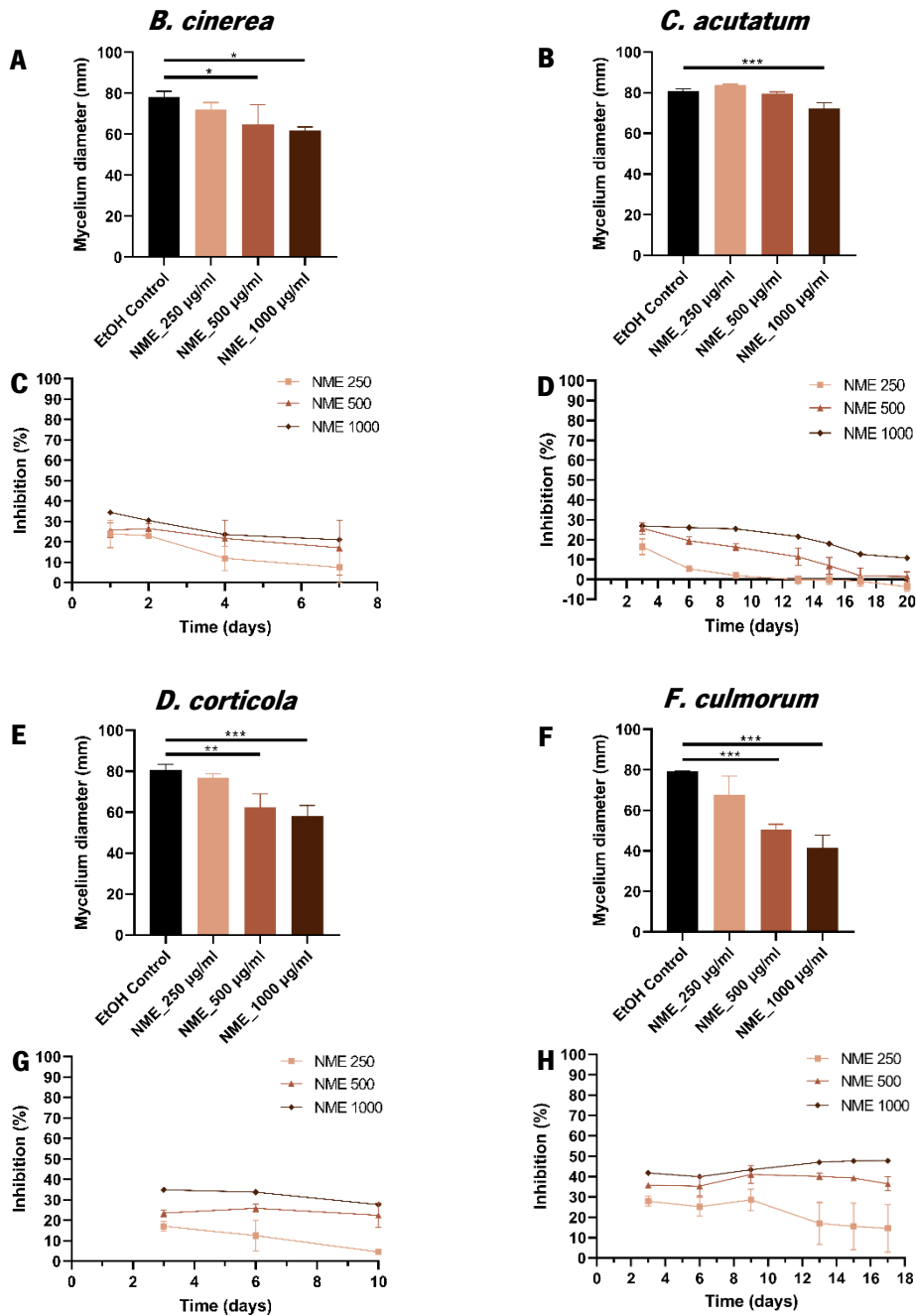


Figure 26 – Mycelium diameter (mm) and mycelium growth inhibition (%) of *Botrytis cinerea*, *Colletotrichum acutatum*, *Diplodia corticola* and *Fusarium culmorum* when exposed to *Myristica fragrans* ethanolic extract (NME). The NME extract was incorporated into molten PDA medium at various concentrations (250, 500, or 1000 µg/mL), alongside control groups where 80% ethanol was adjusted in volume to match the highest concentration of the extract. A mycelium disc was positioned at the center of each plate and incubated in darkness at 25°C until the fungus extended to the edge of the Petri dish. The diameter graphs depict the mycelium diameter measured on the final day of the assay for each fungus (A-B and E-F). Furthermore, graphs illustrating the growth inhibition during the assay period are provided (C-D and G-H) for the fungi *B. cinerea* (A and C), *C. acutatum* (B and D), *D. corticola* (E and G) and *F. culmorum* (F and H). The data for diameter and mycelium growth inhibition represent the mean of three independent experiments ± SD. One-way ANOVA was conducted, followed by the Dunnett test for multiple comparisons: *0.01 < p ≤ 0.05, **0.001 < p ≤ 0.01, ***0.0001 < p ≤ 0.001 and ****p ≤ 0.0001, with significance compared to the respective controls.

In the case of *D. corticola*, there was a significant reduction in diameters following a 10-day incubation period with NME extract at concentrations of 500 µg/mL ($p < 0.01$) and 1000 µg/mL ($p < 0.001$), in comparison to the solvent control (Figure 26E). This reduction was accompanied by growth inhibitions of 22.46% and 27.73%, respectively (Figure 26G). Worth noting is the consistent inhibitory trend at approximately 25.00% with 500 µg/mL and around 34.50% with 1000 µg/mL on days 3 and 6. These findings further substantiate the toxic impact of NME on *D. corticola*. Photographic records reveal a slightly lighter coloration at the edges of the *D. corticola* mycelium, with a central grey tinge, as compared to the uniformly grey appearance of the solvent control. Notably, mycelium appearance remains relatively consistent across all three tested concentrations (Figure 28C). Additionally, a discernible dose-response relationship is observed, confirming the inhibitory effect of the NME extract on mycelium growth.

In the case of *F. culmorum*, there was a significant reduction in diameters following a 17-day incubation period with NME extract at 500 µg/mL ($p < 0.001$) and 1000 µg/mL ($p < 0.001$), when compared to the solvent control (Figure 26F). This reduction led to growth inhibitions of 36.45% and 47.79%, respectively (Figure 26H). This inhibitory trend remained relatively stable until day 9 across all tested concentrations. Subsequently, at 1000 µg/mL, a notable increase in inhibitory percentage was observed on day 13, maintaining consistency until day 17. At 500 µg/mL, the inhibitory percentage remained consistent until day 17, while at 250 µg/mL, the inhibitory percentage decreased on day 13 and remained consistent until day 17. These findings underscore the toxicity of NME towards *F. culmorum* at concentrations of 500 and 1000 µg/mL. Photographic records reveal distinct mycelium colorations: a pink hue at the 250 µg/mL, and a white shade with hints of yellow at the other two tested concentrations. This contrasts with the yellow coloration observed in the solvent control. Furthermore, a clear dose-response pattern is evident (see Figure 28D). This supports the conclusion that the NME extract holds toxicity for *F. culmorum*, capable of inhibiting mycelium growth.

Regarding *P. cactorum*, no significant reduction in diameters was observed following a 24-day incubation period with NME extract at 250, 500, and 1000 µg/mL, as compared to the solvent control (Figure 27A). The highest inhibition recorded was a mere 9.66% at 1000 µg/mL. At the concentrations of 250 and 500 µg/mL even negative inhibition values were found (not significant), suggesting that the oomycete may be resistant/overcoming the extract's mechanisms of action seen in other fungi (Figure 27C). These outcomes indicate that NME does not appear to be toxic to *P. cactorum*, implying that the oomycete might be overcoming the extract's mechanisms of action across all tested concentrations over

time. Photographic records consistently depict the mycelium of *P. cactorum* maintaining the same color and appearance as the solvent control, irrespective of concentration. Together, the absence of an evident effect, confirms that the NME extract does not inhibit the growth of this oomycete's mycelium (see Figure 28E).

Finally, regarding *P. cinnamomi*, a noteworthy reduction in diameters occurred after a 6-day incubation period with NME extract at 250 $\mu\text{g}/\text{mL}$ ($p < 0.05$), 500 $\mu\text{g}/\text{mL}$ ($p < 0.001$), and 1000 $\mu\text{g}/\text{mL}$ ($p < 0.0001$), when compared to the solvent control (Figure 27B). This reduction corresponded to inhibitions of 9.26%, 21.75%, and 25.23%, respectively (Figure 27D). Importantly, the inhibitory effect remained consistent across all concentrations over the observed time frame, displaying a clear dose-response trend. These findings strongly indicate that NME exhibits toxicity towards *P. cinnamomi* at the tested concentrations. Photographic records consistently portray the mycelium of *P. cinnamomi* maintaining the same color and appearance as the solvent control across all concentrations. The clear dose-response pattern is evident, with the highest concentration resulting in the smallest oomycetal growth and the highest inhibition. This pronounced decrease in mycelium growth underscores the substantial inhibitory impact of the NME extract on *P. cinnamomi* mycelium growth (Figure 28F).

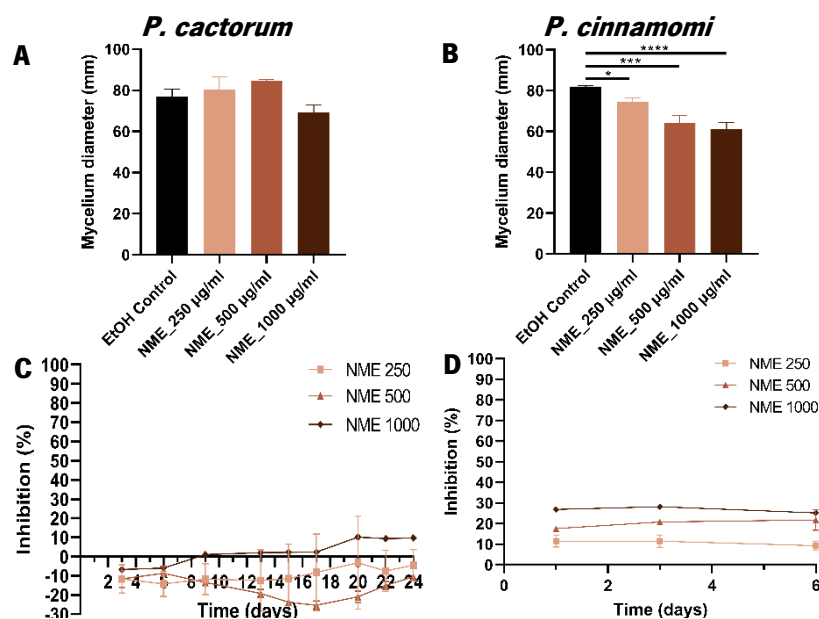


Figure 27 – Mycelium diameter (mm) and mycelium growth inhibition (%) of *Phytophthora cactorum* and *Phytophthora cinnamomi* when exposed to *Myristica fragrans* ethanolic extract (NME). The NME extract was incorporated into molten PDA medium at various concentrations (250, 500, or 1000 $\mu\text{g}/\text{mL}$), alongside control groups where 80% ethanol was adjusted in volume to match the highest concentration of the extract. A mycelium disc was positioned at the center of each plate and incubated in darkness at 25°C until the oomycetes extended to the edge of the Petri dish. The diameter graphs depict the mycelium diameter measured on the final day of the assay for each oomycete (**A and B**). Furthermore, graphs illustrating the growth inhibition during the assay period are provided (**C and D**) for the oomycetes *P. cactorum* (**A and C**) and *P. cinnamomi* (**B and D**). The data for diameter and mycelium growth inhibition represent the mean of three independent experiments \pm SD. One-way ANOVA was conducted, followed by the Dunnett test for multiple comparisons: $*0.01 < p \leq 0.05$, $**0.001 < p \leq 0.01$, $***0.0001 < p \leq 0.001$ and $****p \leq 0.0001$, with significance compared to the respective controls.

Based on these findings, the NME extract demonstrates significant antifungal activity and toxicity against all tested phytopathogenic fungi (*B. cinerea*, *C. acutatum*, *D. corticola* and *F. culmorum*) and only to one oomycete (*P. cinnamomi*). However, additional research is essential to comprehensively understand the observed phenomenon in relation to *P. cactorum*. Gupta et al. (2013) suggested that the antimicrobial activity of nutmeg might be attributed to its diverse array of active compounds. These compounds are believed to contribute to mechanisms such as radical scavenging, metal chelation, inhibition of lipid peroxidation, quenching of singlet oxygen and antioxidation. Nevertheless, further studies are needed to elucidate the precise MOA of these constituents and the extract due to limited existing information, but also to unveil this species-specific mechanism of resistance of *P. cactorum*. Additionally, Radwan *et al.* (2014) demonstrated the mycelial growth inhibition of *C. acutatum*, *C. fragariae* and *C. gloeosporioides* by methanolic nutmeg extract. However, the mechanisms underlying this inhibition were not explored. As such, more comprehensive investigations are warranted to identify the most active compounds within this extract, delineate their mechanisms of action and discern their specific targets. Furthermore, this study is particularly significant as the exploration of this plant bioactivities remains relatively limited compared to others. Despite this, it has exhibited promise over time and has been evaluated against fungi and oomycetes that are not typically associated with sensitivity to this plant species.

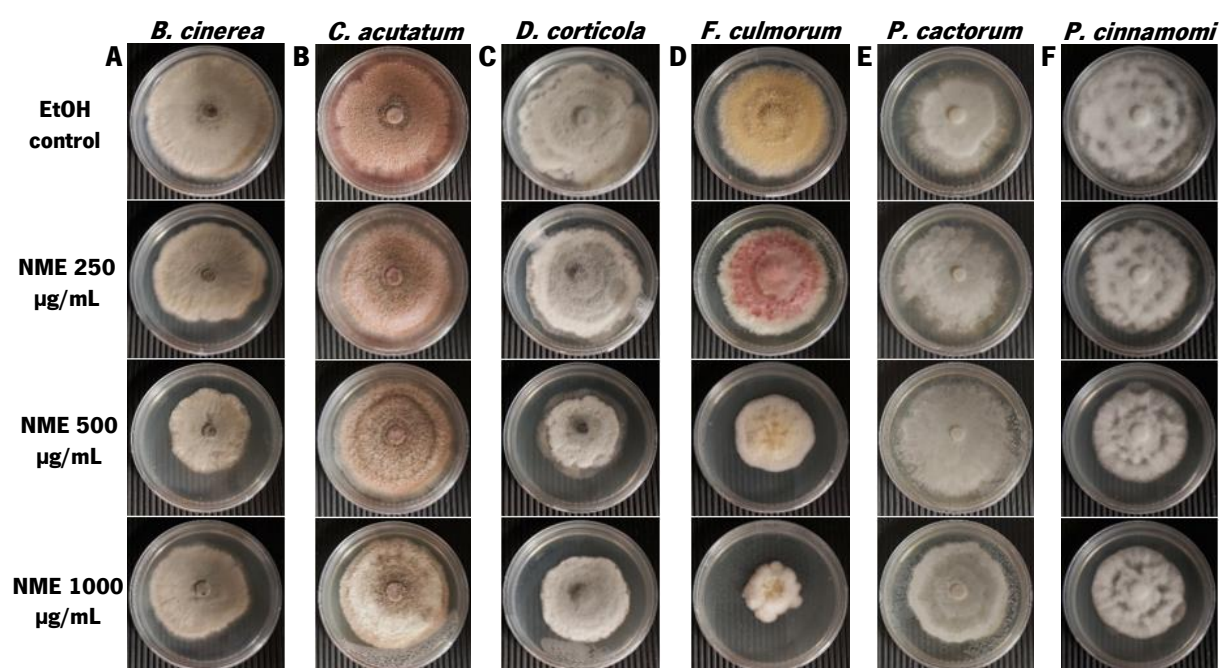


Figure 28 – Photographic record of filamentous fungus exposed to *Myristica fragrans* ethanolic extract (NME). *B. cinerea* (A), *C. acutatum* (B), *D. corticola* (C), *F. culmorum* (D), *P. cactorum* (E) and *P. cinnamomi* (F) were subjected to 250, 500, or 1000 µg/mL of NME extract and incubated in darkness at 25°C until the fungus extended to the edge of the Petri dish. The mycelium images represent three experiments and were taken on the final day of the assay for each fungus.

4.3. Possible mechanisms of action of CE and NME extracts

To comprehend the mechanisms underlying the CE and NME toxicity towards yeasts and filamentous fungi and oomycetes, we exposed two WT strains (BY4741 and W303-1A) as well as eight mutant strains derived from these WTs to varying concentrations of CE and NME. These selected mutants include strains associated with ergosterol biosynthesis (*erg6*, *erg2*, *erg3*, *erg5*, and *erg4* mutants), the cell wall integrity pathway (*bck1* and *mkk1/mkk2* mutants, as identified by Jin et al., 2015), and the apoptotic process (*yca1* mutant, as noted by Khan et al., 2005). It is worth mentioning that the mutant strains have a deletion of a single gene, except for the *mkk1/mkk2* mutant, which involves the deletion of both *MKK1* and *MKK2* genes. In these experiments, the strains were subjected to CE and NME concentrations of 250, 500 and 1000 µg/mL. These treatments provide an insight into the extract's impact on each mutant, indicating whether viability increased or decreased compared to the WT. The viability assessments for the mutants were conducted at various time points using viability assays, as detailed in section 3.3.1.

The biosynthesis of ergosterol is one of the most targeted processes by fungicides, as ergosterol is present in the fungal plasma membrane and plays vital roles in their normal functioning. Furthermore, this molecule is absent in other eukaryotic organisms, which provides an advantage in avoiding toxicity to non-target organisms. Some antifungals have the enzymes present in the final stages of ergosterol biosynthesis as the main targets (Jordá & Puig, 2020). In this pathway, zymosterol is converted to fecosterol through the enzyme sterol C-24 methyltransferase (Erg6), which results from the expression of the *ERG6* gene. Next, episterol is formed by the enzyme sterol C-8 isomerase (Erg2) encoded by the *ERG2* gene, and finally, this molecule is desaturated and reduced by the enzymes sterol C-5 desaturase (Erg3), sterol C-22 desaturase (Erg5), and sterol C-24 reductase (Erg4), which result from the expression of the *ERG3*, *ERG5* and *ERG4* genes, respectively, leading to the formation of ergosterol (Figure 10).

If the CE and NME extracts affect the ergosterol biosynthetic pathway, the sensitivity of *erg6*, *erg2*, *erg3*, *erg5*, and *erg4* mutants to these extracts may differ from that of the WT strain. Notably, the control of *erg6* mutant strain (no treatment) exhibited comparable viability to the control of the WT strain (Figure 22B). In the presence of the CE extract, its viability remained unaffected across all three concentrations (Figure 29A), showing no significant differences compared to the respective control at any of the time points. Furthermore, at the 120-min timepoint, the viability of the *erg6* mutant treatments was significantly higher than that of WT BY4741 treatments (the background strain), showing significant differences at all tested concentrations (see Annex 3). Conversely, exposure to the NME also had no

impact on the viability of the *erg6* mutant (Figure 29B), with no significant differences observed compared to the control at any of the time points. Similarly, at the 120-minute mark, the *erg6* mutant treatments exhibited significantly higher viability than WT BY4741 treatments (Figure 22D), showing significant differences at all tested concentrations (see Annex 3). Considering that Erg6 catalyzes the conversion of zymosterol into fecosterol, the absence or inactivity of Erg6 would result in the accumulation of zymosterol within the cells. According to Jordá & Puig (2020) and Munn *et al.* (1999), this accumulation can trigger the build-up of other sterols due to the catalytic activity of the Erg2, Erg3, and Erg5 enzymes on zymosterol. One example is cholesta-5,7,24-trienol, which, like zymosterol, is found in high percentages within cells. Consequently, if the *erg6* mutant is unaffected in comparison to WT, it implies that both extracts require functional Erg6 enzyme activity to exert their antifungal effects. This suggests that some components of these extracts do not bind to zymosterol, thus lacking antifungal activity against it. Consequently, it can be concluded that fecosterol or other metabolic intermediates up to ergosterol or even Erg6 enzyme likely represents one of the primary targets for these extracts, inhibiting ergosterol synthesis and, consequently, impairing the formation of ergosterol, which impacts the fungal cell's plasma membrane.

The control of mutant strain *erg2* (no treatment) displayed viability similar to the control of the WT strain (Figure 22B and 29C). In the presence of the CE extract, viability was less affected across all three concentrations (Figure 29C) compared to the WT strain (Figure 22B), showing significant differences relatively to the control at 30, 60, 90 and 120 minutes ($p < 0.01$, $p < 0.001$ and $p < 0.0001$), indicating a clear dose-response effect. Furthermore, at 120 minutes, the viability of the *erg2* mutant treatments compared to that of the treatments of the WT BY4741 (the background strain) was significantly higher at all concentrations (see Annex 3). Conversely, when exposed to the NME extract, the *erg2* mutant's viability was also less affected, particularly at the 250 $\mu\text{g}/\text{mL}$ (Figure 29D) compared to the WT strain (Figure 22D). The 500 and 1000 $\mu\text{g}/\text{mL}$ of NME extract displayed a similar behavior to WT. However, significant differences compared to the control were observed at all tested time points ($p < 0.01$, $p < 0.001$ and $p < 0.0001$), indicating a dose-response effect. Moreover, at 120 minutes, differences in viability were observed between the *erg2* mutant treatments and the WT BY4741 treatments, but these differences were only significant at 250 $\mu\text{g}/\text{mL}$ (see Annex 3). Given that Erg2 converts fecosterol into episterol, the absence or inactivity of Erg2 would result in the accumulation of fecosterol within the cells. Considering this, if the mutant is less affected compared to WT, it suggests that both extracts require functional Erg2 enzyme activity, especially the CE extract, to exert their antifungal effects. This implies that the fecosterol must be a partial target of the extracts, with the possibility of having other targets, consequently, displaying

reduced antifungal activity compared to the WT strain, as evident in the results. So, it is possible that some components of these extracts also bind to episterol or other metabolic intermediates up to ergosterol or even to the Erg2 enzyme. Therefore, it can be concluded that these extracts impact ergosterol synthesis and, consequently, the fungal cell's plasma membrane.

The control of *erg3* mutant strain (no treatment) exhibited viability similar to the control of the WT strain (Figure 22B and 29E). In the presence of the CE extract, viability was significantly more affected at all concentrations (Figure 29E) compared to the WT strain (Figure 22B), showing significant differences from the control at 30, 60, 90 and 120 minutes ($p < 0.0001$). However, the dose-response effect was not very clear. Moreover, at 120 minutes, the viability of the *erg3* mutant compared to that of the WT BY4741 treatments (the background strain) was lower at all concentrations, but it only showed a significant difference at 250 $\mu\text{g}/\text{mL}$ (see Annex 3). Conversely, when exposed to the NME extract, the *erg3* mutant's viability was also significantly more affected at all concentrations (Figure 29F), compared to the WT strain (Figure 22D), displaying significant differences compared to the control at all time points ($p < 0.0001$). However, there appeared to be no clear dose-response effect. Furthermore, at 120 minutes, the viability of the *erg3* mutant treatments was lower in comparison to that of the WT BY4741 treatments. However, no significant differences were observed at any of the tested concentrations (see Annex 3). Given that Erg3 desaturates episterol into ergosta-5,7,24(28)-trienol, the absence of Erg3 results in the accumulation of episterol within the cells. Considering this, if the mutant is more affected than the WT, it indicates that both extracts do not require the presence of the Erg3 enzyme to exert their antifungal activity; in fact, they exhibit even stronger activity. This suggests that some components of these extracts have a higher affinity for episterol, interacting with it and demonstrating increased toxicity to the cell. Furthermore, it can be inferred that the extract does not bind to ergosta-5,7,24(28)-trienol, indicating that its toxicity is independent of the presence of this sterol. Consequently, it can be concluded that these extracts do not rely on the Erg3 enzyme for their antifungal activity, suggesting that this enzyme is possibly not among the targets of these extracts. Additionally, in the case of the CE extract at 250 $\mu\text{g}/\text{mL}$, the *erg3* mutant exhibits increased sensitivity to the extract compared to WT BY4741. Therefore, further investigation is needed to elucidate the underlying mechanisms.

The control of *erg5* mutant strain (no treatment) displayed viability similar to the control of the WT strain (Figure 22B and 29G). In the presence of the CE extract, viability was less affected at 250 and 500 $\mu\text{g}/\text{mL}$ (Figure 29G) compared to the WT strain (Figure 22B), showing significant differences from the control at 30, 60, 90 and 120 minutes ($p < 0.01$, $p < 0.001$, and $p < 0.0001$), with a clear dose-

response effect. Furthermore, at 120 minutes, the viability of the *erg5* mutant treatments was similar to that of the WT BY4741 treatments (the background strain) at 500 and 1000 µg/mL, with significance observed only at the 250 µg/mL (see Annex 3). Conversely, when exposed to the NME extract, the viability of the *erg5* mutant was similar to that of the WT at 250 µg/mL and was more affected at 500 and 1000 µg/mL (Figure 29H) compared to the WT strain (Figure 22D), and showing significant differences from the control at all tested time points ($p < 0.0001$), with an unclear dose-response effect. Furthermore, at 120 minutes, the viability of the *erg5* mutant treatments was relatively similar to that of the WT BY4741 treatments at all concentrations tested, with no significant differences observed compared to WT (see Annex 3). Given that Erg5 desaturates ergosta-5,7,24(28)-trienol into ergosta-5,7-22-24(28)-trienol, the absence of Erg5 leads to an accumulation of this molecule within the cells. Regarding the CE extract, if this mutant is less affected compared to WT, it implies that this extract requires the Erg5 enzyme to be functional for its antifungal activity. This suggests that some components of this extract may have a high affinity for ergosta-5,7-22-24(28)-trienol or for other metabolic intermediates or even for the Erg5 enzyme, failing to bind to it and thus demonstrating reduced antifungal activity. In the case of the NME extract, the viability of this mutant was not significantly affected compared to WT, indicating that this extract does not necessitate the presence of the Erg5 enzyme to exert its antifungal activity. This suggests that this extract may bind to metabolic intermediates prior to the reaction catalyzed by the Erg5 enzyme, which is in accordance with the previous results. Consequently, it can be concluded that the CE extract relies on the Erg5 enzyme for enhanced antifungal activity, while the NME extract does not require this enzyme to affect ergosterol synthesis and, consequently, the fungal plasma membrane.

The control of *erg4* mutant strain (no treatment) exhibited viability similar to the control of the WT strain (Figure 22B and 29I). In the presence of the CE extract, viability was less affected at all three concentrations (Figure 29I) compared to the WT strain (Figure 22B), showing significant differences from the control at 30, 60, 90 and 120 minutes ($p < 0.05$, $p < 0.01$, $p < 0.001$ and $p < 0.0001$), with a very clear dose-response effect. Moreover, at 120 minutes, the viability of the *erg4* mutant compared to that of WT BY4741 (the background strain) was higher at all concentrations, with significant differences observed at 250 and 500 µg/mL (see Annex 3). Conversely, when exposed to the NME extract, the *erg4* mutant's viability was also less affected, especially at 250 and 500 µg/mL (Figure 29J), while the 1000 µg/mL concentration exhibited behavior similar to WT (Figure 22D). Nevertheless, significant differences compared to the control were noted at all tested time points ($p < 0.01$, $p < 0.001$ and $p < 0.0001$), and a clear dose-response effect was evident. Furthermore, at 120 minutes, the viability of the *erg4* mutant compared to that of WT BY4741 was higher and exhibited significant differences at all concentrations

tested (see Annex 3). Considering that Erg4 reduces ergosta-5,7-22-24(28)-trienol into ergosterol, the absence or inactivity of Erg4 leads to an accumulation of ergosta-5,7-22-24(28)-trienol within the cells, preventing ergosterol formation. In this context, if the mutant is less affected compared to the WT, it indicates that both extracts require functional Erg4 enzyme activity for their antifungal activity. This suggests that some components of these extracts may have a high affinity for ergosterol or for the Erg4 enzyme, failing to bind to it and thus demonstrating weaker antifungal activity. This also indicates that the extracts bind to prior metabolic intermediates, as demonstrated by the previous results. Therefore, it can be concluded that these extracts depend on the presence of active Erg4 enzyme to exert their activity, affecting ergosterol synthesis, and consequently, the fungal cell's plasma membrane. Also, according to all tested *erg* mutants, it can be inferred that the fecosterol and episterol probably are the major targets of these extracts.

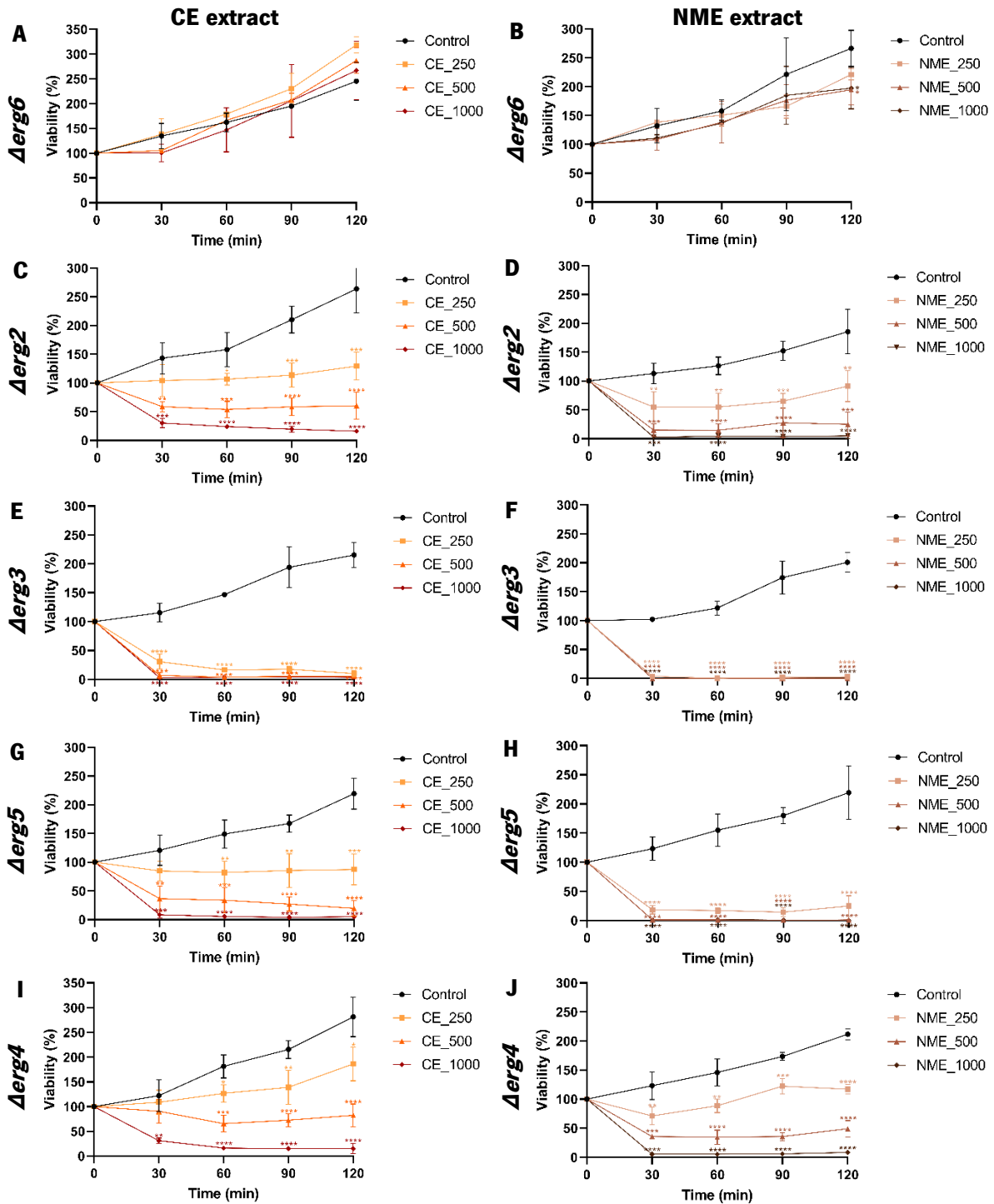


Figure 29 – Mutant strains *erg6*, *erg2*, *erg5*, and *erg4*, exhibited higher resistance, while *erg3* mutant strain displayed higher sensitivity to ethanolic extracts of *Curcuma longa* (CE) and *Myristica fragrans* (NME) compared to their respective wild-type (WT) strains. *Saccharomyces cerevisiae* cells were cultured in YPD at 30 °C and 200 rpm until reaching an OD₆₀₀ within the range of 0.4-0.6 and treatments were applied: CE (A, C, E, G, and I) or NME (B, D, F, H, and J) to mutants *erg6* (A and B), *erg2* (C and D), *erg3* (E and F), *erg5* (G and H), and *erg4* (I and J) mutant strains. The treatments consisted of 2% v/v solvent extract (80% ethanol; control) or CE or NME extracts at concentrations of 250, 500 and 1000 µg/mL. Aliquots were harvested along time, serially diluted up to a factor of 10⁻⁴ and 40 µL drops were plated and incubated for 48 hours at 30 °C. Cell viability percentages were calculated by dividing the average CFUs by the average at 0 minutes. Data are presented as the mean of three independent experiments ± standard deviation (SD). One-way ANOVA was conducted, followed by the Dunnett test for multiple comparisons: *0.01 < p ≤ 0.05, **0.001 < p ≤ 0.01, ***0.0001 < p ≤ 0.001 and ****p ≤ 0.0001, with significance compared to the respective controls.

Maintaining the integrity of the cell wall (CWI) is crucial for the proper functioning of cells. Destabilization of the cell wall can lead to reduced cell viability, often through mechanisms such as cell lysis. In the case of *S. cerevisiae*, the regulation of cell wall integrity is associated with the mitogen-activated protein kinase (MAPK) cascade. This cascade includes key proteins, such as Bck1 (MAPKKK), encoded by the *BCK1* gene, Mkk1 and Mkk2 (MAPKK), encoded by the *MKK1* and *MKK2* genes, and Slit2/Mpk1, which collectively play a pivotal role in strengthening the cell wall and facilitating its repair following stress conditions (Gustin et al., 1998; Levin, 2005; Rispaill et al., 2009). Deletion of a single gene within this MAP kinase cascade in *S. cerevisiae* can result in cell autolysis, heightened sensitivity to mating pheromones and increased vulnerability to agents affecting the cell wall (Levin, 2005). In pathogenic fungi that affect humans and plants, these three MAP kinases are indispensable for maintaining cell wall integrity and also play crucial roles in conidiation and pathogenicity (Chen et al., 2014). Additionally, cell wall integrity is monitored by cell surface sensors such as Wsc1, Wsc2, Wsc3, Mid2 and Mtl1. In *S. cerevisiae*, when confronted with cell wall stress, Wsc1 activates the small G protein Rho1 through Rom2, acting as a guanosine nucleotide exchange factor. Rho1, in turn, triggers the activation of Pkc1, a protein kinase C, which further phosphorylates the downstream kinase of the conserved MAPK cascade – Bck1. Bck1 then transmits the signal to the redundant pair of MAP kinase kinases – Mkk1 and Mkk2. Finally, the MAPK Slit2/Mpk1 is phosphorylated and activated. Slit2/Mpk1 subsequently phosphorylates the transcription factor Rlm1 and the SBF complex to regulate gene expression of genes involved in cell wall remodelling (see Figure 30) (Jendretzki et al., 2011; Levin, 2005, 2011; Sanz et al., 2012, 2016).

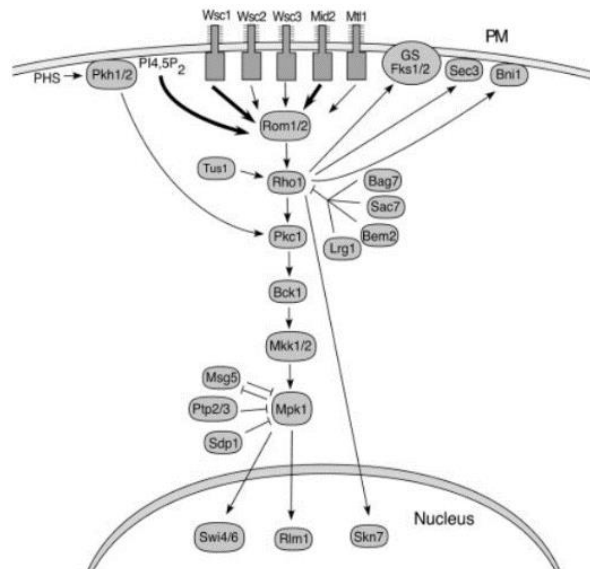


Figura 30 – CWI signaling pathway. The CWI signaling pathway is initiated at the plasma membrane (PM) through cell surface sensors, namely Wsc1, Wsc2, Wsc3, Mid2 and Mtl1. Along with PI4,5P₂, which recruits the Rom1/2 to the plasma membrane, these sensors stimulate nucleotide exchange on Rho1, which in turn, activates five different effectors, including the Pkc1 MAP kinase cascade, β1,3-glucan synthase (GS), the Bni1 formin protein, the exocyst component Sec3 and the Skn7 transcription factor. Additional regulatory inputs come from the Tus1 GEF, inhibitory Rho1 GAPs and the Pkh1/2 protein kinases, which are activated by phytosphingosine (PHS). The MAP kinase cascade consists of Bck1, Mkk1/2 and Mpk1 and is activated by Pkc1. Multiple MAP kinase phosphatases play a role in downregulating Mpk1. Lastly, two transcription factors, Rlm1 and the SBF complex (Swi4/Swi6), are targets of the MAP kinase. Adapted from Levin et al. (2005).

To investigate whether the CE and NME target cell wall or the ability to repair cell wall damage, we opted to employ the *bck1* mutant and the *mkk1/mkk2* mutant strains, which are highly sensitive strains to cell wall stress. If these extracts indeed target cell wall integrity, the *bck1* and *mkk1/mkk2* mutants would be expected to exhibit higher sensitivity to CE and NME compared to the WT strain. The control of *bck1* mutant strain (no treatment) demonstrated growth similar to that of the control of the WT strain (Figure 22B and 31A). However, when exposed to the CE extract, viability was less affected at all three concentrations (Figure 31A) compared to the WT strain (Figure 22B), displaying significant differences compared to the control at 30, 60, 90 and 120 minutes ($p < 0.01$, $p < 0.001$ and $p < 0.0001$), with a clear dose-response effect. Furthermore, at 120 minutes, the viability of the *bck1* mutant treatments compared to WT BY4741 treatments (the background strain) was higher at all concentrations, with significant differences observed only at 250 and 1000 $\mu\text{g}/\text{mL}$ (see Annex 3). Conversely, when the *bck1* mutant was exposed to the NME extract, its viability was also less affected, especially at the 250 $\mu\text{g}/\text{mL}$ (Figure 31B), compared to the WT strain (Figure 22D). However, significant differences from the control were noted at all tested time points ($p < 0.05$ and $p < 0.01$), with a clear dose-response effect. Furthermore, at 120 minutes, the viability of the *bck1* mutant treatments compared to WT BY4741 treatments was statistically similar at all tested concentrations (see Annex 3). These results suggest that

the CE extract may operate through a mechanism associated with the Bck1 protein, indicating a dependency on this functional protein for enhanced antifungal activity. It has been demonstrated that the overactivation of the cell wall integrity pathway is lethal to yeast cells. Specifically, the accumulation of the lipid membrane derivative phosphatidylinositol 3-phosphate has been shown to trigger this lethal overactivation of this signaling pathway (Parrish et al., 2005). The results with CE and the *bck1* mutant are consistent with this observation because the extract exhibits reduced activity when the pathway is inactive. Furthermore, it appears unlikely that the cell wall is the target of the extract since, in that case, the mutant would be more sensitive than the WT. Conversely, for the NME extract, there were no significant differences between the WT strain and the mutant strain, suggesting that the Bck1 protein is not required to be active or functional for the extract's antifungal activity, indicating that this is not one of its MOA.

To confirm results with the *bck1* mutant strain we employed the *mkk1/mkk2* double mutant strain also affected in the cell wall integrity signaling pathway. The control of *mkk1/mkk2* mutant strain exhibited growth similar to the control of the WT strain (Figure 22B and 31C). However, in the presence of the CE extract, viability was less affected at all three concentrations (Figure 31C), compared to the WT strain (Figure 22B), showing significant differences compared to the control at 30, 60, 90 and 120 min ($p < 0.01$, $p < 0.001$ and $p < 0.0001$), with a clear dose-response effect. Moreover, at 120 min, the viability of the *mkk1/mkk2* mutant treatments compared to WT BY4741 treatments (the background strain) was higher at all concentrations, with significant differences observed across all tested concentrations (see Annex 3). Conversely, when the *mkk1/mkk2* mutant was exposed to the NME extract, its viability was also less affected (Figure 31D), compared to the WT strain (Figure 22D). However, significant differences from the control were only noted at 500 and 1000 $\mu\text{g}/\text{mL}$ at 60, 90 and 120 minutes ($p < 0.05$ and $p < 0.01$), displaying a dose-response effect. Furthermore, at 120 minutes, the viability of the *mkk1/mkk2* mutant treatments compared to that of WT BY4741 treatments showed no significant differences at any of the tested concentrations (see Annex 3). These findings suggest that the CE extract indeed targets cell wall integrity, necessitating the presence of functional Mkk1/Mkk2 protein, thus corroborating the results obtained with the *bck1* mutant. Furthermore, the hypothesis that this extract may be correlated with the overactivation of the cell wall integrity pathway is supported by this mutant and aligns with the results obtained with the *bck1* mutant. Concerning the NME extract, although visually the viability of the mutants was less affected compared to that of the WT BY4741, statistically there were no significant differences. So, the results indicate that this extract likely does not rely on cell wall integrity as its primary mechanism of action. Both the *bck1* and *mkk1/mkk2* mutants' treatments

exhibited no significant differences in viability compared to WT BY4741 treatments. Nonetheless, further studies should be conducted to confirm that this extract does not require functional Bck1 and Mkk1/Mkk2 proteins to exhibit antifungal activity.

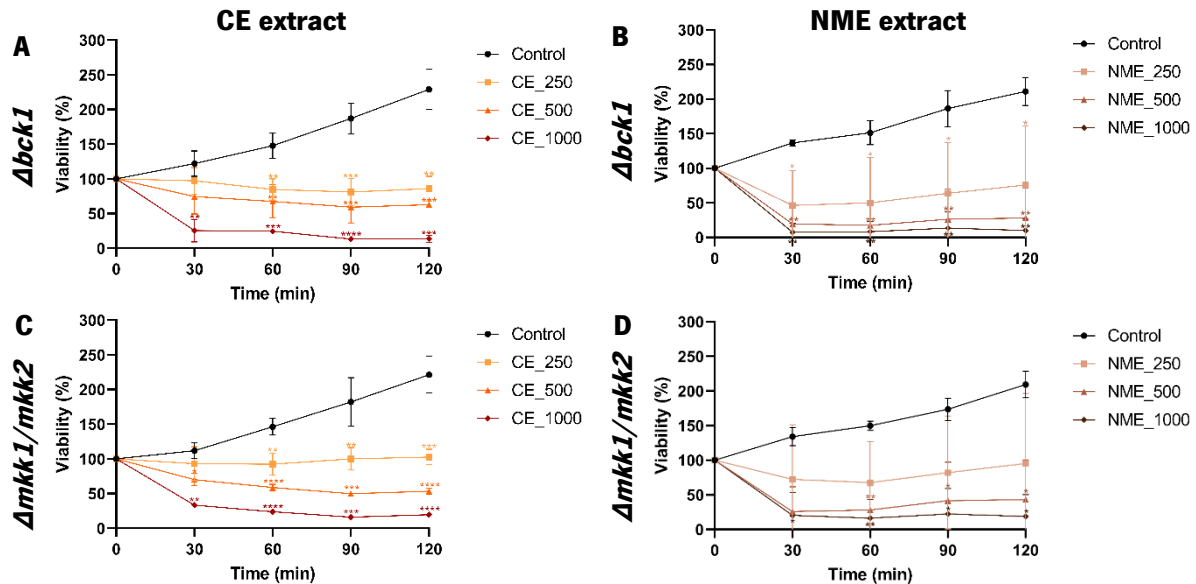


Figure 31 – Mutant strains *bck1*, and *mkk1/mkk2*, exhibited higher resistance to ethanolic extracts of *Curcuma longa* (CE) and *Myristica fragrans* (NME) compared to their respective wild-type (WT) strains. *Saccharomyces cerevisiae* cells were cultured in YPD at 30 °C and 200 rpm until reaching an OD₆₀₀ within the range of 0.4-0.6 and treatments were applied: CE (A and C) or NME (B and D) to mutants *bck1* (A and B) and *mkk1/mkk2* (C and D). The treatments consisted of 2% v/v solvent extract (80% ethanol; control), or CE or NME extracts at concentrations of 250, 500 or 1000 μg/mL. Aliquots were harvested along time, serially diluted up to a factor of 10⁴ and 40 μL drops were plated and incubated for 48 hours at 30 °C. Cell viability percentages were calculated by dividing the average CFUs by the average at 0 minutes. Data are presented as the mean of three independent experiments ± standard deviation (SD). One-way ANOVA was conducted, followed by the Dunnett test for multiple comparisons: *0.01 < p ≤ 0.05, **0.001 < p ≤ 0.01, ***0.0001 < p ≤ 0.001 and ****p ≤ 0.0001, with significance compared to the respective controls.

Programmed cell death (PCD) in *S. cerevisiae* is triggered in response to specific stress conditions, such as oxidative stress, nutrient stress, or DNA stress. This process is mediated by the Yca1 protein, which is encoded by the *YCA1* gene (Guaragnella et al., 2006). Notably, Yca1, a metacaspase, shares similarities with caspases and plays a multifaceted role in the cell. Beyond its involvement in PCD, it also contributes to cell viability and the maintenance of proteostasis (Lee et al., 2010). Moreover, Yca1 has been implicated in limiting protein aggregation in daughter cells during yeast aging studies (Hill et al., 2014). As a member of the cysteine-dependent aspartic protease family, its absence leads to increased retention of aggregated material within the insoluble proteome (Shrestha et al., 2019). Therefore, if the CE and NME extracts induce apoptosis in yeast cells, the *yca1* mutant is expected to exhibit higher resistance to the action of the extracts than the WT strain. This is because the absence of the Yca1 protein disrupts the normal progression of PCD.

In the case of the CE extract, the control of *yca1* mutant strain exhibited growth similar to that of the control of the WT strain (Figure 32A and C). However, in the presence of the CE extract, viability was more affected at 500 and 1000 $\mu\text{g}/\text{mL}$, whereas at 250 $\mu\text{g}/\text{mL}$ the viability was relatively similar to that of the WT (Figure 32A and C). Significant differences from the control were observed at 30, 60, 90 and 120 minutes ($p < 0.01$, $p < 0.001$ and $p < 0.0001$), indicating a dose-response effect. At 120 minutes, the viability of the *yca1* mutant treatments compared to WT W303-1A treatments (the parental strain) was lower at all concentrations, with significant differences observed across all concentrations (see Annex 3). Conversely, when the mutant was exposed to the NME extract, its viability was also more affected at all concentrations compared to the WT strain (Figure 32B and D). Significant differences from the control were observed at all time points ($p < 0.0001$), with an unclear dose-response effect. Furthermore, at 120 minutes, the viability of the *yca1* mutant treatments compared to WT W303-1A treatments was lower at all concentrations, with significant differences noted at all tested concentrations (see Annex 3). In the case of the CE extract, these results suggest that the extract does not require the presence of the functional Yca1 protein. However, in its absence, the extract exerts more toxicity upon the cells. Furthermore, it appears that this extract does not induce PCD since the extract continues to affect viability in the absence of the Yca1 metacaspase. In the case of the NME extract, the WT W303-1A strain is less affected by the extract compared to the WT BY4741 (Figure 22D). Since there are no significant differences within the treatments and the control, it can be said that the WT W303-1A strain is unaffected by this extract. However, when the *YCA1* gene was removed, the extract began to affect cell viability. Therefore, these results need further investigation to unveil the underlying mechanisms at play. While these results are intriguing, we cannot definitively rule out the possibility that the CE and NME extracts induce PCD. PCD can be triggered by various factors, including the generation of reactive oxygen species, mitochondrial fragmentation and dissipation of mitochondrial membrane potential (Fannjiang et al., 2004; Madeo et al., 1999). Additionally, beyond *YCA1* gene, several other genes are involved in intrinsic pathways, such as *AIF1*, *BIR1*, *BXI1* and *NMA111* (Cebulski et al., 2011; Fahrenkrog et al., 2004; Madeo et al., 2002; Walter et al., 2006; Wissing et al., 2004). Therefore, these extracts can cause some of these distinct phenotypical markers or require pre-apoptotic genes, like the *AIF1*, but not the metacaspase Yca1, as shown by Chin *et al.* (2014) with the caspofungin fungicide.

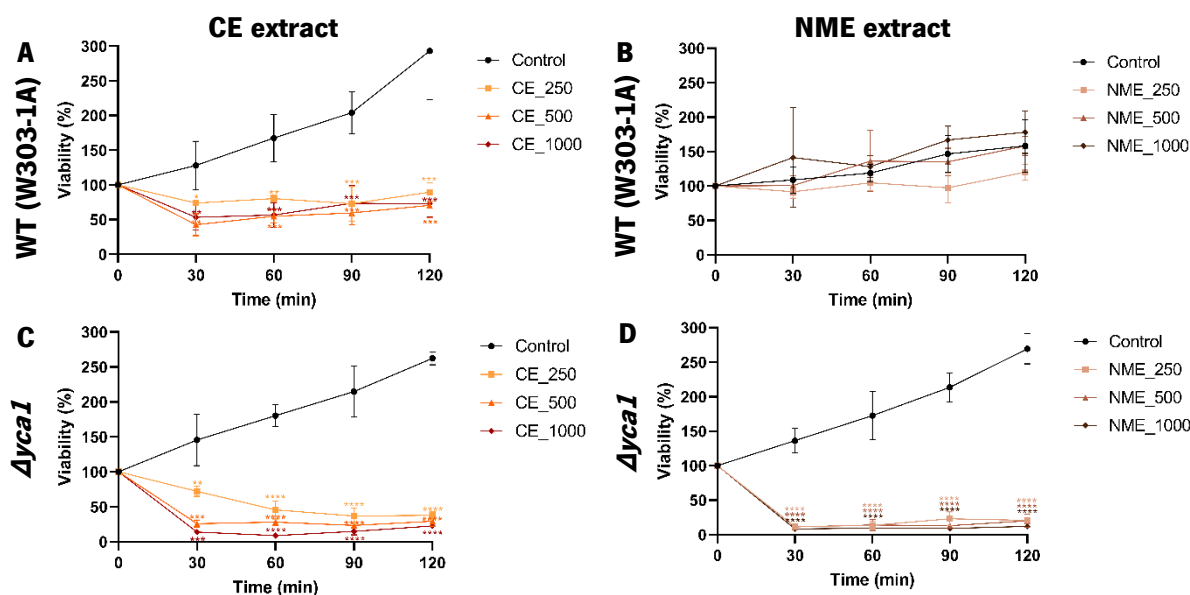


Figure 32 – Mutant strain *yca1* displayed higher sensitivity to ethanolic extracts of *Curcuma longa* (CE) and *Myristica fragrans* (NME) compared to its respective wild-type (WT) strain. *Saccharomyces cerevisiae* cells were cultured in YPD at 30 °C and 200 rpm until reaching an OD₆₀₀ within the range of 0.4-0.6 and treatments were applied: CE (A and C) or NME (B and D) to WT W303-1A (A and B), and mutant *yca1* (C and D). The treatments consisted of 2% v/v solvent extract (80% ethanol; control), or CE or NME extracts at concentrations of 250, 500 or 1000 µg/mL. Aliquots were harvested along time, serially diluted up to a factor of 10⁺ and 40 µL drops were plated and incubated for 48 hours at 30 °C. Cell viability percentages were calculated by dividing the average CFUs by the average at 0 minutes. Data are presented as the mean of three independent experiments ± standard deviation (SD). One-way ANOVA was conducted, followed by the Dunnett test for multiple comparisons: *0.01 < p ≤ 0.05, **0.001 < p ≤ 0.01, ***0.0001 < p ≤ 0.001 and ****p ≤ 0.0001, with significance compared to the respective controls.

4.4. Assessment of viability with propidium iodide by fluorescence microscopy

To assess the viability of plasma membranes when exposed to CE and NME extracts and to discern whether loss of viability (cell death) was due to cellular necrosis or apoptosis, we employed the fluorescent agent propidium iodide (PI). Propidium iodide binds to DNA molecules and can only cross plasma membranes when there is a loss of membrane integrity, so, in the absence of membrane damage there is no incorporation of PI and therefore it serves as an effective indicator of cell viability. Through fluorescence microscopy, we could observe the red fluorescence emitted by PI and determine whether the cells are viable or not. For these experiments, cells from the WT BY4741 strain were subjected to three different conditions: a portion of the cells was exposed to high temperatures (90-100 °C, 10 minutes) to induce cell death, serving as a test for the effectiveness of PI (positive control); another portion of cells was exposed only to the extract solvent (80% EtOH) as a negative control; and the remaining cells were exposed to CE or NME extracts at 500 µg/mL. This concentration was chosen because it resulted in a viability percentage of approximately 20% for the CE extract and 5% for the NME extract. This allowed us to measure viability values both above and below these thresholds. Cell viability was assessed at two

time points: at 0 minutes for the controls and at 120 min for the treatment groups, as described in Section 3.5. The cells in the negative control were the same cells subsequently exposed to the extract. This is why the control was observed only at time 0 and the extract-exposed cells only at time 120. This was also to ensure the viability of cells exposed to the extract upon its addition. Also, a control without solvent was not performed since it was previously demonstrated that the solvent had no impact on cell viability after 120 min (see Annex 1).

If the CE and NME induce cell necrosis, the percentage of marked cells should closely match the percentage of non-viable cells in the viability tests assessed by CFU. However, if they trigger PCD, the percentage of marked cells may be lower than the non-viable cells in the viability tests. When cells were exposed to high temperatures, the results were as expected: all cells observed in the bright field (BF) exhibited PI marking, which means that the integrity of the cell membrane was compromised and cell death occurred (Figure 31A). On the other hand, when cells were exposed to the solvent used in the extracts (80% EtOH, solvent control), none of the visualized cells in the BF displayed fluorescence (Figure 31B). This suggests that the solvent itself is not toxic to the cells and does not affect cell membrane integrity. When the cells were exposed to the extracts, in the case of the CE extract, approximately 70% of the cells observed in the BF were marked with PI (Figure 31C and 31E), i.e. 70% of the cells had their membrane affected and 30% of the cells remained with their membrane intact. The viability tests showed a value of approximately 20% of viable cells, meaning that 80% were dead cells. As the majority of the cells are marked with PI, indicating an affected plasmatic membrane, it suggests that the extract is causing necrosis. The 10% reduction in the number of affected cells in this assay may imply that these cells are dead while retaining an intact membrane, as PI does not mark apoptotic cells with intact membranes. However, the continued loss of viability in the presence of the CE extract by the *yca1* mutant suggests that it is not PCD. This conclusion aligns with the results obtained with the *yca1* mutant, although further studies are needed to determine whether or not this extract is indeed correlated with PCD. For the NME extract, roughly 93% of the cells observed in the BF were marked with PI (Figure 31D and 31F), i.e. 93% of the cells had their membrane affected and 7% of the cells remained with their membrane intact. Furthermore, the viability tests showed a value of approximately 5% of viable cells, meaning that 95% were dead cells. Since the values with the PI are very close to those obtained in the viability tests, these results suggest that the NME extract causes cell necrosis in yeast cells rather than PCD. However, this conclusion does not explain the increased sensitivity of the *yca1* mutant to the extract compared to the WT strain, but at the same time shows that probably it does not directly affect the Yca1 metacaspase,

but possibly another pathway related to cell necrosis. Therefore, additional research is required to confirm and understand the mechanism of cell death induced by this extract.

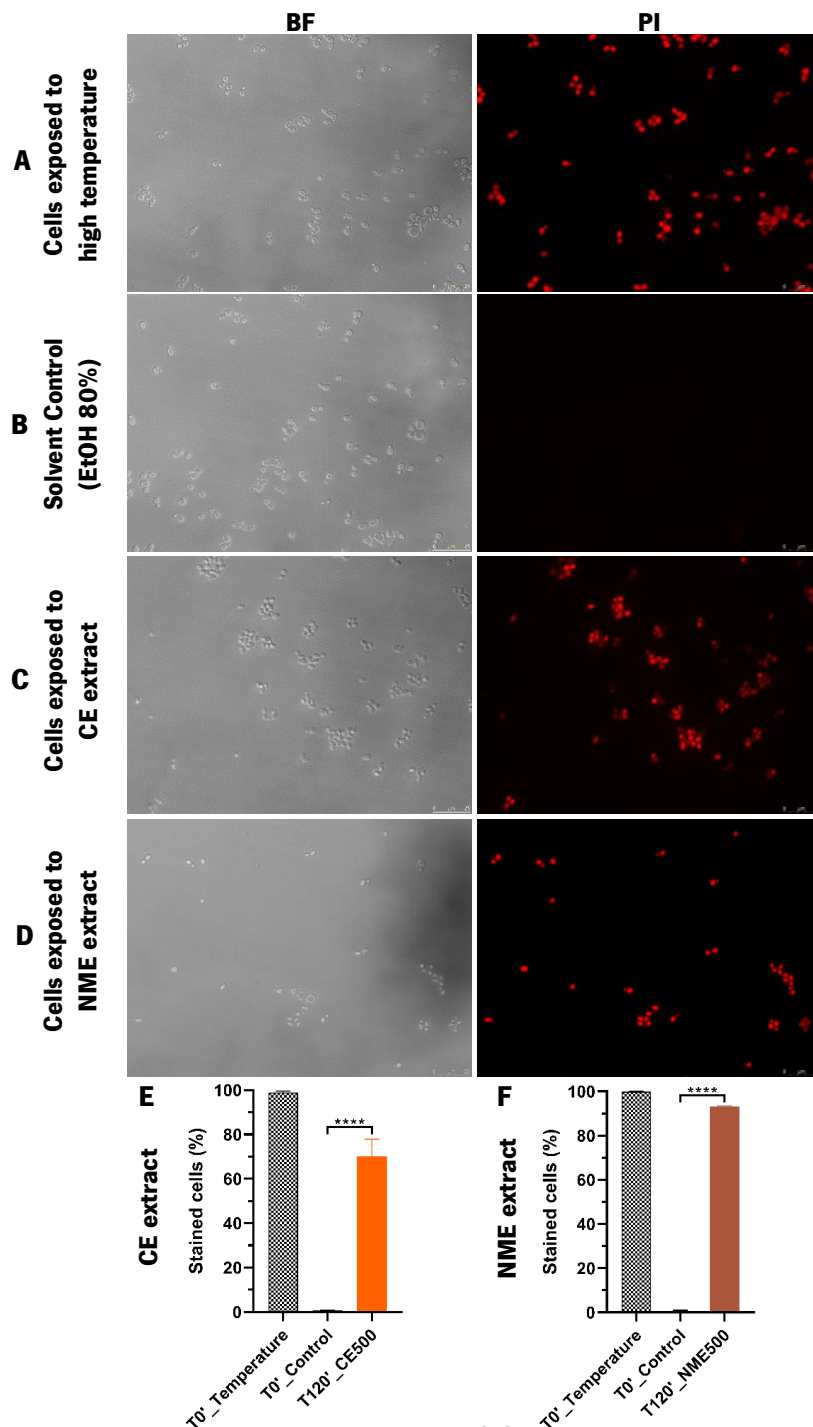


Figure 33 – Plasma membrane integrity and viability of *Saccharomyces cerevisiae* cells exposed to *Curcuma longa* extract (CE) and *Myristica fragrans* extract (NME). *Saccharomyces cerevisiae* cells were cultured in YPD at 30 °C and 200 rpm until reaching an OD₆₀₀ within 0.6-0.8 and treatments were applied: CE (**C and E**) or NME (**D and F**) to BY4741. The treatments consisted of exposure to high temperatures (**A**) or 1.6% v/v ethanol (control) (**B**), or CE or NME extracts at concentrations of 500 µg/mL (**C-F**). An aliquot was collected and centrifuged. Then, the cells were resuspended in 1x PBS and the PI was added. After incubation, the cells were observed under a fluorescence microscope in the bright field (BF) and in PI filters (**A-D**). Cell viability percentages were calculated by dividing the average of stained cells by the total cells at 0 and 120 minutes. Data are presented as the mean of three independent experiments ± standard error of the mean (SEM). One-way ANOVA was conducted, followed by the Dunnett test for multiple comparisons: **** $p \leq 0.0001$, with significance compared to the control at time 0. The cell images are representative of three independent experiments.

4.5. Susceptibility of lettuce seed germination and early growth of lettuce seedlings to the extracts CE and NME

Phytotoxicity tests were conducted using lettuce seeds to assess the potential toxicity of CE and NME extracts in rapid tests of germination and early growth of plantlets *in vitro*. Lettuce seeds were chosen for these tests due to their susceptibility to toxic compounds, making them reliable indicators of toxicity, and for being one of the species recommended by OCDE guidelines (OECD, 2006) more generally used for this type of bioassays by the scientific community. In each Petri dish, 20 seeds were placed under five different conditions: a solvent control (37.50 μL of 80% EtOH, the same volume of the highest extract concentration, resulting in a final concentration of 0.2%), two concentrations of CE extract (250 and 500 $\mu\text{g}/\text{mL}$) and two concentrations of NME extract (250 and 500 $\mu\text{g}/\text{mL}$), where the volumes of extract added were 18.75 μL and 37.50 μL for the 250 and 500 $\mu\text{g}/\text{mL}$ concentrations, respectively. The trial concluded with a photographic record and a comprehensive analysis that included evaluating the percentage of germination, measurement of root length, percentage of seedlings with cotyledons fully expanded, percentage of visible shoot apices ($> 1 \text{ mm}$) and number of leaves of the seedlings, as detailed in Section 3.6.

The germination percentage of lettuce seeds exposed to 250 and 500 $\mu\text{g}/\text{mL}$ concentrations of both CE and NME extracts showed no significant differences compared to the solvent control, indicating that the germination was not affected by the extract (Figure 32A and 32F). However, when evaluating root length after 7 days, we observed significantly higher growth with the 250 and 500 $\mu\text{g}/\text{mL}$ CE extract and with 250 $\mu\text{g}/\text{mL}$ NME extract compared to the control ($p < 0.0001$, $p < 0.01$ and $p < 0.01$, respectively) (Figure 32B). Probably, a higher dispersion of values at 500 $\mu\text{g}/\text{mL}$ NME extract could have masked an eventual effect and no significant differences when compared to the control. Apparently, this result suggests that the extracts at these concentrations promote root growth. However, the wider dispersion of root lengths observed with the extracts in comparison to the control (Figure 32B) seem to suggest that an impact in the germination rate, and therefore on the rate of early plant development, may occur, rendering the analysis less robust. The percentage of seedlings with expanded cotyledons showed no significant differences compared to the control, indicating that the extracts did not impact significantly the normal early enlargement of this embryonic organ (Figure 32C). However, a trend of reduced expanded cotyledons was observed in the NME extract, particularly at 500 $\mu\text{g}/\text{mL}$ (Figure 32F). The presence of shoot apex was also assessed, revealing no significant differences in any concentration of CE extract or 250 $\mu\text{g}/\text{mL}$ NME. However, with 500 $\mu\text{g}/\text{mL}$ NME, significant differences were noted ($p <$

0.05) (Figure 32D), concordant with what was seen for cotyledons and with an impact of this concentration on lettuce plantlet development. Lastly, the number of developed leaves during the destructive sampling analysis showed that both concentrations of NME extract had fewer seeds with developed leaves compared to the control, with significant differences ($p < 0.0001$) (Figure 32E). This shows once again the potential toxicity of the NME extract.

Based on the results of this bioassay, it can be concluded that the CE extract is non-toxic to lettuce seed germination at concentrations of 250 and 500 $\mu\text{g}/\text{mL}$, which is promising for potential future applications. Conversely, the NME extract exhibited toxicity to lettuce seed germination, particularly at the 500 $\mu\text{g}/\text{mL}$ concentration. It is worth noting that this toxicity observed during germination does not necessarily imply toxicity to more mature plants, as the latter possess defense mechanisms that early seedlings lack, being more vulnerable. This is supported by the positive correlation between age and resistance to diseases (Whalen, 2005), which can also apply to the components of the NME extract. Many terms exist to describe the development of resistance during the maturation process of a plant (Hu & Yang, 2019), and several studies have demonstrated an increase in resistance against various pathogens during the transition from the juvenile to the adult phase of a plant. For instance, as documented by Marla et al. (2018), the adult phase of corn is associated with high resistance to common rust (*Puccinia sorghi*) and other diseases. However, the molecular mechanisms underlying this phenomenon are still unknown. Nevertheless, there is growing evidence suggesting that this resistance is controlled by a sophisticated intrinsic regulatory network that enables plants to adjust their immunity in response to predictable biotic stress changes occurring during their life cycles (Hu & Yang, 2019). Therefore, further tests are warranted to confirm the potential toxic effects of the NME extract on juvenile and adult plants.

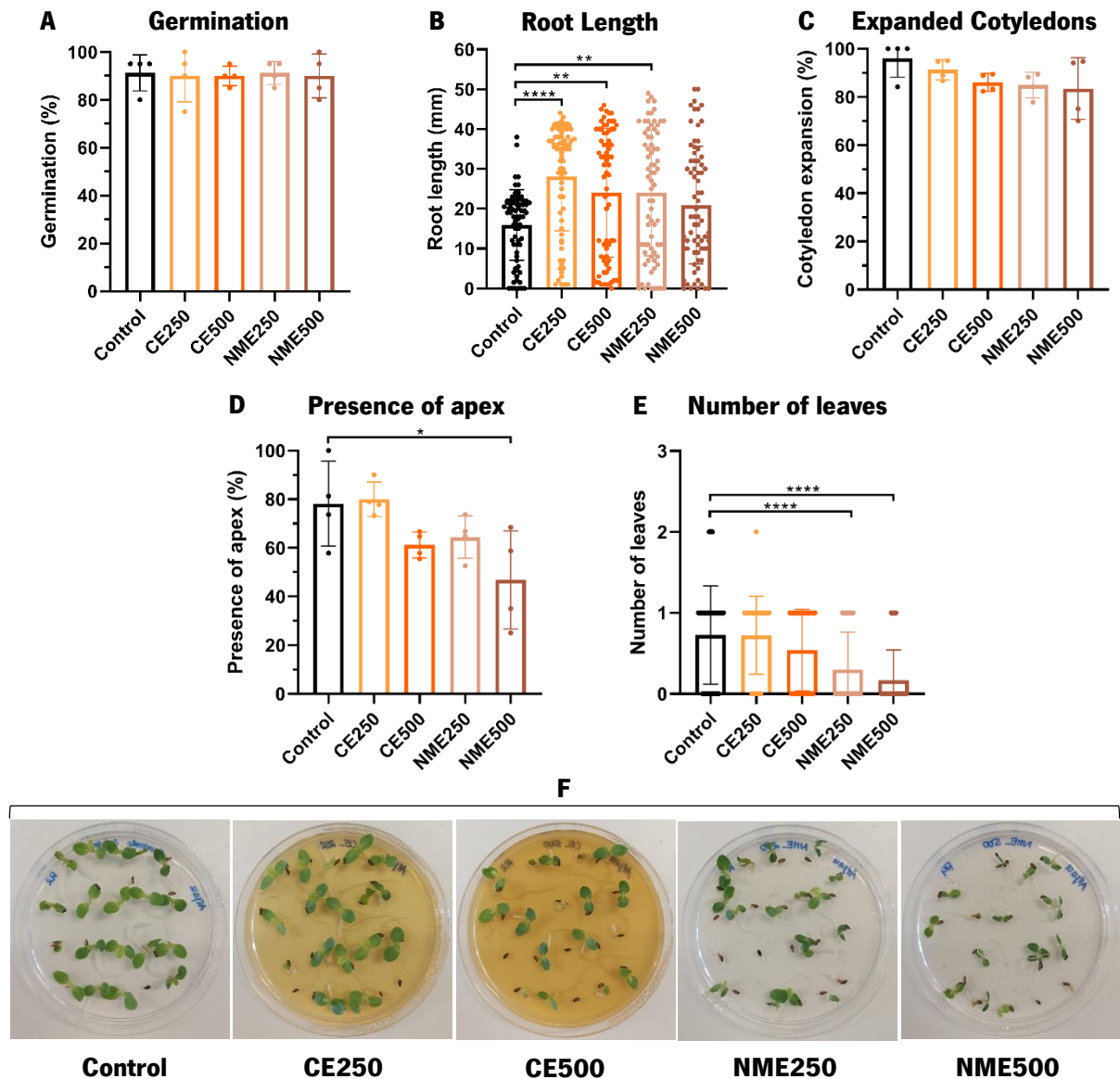


Figure 34 – *Curcuma longa* extract (CE) does not exhibit toxicity towards lettuce seeds, but *Myristica fragrans* extract (NME) appears do be toxic, especially at a concentration of 500 $\mu\text{g}/\text{mL}$. The seeds were washed in 5% bleach for 20 minutes with manual agitation, and rinsed three times with sterile deionized water. A volume of 37.50 μL of 80% EtOH was added to the solvent control and a volume of 18.75 or 37.50 μL of the CE or NME extract at concentrations of 250 and 500 $\mu\text{g}/\text{mL}$, respectively, were incorporated into the MS medium before solidification and poured into Petri dishes. Seeds were carefully placed into the Petri dishes and placed in a plant growth room for 7 days at room temperature. At the end of the trial, a destructive analysis was performed to analyze germination (A), root length (B), expanded cotyledons (C), presence of apex (D), and number of leaves (E). Also, a photographic record was done (F). Germination percentages were calculated by dividing the number of germinated seeds by the total number of seeds in a plate. Cotyledon expansion percentages were calculated by dividing the number of seeds with fully expanded cotyledons by the total number of seeds in a plate. Presence of apex percentages were calculated by dividing the number of seeds with a visible shoot apex by the total number of seeds in a plate. Data are presented as the mean of four independent replicates \pm standard deviation (SD). One-way ANOVA was conducted, followed by the Dunnett test for multiple comparisons: $*0.01 < p \leq 0.05$, $**0.001 < p \leq 0.01$ and $****p \leq 0.0001$, with significance compared to the control. The images of lettuce seeds are representative plates of the four independent replicates.

4.6. Resistance induction potential of the extracts in comparison with itraconazole

To assess the potential induction of resistance to the ITC fungicide and CE extract over time, resistance induction tests were conducted on the BY4741 yeast strain. Initially, as described in Section 3.6.1 a susceptibility test was conducted with the BY4741 strain to determine the MIC value for the synthetic fungicide ITC, which was found to be 0.250 µg/mL. To induce resistance in these cells, they were placed in 10 mL of YM medium containing different concentrations of ITC, as described in Section 3.6.2. The cells were exposed to concentrations under the MIC (0.125 µg/mL), equal to the MIC (0.250 µg/mL) and four times higher than the MIC (1.0 µg/mL). As shown in Table 5, the cells developed varying degrees of ITC resistance depending on the concentrations of ITC in the medium, with resistance beginning to increase after 24 h of exposure. For cells exposed to ITC at 0.125 µg/mL, the MICs increased from 0.250 to 0.500 µg/mL after one day. After two and three days, the MICs further increased to 2.00 µg/mL, and after four days of exposure, it reached a maximum value of 16.0 µg/mL, the highest value for this treatment. In contrast, cells exposed to 0.250 µg/mL ITC saw their MICs increased from 0.250 to 0.500 µg/mL after one day of exposure. However, after two and three days, the MICs increased to 4.00 µg/mL, and after four days, the MICs exceeded 16.0 µg/mL. Yeast cells grown in ITC at 1.00 µg/mL experienced a MIC increase from 0.250 to 1.00 µg/mL after one day of exposure. After two days, the MIC increased to 4.00 µg/mL, and after three days, it reached a value higher than 16.0 µg/mL, remaining stable after four days of exposure. In summary, initially, the cells were susceptible and dose-dependent to ITC but eventually became resistant. This result demonstrates that the cells gained resistance to ITC and underscores the ability of synthetic fungicides to induce resistance in cells, even at concentrations below the MIC, which is of great concern.

Table 5 – MIC values of cells exposed to three different concentrations of itraconazole (ITC).

Days cells were exposed	Cells exposed to ITC at 0.125 µg/mL (µg/mL)	Cells exposed to ITC at 0.250 µg/mL (µg/mL)	Cells exposed to ITC at 1.0 µg/mL (µg/mL)
Day 1	0.500	0.500	1.00
Day 2	2.00	4.00	4.00
Day 3	2.00	4.00	> 16.0
Day 4	16.0	> 16.0	> 16.0

Then, the same procedure was made to the CE extract, so initially, the susceptibility test conducted with the BY4741 strain to determine the MIC value for the CE extract was found to be 12.50

µg/mL. To induce resistance in these cells, they were placed in 10 mL of YM medium containing different concentrations of CE extract: concentrations under the MIC (6.25 µg/mL), equal to the MIC (12.50 µg/mL) and four times higher than the MIC (50 µg/mL). As shown in Table 6, the cells exposed to 6.25 or 12.50 µg/mL CE maintained their initial MIC over four days, showing no development of resistance. However, cells exposed to 50 µg/mL CE initially exhibited increased MIC (12.50 to 25.00 µg/mL) in two days, which remained stable for another day before decreasing to the initial value (12.50 µg/mL) on the fourth day. In summary, cells remained susceptible when exposed to concentrations below or equal to the MIC. Exposure to concentrations four times higher than the initial MIC initially led to resistance, but this resistance did not increase further after three days and was lost by the fourth day, contrary to what happened with ITC. These results suggest that, in general, cells did not develop resistance to CE extract. However, the temporary increase in resistance when exposed to concentrations four times higher than the MIC, along with the subsequent decrease in MIC to its original value on the fourth day, warrants further investigation to better understand the underlying factors.

Table 6 – MIC values of cells exposed to three different concentrations of *Curcuma longa* (CE) extract.

Days cells were exposed	Cells exposed to CE at 6.25 µg/mL (µg/mL)	Cells exposed to CE at 12.50 µg/mL (µg/mL)	Cells exposed to CE at 50 µg/mL (µg/mL)
Day 1	ND	ND	ND
Day 2	12.50	12.50	25.00
Day 3	12.50	12.50	25.00
Day 4	12.50	12.50	12.50

*ND – Not determined

Barchiesi et al. (2000) demonstrated that *Candida tropicalis* gained resistance to fluconazole after two days of exposure and reached the highest MIC value after six days, which is consistent with the results obtained in this assay with the ITC. They also revealed that the expression of multidrug transporter genes like *CtMDR1* (encoding major facilitators) and *CDR1* (encoding ABC transporters) is correlated with the increase in fluconazole MICs. Once they are upregulated in the resistant phenotypes, the authors suggest that drug efflux from the cell could be one of the mechanisms of resistance in *Candida* sp. Therefore, it is possible that *S. cerevisiae* employs similar resistance mechanisms, however, further investigation is required to uncover the underlying mechanisms.

4.7. Chemical characterization of CE and NME extracts

4.7.1. Compounds present in CE extract

In this study, an ATR–FTIR vibrational characterization and a GC–MS analysis of the CE extract was conducted to identify its constituents. The ATR–FTIR vibrational characterization spectrum (Annex 4: Figure 40 and Table 7) revealed several important vibrational features, such as: stretching vibrations of O–H groups, alkenes (C=C) and carbonyl (C=O) groups; a highly intense band at 1509 cm^{-1} that represented not only carbonyl bonds, but also in-plane bending vibrations around aliphatic ($\delta\text{ CC–C}$ and $\delta\text{ CC=O}$) and aromatic ($\delta\text{ CC–H}$) of keto and enol configurations and stretching vibrations of aromatic (νCC) bonds in keto and enolic forms. Finally, the intense band at 1267 cm^{-1} was attributed to the bending vibration of the phenolic band ($\nu\text{C–O}$) (Ismail et al., 2014). In addition, the chromatogram obtained in the GC–MS analysis of the CE extract (Annex 5: Figure 41) revealed the following main phytochemicals: (+)- β -turmerone, a sesquiterpenoid (28.9%); α -turmerone, an enone (13.3%); (+)-(S)-*ar*-turmerone, a bisabolane sesquiterpenoid (15.3%) and α -atlantone, a bisabolane-type sesquiterpenoid (3.0%) (Figure 35). Minor phytoconstituents included γ -curcumene, a bisabolone sesquiterpene (0.34%); zingiberene or α -sesqui phellandrene, a monocyclic sesquiterpene (0.43%); isoelemicin, a phenylpropanoid (1.48%) and gibberellin A3, a pentacyclic diterpenoid (0.55%). A comprehensive list of all identified constituents via GC–MS is in Annex 5: Table 8.

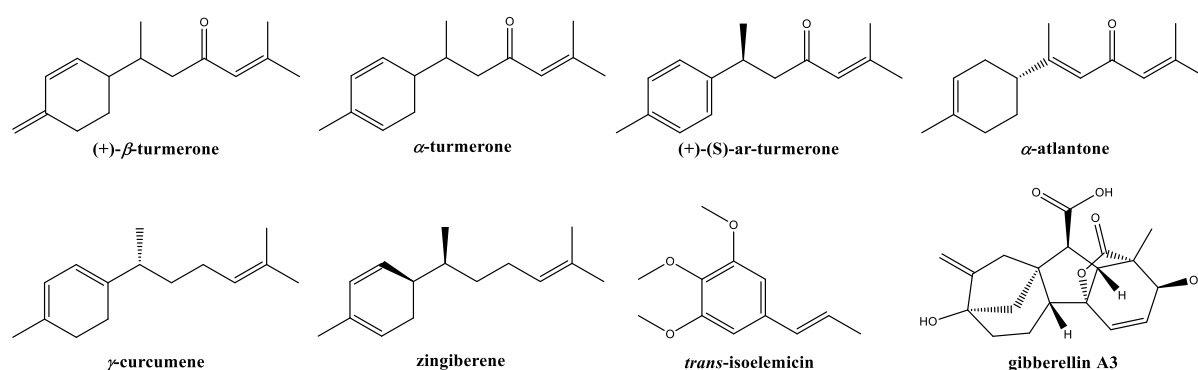


Figure 35 – Chemical structures of phytochemicals identified in *Curcuma longa* (CE) extract by GC–MS. The main compounds present in the composition of the CE extract are: (+)- β -turmerone, that is a sesquiterpenoid; α -turmerone, that is an enone; (+)-(S)-*ar*-turmerone, that is a bisabolane sesquiterpenoid that is 2-methylhept-2-en-4-one substituted by a 4-methylphenyl group at position 6; and α -atlantone, that is a bisabolane-type sesquiterpenoid. Some of the minor constituents are: γ -curcumene, which is a bisabolone sesquiterpene; zingiberene or α -sesqui phellandrene, which is a monocyclic sesquiterpene; isoelemicin, which is a phenylpropanoid; and gibberellin A3, which is a pentacyclic diterpenoid.

Considering the chemical structure, the presence of a benzylic stereogenic center in bisabolanes allows for the asymmetric hydrovinylation conversion of 4-methylstyrene into curcumene, *ar*-turmerone, and other identified phytoconstituents. These compounds exhibit subtle stereochemical differences. Given the structural similarities among these closely related substances in the mixture, it is reasonable to expect that they may share similar biological activities. Consequently, we advocate for conducting activity studies not on individual constituents but rather on the crude extract, in which these compounds are the primary components. This approach offers several advantages, including cost-effectiveness, prolonged effectiveness (multi-compound products can deter the development of resistance in pathogens, as they struggle to adapt to multiple simultaneous actions), and a broader range of applications against various pests and diseases. This is because the compounds often work synergistically (Lee et al., 2007), providing protection against diverse pathogens, while a single refined product may only address specific pests, potentially leaving the crop vulnerable to additional risks.

The obtained results are in line with the findings of Alvindia et al. (2022), who identified *ar*-turmerone (50.63%), curlone (15.42%), α -curcumene (6.48%) and 3-octanol (5.88%) as the primary components in *C. longa* crude extract. Additionally, Braga et al. (2003) demonstrated that the key compounds of *C. longa* rhizomes' ethanolic extract included *ar*-turmerone, (Z)- and (E)- γ -atlantone, with smaller amounts of *ar*-curcumene, α -zingiberene, β -sesquiphellandrene and *ar*-turmerol (<2.4%). Furthermore, Singh et al. (2010) revealed differences in the chemical composition of ethanol oleoresin obtained from fresh and dry rhizomes of *C. longa*. Fresh rhizomes contained α -turmerone (53.4%), β -turmerone (18.1%) and aromatic-turmerone (6.2%) as the major components, while dry rhizomes had aromatic-turmerone (9.6%), α -santalene (7.8%) and α -turmerone (6.5%) as the main chemical species. The variability in the compounds and their relative proportions in *C. longa* extracts can be attributed to the different responses of these compounds to various solvents and extraction process factors. Age, physiological state and environmental conditions also play a crucial role in extracting different constituents (Pandey et al., 2021). Oxygenated sesquiterpenes and sesquiterpene hydrocarbons found in the composition of the CE extract are often present in essential oils obtained from *C. longa* rhizomes via various extraction methods, as reviewed by Ibáñez & Blázquez, (2020). This fact is noteworthy because it is uncommon: ethanolic extracts can capture a wide range of compounds, including both polar and nonpolar ones, while preserving more heat-sensitive compounds. In contrast, essential oils consist primarily of volatile and lipophilic compounds. So, different extraction methods typically yield distinct phytochemical compositions. This highlights the advantages of extracting similar constituents using

regular ethanolic extraction over essential oils, including reduced volatility, easier standardization and improved sustainability.

Turmerones are sesquiterpenoid α,β -unsaturated ketones characterized by the presence of a carbonyl group. In general, they exhibit strong antibacterial, antifungal and cytotoxic activities. Notably, *ar*-turmerone has been reported to possess strong antibacterial and antifungal properties against *Clostridium perfringens* and *A. flavus*, respectively (Lee, 2006; Dhingra et al., 2007). According to Kumar et al. (2016), turmerones found in *C. longa* essential oil are responsible for its antifungal activity against *F. graminearum*. These sesquiterpenoids induce changes in the fatty acid composition and permeability of the fungal cell membrane. Moreover, the α,β -unsaturation of turmerones increases the polarizability of the molecule, enabling binding with amino acids and nucleic acids, which, in turn, affects various metabolic pathways in fungi (Herrera et al., 2015; LoPachin & Gavin, 2016). Therefore, the observed antimicrobial activity in the CE extract can be attributed to its high proportion of turmerones, including (+)- β -turmerone, α -turmerone and (+)-(S)-*ar*-turmerone.

4.7.2. Compounds present in NME extract

In this study, an ATR–FTIR vibrational characterization and a GC-MS analysis of the NME extract was also performed to identify its constituents. The ATR–FTIR spectrum (Annex 6: Figure 42 and Table 9) exhibited characteristic bands associated with fatty acids, as well as bands corresponding to eugenol derivatives (Kuo et al., 2009), specifically at 1428 cm^{-1} (indicative of C=C aromatic stretching) and 1235 cm^{-1} (representing C–O–C vibrations). The presence of a peak at 1330 cm^{-1} (related to C–O stretching vibration of the methoxy group) suggests the possible presence of methoxyeugenol (2,6-dimethoxy-4-allylphenol or 4-allyl-2,6-dimethoxy phenol), which is a phenylpropene, a methoxyphenol and a derivative of eugenol. Additionally, in the chromatogram of the NME extract (Annex 7: Figure 43 and Table 10), the primary phytochemicals identified were fatty acids, constituting 40.4% of the composition. These fatty acids included tetradecanoic acid or myristic acid (21.3%), 9-octadecenoic acid or oleic acid (10%), *n*-hexadecanoic acid or palmitic acid (4.8%), dodecanoic acid or lauric acid and its ethyl ester (2.9%) and octadecanoic acid or stearic acid (1.3%). Additional constituents included methoxyeugenol, trans-isoeugenol and trans-methyl isoeugenol (11.1%); elemicin or 3,4,5-trimethoxyallylbenzene, a phenylpropene and trans-isoelemicin (6.7%); 1,4,6-trimethyl-2-azafluorene (5.2%); gelsivirine, an indole alkaloid (2%); veratone or veratryl acetone, an aromatic ketone capable of forming hydrogen bonds with

enzymes and other molecules (1.6%); and montanine or 20-hydroxy-voaluteine, an alkaloid (1.1%), as illustrated in Annex 7: Figure 43. Regarding 1,4,6-trimethyl-2-azafluorene, it's worth noting that the Qual value is low (64) and the assignment may be inaccurate. An alternative assignment could be to 4-methyl-acridone.

In the literature, the four main phytoconstituents identified by GC-MS in the *M. fragans* ethanolic extract are: myristicin (64.5%), myristic acid (18.7%), terpinen-4-ol (8.8%) and methoxyeugenol (8.1%) (Barman et al., 2021; López et al., 2015). However, in this study, myristicin was not detected. On the other hand, the typically reported alkenylbenzenes (viz. elemicin and isoelemicin) were present instead. Myristic acid's presence has been documented in *M. fragans* oleoresins (Morsy, 2016), as well as in extracts or essential oils from *Myristica malabarica* and other members of the Myristicaceae family, including *Horsfieldia irya*, *Iryanthera juruensis*, and *Virola bicuhyba* (Sanford & Heinz, 1971). According to Barman et al. (2021), myristic acid is a common constituent of both nutmeg and wild nutmeg butter, alongside oleic, palmitic, lauric and stearic acids, all of which were detected in the extract under study. Conversely, safrole and virolane phenylpropanoids that usually appear in the constitution of the *M. fragans* extracts were not found. In terms of hydrocarbon and oxygenated monoterpenes and sesquiterpenes (such as α - and β -pinene or sabinene), as well as terpene alcohols (including linalool, geraniol, or 4-terpineol), only small amounts of α -terpinolene and γ -terpinene monoterpene hydrocarbons and selinene sesquiterpene were detected. Methoxyeugenol, trans-isoeugenol and methyl isoeugenol have also been previously identified in *M. fragans* extracts (López et al., 2015) and essential oils (Barman et al., 2021). While gelsemine and montanine have not been reported in *M. fragans* before, other indole alkaloids have been described in other members of the Myristicaceae family. To the best of our knowledge, there are no reports of veratone in the Myristicaceae family; however, it is worth noting that it shares structural similarities with alkenylbenzenes (see Figure 36). Sanford & Heinz, (1971) suggest that the variations observed in the composition of the *M. fragans* extract should not solely be attributed to the extraction method; rather, they can be attributed to a multitude of factors, including differences in cultivation practices, maturity at the time of harvest, pre-shipping storage conditions and genetic mutations.

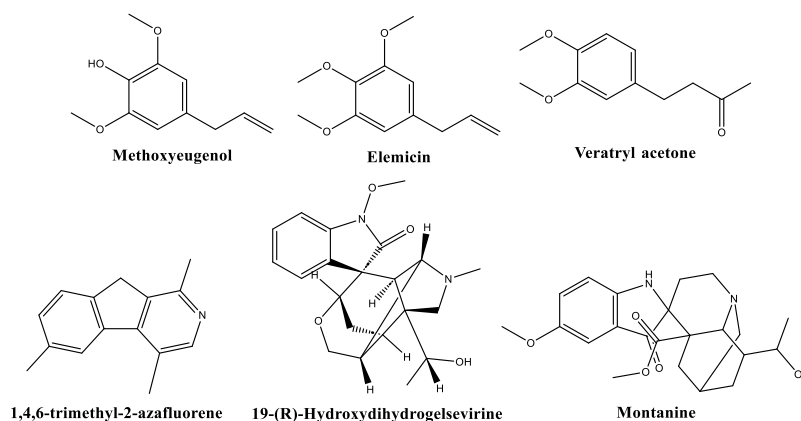


Figure 36 – Chemical structures of some of the phytochemicals found in *Myristica fragrans* (NME) extract.

The main compounds present in the composition of the NME extract are: myristic acid, a fatty acid (21.3%), as methoxyeugenol, trans-isoeugenol and trans-methyl isoeugenol (11.1%). Other constituents are elemicin, a phenylpropene and trans-isoelemicin (6.7%); 1,4,6-trimethyl-2-azafluorene (5.2%); gelsivirine, an indole alkaloid (2%); veratryl acetone, an aromatic ketone (1.6%); and montanine, an alkaloid (1.1%).

Liu et al. (2008) demonstrated that saturated fatty acids like myristic acid, palmitic acid and lauric acid exhibit antifungal activity against various fungi, including *Alternaria solani*, *Colletotrichum lagenarium*, *Fusarium oxysporum* f. sp. *cucumerinum* and *Fusarium oxysporum* f. sp. *lycopersici*. Unsaturated fatty acids, such as oleic acid, have also been reported to have antifungal activity against *Pythium ultimum* and *Crinipellis pernicioso* (Walters et al., 2004). Eugenol, a phenolic compound, is known for its antifungal activity due to its lipophilic character, enabling it to penetrate fungal cell walls. Eugenol also has a free –OH group that allows it to form hydrogen bonds with other molecules, such as enzymes, disrupting their normal activity (Pandey et al., 2016; Knobloch et al., 1989). Methoxyeugenol, a derivative of eugenol present in the NME extract, may have similar properties, making it a potential compound with antifungal activity. However, further studies are needed to understand its role. Elemicin, another phenylpropene, has been reported to have strong antibacterial and antifungal activities against various fungi, including *C. tropicalis* and *A. flavus* (Al-Qahtani et al., 2022). The MOA of this compound is not yet elucidated. Therefore, it can be inferred that the NME extract has antifungal activity due to these compounds and their potential interactions. It is important to note that gelsimine, veratone and montanine have no reported antifungal or anti-oomycetal activities. While some of these compounds may possess antifungal and/or anti-oomycetal properties, further investigation is required to draw a definitive conclusion.

5. CONCLUSIONS AND FUTURE PERSPECTIVES

The main goal of this study is to create natural antifungal agents that can efficiently substitute traditional fungicides while avoiding their associated downsides, against filamentous fungi and oomycetes known to devastate crops in Portugal and other countries. We aimed to elucidate the mechanisms of action responsible for the antifungal properties in plant extracts and to discover their cellular targets. Additionally, we assessed the extracts for toxicity in plants, using the lettuce *in vitro* germination model, while also exploring their potential to induce microbial resistance in yeasts and fungi, as happens with conventional fungicides. Ultimately, our goal is to contribute to sustainable agricultural practices by harnessing the potential of these extracts.

Based on the results obtained in viability assays conducted on *S. cerevisiae* using aqueous and ethanolic extracts of *C. longa*, *M. fragrans*, and *O. basilicum*, it was determined that only the ethanolic extracts of *C. longa* and *M. fragrans* exhibited toxicity towards this yeast. Chemical analysis conducted by Eva Sánchez at the University of Valladolid revealed that the toxic properties of the CE extract are attributed to sesquiterpenoids, such as (+)- β -turmerone, α -turmerone and (+)-(S)-*a*-turmerone. Conversely, for the NME extract, toxic properties are linked to myristic acid, methoxyeugenol and elemicin. Consequently, it is advisable to consider isolating these compounds with higher toxicity and conducting further tests to investigate their efficacy against filamentous fungi and oomycetes. This will help ascertain whether these compounds exhibit enhanced antifungal activity when isolated.

To assess the antifungal activity of the CE and NME extracts, we exposed phytopathogenic filamentous fungi and oomycetes to three different concentrations of each extract. Once each fungus or oomycete reached the edge of the Petri dish, we observed inhibition of mycelium growth with both extracts tested. For the CE extract, we observed maximum inhibitions in *B. cinerea* (36.14%), *C. acutatum* (23.23%), *D. corticola* (34.32%), *P. cactorum* (41.29%) and *P. cinnamomi* (65.88%). Especially, the fungus *F. culmorum* did not show significant inhibition. In all cases where inhibition occurred, a dose-response effect was consistently visible. For the NME extract, maximum inhibition of mycelium growth was also observed in *B. cinerea* (21.00%), *C. acutatum* (10.74%), *D. corticola* (27.73%), *F. culmorum* (47.79%) and *P. cinnamomi* (25.23%). In general, NME was less efficient in inhibiting mycelium radial growth, although a dose-response effect was also consistently observed in cases of inhibition. However, differently from the CE extract, the NME did not inhibit the oomycete *P. cactorum* and induce a high inhibition on *F. culmorum* mycelium growth. This suggests that the efficacy of a plant extract could be very species-specific, with certain phytopathogens being particularly susceptible to specific compounds/MOA.

From these results, it is evident that the CE extract tends to inhibit the growth of oomycetes, as the highest inhibition values were observed for the two oomycetes exposed to the highest concentration. Both of these oomycetes are soil-borne and employ the same infection mechanism via zoospores. Throughout the infection process, these zoospores end up aggregating and producing degrading enzymes to help penetrate and colonize the tissues. One plausible explanation is that this extract affects these enzymes, either by inhibiting their synthesis, growth or action, particularly in the case of *P. cinnamomi*, as it was the organism more susceptible to the action of the CE extract. Notably, *P. cactorum* differs from *P. cinnamomi* in producing caducous sporangia, which play a crucial role in its pathogenicity. This difference might account for the varying toxicity of the extract towards these two *Phytophthora* species, although further investigation is needed to clarify this. Therefore, it would be interesting in the future to address this issue and find out which mechanisms lead the CE extract to inhibit these oomycetes more easily and, perhaps, test it on more oomycetes to see if this trend is maintained in all oomycetes or only in oomycetes of the genus *Phytophthora*. As for the NME extract, there appears to be a trend towards greater inhibition specifically against the *F. culmorum* fungus, as the highest inhibition value achieved by this extract was with *F. culmorum* at the highest concentration, a fungus that was not susceptible to CE. These findings raise questions about the extract's mechanisms of toxicity, particularly its selectivity against *F. culmorum*, and warrant further investigation. Therefore, it would be appropriate to try to understand what mechanisms lead to this extract being more toxic to this filamentous fungus and to try to understand why its inhibition capacity was not as strong for the other filamentous fungi.

In the viability assessment of *erg6*, *erg2*, *erg5*, *erg4*, *bck1* and *mkk1/mkk2* mutants, increased resistance was observed when exposed to both extracts when compared with the WT. This suggests that these extracts may affect the ergosterol biosynthetic pathway and the cell wall integrity pathway. Additionally, it was observed that both extracts might require sterol C-24 methyltransferase enzyme (encoded by the *ERG6* gene) to be functional, since their activity is compromised in its absence. This indicates that this enzyme could be one of the main targets of certain compounds present in these extracts, potentially serving as allosteric modulators of this enzyme, preventing the conversion of zymosterol into fecosterol and thus leading to the interruption of the ergosterol biosynthetic pathway. Furthermore, this also indicates that fecosterol is one of the targets. However, it is worth noting that the Erg2, Erg5 and Erg4 enzymes can also be important targets for the antifungal activity of the CE and NME extracts, although viability of the corresponding mutants was not affected to the same extent as the *erg6* mutant, probably because the targets of the extracts could be mainly fecosterol and episterol, the metabolic intermediates potentially accumulated in *erg2*, *erg5* and *erg4* mutants and absent in the *erg6*

mutant. The *bck1* and *mkk1/mkk2* mutants showed that the CE extract may be correlated with the overactivation of the cell wall integrity pathway, but not the NME extract. To validate these findings, further tests could be conducted using other mutants, particularly those involved in the cell wall integrity pathway, such as *Pkc1* and *Slit2/Mpk1*. This approach will enhance our comprehension of the mechanisms underlying the action of these extracts. Furthermore, it would be valuable to investigate whether any of the compounds within the CE and NME extracts have a direct affinity for membrane ergosterol, similar to certain synthetic fungicides.

Beyond the mutants mentioned above, the viability of the *erg3* and *yca1* mutants, which exhibited heightened sensitivity to the extracts, was also examined. In the case of the *erg3* mutant, this suggests that the extracts do not necessarily rely on the sterol C-5 desaturase enzyme encoded by the *ERG3* gene to exert their activity on yeasts. However, it is noteworthy that the antifungal activity is even more pronounced in the absence of this enzyme, suggesting that episterol, the *Erg3* substrate, might be a target of the extracts. Regarding the *yca1* mutant, the extracts did not appear to directly induce apoptosis but rather affect this pathway. Fluorescence microscopy tests made to assess viability with PI (see Figure 31) indicated that the CE and NME extracts lead to necrosis. Nevertheless, additional studies are necessary to fully comprehend the mechanisms associated with this pathway. Potential tests include evaluating mitochondrial membrane depolarization, a phenomenon occurring in various cellular processes, including apoptosis, using flow cytometry. Additionally, considering the research by Chin *et al.* (2014), investigating the response of the *aif1* mutant could provide insights into whether the extracts are involved with PCD, because certain fungicides do not need the *YCA1* gene to induce PCD. As an example, caspofungin, only needs the pro-apoptotic *AIF1* gene to induce PCD. If the *aif1* mutant demonstrates resistance, it may suggest that the CE extract induces PCD. Conversely, if it remains unaffected or becomes more sensitive, this would suggest another mechanism of action.

According to the phytotoxicity tests, it was concluded that the CE extract was not toxic at the tested concentrations (250 and 500 µg/mL) when applied to germinating lettuce seeds. In contrast, the NME extract exhibited a toxic effect impairing the early development of the seedlings, particularly at the concentration of 500 µg/mL. This finding suggests that caution should be exercised when considering the use of the NME extract as a pre-germination treatment. Instead, it may be more suitable for post-germination applications, namely in mature organs and adult plants. To substantiate the observed toxic effect of the NME extract and this hypothesis, further investigation is warranted. One avenue for exploration is to conduct tests on mature or more developed plants. Mature plants typically possess more

robust defense mechanisms compared to germinating seeds. If mature plants are not adversely affected by the NME extract, it could potentially find utility during plant growth or as a post-harvest treatment. Furthermore, it would be interesting to evaluate the potential toxicity in human cellular lines and in animal models.

The susceptibility tests revealed that the MIC value for ITC is 0.250 $\mu\text{g}/\text{mL}$, while for the CE extract, it is 12.50 $\mu\text{g}/\text{mL}$. In the case of ITC, when cells were exposed to three different concentrations for four days, the MIC increased to a value higher than 16 $\mu\text{g}/\text{mL}$. So, it can be concluded that cells can overcome the MOA and develop resistance to the synthetic fungicide ITC. In the case of the CE extract, cells exposed to concentrations below or equal to the MIC did not develop resistance after four days. Cells exposed to concentrations higher than the initial MIC did gain resistance up to 25.00 $\mu\text{g}/\text{mL}$, but on the fourth day, this value decreased to the original MIC value. This indicates that cells were unable to develop lasting resistance against the MOA of the CE extract.

With the ultimate goal of formulating a natural fungicide derived from CE and NME extracts, several promising approaches can be considered. One such avenue is the application of nanotechnology to encapsulate these extracts, potentially enhancing their efficacy and stability. Additionally, the isolation and extraction of the most active compounds within these extracts or their combination to harness synergistic effects warrants further investigation. These strategies can serve to amplify the antimicrobial activity of these extracts and contribute to the development of effective natural fungicides.

In conclusion, this study has unveiled the antimicrobial potential of extracts from commonly used culinary plants, *C. longa* and *M. fragrans*, particularly against fungi, oomycetes and yeasts. The CE extract's antimicrobial properties are attributed to sesquiterpenoids, including (+)- β -turmerone, α -turmerone, and (+)-(S)-*ar*-turmerone, while the NME extract relies on fatty acids (myristic acid), methoxyeugenol, and elemicin. When harnessed wisely, these extracts could offer a sustainable alternative to synthetic fungicides, potentially mitigating the significant economic impact caused by these microorganisms across a range of crops. Furthermore, the diverse mechanisms of action exhibited by these extracts may help deter the development of resistance in target microorganisms, thereby simplifying fungal treatment not only in agriculture but also in fields like medicine. This study has laid the foundation for further inquiry, raising pertinent questions. Continued research in this area promises to unveil new insights and opportunities, rendering this study a valuable asset for future investigations.

6. BIBLIOGRAPHY

- Abbas**, H. K., Yoshizawa, T., & Shier, W. T. (2013). Cytotoxicity and phytotoxicity of trichothecene mycotoxins produced by *Fusarium* spp. *Toxicon*, *74*, 68–75. <https://doi.org/10.1016/j.toxicon.2013.07.026>
- Adeyemi**, J. O., & **Onwudiwe**, D. C. (2020). Chemistry and Some Biological Potential of Bismuth and Antimony Dithiocarbamate Complexes. *Molecules (Basel, Switzerland)*, *25*(2), 305-327. <https://doi.org/10.3390/molecules25020305>
- Ahmad**, R., Srivastava, S. P., Maurya, R., Rajendran, S. M., & Nbsp, K. R. A. and A. K. S. (2008). Mild antihyperglycaemic activity in *Eclipta alba*, *Berberis aristata*, *Betula utilis*, *Cedrus deodara*, *Myristica fragrans* and *Terminalia chebula*. *Indian Journal of Science and Technology*, *1*(5), 1–6. <https://doi.org/10.17485/ijst/2008/v1i5.1>
- Ajiboye**, T. O., Ajiboye, T. T., Marzouki, R., & Onwudiwe, D. C. (2022). The Versatility in the Applications of Dithiocarbamates. *International Journal of Molecular Sciences*, *23*(3), 1317-1353. <https://doi.org/10.3390/ijms23031317>
- Aktar**, Md. W., Sengupta, D., & Chowdhury, A. (2009). Impact of pesticides use in agriculture: Their benefits and hazards. *Interdisciplinary Toxicology*, *2*(1), 1–12. <https://doi.org/10.2478/v10102-009-0001-7>
- Al Aboody**, M. S., & **Mickymaray**, S. (2020). Anti-Fungal Efficacy and Mechanisms of Flavonoids. *Antibiotics*, *9*(2), 45-87. <https://doi.org/10.3390/antibiotics9020045>
- Aldred**, D., & **Magan**, N. (2004). Prevention strategies for trichothecenes. *Toxicology Letters*, *153*(1), 165–171. <https://doi.org/10.1016/j.toxlet.2004.04.031>
- Al-Qahtani**, W. H., Dinakarkumar, Y., Arokiyaraj, S., Saravanakumar, V., Rajabathar, J. R., Arjun, K., Gayathri, P. K., Appaturi, J. N. (2022). Phyto-chemical and biological activity of *Myristica fragrans*, an ayurvedic medicinal plant in Southern India and its ingredient analysis. *Saudi Journal of Biological Sciences*, *29*, 3815-3821. <https://doi.org/10.1016/j.sjbs.2022.02.043>
- Alvindia**, D. de G., Mangoba, M. A. A., Abduzukhurov, J. T., & Santiago, E. F. (2022). Biocidal activities of *Curcuma longa* L. against anthracnose of mango fruits caused by *Colletotrichum gloeosporioides* (Penz.) Penz. And Sacc. *Archives of Phytopathology and Plant Protection*, *55*(5), 515–526. <https://doi.org/10.1080/03235408.2022.2035155>
- Amalraj**, A., Pius, A., Gopi, S., & Gopi, S. (2017). Biological activities of curcuminoids, other biomolecules from turmeric and their derivatives – A review. *Journal of Traditional and Complementary Medicine*, *7*(2), 205–233. <https://doi.org/10.1016/j.jtcme.2016.05.005>
- Amundson**, R., Berhe, A. A., Hopmans, J. W., Olson, C., Szein, A. E., & Sparks, D. L. (2015). Soil and human security in the 21st century. *Science*, *348*(6235), 1261071-1, 1-6. <https://doi.org/10.1126/science.1261071>
- Annunziata**, F., Pinna, C., Dallavalle, S., Tamborini, L., & Pinto, A. (2020). An Overview of Coumarin as a Versatile and Readily Accessible Scaffold with Broad-Ranging Biological Activities. *International Journal of Molecular Sciences*, *21*(4618), 1-81. <https://doi.org/10.3390/ijms21134618>
- Arif**, T., Bhosale, J. D., Kumar, N., Mandal, T. K., Bendre, R. S., Lavekar, G. S., & Dabur, R. (2009). Natural products—Antifungal agents derived from plants. *Journal of Asian Natural Products Research*, *11*(7), 621–638. <https://doi.org/10.1080/10286020902942350>
- Arumugam**, G., Purushotham, B., & Swamy, M. K. (2019). *Myristica fragrans* Houtt.: Botanical, Pharmacological, and Toxicological Aspects. In M. K. Swamy & M. S. Akhtar (Eds.), *Natural Bio-active Compounds: Volume 2: Chemistry, Pharmacology and Health Care Practices* (pp. 81–106). Springer. https://doi.org/10.1007/978-981-13-7205-6_4

- Assress**, H. A., Selvarajan, R., Nyoni, H., Mamba, B. B., & Msagati, T. A. M. (2021). Antifungal azoles and azole resistance in the environment: Current status and future perspectives—a review. *Reviews in Environmental Science and Bio/Technology*, 20(4), 1011–1041. <https://doi.org/10.1007/s11157-021-09594-w>
- Avanço**, G. B., Ferreira, F. D., Bomfim, N. S., Santos, P. A. de S. R. dos, Peralta, R. M., Brugnari, T., Mallmann, C. A., Abreu Filho, B. A. de, Mikcha, J. M. G., & Machinski Jr., M. (2017). Curcuma longa L. essential oil composition, antioxidant effect, and effect on Fusarium verticillioides and fumonisin production. *Food Control*, 73, 806–813. <https://doi.org/10.1016/j.foodcont.2016.09.032>
- Azevedo**, M.-M., Faria-Ramos, I., Cruz, L. C., Pina-Vaz, C., & Rodrigues, A. G. (2015). Genesis of Azole Antifungal Resistance from Agriculture to Clinical Settings. *Journal of Agricultural and Food Chemistry*, 63(34), 7463–7468. <https://doi.org/10.1021/acs.jafc.5b02728>
- Backman**, P. A., & Sikora, R. A. (2008). Endophytes: An emerging tool for biological control. *Biological Control*, 46(1), 1–3. <https://doi.org/10.1016/j.biocontrol.2008.03.009>
- Baćmaga**, M., Wyszowska, J., & Kucharski, J. (2018). The influence of chlorothalonil on the activity of soil microorganisms and enzymes. *Ecotoxicology (London, England)*, 27(9), 1188–1202. <https://doi.org/10.1007/s10646-018-1968-7>
- Baggio**, J. S., Marin, M. V., & Peres, N. A. (2021). Phytophthora Crown Rot of Florida Strawberry: Inoculum Sources and Thermotherapy of Transplants for Disease Management. *Plant Disease*, 105(11), 3496–3502. <https://doi.org/10.1094/PDIS-11-20-2476-RE>
- Bai**, G. H., Desjardins, A. E., & Plattner, R. D. (2002). Deoxynivalenol-nonproducing fusarium graminearum causes initial infection, but does not cause disease spread in wheat spikes. *Mycopathologia*, 153(2), 91–98. <https://doi.org/10.1023/a:1014419323550>
- Bajpai**, V. K., & Chul, S. (2012). In vitro and in vivo inhibition of plant pathogenic fungi by essential oil and extracts of Magnolia liliflora Desr. *Journal of Agricultural Science and Technology*, 14, 845–856.
- Barchiesi**, F., Calabrese, D., Sanglard, D., Falconi Di Francesco, L., Caselli, F., Giannini, D., Giacometti, A., Gavaudan, S., & Scalise, G. (2000). Experimental Induction of Fluconazole Resistance in Candida tropicalis ATCC 750. *Antimicrobial Agents and Chemotherapy*, 44(6), 1578–1584.
- Barman**, R., Bora, P. K., Saikia, J., Kemprai, P., Saikia, S. P., Haldar, S., & Banik, D. (2021). Nutmegs and wild nutmegs: An update on ethnomedicines, phytochemicals, pharmacology, and toxicity of the Myristicaceae species. *Phytotherapy Research: PTR*, 35(9), 4632–4659. <https://doi.org/10.1002/ptr.7098>
- Barradas**, C., Phillips, A. J. L., Correia, A., Diogo, E., Bragança, H., & Alves, A. (2016). Diversity and potential impact of Botryosphaeriaceae species associated with Eucalyptus globulus plantations in Portugal. *European Journal Of Plant Pathology*, 146(2), 245–257. <https://doi.org/10.1007/s10658-016-0910-1>
- Bateman**, G. L., Murray, G., Gutteridge, R. J., & Coskun, H. (1998). Effects of method of straw disposal and depth of cultivation on populations of Fusarium spp. In soil and on brown foot rot in continuous winter wheat. *Annals of Applied Biology - AAB*, 132(1), 35–47. <https://doi.org/10.1111/j.1744-7348.1998.tb05183.x>
- Beakes**, G. W., Glockling, S. L., & Sekimoto, S. (2012). The evolutionary phylogeny of the oomycete «fungi». *Protoplasma*, 249(1), 3–19. <https://doi.org/10.1007/s00709-011-0269-2>
- Beccari**, G., Covarelli, L., & Nicholson, P. (2011). Infection processes and soft wheat response to root rot and crown rot caused by Fusarium culmorum. *Plant Pathology*, 60(4), 671–684. <https://doi.org/10.1111/j.1365-3059.2011.02425.x>
- Belisle**, R. J., Hao, W., McKee, B., Arpaia, M. L., Manosalva, P., & Adaskaveg, J. E. (2019). New Oomycota Fungicides With Activity Against Phytophthora cinnamomi and Their Potential Use for

- Managing Avocado Root Rot in California. *Plant Disease*, 103(8), 2024–2032. <https://doi.org/10.1094/PDIS-09-18-1698-RE>
- Bentley**, A. R., Cromey, M. G., Farrokhi-Nejad, R., Leslie, J. F., Summerell, B. A., & Burgess, L. W. (2006). Fusarium crown and root rot pathogens associated with wheat and grass stem bases on the South Island of New Zealand. *Australasian Plant Pathology*, 35(5), 495–502. <https://doi.org/10.1071/AP06053>
- Berger**, S., El Chazli, Y., Babu, A. F., & Coste, A. T. (2017). Azole Resistance in *Aspergillus fumigatus*: A Consequence of Antifungal Use in Agriculture? *Frontiers in Microbiology*, 8:1024, 1-6. <https://doi.org/10.3389/fmicb.2017.01024>
- Bérubé**, J. A., Gagné, P., Ponchart, J. P., Tremblay, E., & Bilodeau, G. J. (2018). Detection of *Diplodia corticola* spores in Ontario and Québec based on High Throughput Sequencing (HTS) methods. 4(3), 378–386. <https://doi.org/10.1080/07060661.2018.1498394>
- Bhattacharya**, S., Esquivel, B. D., & White, T. C. (2018). Overexpression or Deletion of Ergosterol Biosynthesis Genes Alters Doubling Time, Response to Stress Agents, and Drug Susceptibility in *Saccharomyces cerevisiae*. *mBio*, 9(4), e01291-18, 1-14. <https://doi.org/10.1128/mbio.01291-18>
- Bhattacharya**, S., Sae-Tia, S., & Fries, B. C. (2020). Candidiasis and Mechanisms of Antifungal Resistance. *Antibiotics*, 9(6), 312, 1-19. <https://doi.org/10.3390/antibiotics9060312>
- Birr**, T., Hasler, M., Verreet, J.-A., & Klink, H. (2020). Composition and Predominance of Fusarium Species Causing Fusarium Head Blight in Winter Wheat Grain Depending on Cultivar Susceptibility and Meteorological Factors. *Microorganisms*, 8, 617, 1-24. <https://doi.org/10.3390/microorganisms8040617>
- Błaszczyk**, L., Ćwiek-Kupczyńska, H., Hoppe Gromadzka, K., Basińska-Barczak, A., Stępień, Ł., Kaczmarek, J., & Lenc, L. (2023). Containment of *Fusarium culmorum* and Its Mycotoxins in Various Biological Systems by Antagonistic *Trichoderma* and *Clonostachys* Strains. *Journal of Fungi (Basel, Switzerland)*, 9, 289, 1-25. <https://doi.org/10.3390/jof9030289>
- Boller**, T., & Felix, G. (2009). A renaissance of elicitors: Perception of microbe-associated molecular patterns and danger signals by pattern-recognition receptors. *Annual Review of Plant Biology*, 60, 379–406. <https://doi.org/10.1146/annurev.arplant.57.032905.105346>
- Bora**, K. S., Arora, S., & Shri, R. (2011). Role of *Ocimum basilicum* L. in prevention of ischemia and reperfusion-induced cerebral damage, and motor dysfunctions in mice brain. *Journal of Ethnopharmacology*, 137(3), 1360–1365. <https://doi.org/10.1016/j.jep.2011.07.066>
- Braga**, M. E. M., Leal, P. F., Carvalho, J. E., & Meireles, M. A. A. (2003). Comparison of yield, composition, and antioxidant activity of turmeric (*Curcuma longa* L.) extracts obtained using various techniques. *Journal of Agricultural and Food Chemistry*, 51(22), 6604–6611. <https://doi.org/10.1021/jf0345550>
- Brauer**, V. S., Rezende, C. P., Pessoni, A. M., De Paula, R. G., Rangappa, K. S., Nayaka, S. C., Gupta, V. K., & Almeida, F. (2019). Antifungal Agents in Agriculture: Friends and Foes of Public Health. *Biomolecules*, 9, 521, 1-21. <https://doi.org/10.3390/biom9100521>
- Breeze**, E. (2019). 97 Shades of Gray: Genetic Interactions of the Gray Mold, *Botrytis cinerea*, with Wild and Domesticated Tomato. *The Plant Cell*, 31(2), 280–281. <https://doi.org/10.1105/tpc.19.00030>
- Brown**, M. S., Baysal-Gurel, F., Oliver, J. B., & Adesso, K. M. (2019). Comparative Performance of Fungicides, Biofungicides, and Host Plant Defense Inducers in Suppression of *Phytophthora* Root Rot in Flowering Dogwood During Simulated Root Flooding Events. *Plant Disease*, 103(7), 1703–1711. <https://doi.org/10.1094/PDIS-09-18-1597-RE>
- Burgess**, T. I., Scott, J. K., McDougall, K. L., Stukely, M. J. C., Crane, C., Dunstan, W. A., Brigg, F., Andjic, V., White, D., Rudman, T., Arentz, F., Ota, N., & Hardy, G. E. S. J. (2017). Current and

- projected global distribution of *Phytophthora cinnamomi*, one of the world's worst plant pathogens. *Global Change Biology*, 23(4), 1661–1674. <https://doi.org/10.1111/gcb.13492>
- Burki**, F., Roger, A. J., Brown, M. W., & Simpson, A. G. B. (2020). The New Tree of Eukaryotes. *Trends in Ecology & Evolution*, 35(1), 43–55. <https://doi.org/10.1016/j.tree.2019.08.008>
- Cahill**, D. M., Cope, M., & Hardham, A. R. (1996). Thrust reversal by tubular mastigonemes: Immunological evidence for a role of mastigonemes in forward motion of zoospores of *Phytophthora cinnamomi*. *Protoplasma*, 194(1), 18–28. <https://doi.org/10.1007/BF01273164>
- Cai**, W. Y., Tian, H., Liu, J. R., Fang, X. L., & Nan, Z. B. (2021). *Phytophthora cactorum* as a Pathogen Associated with Root Rot on Alfalfa (*Medicago sativa*) in China. *Plant Disease*, 105(1), 231. <https://doi.org/10.1094/PDIS-04-20-0815-PDN>
- Callaway**, E. (2016). Devastating wheat fungus appears in Asia for first time. *Nature*, 532, 421–422. <https://doi.org/10.1038/532421a>
- Cannon**, P. F., Damm, U., Johnston, P. R., & Weir, B. S. (2012). *Colletotrichum*: Current status and future directions. *Studies in Mycology*, 73(1), 181–213. <https://doi.org/10.3114/sim0014>
- Card**, S., Johnson, L., Teasdale, S., & Caradus, J. (2016). Deciphering endophyte behaviour: The link between endophyte biology and efficacious biological control agents. *FEMS Microbiology Ecology*, 92(8), 1–19. <https://doi.org/10.1093/femsec/fiw114>
- Carlucci**, A., & Frisullo, S. (2009). First report of *Diplodia corticola* on grapevine in Italy. *Journal of Plant Pathology*, 91, 233. <https://fair.unifg.it/handle/11369/16468>
- Carraro**, G. (1997). *AGROTÓXICO E MEIO AMBIENTE: Uma proposta de Ensino de Ciências e de Química*. Porto Alegre, 1–95.
- Cebulski**, J., Malouin, J., Pinches, N., Cascio, V., & Austriaco, N. (2011). Yeast Bax inhibitor, Bxi1p, is an ER-localized protein that links the unfolded protein response and programmed cell death in *Saccharomyces cerevisiae*. *PloS One*, 6(6), e20882, 1–7. <https://doi.org/10.1371/journal.pone.0020882>
- Ceci**, A., Pinzari, F., Riccardi, C., Maggi, O., Pierro, L., Petrangeli Papini, M., Gadd, G. M., & Persiani, A. M. (2018). Metabolic synergies in the biotransformation of organic and metallic toxic compounds by a saprotrophic soil fungus. *Applied Microbiology and Biotechnology*, 102(2), 1019–1033. <https://doi.org/10.1007/s00253-017-8614-9>
- Ceci**, A., Pinzari, F., Russo, F., Persiani, A. M., & Gadd, G. M. (2019). Roles of saprotrophic fungi in biodegradation or transformation of organic and inorganic pollutants in co-contaminated sites. *Applied Microbiology and Biotechnology*, 103(1), 53–68. <https://doi.org/10.1007/s00253-018-9451-1>
- Celiz**, M. D., Tso, J., & Aga, D. S. (2009). Pharmaceutical metabolites in the environment: Analytical challenges and ecological risks. *Environmental Toxicology and Chemistry*, 28(12), 2473–2484. <https://doi.org/10.1897/09-173.1>
- Chatterjee**, S., Kuang, Y., Splivallo, R., Chatterjee, P., & Karlovsky, P. (2016). Interactions among filamentous fungi *Aspergillus niger*, *Fusarium verticillioides* and *Clonostachys rosea*: Fungal biomass, diversity of secreted metabolites and fumonisin production. *BMC Microbiology*, 16(83), 1–13. <https://doi.org/10.1186/s12866-016-0698-3>
- Chen**, C., Long, L., Zhang, F., Chen, Q., Chen, C., Yu, X., Liu, Q., Bao, J., & Long, Z. (2018). Antifungal activity, main active components and mechanism of *Curcuma longa* extract against *Fusarium graminearum*. *PloS One*, 13(3), e0194284, 1–19. <https://doi.org/10.1371/journal.pone.0194284>
- Chen**, I.-N., Chang, C.-C., Ng, C.-C., Wang, C.-Y., Shyu, Y.-T., & Chang, T.-L. (2008). Antioxidant and Antimicrobial Activity of Zingiberaceae Plants in Taiwan. *Plant Foods for Human Nutrition*, 63(1), 15–20. <https://doi.org/10.1007/s11130-007-0063-7>

- Chen**, X.-R., Huang, S.-X., Zhang, Y., Sheng, G.-L., Zhang, B.-Y., Li, Q.-Y., Zhu, F., & Xu, J.-Y. (2018). Transcription profiling and identification of infection-related genes in *Phytophthora cactorum*. *Molecular Genetics and Genomics: MGG*, *293*(2), 541–555. <https://doi.org/10.1007/s00438-017-1400-7>
- Chen**, Y., Zhu, J., Ying, S.-H., & Feng, M.-G. (2014). Three mitogen-activated protein kinases required for cell wall integrity contribute greatly to biocontrol potential of a fungal entomopathogen. *PLoS One*, *9*(2), e87948, 1-11. <https://doi.org/10.1371/journal.pone.0087948>
- Chin**, C., Donaghey, F., Helming, K., McCarthy, M., Rogers, S., & Austriaco, N. (2014). Deletion of AIF1 but not of YCA1/MCA1 protects *Saccharomyces cerevisiae* and *Candida albicans* cells from caspofungin-induced programmed cell death. *Microbial Cell (Graz, Austria)*, *1*(2), 58–63. <https://doi.org/10.15698/mic2014.01.119>
- Chung**, H.-C., Kim, M.-S., Mun, S.-Y., Sa, B.-K., Chung, J.-Y., Kim, D.-U., & Hwang, J.-K. (2012). Effect of oral administration of nutmeg extract on american house dust mite (*Dermatophagoides farinae*) extract-induced atopic dermatitis-like skin lesions in NC/Nga mice. *Food Science and Biotechnology*, *21*(2), 559–564. <https://doi.org/10.1007/s10068-012-0071-8>
- Cimmino**, A., Maddau, L., Masi, M., Evidente, M., Linaldeddu, B., & Evidente, A. (2016). Further secondary metabolites produced by *Diplodia corticola*, a fungal pathogen involved in cork oak decline. *Tetrahedron*, *72*(43), 6788-6793. <https://doi.org/10.1016/j.tet.2016.09.008>
- Cook**, R. J. (1980). Fusarium foot rot of wheat and its control in the Pacific Northwest. *Plant Disease*, *64*(12), 1061–1066. <https://doi.org/10.1094/PD-64-1061>
- Corcobado**, T., Cubera, E., Juárez, E., Moreno, G., & Solla, A. (2014). Drought events determine performance of *Quercus ilex* seedlings and increase their susceptibility to *Phytophthora cinnamomi*. *Agricultural and Forest Meteorology*, *192–193*, 1–8. <https://doi.org/10.1016/j.agrformet.2014.02.007>
- Covarelli**, L., Beccari, G., Steed, A., & Nicholson, P. (2012). Colonization of soft wheat following infection of the stem base by *Fusarium culmorum* and translocation of deoxynivalenol to the head. *Plant Pathology*, *61*(6), 1121–1129. <https://doi.org/10.1111/j.1365-3059.2012.02600.x>
- Creusot**, N., Casado-Martinez, C., Chiaia-Hernandez, A., Kiefer, K., Ferrari, B. J. D., Fu, Q., Munz, N., Stamm, C., Tlili, A., & Hollender, J. (2020). Retrospective screening of high-resolution mass spectrometry archived digital samples can improve environmental risk assessment of emerging contaminants: A case study on antifungal azoles. *Environment International*, *139*, 105708, 1-10. <https://doi.org/10.1016/j.envint.2020.105708>
- Crone**, M., McComb, J. A., O'Brien, P. A., & Hardy, G. E. S. J. (2013). Survival of *Phytophthora cinnamomi* as oospores, stromata, and thick-walled chlamydospores in roots of symptomatic and asymptomatic annual and herbaceous perennial plant species. *Fungal Biology*, *117*(2), 112–123. <https://doi.org/10.1016/j.funbio.2012.12.004>
- Cuzick**, A., Maguire, K., & Hammond-Kosack, K. E. (2009). Lack of the plant signalling component SGT1b enhances disease resistance to *Fusarium culmorum* in *Arabidopsis* buds and flowers. *The New Phytologist*, *181*(4), 901–912. <https://doi.org/10.1111/j.1469-8137.2008.02712.x>
- D'Addabbo**, T., Argentieri, M. P., Żuchowski, J., Biazzini, E., Tava, A., Oleszek, W., & Avato, P. (2020). Activity of Saponins from *Medicago* Species against Phytoparasitic Nematodes. *Plants*, *9*, 443, 1-19. <https://doi.org/10.3390/plants9040443>
- Damm**, U., Cannon, P. F., Woudenberg, J. H. C., & Crous, P. W. (2012). The *Colletotrichum acutatum* species complex. *Studies in Mycology*, *73*(1), 37–113. <https://doi.org/10.3114/sim0010>
- Dao**, T. T., Nguyen, P. H., Won, H. K., Kim, E. H., Park, J., Won, B. Y., & Oh, W. K. (2012). Curcuminoids from *Curcuma longa* and their inhibitory activities on influenza A neuraminidases. *Food Chemistry*, *134*(1), 21–28. <https://doi.org/10.1016/j.foodchem.2012.02.015>

- Davidse**, L. C. (1973). Antimitotic activity of methyl benzimidazol-2-yl carbamate (MBC) in *Aspergillus nidulans*. *Pesticide Biochemistry and Physiology*, *3*(3), 317–325. [https://doi.org/10.1016/0048-3575\(73\)90030-8](https://doi.org/10.1016/0048-3575(73)90030-8)
- Davidse**, L. C., & **Flach**, W. (1977). Differential binding of methyl benzimidazol-2-yl carbamate to fungal tubulin as a mechanism of resistance to this antimitotic agent in mutant strains of *Aspergillus nidulans*. *The Journal of Cell Biology*, *72*(1), 174–193. <https://doi.org/10.1083/jcb.72.1.174>
- Davis**, E. M., & **Croteau**, R. (2000). Cyclization Enzymes in the Biosynthesis of Monoterpenes, Sesquiterpenes, and Diterpenes. *Topics in Current Chemistry*, *209*, 1–43. https://doi.org/10.1007/3-540-48146-X_2
- Dean**, R., Van Kan, J. A. L., Pretorius, Z. A., Hammond-Kosack, K. E., Di Pietro, A., Spanu, P. D., Rudd, J. J., Dickman, M., Kahmann, R., Ellis, J., & Foster, G. D. (2012). The Top 10 fungal pathogens in molecular plant pathology. *Molecular Plant Pathology*, *13*(4), 414–430. <https://doi.org/10.1111/j.1364-3703.2011.00783.x>
- Dell**, B., Vear, K., & Carter, R. (2004). *Arresting Phytophthora Dieback: The Biological Bulldozer*. WWF Australia and Dieback Consultative Council, 1-22.
- Demestichas**, K., Peppes, N., & Alexakis, T. (2020). Survey on Security Threats in Agricultural IoT and Smart Farming. *Sensors*, *20*, 6458, 1-17. <https://doi.org/10.3390/s20226458>
- Denning**, D. W., Pleuvry, A., & Cole, D. C. (2013). Global burden of allergic bronchopulmonary aspergillosis with asthma and its complication chronic pulmonary aspergillosis in adults. *Medical Mycology*, *51*(4), 361–370. <https://doi.org/10.3109/13693786.2012.738312>
- Deshmukh**, S. K., Gupta, M. K., Prakash, V., & Saxena, S. (2018). Endophytic Fungi: A Source of Potential Antifungal Compounds. *Journal of Fungi*, *4*, 77, 1-42. <https://doi.org/10.3390/jof4030077>
- Dey**, P., Kundu, A., Kumar, A., Gupta, M., Lee, B. M., Bhakta, T., Dash, S., & Kim, H. S. (2020). Analysis of alkaloids (indole alkaloids, isoquinoline alkaloids, tropane alkaloids). *Recent Advances in Natural Products Analysis*, 505–567. <https://doi.org/10.1016/B978-0-12-816455-6.00015-9>
- Dhingra**, O., Jham, G. N., Barcelos, R. C., Mendonça, F. A. & Ghiviriga, I. (2007). Isolation and Identification of the Principal Fungitoxic Component of Turmeric Essential Oil. *Journal of Essential Oil Research*, *19*(4), 387-391. <https://doi.org/10.1080/10412905.2007.9699312>
- Dingley**, J., & **Gilmour**, J. (1972). *Colletotrichum acutatum* Simms. F.sp. Pine associated with «terminal crook» disease of *Pinus* spp. *New Zealand journal of forestry science*, *2*(2), 192-201.
- Dong**, S., Stam, R., Cano, L. M., Song, J., Sklenar, J., Yoshida, K., Bozkurt, T. O., Oliva, R., Liu, Z., Tian, M., Win, J., Banfield, M. J., Jones, A. M. E., van der Hoorn, R. A. L., & Kamoun, S. (2014). Effector specialization in a lineage of the Irish potato famine pathogen. *Science (New York, N.Y.)*, *343*(6170), 552–555. <https://doi.org/10.1126/science.1246300>
- Dou**, D., & **Zhou**, J.-M. (2012). Phytopathogen effectors subverting host immunity: Different foes, similar battleground. *Cell Host & Microbe*, *12*(4), 484–495. <https://doi.org/10.1016/j.chom.2012.09.003>
- Dreaden**, T. J., Shin, K., & Smith, J. A. (2011). First Report of *Diplodia corticola* Causing Branch Cankers on Live Oak (*Quercus virginiana*) in Florida. *Plant Disease*, *95*(8), 1027-1027. <https://doi.org/10.1094/PDIS-02-11-0123>
- Duina**, A. A., Miller, M. E., & Keeney, J. B. (2014). Budding Yeast for Budding Geneticists: A Primer on the *Saccharomyces cerevisiae* Model System. *Genetics*, *197*(1), 33–48. <https://doi.org/10.1534/genetics.114.163188>
- Efimova**, S. S., & **Ostroumova**, O. S. (2021). Is the Membrane Lipid Matrix a Key Target for Action of Pharmacologically Active Plant Saponins? *International Journal of Molecular Sciences*, *22*, 3167, 1-17. <https://doi.org/10.3390/ijms22063167>

- Ehrenpreis**, J. E., DesLauriers, C., Lank, P., Armstrong, P. K., & Leikin, J. B. (2014). Nutmeg Poisonings: A Retrospective Review of 10 Years Experience from the Illinois Poison Center, 2001–2011. *Journal of Medical Toxicology*, *10*, 148–151. <https://doi.org/10.1007/s13181-013-0379-7>
- Eifler**, J., Martinelli, E., Santonico, M., Capuano, R., Schild, D., & Di Natale, C. (2011). Differential detection of potentially hazardous *Fusarium* species in wheat grains by an electronic nose. *PLoS One*, *6*(6), e21026, 1-6. <https://doi.org/10.1371/journal.pone.0021026>
- El-Sayed**, M., & Verpoorte, R. (2007). Catharanthus terpenoid indole alkaloids: Biosynthesis and regulation. *Phytochemistry Reviews*, *6*(2), 277–305. <https://doi.org/10.1007/s11101-006-9047-8>
- Erwin**, D. C., & Ribeiro, O. K. (1996). Phytophthora diseases worldwide. *American Phytopathological Society (APS Press)*, 562. ISBN: 9780890542125
- Fahrenkrog**, B., Sauder, U., & Aebi, U. (2004). The *S. cerevisiae* HtrA-like protein Nma111p is a nuclear serine protease that mediates yeast apoptosis. *Journal of Cell Science*, *117*(Pt 1), 115–126. <https://doi.org/10.1242/jcs.00848>
- Fannjiang**, Y., Cheng, W.-C., Lee, S. J., Qi, B., Pevsner, J., McCaffery, J. M., Hill, R. B., Basañez, G., & Hardwick, J. M. (2004). Mitochondrial fission proteins regulate programmed cell death in yeast. *Genes & Development*, *18*(22), 2785–2797. <https://doi.org/10.1101/gad.1247904>
- FAO**, I. (2021). *The State of Food Security and Nutrition in the World 2021: Transforming food systems for food security, improved nutrition and affordable healthy diets for all*. FAO. <https://doi.org/10.4060/cb4474en>
- FAOSTAT**. (2022). <https://www.fao.org/faostat/en/#compare>
- Farias**, S. A. de S., Costa, K. S. da, & Martins, J. B. L. (2021). Analysis of Conformational, Structural, Magnetic, and Electronic Properties Related to Antioxidant Activity: Revisiting Flavan, Anthocyanidin, Flavanone, Flavonol, Isoflavone, Flavone, and Flavan-3-ol. *ACS Omega*, *6*(13), 8908–8918. <https://doi.org/10.1021/acsomega.0c06156>
- Farzana**, Abid, M., & Hussain, F. (2022). Screening of ethnomedicinal plants for their antifungal and nematocidal activities against soil-borne phytopathogens. *South African Journal of Botany*, *147*, 18–23. <https://doi.org/10.1016/j.sajb.2021.12.003>
- Fawke**, S., Doumane, M., & Schornack, S. (2015). Oomycete Interactions with Plants: Infection Strategies and Resistance Principles. *Microbiology and Molecular Biology Reviews: MMBR*, *79*(3), 263–280. <https://doi.org/10.1128/MMBR.00010-15>
- Ferguson**, L. R. (2001). Role of plant polyphenols in genomic stability. *Mutation Research*, *475*(1–2), 89–111. [https://doi.org/10.1016/s0027-5107\(01\)00073-2](https://doi.org/10.1016/s0027-5107(01)00073-2)
- Fernandes**, I. O. (2015). *Infection mechanism of Diplodia corticola* [doctoralThesis, Universidade de Aveiro]. <https://ria.ua.pt/handle/10773/15487>
- Ferreira**, F. D., Mossini, S. A. G., Dias Ferreira, F. M., Arrotéia, C. C., da Costa, C. L., Nakamura, C. V., & Machinski, M. (2013). The inhibitory effects of *Curcuma longa* L. essential oil and curcumin on *Aspergillus flavus* link growth and morphology. *TheScientificWorldJournal*, *2013*, 343804, 1-6. <https://doi.org/10.1155/2013/343804>
- Ferreira**, M. L. F. L., Rius, S. P., & Casati, P. (2012). Flavonoids: Biosynthesis, biological functions, and biotechnological applications. *Frontiers in Plant Science*, *3*, 222, 1-15. <https://doi.org/10.3389/fpls.2012.00222>
- Forget**, G. (1993). Balancing the need for pesticides with the risk to human health. *IDRC Ottawa*, 2-16.
- Giraldo**, M. C., Dagdas, Y. F., Gupta, Y. K., Mentlak, T. A., Yi, M., Martinez-Rocha, A. L., Saitoh, H., Terauchi, R., Talbot, N. J., & Valent, B. (2013). Two distinct secretion systems facilitate tissue invasion by the rice blast fungus *Magnaporthe oryzae*. *Nature Communications*, *4*, 1996, 1-12. <https://doi.org/10.1038/ncomms2996>

- Grassini**, P., Eskridge, K. M., & Cassman, K. G. (2013). Distinguishing between yield advances and yield plateaus in historical crop production trends. *Nature Communications*, *4*, 2918, 1-11. <https://doi.org/10.1038/ncomms3918>
- Greig**, D., & **Leu**, J.-Y. (2009). Natural history of budding yeast. *Current Biology: CB*, *19*(19), R886-890. <https://doi.org/10.1016/j.cub.2009.07.037>
- Gromadzka**, K., Chelkowski, J., Stepien, L., & Golinski, P. (2008). Occurrence of zearalenone in wheat and maize grain in Poland. *Cereal Research Communications*, *36*, 361–363.
- Guaragnella**, N., Pereira, C., Sousa, M. J., Antonacci, L., Passarella, S., Côte-Real, M., Marra, E., & Giannattasio, S. (2006). YCA1 participates in the acetic acid induced yeast programmed cell death also in a manner unrelated to its caspase-like activity. *FEBS Letters*, *580*(30), 6880–6884. <https://doi.org/10.1016/j.febslet.2006.11.050>
- Gul**, W., & **Hamann**, M. T. (2005). Indole alkaloid marine natural products: An established source of cancer drug leads with considerable promise for the control of parasitic, neurological and other diseases. *Life Sciences*, *78*(5), 442–453. <https://doi.org/10.1016/j.lfs.2005.09.007>
- Gupta**, A. D., Bansal, V. K., Babu, V., & Maithil, N. (2013). Chemistry, antioxidant and antimicrobial potential of nutmeg (*Myristica fragrans* Houtt). *Journal of Genetic Engineering and Biotechnology*, *11*(1), 25–31. <https://doi.org/10.1016/j.jgeb.2012.12.001>
- Gustin**, M. C., Albertyn, J., Alexander, M., & Davenport, K. (1998). MAP kinase pathways in the yeast *Saccharomyces cerevisiae*. *Microbiology and Molecular Biology Reviews: MMBR*, *62*(4), 1264–1300. <https://doi.org/10.1128/MMBR.62.4.1264-1300.1998>
- Ha**, M. T., Vu, N. K., Tran, T. H., Kim, J. A., Woo, M. H., & Min, B. S. (2020). Phytochemical and pharmacological properties of *Myristica fragrans* Houtt.: An updated review. *Archives of Pharmacal Research*, *43*(11), 1067–1092. <https://doi.org/10.1007/s12272-020-01285-4>
- Hamdi**, O. A. A., Awang, K., Hadi, A. H. A., Syamsir, D. R., & Ng, S. W. (2010). Curcumenol from *Curcuma zedoaria*: A second monoclinic modification. *Acta Crystallographica. Section E, Structure Reports Online*, *66*, o2844, 1-11. <https://doi.org/10.1107/S1600536810040559>
- Han**, J. W., Shim, S. H., Jang, K. S., Choi, Y. H., Dang, Q. L., Kim, H., & Choi, G. J. (2018). In vivo assessment of plant extracts for control of plant diseases: A sesquiterpene ketolactone isolated from *Curcuma zedoaria* suppresses wheat leaf rust. *Journal of Environmental Science and Health. Part B, Pesticides, Food Contaminants, and Agricultural Wastes*, *53*(2), 135–140. <https://doi.org/10.1080/03601234.2017.1397448>
- Hardham**, A. R. (2005). *Phytophthora cinnamomi*. *Molecular Plant Pathology*, *6*(6), 589–604. <https://doi.org/10.1111/j.1364-3703.2005.00308.x>
- Hardham**, A. R., & **Blackman**, L. M. (2018). *Phytophthora cinnamomi*. *Molecular Plant Pathology*, *19*(2), 260–285. <https://doi.org/10.1111/mpp.12568>
- He**, Q., McLellan, H., Boevink, P. C., & Birch, P. R. J. (2020). All Roads Lead to Susceptibility: The Many Modes of Action of Fungal and Oomycete Intracellular Effectors. *Plant Communications*, *1*, 100050, 1-12. <https://doi.org/10.1016/j.xplc.2020.100050>
- Herrera**, J. M., Zunino, M. P., Dambolena, J. S., Pizzolitto, R. P., Gañan, N. A., Lucini, E. I. & Zygadlo, J. A. (2015). Terpene ketones as natural insecticides against *Sitophilus zeamais*. *Industrial Crops and Products*, *70*, 435-442. <https://doi.org/10.1016/j.indcrop.2015.03.074>
- Herrick**, E. J., & **Hashmi**, M. F. (2023). Antifungal Ergosterol Synthesis Inhibitors. *StatPearls Publishing*. <http://www.ncbi.nlm.nih.gov/books/NBK551581/>
- Hill**, S. M., Hao, X., Liu, B., & Nyström, T. (2014). Life-span extension by a metacaspase in the yeast *Saccharomyces cerevisiae*. *Science (New York, N.Y.)*, *344*(6190), 1389–1392. <https://doi.org/10.1126/science.1252634>

- Hof**, H. (2001). Critical Annotations to the Use of Azole Antifungals for Plant Protection. *Antimicrobial Agents and Chemotherapy*, 45(11), 2987–2990. <https://doi.org/10.1128/AAC.45.11.2987-2990.2001>
- Hohl**, H. R., & **Stössel**, P. (1976). Host–parasite interfaces in a resistant and a susceptible cultivar of *Solanum tuberosum* inoculated with *Phytophthora infestans*: Tuber tissue. *Canadian Journal of Botany*, 54(9), 900–912. <https://doi.org/10.1139/b76-094>
- Horbach**, R., Navarro-Quesada, A. R., Knogge, W., & Deising, H. B. (2011). When and how to kill a plant cell: Infection strategies of plant pathogenic fungi. *Journal of Plant Physiology*, 168(1), 51–62. <https://doi.org/10.1016/j.jplph.2010.06.014>
- Hsu**, H., Sheth, C. C., & Veses, V. (2021). Herbal Extracts with Antifungal Activity against *Candida albicans*: A Systematic Review. *Mini-Reviews in Medicinal Chemistry*, 21(1), 90–117. <https://doi.org/10.2174/1389557520666200628032116>
- Hu**, L., & Yang, L. (2019). Time to Fight: Molecular Mechanisms of Age-Related Resistance. *Phytopathology*, 109(9), 1500–1508. <https://doi.org/10.1094/PHYTO-11-18-0443-RVW>
- Hu**, Y., Zhang, J., Kong, W., Zhao, G., & Yang, M. (2017). Mechanisms of antifungal and anti-aflatoxigenic properties of essential oil derived from turmeric (*Curcuma longa* L.) on *Aspergillus flavus*. *Food Chemistry*, 220, 1–8. <https://doi.org/10.1016/j.foodchem.2016.09.179>
- Ibáñez**, M. D., & **Blázquez**, M. A. (2020). *Curcuma longa* L. Rhizome Essential Oil from Extraction to Its Agri-Food Applications. A Review. *Plants*, 10, 44-75. <https://doi.org/10.3390/plants10010044>
- Ijaz**, M., Mahmood, K., & Honermeier, B. (2015). Interactive Role of Fungicides and Plant Growth Regulator (Trinexapac) on Seed Yield and Oil Quality of Winter Rapeseed. *Agronomy*, 5, 435-446. <https://doi.org/10.3390/agronomy5030435>
- Ismail**, E., Sabry, D., Younis, H., & Khalil, M. (2014). Synthesis and Characterization of some Ternary Metal Complexes of Curcumin with 1,10-phenanthroline and their Anticancer Applications. *Journal of Scientific Research*, 6(3), 509-519. <https://doi.org/10.3329/jsr.v6i3.18750>
- Iyer**, M., Gujjari, A. K., Gowda, V., & Angadi, S. (2017). Antifungal response of oral-associated candidal reference strains (American Type Culture Collection) by supercritical fluid extract of nutmeg seeds for geriatric denture wearers: An in vitro screening study. *The Journal of the Indian Prosthodontic Society*, 17(3), 267–272. https://doi.org/10.4103/jips.jips_10_17
- Jachak**, G. R., Ramesh, R., Sant, D. G., Jorwekar, S. U., Jadhav, M. R., Tupe, S. G., Deshpande, M. V., & Reddy, D. S. (2015). Silicon Incorporated Morpholine Antifungals: Design, Synthesis, and Biological Evaluation. *ACS Medicinal Chemistry Letters*, 6(11), 1111–1116. <https://doi.org/10.1021/acsmedchemlett.5b00245>
- Jayasinghe**, C., Gotoh, N., Aoki, T., & Wada, S. (2003). Phenolics composition and antioxidant activity of sweet basil (*Ocimum basilicum* L.). *Journal of Agricultural and Food Chemistry*, 51(15), 4442–4449. <https://doi.org/10.1021/jf034269o>
- Jendretzki**, A., Wittland, J., Wilk, S., Straede, A., & Heinisch, J. J. (2011). How do I begin? Sensing extracellular stress to maintain yeast cell wall integrity. *European Journal of Cell Biology*, 90(9), 740–744. <https://doi.org/10.1016/j.ejcb.2011.04.006>
- Jiménez-Reyes**, M. F., Carrasco, H., Olea, A. F., & Silva-Moreno, E. (2019). Natural Compounds: A Sustainable Alternative To The Phytopathogens Control. *Journal of the Chilean Chemical Society*, 64(2), 4459–4465. <https://doi.org/10.4067/S0717-97072019000204459>
- Jin**, D.-Q., Lim, C. S., Hwang, J. K., Ha, I., & Han, J.-S. (2005). Anti-oxidant and anti-inflammatory activities of macelignan in murine hippocampal cell line and primary culture of rat microglial cells. *Biochemical and Biophysical Research Communications*, 331(4), 1264–1269. <https://doi.org/10.1016/j.bbrc.2005.04.036>

- Johnston, P. R., & Jones, D.** (1997). Relationships among Colletotrichum isolates from fruit-rots assessed using rDNA sequences. *Mycologia*, *89*(3), 420–430. <https://doi.org/10.1080/00275514.1997.12026801>
- Jones, J. D. G., & Dangl, J. L.** (2006). The plant immune system. *Nature*, *444*(7117), 323–329. <https://doi.org/10.1038/nature05286>
- Jonge, R., Bolton, M. D., & Thomma, B. P. H. J.** (2011). How filamentous pathogens co-opt plants: The ins and outs of fungal effectors. *Current Opinion in Plant Biology*, *14*(4), 400–406. <https://doi.org/10.1016/j.pbi.2011.03.005>
- Jordá, T., & Puig, S.** (2020). Regulation of Ergosterol Biosynthesis in *Saccharomyces cerevisiae*. *Genes*, *11*, 795–813. <https://doi.org/10.3390/genes11070795>
- Judelson, H. S., & Blanco, F. A.** (2005). The spores of Phytophthora: Weapons of the plant destroyer. *Nature Reviews Microbiology*, *3*, 47–58. <https://doi.org/10.1038/nrmicro1064>
- Kachroo, A. H., Laurent, J. M., Yellman, C. M., Meyer, A. G., Wilke, C. O., & Marcotte, E. M.** (2015). Evolution. Systematic humanization of yeast genes reveals conserved functions and genetic modularity. *Science (New York, N.Y.)*, *348*(6237), 921–925. <https://doi.org/10.1126/science.aaa0769>
- Kammoun, L. G., Gargouri, S., Barreau, C., Richard-Forget, F., & Hajlaoui, M. R.** (2010). Trichothecene chemotypes of *Fusarium culmorum* infecting wheat in Tunisia. *International Journal of Food Microbiology*, *140*(1), 84–89. <https://doi.org/10.1016/j.ijfoodmicro.2010.01.040>
- Kamoun, S.** (2009). Plant Pathogens: Oomycetes (water mold). Em M. Schaechter (Ed.), *Encyclopedia of Microbiology (Third Edition)* (pp. 689–695). Academic Press. <https://doi.org/10.1016/B978-012373944-5.00349-7>
- Kamoun, S., Furzer, O., Jones, J. D. G., Judelson, H. S., Ali, G. S., Dalio, R. J. D., Roy, S. G., Schena, L., Zambounis, A., Panabières, F., Cahill, D., Ruocco, M., Figueiredo, A., Chen, X.-R., Hulvey, J., Stam, R., Lamour, K., Gijzen, M., Tyler, B. M., ... Govers, F.** (2015). The Top 10 oomycete pathogens in molecular plant pathology. *Molecular Plant Pathology*, *16*(4), 413–434. <https://doi.org/10.1111/mpp.12190>
- Kauppinen, M., Saikkonen, K., Helander, M., Pirttilä, A. M., & Wäli, P. R.** (2016). Epichloë grass endophytes in sustainable agriculture. *Nature Plants*, *2*, 15224. <https://doi.org/10.1038/nplants.2015.224>
- Kennedy, D., & Wightman, E.** (2011). Herbal Extracts and Phytochemicals: Plant Secondary Metabolites and the Enhancement of Human Brain Function. *Advances in Nutrition*, *2*, 32–50. <https://doi.org/10.3945/an.110.000117>
- Khan, R. A. A., Najeeb, S., Hussain, S., Xie, B., & Li, Y.** (2020). Bioactive Secondary Metabolites from *Trichoderma* spp. Against Phytopathogenic Fungi. *Microorganisms*, *8*, 817–839. <https://doi.org/10.3390/microorganisms8060817>
- Khang, C. H., Berruyer, R., Giraldo, M. C., Kankanala, P., Park, S.-Y., Czymmek, K., Kang, S., & Valent, B.** (2010). Translocation of *Magnaporthe oryzae* Effectors into Rice Cells and Their Subsequent Cell-to-Cell Movement. *The Plant Cell*, *22*(4), 1388–1403. <https://doi.org/10.1105/tpc.109.069666>
- Knobloch, K., Pauli, A., Iberl, B., Weigand, H. & Weis, N.** (1989). Antibacterial and Antifungal Properties of Essential Oil Components. *Journal of Essential Oil Research*, *1*(3), 119–128. <https://doi.org/10.1080/10412905.1989.9697767>
- Knunyants, I., & Zefirov, N.** (1988). Chemical Encyclopedia. *Sov. Entsikl*, *1*, 623.
- Kodedová, M., & Sychrová, H.** (2015). Changes in the Sterol Composition of the Plasma Membrane Affect Membrane Potential, Salt Tolerance and the Activity of Multidrug Resistance Pumps in *Saccharomyces cerevisiae*. *PLOS ONE*, *10*(9), e0139306, 1–19. <https://doi.org/10.1371/journal.pone.0139306>

- Koh**, S., André, A., Edwards, H., Ehrhardt, D., & Somerville, S. (2005). Arabidopsis thaliana subcellular responses to compatible Erysiphe cichoracearum infections. *The Plant Journal: For Cell and Molecular Biology*, 44(3), 516–529. <https://doi.org/10.1111/j.1365-313X.2005.02545.x>
- Kosmidis**, C., & **Denning**, D. W. (2015). The clinical spectrum of pulmonary aspergillosis. *Thorax*, 70(3), 270–277. <https://doi.org/10.1136/thoraxjnl-2014-206291>
- Kristan**, K., & **Rižner**, T. L. (2012). Steroid-transforming enzymes in fungi. *The Journal of Steroid Biochemistry and Molecular Biology*, 129(1), 79–91. <https://doi.org/10.1016/j.jsbmb.2011.08.012>
- Kumar**, K. N., Venkataramana, M., Allen, J. A., Chandranayaka, S., Murali, H. S. & Batra, H. V. (2016). Role of Curcuma longa L. essential oil in controlling the growth and zearalenone production of Fusarium graminearum. *LWT - Food Science and Technology*, 69, 522-528. <https://doi.org/10.1016/j.lwt.2016.02.005>
- Kuntzmann**, P., Villaume, S., & Bertsch, C. (2009). Conidia dispersal of Diplodia species in a French vineyard. *Phytopathologia Mediterranea*, 48, 150-154. https://doi.org/10.14601/Phytopathol_Mediterr-2885
- Kuo**, S.-C., Chuang, S.-K., Lin, H.-Y., & Wang, L.-H. (2009). Study of the aerosol fragrances of eugenol derivatives in Cananga odorata using diffuse reflectance infrared Fourier transform spectroscopy and gas chromatography. *Analytica Chimica Acta*, 653(1), 91–96. <https://doi.org/10.1016/j.aca.2009.08.034>
- Lakshmi**, S., Padmaja, G., & Remani, P. (2011). Antitumour Effects of Isocurcumenol Isolated from Curcuma zedoaria Rhizomes on Human and Murine Cancer Cells. *International Journal of Medicinal Chemistry*, 2011, e253962, 1-13. <https://doi.org/10.1155/2011/253962>
- Leber**, R., Landl, K., Zinser, E., Ahorn, H., Spök, A., Kohlwein, S. D., Turnowsky, F., & Daum, G. (1998). Dual Localization of Squalene Epoxidase, Erg1p, in Yeast Reflects a Relationship between the Endoplasmic Reticulum and Lipid Particles. *Molecular Biology of the Cell*, 9(2), 375–386. <https://doi.org/10.1091/mbc.9.2.375>
- Lecce**, R. D., Masi, M., Linaldeddu, B. T., Pescitelli, G., Maddau, L., & Evidente, A. (2021). Bioactive secondary metabolites produced by the emerging pathogen Diplodia olivarum. *Phytopathologia Mediterranea*, 60(1), 129-138. <https://doi.org/10.36253/phyto-12170>
- Lee**, D., Kim, D.-H., Jeon, Y.-A., Uhm, J., & Hong, S.-B. (2007). Molecular and Cultural Characterization of Colletotrichum spp. Causing Bitter Rot of Apples in Korea. *The Plant Pathology Journal*, 23(2), 37-44. <https://doi.org/10.5423/PPJ.2007.23.2.037>
- Lee**, H.-S. (2006). Antimicrobial Property of Turmeric (Curcuma longa L.) Rhizome-Derived ar-Turmerone and Curcumin. *Food Science and Biotechnology*, 15, 559-563.
- Lee**, R. E. C., Brunette, S., Puente, L. G., & Megeney, L. A. (2010). Metacaspase Yca1 is required for clearance of insoluble protein aggregates. *Proceedings of the National Academy of Sciences*, 107(30), 13348–13353. <https://doi.org/10.1073/pnas.1006610107>
- Lee**, S.-H., Chang, K.-S., Su, M.-S., Huang, Y.-S., & Jang, H.-D. (2007). Effects of some Chinese medicinal plant extracts on five different fungi. *Food Control*, 18, 1547–1554. <https://doi.org/10.1016/j.foodcont.2006.12.005>
- Lee**, Y., Robbins, N., & Cowen, L. E. (2023). Molecular mechanisms governing antifungal drug resistance. *Npj Antimicrobials and Resistance*, 1(5), 1-9. <https://doi.org/10.1038/s44259-023-00007-2>
- Levin**, D. E. (2005). Cell Wall Integrity Signaling in Saccharomyces cerevisiae. *Microbiology and Molecular Biology Reviews*, 69(2), 262–291. <https://doi.org/10.1128/MMBR.69.2.262-291.2005>
- Levin**, D. E. (2011). Regulation of Cell Wall Biogenesis in Saccharomyces cerevisiae: The Cell Wall Integrity Signaling Pathway. *Genetics*, 189(4), 1145–1175. <https://doi.org/10.1534/genetics.111.128264>

- Li, J.**, Gu, F., Wu, R., Yang, J., & Zhang, K.-Q. (2017). Phylogenomic evolutionary surveys of subtilase superfamily genes in fungi. *Scientific Reports*, *7*(45456), 1-15. <https://doi.org/10.1038/srep45456>
- Li, M.**, Asano, T., Suga, H., & Kageyama, K. (2011). A Multiplex PCR for the Detection of *Phytophthora nicotianae* and *P. cactorum*, and a Survey of Their Occurrence in Strawberry Production Areas of Japan. *Plant Disease*, *95*(10), 1270–1278. <https://doi.org/10.1094/PDIS-01-11-0076>
- Li, S.**, Yuan, W., Deng, G., Wang, P., Yang, P., & Aggarwal, B. B. (2011). Chemical Composition and Product Quality Control of Turmeric (*Curcuma longa* L.). *Pharmaceutical Crops*, *2*, 28-54. <https://benthamopen.com/ABSTRACT/TOPHARMCJ-2-28>
- Li, X. C.**, ElSohly, H. N., Nimrod, A. C., & Clark, A. M. (1999). Antifungal jujubogenin saponins from *Colubrina retusa*. *Journal of Natural Products*, *62*(5), 674–677. <https://doi.org/10.1021/np9803169>
- Liberto**, M. D., Svetaz, L., Furlán, R. L. E., Zacchino, S. A., Delporte, C., Novoa, M. A., Asencio, M., & Cassels, B. K. (2010). Antifungal activity of saponin-rich extracts of *Phytolacca dioica* and of the saponins obtained through hydrolysis. *Natural Product Communications*, *5*(7), 1013–1018.
- Lieberman, A., & Curtis, L.** (2018). Severe Adverse Reactions Following Ketoconazole, Fluconazole, and Environmental Exposures: A Case Report. *Drug Safety - Case Reports*, *5*, 18-23. <https://doi.org/10.1007/s40800-018-0083-2>
- Linaldeddu, B. T.**, Scanu, B., Maddau, L., & Franceschini, A. (2014). *Diplodia corticola* and *Phytophthora cinnamomi*: The main pathogens involved in holm oak decline on Caprera Island (Italy). *Forest Pathology*, *44*(3), 191–200. <https://doi.org/10.1111/efp.12081>
- Liu, S.**, Fu, L., Tan, H., Jiang, J., Che, Z., Tian, Y., & Chen, G. (2021). Resistance to Boscalid in *Botrytis cinerea* From Greenhouse-Grown Tomato. *Plant Disease*, *105*(3), 628–635. <https://doi.org/10.1094/PDIS-06-20-1191-RE>
- Liu, S.**, Hai, F., & Jiang, J. (2017). Sensitivity to Fludioxonil of *Botrytis cinerea* Isolates from Tomato in Henan Province of China and Characterizations of Fludioxonil-resistant Mutants. *Journal of Phytopathology*, *165*(2), 98-104. <https://doi.org/10.1111/jph.12542>
- Liu, S.**, Ruan, W., Li, J., Xu, H., Wang, J., Gao, Y. & Wang, J. (2008). Biological Control of Phytopathogenic Fungi by Fatty Acids. *Mycopathologia*, *166*, 93-102. <https://doi.org/10.1007/s11046-008-9124-1>
- LoPachin, R. M. & Gavin, T.** (2016). Reactions of electrophiles with nucleophilic thiolate sites: relevance to pathophysiological mechanisms and remediation. *Free Radical Research*, *50*(2), 195-205. <https://doi.org/10.3109/10715762.2015.1094184>
- López, V.**, Gerique, J., Langa, E., Berzosa, C., Valero, M. S., & Gómez-Rincón, C. (2015). Antihelmintic effects of nutmeg (*Myristica fragans*) on *Anisakis simplex* L3 larvae obtained from *Micromesistius potassou*. *Research in Veterinary Science*, *100*, 148–152. <https://doi.org/10.1016/j.rvsc.2015.03.033>
- Lourenço, D.**, Leon, P., Santos, L., Choupina, A. B., & Marques, P. (2019). Molecular factors associated with pathogenicity of *Phytophthora cinnamomi*: Fatores moleculares associados com a patogenicidade de *Phytophthora cinnamomi*. *Revista de Ciências Agrárias*, *42*(4), 1059-1070. <https://doi.org/10.19084/rca.18577>
- Lowe, R.**, Jubault, M., Canning, G., Urban, M., & Hammond-Kosack, K. E. (2012). The induction of mycotoxins by trichothecene producing *Fusarium* species. *Methods in Molecular Biology (Clifton, N.J.)*, *835*, 439–455. https://doi.org/10.1007/978-1-61779-501-5_27
- Lynch, S. C.**, Eskalen, A., Zambino, P. J., Mayorquin, J. S., & Wang, D. H. (2013). Identification and pathogenicity of *Botryosphaeriaceae* species associated with coast live oak (*Quercus agrifolia*) decline in southern California. *Mycologia*, *105*(1), 125–140. <https://doi.org/10.3852/12-047>
- Maas, J. L.** (1998). Compendium of strawberry diseases (2nd ed). *APS Press*, 1-98.

- Macías-Rubalcava, M. L., & Sánchez-Fernández, R. E.** (2016). Secondary metabolites of endophytic Xylaria species with potential applications in medicine and agriculture. *World Journal of Microbiology and Biotechnology*, *33*, 15. <https://doi.org/10.1007/s11274-016-2174-5>
- Madeo, F., Fröhlich, E., Ligr, M., Grey, M., Sigrist, S. J., Wolf, D. H., & Fröhlich, K. U.** (1999). Oxygen stress: A regulator of apoptosis in yeast. *The Journal of Cell Biology*, *145*(4), 757–767. <https://doi.org/10.1083/jcb.145.4.757>
- Madeo, F., Herker, E., Maldener, C., Wissing, S., Lächelt, S., Herlan, M., Fehr, M., Lauber, K., Sigrist, S. J., Wesselborg, S., & Fröhlich, K. U.** (2002). A caspase-related protease regulates apoptosis in yeast. *Molecular Cell*, *9*(4), 911–917. [https://doi.org/10.1016/s1097-2765\(02\)00501-4](https://doi.org/10.1016/s1097-2765(02)00501-4)
- Madhumitha, G., & Saral, A.** (2011). Preliminary phytochemical analysis, antibacterial, antifungal and anticandidal activities of successive extracts of *Crossandra infundibuliformis*. *Asian Pacific Journal of Tropical Medicine*, *4*(3), 192–195. [https://doi.org/10.1016/S1995-7645\(11\)60067-9](https://doi.org/10.1016/S1995-7645(11)60067-9)
- Mahato, S. B., & Sen, S.** (1997). Advances in triterpenoid research, 1990-1994. *Phytochemistry*, *44*(7), 1185–1236. [https://doi.org/10.1016/s0031-9422\(96\)00639-5](https://doi.org/10.1016/s0031-9422(96)00639-5)
- Malcolm, J. R., Liu, C., Neilson, R. P., Hansen, L., & Hannah, L.** (2006). Global warming and extinctions of endemic species from biodiversity hotspots. *Conservation Biology: The Journal of the Society for Conservation Biology*, *20*(2), 538–548. <https://doi.org/10.1111/j.1523-1739.2006.00364.x>
- Manire, C. A., Rhinehart, H. L., Sutton, D. A., Thompson, E. H., Rinaldi, M. G., Buck, J. D., & Jacobson, E.** (2002). Disseminated mycotic infection caused by *Colletotrichum acutatum* in a Kemp's ridley sea turtle (*Lepidochelys kempi*). *Journal of Clinical Microbiology*, *40*(11), 4273–4280. <https://doi.org/10.1128/JCM.40.11.4273-4280.2002>
- Manning, V. A., Andrie, R. M., Trippe, A. F., & Ciuffetti, L. M.** (2004). Ptr ToxA requires multiple motifs for complete activity. *Molecular Plant-Microbe Interactions: MPMI*, *17*(5), 491–501. <https://doi.org/10.1094/MPMI.2004.17.5.491>
- Marcelino, J., Giordano, R., Gouli, S., Gouli, V., Parker, B. L., Skinner, M., TeBeest, D., & Cesnik, R.** (2008). *Colletotrichum acutatum* var. *fioriniae* (Teleomorph: *Glomerella acutata* var. *fioriniae* var. nov.) Infection of a Scale Insect. *Mycologia*, *100*(3), 353–374.
- Marín-Menguiano, M., Moreno-Sánchez, I., Barrales, R. R., Fernández-Álvarez, A., & Ibeas, J. I.** (2019). N-glycosylation of the protein disulfide isomerase Pdi1 ensures full *Ustilago maydis* virulence. *PLoS Pathogens*, *15*(11), e1007687, 1-29. <https://doi.org/10.1371/journal.ppat.1007687>
- Marla, S. R., Chu, K., Chintamanani, S., Multani, D. S., Klempien, A., DeLeon, A., Bong-Suk, K., Dunkle, L. D., Dilkes, B. P., & Johal, G. S.** (2018). Adult plant resistance in maize to northern leaf spot is a feature of partial loss-of-function alleles of Hm1. *PLoS Pathogens*, *14*(10), e1007356, 1-24. <https://doi.org/10.1371/journal.ppat.1007356>
- Martinez-Correa, H. A., Paula, J. T., Kayano, A. C. A. V., Queiroga, C. L., Magalhães, P. M., Costa, F. T. M., & Cabral, F. A.** (2017). Composition and antimalarial activity of extracts of *Curcuma longa* L. obtained by a combination of extraction processes using supercritical CO₂, ethanol and water as solvents. *The Journal of Supercritical Fluids*, *119*, 122–129. <https://doi.org/10.1016/j.supflu.2016.08.017>
- Masi, M., Maddau, L., Linaldeddu, B. T., Cimmino, A., D'Amico, W., Scanu, B., Evidente, M., Tuzi, A., & Evidente, A.** (2016). Bioactive Secondary Metabolites Produced by the Oak Pathogen *Diplodia corticola*. *Journal of Agricultural and Food Chemistry*, *64*(1), 217–225. <https://doi.org/10.1021/acs.jafc.5b05170>
- McGovern, P. E., Glusker, D. L., Exner, L. J., & Voigt, M. M.** (1996). Neolithic resinated wine. *Nature*, *381*(6582), 480–481. <https://doi.org/10.1038/381480a0>

- McGowan, J., & Fitzpatrick, D. A.** (2020). Chapter Five—Recent advances in oomycete genomics. Em D. Kumar (Ed.), *Advances in Genetics* (Vol. 105, pp. 175–228). Academic Press. <https://doi.org/10.1016/bs.adgen.2020.03.001>
- Micali, C. O., Neumann, U., Grunewald, D., Panstruga, R., & O'Connell, R.** (2011). Biogenesis of a specialized plant-fungal interface during host cell internalization of *Golovinomyces orontii* haustoria. *Cellular Microbiology*, *13*(2), 210–226. <https://doi.org/10.1111/j.1462-5822.2010.01530.x>
- Moricca, S., Linaldeddu, B. T., Ginetti, B., Scanu, B., Franceschini, A., & Ragazzi, A.** (2016). Endemic and Emerging Pathogens Threatening Cork Oak Trees: Management Options for Conserving a Unique Forest Ecosystem. *Plant Disease*, *100*(11), 2184–2193. <https://doi.org/10.1094/PDIS-03-16-0408-FE>
- Morsy, N. F. S.** (2016). A comparative study of nutmeg (*Myristica fragrans* Houtt.) oleoresins obtained by conventional and green extraction techniques. *Journal of Food Science and Technology*, *53*(10), 3770–3777. <https://doi.org/10.1007/s13197-016-2363-0>
- Mortimer, R. K.** (2000). Evolution and variation of the yeast (*Saccharomyces*) genome. *Genome Research*, *10*(4), 403–409. <https://doi.org/10.1101/gr.10.4.403>
- Moser, R., Pertot, I., Elad, Y., & Raffaelli, R.** (2008). Farmers' attitudes toward the use of biocontrol agents in IPM strawberry production in three countries. *Biological Control*, *47*, 125–132. <https://doi.org/10.1016/j.biocontrol.2008.07.012>
- Munn, A. L., Heese-Peck, A., Stevenson, B. J., Pichler, H., & Riezman, H.** (1999). Specific Sterols Required for the Internalization Step of Endocytosis in Yeast. *Molecular Biology of the Cell*, *10*(11), 3943–3957.
- Muñoz-Adalia, E. J., & Colinas, C.** (2021). Susceptibility of cork oak (*Quercus suber*) to canker disease caused by *Diplodia corticola*: When time is of the essence. *New Forests*, *52*, 863–873. <https://doi.org/10.1007/s11056-020-09829-8>
- Muñoz-Adalia, E. J., Meijer, A., & Colinas, C.** (2022). New qPCR protocol to detect *Diplodia corticola* shows phoretic association with the oak pinhole borer *Platypus cylindrus*. *Pest Management Science*, *78*(8), 3534–3539. <https://doi.org/10.1002/ps.6994>
- Nešić, K., Habschied, K., & Mastanjević, K.** (2021). Possibilities for the Biological Control of Mycotoxins in Food and Feed. *Toxins*, *13*, 198–213. <https://doi.org/10.3390/toxins13030198>
- Nielsen, J.** (2015). Bioengineering. Yeast cell factories on the horizon. *Science (New York, N.Y.)*, *349*(6252), 1050–1051. <https://doi.org/10.1126/science.aad2081>
- Nielsen, J.** (2019). Yeast Systems Biology: Model Organism and Cell Factory. *Biotechnology Journal*, *14*(9), e1800421, 1–23. <https://doi.org/10.1002/biot.201800421>
- Nielsen, L. K., Jensen, J. D., Nielsen, G. C., Jensen, J. E., Spliid, N. H., Thomsen, I. K., Justesen, A. F., Collinge, D. B., & Jørgensen, L. N.** (2011). Fusarium Head Blight of Cereals in Denmark: Species Complex and Related Mycotoxins. *Phytopathology*, *101*(8), 960–969. <https://doi.org/10.1094/PHTO-07-10-0188>
- Nofiani, R., de Mattos-Shiple, K., Lebe, K. E., Han, L.-C., Iqbal, Z., Bailey, A. M., Willis, C. L., Simpson, T. J., & Cox, R. J.** (2018). Strobilurin biosynthesis in Basidiomycete fungi. *Nature Communications*, *9*, 3940, 1–11. <https://doi.org/10.1038/s41467-018-06202-4>
- O'Connell, R. J., & Panstruga, R.** (2006). Tête à tête inside a plant cell: Establishing compatibility between plants and biotrophic fungi and oomycetes. *The New Phytologist*, *171*(4), 699–718. <https://doi.org/10.1111/j.1469-8137.2006.01829.x>
- O'Donnell, K., Rooney, A. P., Proctor, R. H., Brown, D. W., McCormick, S. P., Ward, T. J., Frandsen, R. J. N., Lysøe, E., Rehner, S. A., Aoki, T., Robert, V. A. R. G., Crous, P. W., Groenewald, J. Z., Kang, S., & Geiser, D. M.** (2013). Phylogenetic analyses of RPB1 and RPB2 support a middle

- Cretaceous origin for a clade comprising all agriculturally and medically important fusaria. *Fungal Genetics and Biology: FG & B*, 52, 20–31. <https://doi.org/10.1016/j.fgb.2012.12.004>
- OECD.** (2006). *Test No. 208: Terrestrial Plant Test: Seedling Emergence and Seedling Growth Test*. Organisation for Economic Co-operation and Development. https://www.oecd-ilibrary.org/environment/test-no-208-terrestrial-plant-test-seedling-emergence-and-seedling-growth-test_9789264070066-en
- O’Gara**, E., Howard, K., Mccomb, J. A., Colquhoun, I., & Hardy, G. (2014). Penetration of suberised periderm of a woody host by *Phytophthora cinnamomi*. *Plant Pathology*, 64(1), 207-215. <https://doi.org/10.1111/ppa.12244>
- Okmen**, B., & **Doehlemann**, G. (2014). Inside plant: Biotrophic strategies to modulate host immunity and metabolism. *Current Opinion in Plant Biology*, 20, 19–25. <https://doi.org/10.1016/j.pbi.2014.03.011>
- Oliveira-Garcia**, E., & **Deising**, H. B. (2013). Infection structure-specific expression of β -1,3-glucan synthase is essential for pathogenicity of *Colletotrichum graminicola* and evasion of β -glucan-triggered immunity in maize. *The Plant Cell*, 25(6), 2356–2378. <https://doi.org/10.1105/tpc.112.103499>
- Pancaldi**, D., Tonti, S., Prodi, A., Salomoni, D., Dal Prà, M., Nipoti, P., Alberti, I., & Pisi, A. (2010). Survey of the main causal agents of fusarium head blight of durum wheat around Bologna, northern Italy. *Phytopathologia Mediterranea*, 49(2), 258–266.
- Pandey**, A. K., Kumar, P., Singh, P., Tripathi, N. N. & Bajpai, V. K. (2017). Essential Oils: Sources of Antimicrobials and Food Preservatives. *Front. Microbiol.*, 7, 2161-2175. <https://doi.org/10.3389/fmicb.2016.02161>
- Pandey**, A. K., Silva, A. S., Varshney, R., Chávez-González, M. L., & Singh, P. (2021). Curcuma-based botanicals as crop protectors: From knowledge to application in food crops. *Current Research in Biotechnology*, 3, 235–248. <https://doi.org/10.1016/j.crbiot.2021.07.004>
- Paoletti**, E., Anselmi, N., & Franceschini, A. (2007). Pre-exposure to ozone predisposes oak leaves to attacks by *Diplodia corticola* and *Biscogniauxia mediterranea*. *TheScientificWorldJournal*, 7(1), 222–230. <https://doi.org/10.1100/tsw.2007.22>
- Parreira**, D. F., Neves, W. dos S., & Zambolim, L. (2010). Artigo De Revisão: Resistência De Fungos A Fungicidas Inibidores De Quinona. *Revista Trópica: Ciências Agrárias e Biológicas*, 3(2), 24-35. <https://doi.org/10.0000/rtcab.v3i2.36>
- Parrish**, W. R., Stefan, C. J., & Emr, S. D. (2005). PtdIns(3)P accumulation in triple lipid-phosphatase-deletion mutants triggers lethal hyperactivation of the Rho1p/Pkc1p cell-integrity MAP kinase pathway. *Journal of Cell Science*, 118(23), 5589–5601. <https://doi.org/10.1242/jcs.02649>
- Pasquali**, M., Beyer, M., Logrieco, A., Audenaert, K., Balmas, V., Basler, R., Boutigny, A.-L., Chrpová, J., Czembor, E., Gagkaeva, T., González-Jaén, M. T., Hofgaard, I. S., Köycü, N. D., Hoffmann, L., Lević, J., Marin, P., Miedaner, T., Migheli, Q., Moretti, A., ... Vogelgsang, S. (2016). A European Database of *Fusarium graminearum* and *F. culmorum* Trichothecene Genotypes. *Frontiers in Microbiology*, 7, 406-417. <https://www.frontiersin.org/articles/10.3389/fmicb.2016.00406>
- Paul**, S., Shaw, D., Joshi, H., Singh, S., Chakrabarti, A., Rudramurthy, S. M., & Ghosh, A. K. (2022). Mechanisms of azole antifungal resistance in clinical isolates of *Candida tropicalis*. *PLOS ONE*, 17(7), e0269721, 1-14. <https://doi.org/10.1371/journal.pone.0269721>
- Peng**, Y., Li, S. J., Yan, J., Tang, Y., Cheng, J. P., Gao, A. J., Yao, X., Ruan, J. J., & Xu, B. L. (2021). Research Progress on Phytopathogenic Fungi and Their Role as Biocontrol Agents. *Frontiers in Microbiology*, 12, 670135, 1-13. <https://www.frontiersin.org/article/10.3389/fmicb.2021.670135>
- Peres**, N. A., & **Baggio**, J. S. (2019). *Phytophthora Crown Rot of Strawberry*. <https://edis.ifas.ufl.edu/publication/PP350>

- Peres**, N. A., Mackenzie, S. J., Peever, T. L., & Timmer, L. W. (2008). Postbloom fruit drop of citrus and key lime anthracnose are caused by distinct phylogenetic lineages of *Colletotrichum acutatum*. *Phytopathology*, *98*(3), 345–352. <https://doi.org/10.1094/PHYTO-98-3-0345>
- Persiani**, A. M., Maggi, O., Montalvo, J., Casado, M. A., & Pineda, F. D. (2008). Mediterranean grassland soil fungi: Patterns of biodiversity, functional redundancy and soil carbon storage. *Plant Biosystems - An International Journal Dealing with all Aspects of Plant Biology*, *142*(1), 111–119. <https://doi.org/10.1080/11263500701872713>
- Petit**, A.-N., Fontaine, F., Vatsa, P., Clément, C., & Vaillant-Gaveau, N. (2012). Fungicide impacts on photosynthesis in crop plants. *Photosynthesis Research*, *111*(3), 315–326. <https://doi.org/10.1007/s11120-012-9719-8>
- Pettitt**, T., & Parry, D. (2001). Effect of temperature on Fusarium foot rot of wheat. *American Phytopathological Society Press*, 145–160.
- Pettitt**, T., & Pegg, G. (2008). Sources of crown rot (*Phytophthora cactorum*) infection in strawberry and the effect of cold storage on susceptibility to the disease. *Annals of Applied Biology*, *125*, 279–292. <https://doi.org/10.1111/j.1744-7348.1994.tb04969.x>
- Pfordt**, A., Ramos Romero, L., Schiwiek, S., Karlovsky, P., & von Tiedemann, A. (2020). Impact of Environmental Conditions and Agronomic Practices on the Prevalence of Fusarium Species Associated with Ear- and Stalk Rot in Maize. *Pathogens*, *9*, 236-253. <https://doi.org/10.3390/pathogens9030236>
- Phillips**, A. J. L., Alves, A., Abdollahzadeh, J., Slippers, B., Wingfield, M. J., Groenewald, J. Z., & Crous, P. W. (2013). The Botryosphaeriaceae: Genera and species known from culture. *Studies in Mycology*, *76*, 51–167. <https://doi.org/10.3114/sim0021>
- Pinto**, A. P., Serrano, C., Pires, T., Mestrinho, E., Dias, L., Teixeira, D. M., & Caldeira, A. T. (2012). Degradation of terbuthylazine, difenoconazole and pendimethalin pesticides by selected fungi cultures. *The Science of the Total Environment*, *435–436*, 402–410. <https://doi.org/10.1016/j.scitotenv.2012.07.027>
- Piyo**, A., Udomsilp, J., Khang-Khun, P., & Thobunluepop, P. (2009). Antifungal activity of essential oils from Basil (*Ocimum basilicum* Linn.) and Sweet Fennel (*Ocimum gratissimum* Linn.): Alternative strategies to control pathogenic fungi in organic rice. *Asian Journal of Food and Agro-Industry*, *2*(Special Issue). <https://www.cabdirect.org/cabdirect/abstract/20123113813>
- Polashock**, J. J., Caruso, F. L., Oudemans, P. V., McManus, P. S., & Crouch, J. A. (2009). The North American cranberry fruit rot fungal community: A systematic overview using morphological and phylogenetic affinities. *Plant Pathology*, *58*(6), 1116–1127. <https://doi.org/10.1111/j.1365-3059.2009.02120.x>
- Porquier**, A., Tisserant, C., Salinas, F., Glassl, C., Wange, L., Enard, W., Hauser, A., Hahn, M., & Weiberg, A. (2021). Retrotransposons as pathogenicity factors of the plant pathogenic fungus *Botrytis cinerea*. *Genome Biology*, *22*, 225-244. <https://doi.org/10.1186/s13059-021-02446-4>
- Porsche**, F. M., Molitor, D., Beyer, M., Charton, S., André, C., & Kollar, A. (2018). Antifungal Activity of Saponins from the Fruit Pericarp of *Sapindus mukorossi* against *Venturia inaequalis* and *Botrytis cinerea*. *Plant Disease*, *102*(5), 991–1000. <https://doi.org/10.1094/PDIS-06-17-0906-RE>
- Prasad**, R., Nair, R., & Banerjee, A. (2019). Multidrug transporters of *Candida* species in clinical azole resistance. *Fungal Genetics and Biology: FG & B*, *132*, 103252, 1-8. <https://doi.org/10.1016/j.fgb.2019.103252>
- Presti**, L. L., Lanver, D., Schweizer, G., Tanaka, S., Liang, L., Tollot, M., Zuccaro, A., Reissmann, S., & Kahmann, R. (2015). Fungal effectors and plant susceptibility. *Annual Review of Plant Biology*, *66*, 513–545. <https://doi.org/10.1146/annurev-arplant-043014-114623>

- Price**, C. L., Parker, J. E., Warrilow, A. G. S., Kelly, D. E., & Kelly, S. L. (2015). Azole fungicides—Understanding resistance mechanisms in agricultural fungal pathogens. *Pest Management Science*, *71*(8), 1054–1058. <https://doi.org/10.1002/ps.4029>
- Pristov**, K. E., & **Ghannoum**, M. A. (2019). Resistance of *Candida* to azoles and echinocandins worldwide. *Clinical Microbiology and Infection*, *25*(7), 792–798. <https://doi.org/10.1016/j.cmi.2019.03.028>
- Pusztahelyi**, T., Holb, I. J., & Pócsi, I. (2015). Secondary metabolites in fungus-plant interactions. *Frontiers in Plant Science*, *6*, 573, 1-23. <https://doi.org/10.3389/fpls.2015.00573>
- Quintanilha-Peixoto**, G., Torres, R. O., Reis, I. M. A., Oliveira, T. A. S. de, Bortolini, D. E., Duarte, E. A. A., Ariston de Carvalho Azevedo, V., Brenig, B., Aguiar, E. R. G. R., Soares, A. C. F., Góes-Neto, A., & Branco, A. (2019). Calm Before the Storm: A Glimpse into the Secondary Metabolism of *Aspergillus welwitschiae*, the Etiologic Agent of the Sisal Bole Rot. *Toxins*, *11*, 631-644. <https://doi.org/10.3390/toxins11110631>
- Radwan**, M. M., Tabanca, N., Wedge, D. E., Tarawneh, A. H., & Cutler, S. J. (2014). Antifungal compounds from turmeric and nutmeg with activity against plant pathogens. *Fitoterapia*, *99*, 341–346. <https://doi.org/10.1016/j.fitote.2014.08.021>
- Rao**, A., Zhang, Y., Muend, S., & Rao, R. (2010). Mechanism of antifungal activity of terpenoid phenols resembles calcium stress and inhibition of the TOR pathway. *Antimicrobial Agents and Chemotherapy*, *54*(12), 5062–5069. <https://doi.org/10.1128/AAC.01050-10>
- Redondo**, M., Pérez-Sierra, A., Abad-Campos, P., Torres, L., Solla, A., Reig Armiñana, J., & García Breijo, F. (2015). Histology of *Quercus ilex* roots during infection by *Phytophthora cinnamomi*. *Trees*, *29*, 1943–1957. <https://doi.org/10.1007/s00468-015-1275-3>
- Reganold**, J., & **Wachter**, J. (2016). Organic agriculture in the twenty-first century. *Nature Plants*, *2*, 15221, 1-7. <https://doi.org/10.1038/nplants.2015.221>
- Rep**, M., & Kistler, H. C. (2010). The genomic organization of plant pathogenicity in *Fusarium* species. *Current Opinion in Plant Biology*, *13*(4), 420–426. <https://doi.org/10.1016/j.pbi.2010.04.004>
- Rich**, M. K., Schorderet, M., & Reinhardt, D. (2014). The role of the cell wall compartment in mutualistic symbioses of plants. *Frontiers in Plant Science*, *5*(238), 1-15. <https://www.frontiersin.org/articles/10.3389/fpls.2014.00238>
- Richards**, T. A., Dacks, J. B., Jenkinson, J. M., Thornton, C. R., & Talbot, N. J. (2006). Evolution of filamentous plant pathogens: Gene exchange across eukaryotic kingdoms. *Current Biology: CB*, *16*(18), 1857–1864. <https://doi.org/10.1016/j.cub.2006.07.052>
- Rispail**, N., Soanes, D. M., Ant, C., Czajkowski, R., Grünler, A., Huguet, R., Perez-Nadales, E., Poli, A., Sartorel, E., Valiante, V., Yang, M., Beffa, R., Brakhage, A. A., Gow, N. A. R., Kahmann, R., Lebrun, M.-H., Lenasi, H., Perez-Martin, J., Talbot, N. J., ... Di Pietro, A. (2009). Comparative genomics of MAP kinase and calcium-calcieneurin signalling components in plant and human pathogenic fungi. *Fungal Genetics and Biology: FG & B*, *46*(4), 287–298. <https://doi.org/10.1016/j.fgb.2009.01.002>
- Robbins**, N., Caplan, T., & Cowen, L. E. (2017). Molecular Evolution of Antifungal Drug Resistance. *Annual Review of Microbiology*, *71*(1), 753–775. <https://doi.org/10.1146/annurev-micro-030117-020345>
- Rockström**, J., Steffen, W., Noone, K., Persson, Å., Chapin, F. S., Lambin, E. F., Lenton, T. M., Scheffer, M., Folke, C., Schellnhuber, H. J., Nykvist, B., de Wit, C. A., Hughes, T., van der Leeuw, S., Rodhe, H., Sörlin, S., Snyder, P. K., Costanza, R., Svedin, U., ... Foley, J. A. (2009). A safe operating space for humanity. *Nature*, *461*, 472-475. <https://doi.org/10.1038/461472a>
- Ropejko**, K., & **Twarużek**, M. (2021). Zearalenone and Its Metabolites—General Overview, Occurrence, and Toxicity. *Toxins*, *13*, 35-47. <https://doi.org/10.3390/toxins13010035>

- Ruiz Gómez**, F. J., Navarro-Cerrillo, R. M., Sánchez-Cuesta, R., & Pérez-de-Luque, A. (2015). Histopathology of infection and colonization of *Quercus ilex* fine roots by *Phytophthora cinnamomi*. *Plant Pathology*, *64*(3), 605–616. <https://doi.org/10.1111/ppa.12310>
- Sagi**, S., Avula, B., Wang, Y.-H., & Khan, I. A. (2016). Quantification and characterization of alkaloids from roots of *Rauwolfia serpentina* using ultra-high performance liquid chromatography-photo diode array-mass spectrometry. *Analytical and Bioanalytical Chemistry*, *408*(1), 177–190. <https://doi.org/10.1007/s00216-015-9093-4>
- Sakka Rouis-Soussi**, L., Boughelleb-M'Hamdi, N., El Ayeb-Zakhama, A., Flamini, G., Ben Jannet, H., & Harzallah-Skhiri, F. (2014). Phytochemicals, antioxidant and antifungal activities of *Allium roseum* var. *Grandiflorum* subvar. *Typicum* Regel. *South African Journal of Botany*, *91*, 63–70. <https://doi.org/10.1016/j.sajb.2013.12.005>
- Salvatore**, M. M., Di Lelio, I., DellaGreca, M., Nicoletti, R., Salvatore, F., Russo, E., Volpe, G., Becchimanzi, A., Mahamedi, A. E., Berraf-Tebbal, A., & Andolfi, A. (2022). Secondary Metabolites, including a New 5,6-Dihydropyran-2-One, Produced by the Fungus *Diplodia corticola*. Aphicidal Activity of the Main Metabolite, Sphaeropsidin A. *Molecules (Basel, Switzerland)*, *27*, 2327-2336. <https://doi.org/10.3390/molecules27072327>
- Sanford**, K. J., & **Heinz**, D. E. (1971). Effects of storage on the volatile composition of nutmeg. *Phytochemistry*, *10*(6), 1245–1250. [https://doi.org/10.1016/S0031-9422\(00\)84325-3](https://doi.org/10.1016/S0031-9422(00)84325-3)
- Sangalli**, B. C., Sangalli, B., & Chiang, W. (2000). Toxicology of Nutmeg Abuse. *Journal of Toxicology: Clinical Toxicology*, *38*(6), 671–678. <https://doi.org/10.1081/CLT-100102020>
- Sanz**, A. B., García, R., Rodríguez-Peña, J. M., Díez-Muñiz, S., Nombela, C., Peterson, C. L., & Arroyo, J. (2012). Chromatin remodeling by the SWI/SNF complex is essential for transcription mediated by the yeast cell wall integrity MAPK pathway. *Molecular Biology of the Cell*, *23*(14), 2805–2817. <https://doi.org/10.1091/mbc.E12-04-0278>
- Sanz**, A. B., García, R., Rodríguez-Peña, J. M., Nombela, C., & Arroyo, J. (2016). Cooperation between SAGA and SWI/SNF complexes is required for efficient transcriptional responses regulated by the yeast MAPK Sit2. *Nucleic Acids Research*, *44*(15), 7159–7172. <https://doi.org/10.1093/nar/gkw324>
- Savory**, A. I. M., Grenville-Briggs, L. J., Wawra, S., van West, P., & Davidson, F. A. (2014). Auto-aggregation in zoospores of *Phytophthora infestans*: The cooperative roles of bioconvection and chemotaxis. *Journal of the Royal Society Interface*, *11*, 20140017, 1-8. <https://doi.org/10.1098/rsif.2014.0017>
- Scherm**, B., Balmas, V., Spanu, F., Pani, G., Delogu, G., Pasquali, M., & Migheli, Q. (2013). *Fusarium culmorum*: Causal agent of foot and root rot and head blight on wheat. *Molecular Plant Pathology*, *14*(4), 323–341. <https://doi.org/10.1111/mpp.12011>
- Schiller**, M., Lübeck, M., Sundelin, T., Meléndez, L., Danielsen, S., Jensen, D., & Madriz-Ordeñana, K. (2006). Two subpopulations of *Colletotrichum acutatum* are responsible for anthracnose in strawberry and leatherleaf fern in Costa Rica. *European Journal of Plant Pathology*, *116*, 107–118. <https://doi.org/10.1007/s10658-006-9045-0>
- Schouten**, A., van den Berg, G., Edel-Hermann, V., Steinberg, C., Gautheron, N., Alabouvette, C., de Vos, C. H. (Ric), Lemanceau, P., & Raaijmakers, J. M. (2004). Defense Responses of *Fusarium oxysporum* to 2,4-Diacetylphloroglucinol, a Broad-Spectrum Antibiotic Produced by *Pseudomonas fluorescens*. *Molecular Plant-Microbe Interactions®*, *17*(11), 1201–1211. <https://doi.org/10.1094/MPMI.2004.17.11.1201>
- Scognamiglio**, M., Graziani, V., Tsfantakis, N., Esposito, A., Fiorentino, A., & D'Abrosca, B. (2019). NMR-based metabolomics and bioassays to study phytotoxic extracts and putative phytotoxins from Mediterranean plant species. *Phytochemical Analysis: PCA*, *30*(5), 512–523. <https://doi.org/10.1002/pca.2842>

- Senter**, L. H., Sanson, D. R., Corley, D. G., Tempesta, M. S., Rottinghaus, A. A., & Rottinghaus, G. E. (1991). Cytotoxicity of trichothecene mycotoxins isolated from *Fusarium sporotrichioides* (MC-72083) and *Fusarium sambucinum* in baby hamster kidney (BHK-21) cells. *Mycopathologia*, *113*(2), 127–131. <https://doi.org/10.1007/BF00442425>
- Serrano**, M. S., Romero, M. A., Jiménez, J. J., De Vita, P., Ávila, A., Trapero, A., & Sánchez, M. E. (2015). Preventive control of *Botryosphaeria* canker affecting *Quercus suber* in southern Spain. *Forestry: An International Journal of Forest Research*, *88*(4), 500–507. <https://doi.org/10.1093/forestry/cpv016>
- Sestili**, P., Ismail, T., Calcabrini, C., Guescini, M., Catanzaro, E., Turrini, E., Layla, A., Akhtar, S., & Fimognari, C. (2018). The potential effects of *Ocimum basilicum* on health: A review of pharmacological and toxicological studies. *Expert Opinion on Drug Metabolism & Toxicology*, *14*(7), 679–692. <https://doi.org/10.1080/17425255.2018.1484450>
- Seyed**, M. A., Ayesha, S., Azmi, N., Al-Rabae, F. M., Al-Alawy, A. I., Al-Zahrani, O. R., & Hawsawi, Y. (2021). The neuroprotective attribution of *Ocimum basilicum*: A review on the prevention and management of neurodegenerative disorders. *Future Journal of Pharmaceutical Sciences*, *7*, 139–153. <https://doi.org/10.1186/s43094-021-00295-3>
- Shahrajabian**, M. H., Sun, W., & Cheng, Q. (2020). Chemical components and pharmacological benefits of Basil (*Ocimum basilicum*): A review. *International Journal of Food Properties*, *23*(1), 1961–1970. <https://doi.org/10.1080/10942912.2020.1828456>
- Shang**, Y., Xiao, G., Zheng, P., Cen, K., Zhan, S., & Wang, C. (2016). Divergent and Convergent Evolution of Fungal Pathogenicity. *Genome Biology and Evolution*, *8*(5), 1374–1387. <https://doi.org/10.1093/gbe/evw082>
- Shapiro**, R. S., Robbins, N., & Cowen, L. E. (2011). Regulatory Circuitry Governing Fungal Development, Drug Resistance, and Disease. *Microbiology and Molecular Biology Reviews*, *75*(2), 213–267. <https://doi.org/10.1128/mmb.00045-10>
- Sharma**, I. (2021). Chapter 7—Phytopathogenic fungi and their biocontrol applications. Em V. K. Sharma, M. P. Shah, S. Parmar, & A. Kumar (Eds.), *Fungi Bio-Prospect in Sustainable Agriculture, Environment and Nano-Technology* (pp. 155–188). Academic Press. <https://doi.org/10.1016/B978-0-12-821394-0.00007-X>
- Sharma**, R., Mishra, B., Runge, F., & Thines, M. (2014). Gene loss rather than gene gain is associated with a host jump from monocots to dicots in the Smut Fungus *Melanopsichium pennsylvanicum*. *Genome Biology and Evolution*, *6*(8), 2034–2049. <https://doi.org/10.1093/gbe/evu148>
- Sharma**, S., Marin, M. V., Lee, M. B., Baggio, J. S., Peres, N. A., & Lee, S. (2022). Genomic approaches for improving resistance to *Phytophthora* crown rot caused by *P. cactorum* in strawberry (*Fragaria × ananassa*). *Frontiers in Agronomy*, *4*, 941111, 1–16. <https://www.frontiersin.org/articles/10.3389/fagro.2022.941111>
- Shearer**, B. L., Crane, C., Barrett, S. R., & Cochrane, A. (1994). The major plant pathogens occurring in native ecosystems of south-western Australia. *Journal of the Royal Society of Western Australia*, *77*, 113–122. <https://doi.org/10.1071/BT06019>
- Shlezinger**, N., Minz, A., Gur, Y., Hatam, I., Dagdas, Y. F., Talbot, N. J., & Sharon, A. (2011). Anti-apoptotic machinery protects the necrotrophic fungus *Botrytis cinerea* from host-induced apoptotic-like cell death during plant infection. *PLoS Pathogens*, *7*(8), e1002185, 1–12. <https://doi.org/10.1371/journal.ppat.1002185>
- Shrestha**, A., Brunette, S., Stanford, W. L., & Megeney, L. A. (2019). The metacaspase Yca1 maintains proteostasis through multiple interactions with the ubiquitin system. *Cell Discovery*, *5*, 6–19. <https://doi.org/10.1038/s41421-018-0071-9>

- Siddiqui**, B. S., Aslam, H., Ali, S. T., Begum, S., & Khatoon, N. (2007). Two new triterpenoids and a steroidal glycoside from the aerial parts of *Ocimum basilicum*. *Chemical & Pharmaceutical Bulletin*, *55*(4), 516–519. <https://doi.org/10.1248/cpb.55.516>
- Simmonds**. (1965). A study of the species of *Colletotrichum* causing ripe fruit rots in Queensland. *Queensland Journal of Agricultural and Animal Sciences*, *22*(4), 437–459.
- Singh**, A., Kumar, J., Sharma, V. K., Singh, D. K., Kumari, P., Nishad, J. H., Gautam, V. S., & Kharwar, R. N. (2021). Phytochemical analysis and antimicrobial activity of an endophytic *Fusarium proliferatum* (ACQR8), isolated from a folk medicinal plant *Cissus quadrangularis* L. *South African Journal of Botany*, *140*, 87–94. <https://doi.org/10.1016/j.sajb.2021.03.004>
- Singh**, G., Kapoor, I. P. S., Singh, P., de Heluani, C. S., de Lampasona, M. P., & Catalan, C. A. N. (2010). Comparative study of chemical composition and antioxidant activity of fresh and dry rhizomes of turmeric (*Curcuma longa* Linn.). *Food and Chemical Toxicology: An International Journal Published for the British Industrial Biological Research Association*, *48*(4), 1026–1031. <https://doi.org/10.1016/j.fct.2010.01.015>
- Singh**, V., Kaur, K., Kaur, S., Shri, R., Singh, T. G., & Singh, M. (2022). Trimethoxyflavones from *Ocimum basilicum* L. leaves improve long term memory in mice by modulating multiple pathways. *Journal of Ethnopharmacology*, *295*, 115438, 1-12. <https://doi.org/10.1016/j.jep.2022.115438>
- Soares**, D. F., Faria, A. M., & Rosa, A. H. (2016). Análise de risco de contaminação de águas subterrâneas por resíduos de agrotóxicos no município de Campo Novo do Parecis (MT), Brasil. *Engenharia Sanitaria e Ambiental*, *22*(2), 277–284. <https://doi.org/10.1590/s1413-41522016139118>
- Sousa**, B. C. M. de, Barata, L. E. S., Macêdo, C. G., Fraga, S. S., Kasper, A. A. M., Lourido, K. A., Paulino, G. da S., Almeida, E. C. de, Sartoratto, A., & Lustosa, D. C. (2018). Avaliação do teor de Cumarina e atividade antifúngica de frações de Óleo de Cumarú. *Revista Ibero-Americana de Ciências Ambientais*, *9*(6), 63-69. <https://doi.org/10.6008/CBPC2179-6858.2018.006.0008>
- Soyer**, J. L., Hamiot, A., Ollivier, B., Balesdent, M., Rouxel, T., & Fudal, I. (2015). The APSES transcription factor LmStuA is required for sporulation, pathogenic development and effector gene expression in *Leptosphaeria maculans*. *Molecular Plant Pathology*, *16*(9), 1000–1005. <https://doi.org/10.1111/mpp.12249>
- Sparg**, S. G., Light, M. E., & van Staden, J. (2004). Biological activities and distribution of plant saponins. *Journal of Ethnopharmacology*, *94*(2), 219–243. <https://doi.org/10.1016/j.jep.2004.05.016>
- Srivastava**, J. N., Singh, A. K., & Sharma, R. K. (2020). Diseases of Apples and Their Management. Em *Diseases of Fruits and Vegetable Crops* (1st Edition, p. 21). Apple Academic Press.
- Stadnicka-Michalak**, J., Schirmer, K., & Ashauer, R. (2015). Toxicology across scales: Cell population growth in vitro predicts reduced fish growth. *Science Advances*, *1*, e1500302, 1-8. <https://doi.org/10.1126/sciadv.1500302>
- Stensvand**, A., Herrero, M. L., & Talgø, V. (1999). Crown rot caused by *Phytophthora cactorum* in Norwegian strawberry production. *EPPO Bulletin*, *29*(1–2), 155–158. <https://doi.org/10.1111/j.1365-2338.1999.tb00809.x>
- Sudakin**, D. L. (2003). Trichothecenes in the environment: Relevance to human health. *Toxicology Letters*, *143*(2), 97–107. [https://doi.org/10.1016/s0378-4274\(03\)00116-4](https://doi.org/10.1016/s0378-4274(03)00116-4)
- Sundheim**, L., Brodal, G., Hofgaard, I. S., & Rafoss, T. (2013). Temporal Variation of Mycotoxin Producing Fungi in Norwegian Cereals. *Microorganisms*, *1*, 188-198. <https://doi.org/10.3390/microorganisms1010188>
- Suzuki**, T., & Iwahashi, Y. (2014). Phytotoxicity Evaluation of Type B Trichothecenes Using a *Chlamydomonas reinhardtii* Model System. *Toxins*, *6*, 453-463. <https://doi.org/10.3390/toxins6020453>

- Talhinhas**, P., Mota-Capitão, C., Martins, S., Ramos, A. P., Neves-Martins, J., Guerra-Guimarães, L., Várzea, V., Silva, M. C., Sreenivasaprasad, S., & Oliveira, H. (2011). Epidemiology, histopathology and aetiology of olive anthracnose caused by *Colletotrichum acutatum* and *C. gloeosporioides* in Portugal. *Plant Pathology*, *60*(3), 483–495. <https://doi.org/10.1111/j.1365-3059.2010.02397.x>
- Tao**, M., Zhao, Y., Hu, T., Zhang, Q., Feng, H., Lu, Y., Guo, Z., & Yang, B. (2023). Screening of Alfalfa Varieties Resistant to *Phytophthora cactorum* and Related Resistance Mechanism. *Plants*, *12*, 702–715. <https://doi.org/10.3390/plants12040702>
- Tava**, A., & **Avato**, P. (2006). Chemical and Biological Activity of Triterpene Saponins from *Medicago* Species. *Natural Product Communications*, *1*(12), 1159–1180. <https://doi.org/10.1177/1934578X0600101217>
- Teng**, P. S., Shane, W. W., & MacKenzie, D. R. (1984). Crop losses due to plant pathogens. *Critical Reviews in Plant Sciences*, *2*(1), 21–47. <https://doi.org/10.1080/07352688409382187>
- Thines**, M., & **Kamoun**, S. (2010). Oomycete-plant coevolution: Recent advances and future prospects. *Current Opinion in Plant Biology*, *13*(4), 427–433. <https://doi.org/10.1016/j.pbi.2010.04.001>
- Thynne**, E., Saur, I. M. L., Simbaqueba, J., Ogilvie, H. A., Gonzalez-Cendales, Y., Mead, O., Taranto, A., Catanzariti, A., McDonald, M. C., Schwessinger, B., Jones, D. A., Rathjen, J. P., & Solomon, P. S. (2016). Fungal phytopathogens encode functional homologues of plant rapid alkalization factor (RALF) peptides. *Molecular Plant Pathology*, *18*(6), 811–824. <https://doi.org/10.1111/mpp.12444>
- Tian**, J., Ban, X., Zeng, H., He, J., Chen, Y., & Wang, Y. (2012). The Mechanism of Antifungal Action of Essential Oil from Dill (*Anethum graveolens* L.) on *Aspergillus flavus*. *PLOS ONE*, *7*(1), e30147, 1–10. <https://doi.org/10.1371/journal.pone.0030147>
- Tomas-Grau**, R. H., Di Peto, P., Chalfoun, N. R., Grellet-Bournonville, C. F., Martos, G. G., Debes, M., Arias, M. E., & Díaz-Ricci, J. C. (2019). *Colletotrichum acutatum* M11 can suppress the defence response in strawberry plants. *Planta*, *250*(4), 1131–1145. <https://doi.org/10.1007/s00425-019-03203-5>
- Tucker**, S. L., & Talbot, N. J. (2001). Surface attachment and pre-penetration stage development by plant pathogenic fungi. *Annual Review of Phytopathology*, *39*, 385–417. <https://doi.org/10.1146/annurev.phyto.39.1.385>
- Tunçbilek**, M., Kiper, T., & Altanlar, N. (2009). Synthesis and in vitro antimicrobial activity of some novel substituted benzimidazole derivatives having potent activity against MRSA. *European Journal of Medicinal Chemistry*, *44*(3), 1024–1033. <https://doi.org/10.1016/j.ejmech.2008.06.026>
- Ultee**, A., Bennis, M. H. J., & Moezelaar, R. (2002). The Phenolic Hydroxyl Group of Carvacrol Is Essential for Action against the Food-Borne Pathogen *Bacillus cereus*. *Applied and Environmental Microbiology*, *68*(4), 1561–1568. <https://doi.org/10.1128/AEM.68.4.1561-1568.2002>
- Uma**, B., Rani, T. S., & Podile, A. R. (2011). Warriors at the gate that never sleep: Non-host resistance in plants. *Journal of Plant Physiology*, *168*(18), 2141–2152. <https://doi.org/10.1016/j.jplph.2011.09.005>
- Ungphaiboon**, S., Tanomjit, S., Pechnoi, S., Supreedee, S., Pranee, R., & Itharat, A. (2005). Study on antioxidant and antimicrobial activities of turmeric clear liquid soap for wound treatment of HIV patients. *Songklanakarin Journal of Science and Technology*, *27*(2), 569–578.
- Úrbez-Torres**, J. R., Adams, P., Kamas, J., & Gubler, W. (2009). Identification, Incidence, and Pathogenicity of Fungal Species Associated with Grapevine Dieback in Texas. *American Journal of Enology and Viticulture*, *60*, 497–507. <https://doi.org/10.5344/ajev.2009.60.4.497>
- Úrbez-Torres**, J. R., Peduto, F., Rooney-Latham, S., & Gubler, W. D. (2010). First Report of *Diplodia corticola* Causing Grapevine (*Vitis vinifera*) Cankers and Trunk Cankers and Dieback of Canyon

- Live Oak (*Quercus chrysolepis*) in California. *Plant Disease*, 94(6), 785-785. <https://doi.org/10.1094/PDIS-94-6-0785A>
- Van Baarlen**, P., Woltering, E. J., Staats, M., & VAN Kan, J. A. L. (2007). Histochemical and genetic analysis of host and non-host interactions of *Arabidopsis* with three *Botrytis* species: An important role for cell death control. *Molecular Plant Pathology*, 8(1), 41–54. <https://doi.org/10.1111/j.1364-3703.2006.00367.x>
- Varela**, C. P., Fernández, V. R., Casal, O. A., & Vázquez, J. P. M. (2011). First Report of Cankers and Dieback Caused by *Neofusicoccum mediterraneum* and *Diplodia corticola* on Grapevine in Spain. *Plant Disease*, 95(10), 1315-1315. <https://doi.org/10.1094/PDIS-05-11-0429>
- Vinale**, F., Sivasithamparam, K., Ghisalberti, E. L., Woo, S. L., Nigro, M., Marra, R., Lombardi, N., Pascale, A., Ruocco, M., Lanzuise, S., Manganiello, G., & Lorito, M. (2014). Trichoderma Secondary Metabolites Active on Plants and Fungal Pathogens. *The Open Mycology Journal*, 8(1), 127-139. <https://benthamopen.com/ABSTRACT/TOMYCJ-8-127>
- Wagacha**, J. M., & Muthomi, J. W. (2007). *Fusarium culmorum*: Infection process, mechanisms of mycotoxin production and their role in pathogenesis in wheat. *Crop Protection*, 26(7), 877–885. <https://doi.org/10.1016/j.cropro.2006.09.003>
- Walter**, D., Wissing, S., Madeo, F., & Fahrenkrog, B. (2006). The inhibitor-of-apoptosis protein Bir1p protects against apoptosis in *S. cerevisiae* and is a substrate for the yeast homologue of Omi/HtrA2. *Journal of Cell Science*, 119(9), 1843–1851. <https://doi.org/10.1242/jcs.02902>
- Walters**, D., Raynor, L., Mitchell, A., Walker, R. & Walker, K. (2004). Antifungal activities of four fatty acids against plant pathogenic fungi. *Mycopathologia*, 157(1), 87-90. <https://doi.org/10.1023/b:myco.0000012222.68156.2c>
- Whalen**, M. C. (2005). Host defence in a developmental context. *Molecular Plant Pathology*, 6(3), 347–360. <https://doi.org/10.1111/j.1364-3703.2005.00286.x>
- Whaley**, S. G., Berkow, E. L., Rybak, J. M., Nishimoto, A. T., Barker, K. S., & Rogers, P. D. (2017). Azole Antifungal Resistance in *Candida albicans* and Emerging Non-*albicans* *Candida* Species. *Frontiers in Microbiology*, 7, 2173, 1-12. <https://doi.org/10.3389/fmicb.2016.02173>
- Wharton**, P., & Schilder, A. M. C. (2007). Novel infection strategies of *Colletotrichum acutatum* on ripe blueberry fruit. *Plant Pathology*, 57, 122–134. <https://doi.org/10.1111/j.1365-3059.2007.01698.x>
- Williamson**, B., Tudzynski, B., Tudzynski, P., & van Kan, J. A. L. (2007). *Botrytis cinerea*: The cause of grey mould disease. *Molecular Plant Pathology*, 8(5), 561–580. <https://doi.org/10.1111/j.1364-3703.2007.00417.x>
- Wink**, M. (2003). Evolution of secondary metabolites from an ecological and molecular phylogenetic perspective. *Phytochemistry*, 64(1), 3–19. [https://doi.org/10.1016/S0031-9422\(03\)00300-5](https://doi.org/10.1016/S0031-9422(03)00300-5)
- Wissing**, S., Ludovico, P., Herker, E., Büttner, S., Engelhardt, S. M., Decker, T., Link, A., Proksch, A., Rodrigues, F., Corte-Real, M., Fröhlich, K.-U., Manns, J., Candé, C., Sigrist, S. J., Kroemer, G., & Madeo, F. (2004). An AIF orthologue regulates apoptosis in yeast. *The Journal of Cell Biology*, 166(7), 969–974. <https://doi.org/10.1083/jcb.200404138>
- Wu**, H., Guo, J., Chen, S., Liu, X., Zhou, Y., Zhang, X., & Xu, X. (2013). Recent developments in qualitative and quantitative analysis of phytochemical constituents and their metabolites using liquid chromatography-mass spectrometry. *Journal of Pharmaceutical and Biomedical Analysis*, 72, 267–291. <https://doi.org/10.1016/j.jpba.2012.09.004>
- Xin-Mei**, P., Gl, D., & C, Z. (2013). Current developments of coumarin compounds in medicinal chemistry. *Current Pharmaceutical Design*, 19(21), 3884-930. <https://doi.org/10.2174/1381612811319210013>

- Xu, K., Wang, J. L., Chu, M. P., & Jia, C. (2019).** Activity of coumarin against *Candida albicans* biofilms. *Journal De Mycologie Medicale*, *29*(1), 28–34. <https://doi.org/10.1016/j.mycmed.2018.12.003>
- Yin, Z., Ke, X., Kang, Z., & Huang, L. (2016).** Apple resistance responses against *Valsa mali* revealed by transcriptomics analyses. *Physiological and Molecular Plant Pathology*, *93*, 85–92. <https://doi.org/10.1016/J.PMPP.2016.01.004>
- Yörüç, E., & Albayrak, G. (2012).** Chemotyping of *Fusarium graminearum* and *F. culmorum* isolates from Turkey by PCR assay. *Mycopathologia*, *173*(1), 53–61. <https://doi.org/10.1007/s11046-011-9462-2>
- You, M. P., Lamichhane, J. R., Aubertot, J.-N., & Barbetti, M. J. (2020).** Understanding Why Effective Fungicides Against Individual Soilborne Pathogens Are Ineffective with Soilborne Pathogen Complexes. *Plant Disease*, *104*(3), 904–920. <https://doi.org/10.1094/PDIS-06-19-1252-RE>
- Yumnam, D., Dutta, B., Paul, S., & Choudhury, S. (2014).** The effect of Paraquat and Fipronil on the soil and rhizosphere microflora of tea (*Camellia sinensis* (L) O. kuntze). *International Journal of Innovation and Applied Studies*, *7*(4), 1534–1543.
- Zeilinger, S., Gupta, V. K., Dahms, T. E. S., Silva, R. N., Singh, H. B., Upadhyay, R. S., Gomes, E. V., Tsui, C. K.-M., & Nayak S, C. (2016).** Friends or foes? Emerging insights from fungal interactions with plants. *FEMS Microbiology Reviews*, *40*(2), 182–207. <https://doi.org/10.1093/femsre/fuv045>
- Zhou, Y., Xu, J., Zhu, Y., Duan, Y., & Zhou, M. (2016).** Mechanism of Action of the Benzimidazole Fungicide on *Fusarium graminearum*: Interfering with Polymerization of Monomeric Tubulin But Not Polymerized Microtubule. *Phytopathology*, *106*(8), 807–813. <https://doi.org/10.1094/PHYTO-08-15-0186-R>
- Ziegler, J., & Facchini, P. J. (2008).** Alkaloid biosynthesis: Metabolism and trafficking. *Annual Review of Plant Biology*, *59*, 735–769. <https://doi.org/10.1146/annurev.arplant.59.032607.092730>
- Zinedine, A., Soriano, J. M., Moltó, J. C., & Mañes, J. (2007).** Review on the toxicity, occurrence, metabolism, detoxification, regulations and intake of zearalenone: An oestrogenic mycotoxin. *Food and Chemical Toxicology*, *45*(1), 1–18. <https://doi.org/10.1016/j.fct.2006.07.030>
- Zuccaro, A., Lahrman, U., & Langen, G. (2014).** Broad compatibility in fungal root symbioses. *Current Opinion in Plant Biology*, *20*, 135–145. <https://doi.org/10.1016/j.pbi.2014.05.013>
- Zweytick, D., Leitner, E., Kohlwein, S. D., Yu, C., Rothblatt, J., & Daum, G. (2000).** Contribution of Are1p and Are2p to sterol ester synthesis in the yeast *Saccharomyces cerevisiae*. *European Journal of Biochemistry*, *267*(4), 1075–1082. <https://doi.org/10.1046/j.1432-1327.2000.01103.x>

7. ANNEXES

Annex 1

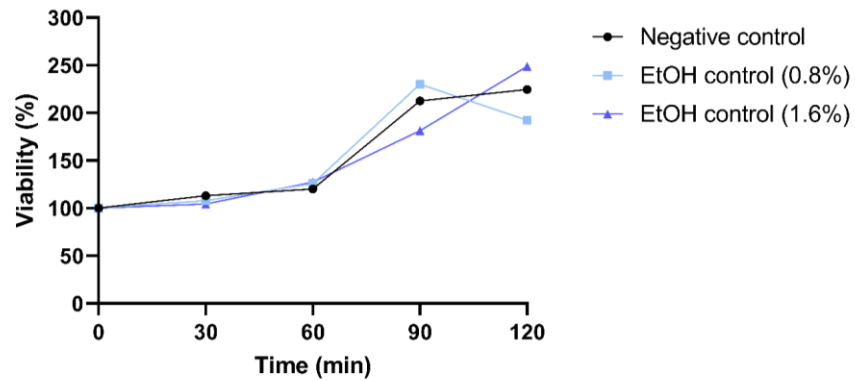


Figure 37 – The viability of *Saccharomyces cerevisiae* remains unaffected by the solvent extracts (80% ethanol; EtOH). *Saccharomyces cerevisiae* cells were cultured in YPD at 30 °C and 200 rpm until reaching an OD₆₀₀ within the range of 0.4-0.6 and treatments were applied: 2% liquid YPD medium (negative control) or 0.8% or 1.6% EtOH (solvent control). Aliquots were harvested along time, serially diluted up to a factor of 10⁻⁴ and 40 µL drops were plated and incubated for 48 hours at 30 °C. The percentage of cell viability was calculated by dividing the average CFU value by the average value at 0 minutes. The data are presented as a result of a single independent experiment.

Annex 2

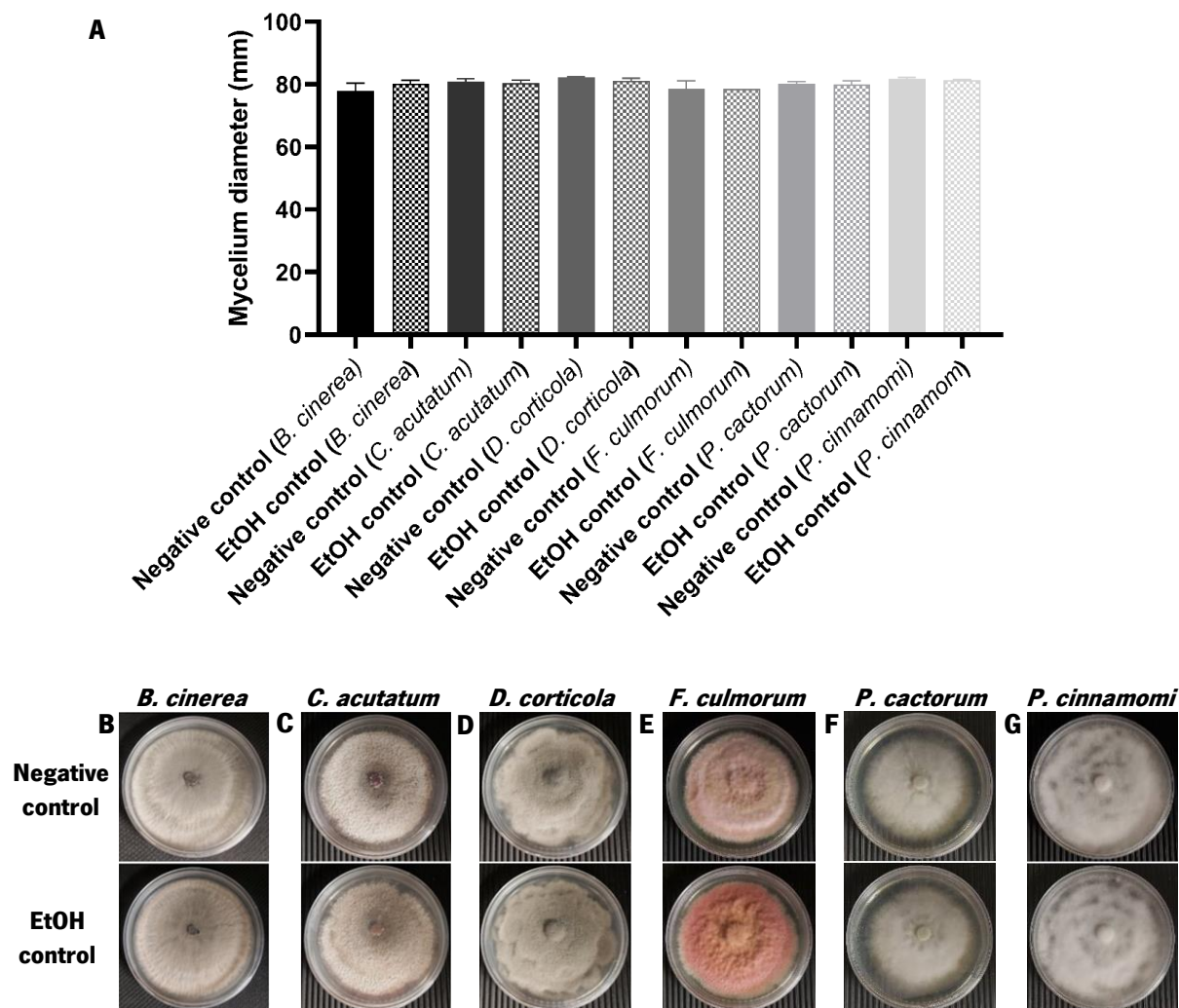
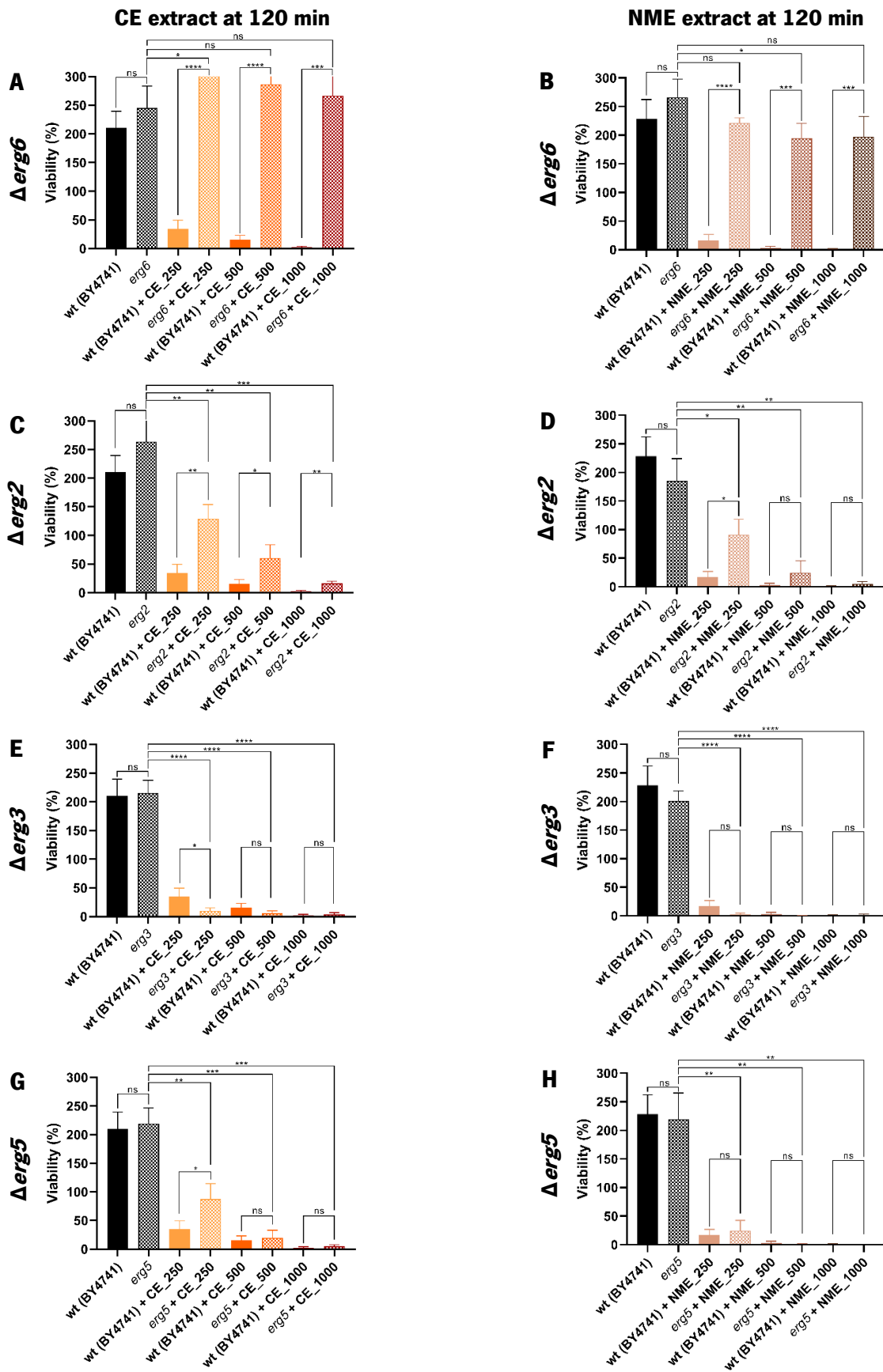
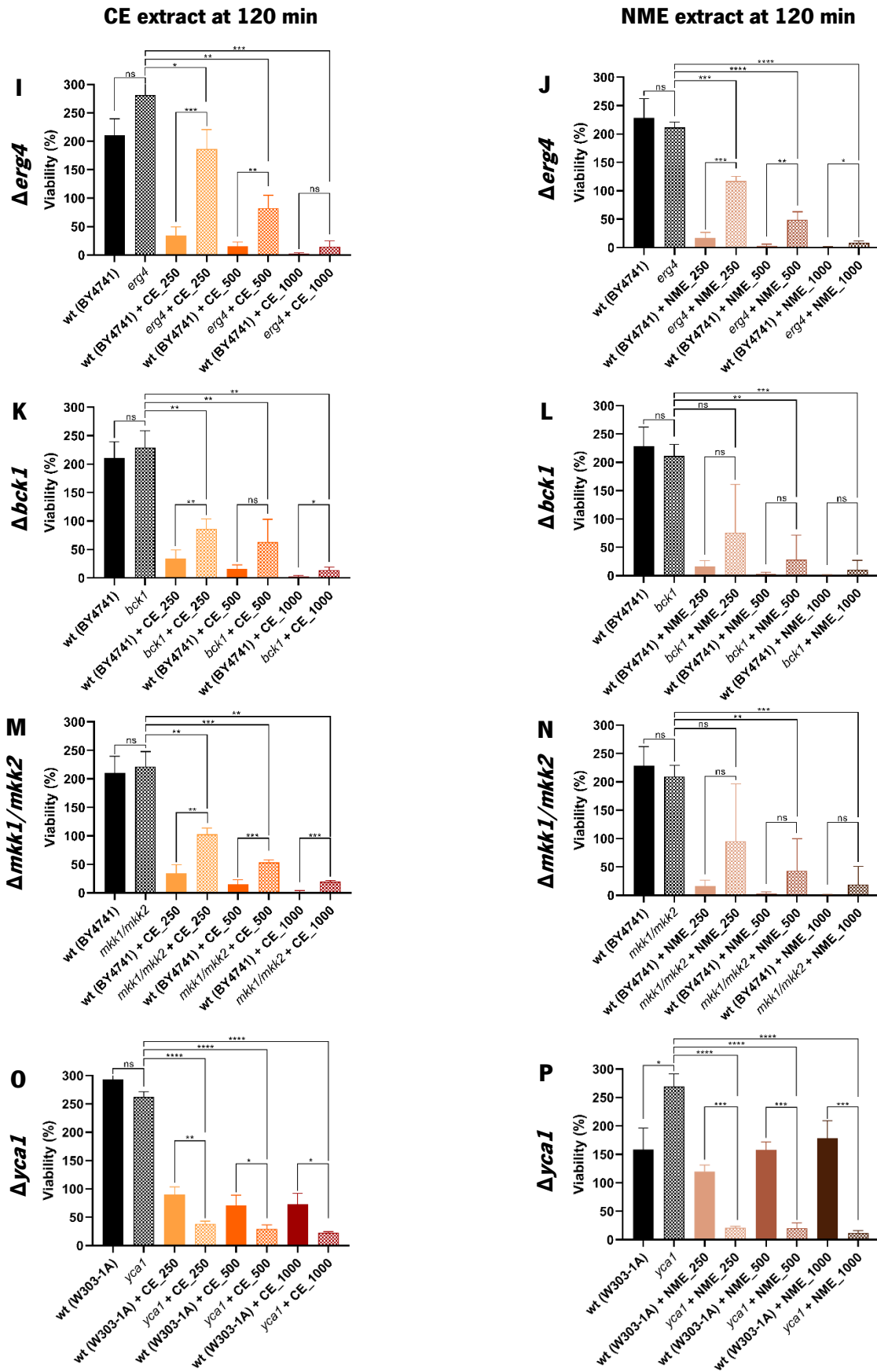


Figure 38 – The mycelium growth of *Botrytis cinerea*, *Colletotrichum acutatum*, *Diplodia corticola*, *Fusarium culmorum*, *Phytophthora cactorum* and *Phytophthora cinnamomi* remains unaltered by the solvent extracts (80% ethanol; EtOH). The treatments were incorporated into the PDA medium: H₂O (negative control) and EtOH (solvent control). The volume of water used equates to the maximum volume of EtOH employed in the viability assays involving filamentous fungi. For each plate, a mycelium disc of one fungus was centered and incubated at 25 °C in the absence of light until the fungus reached the edge of the Petri dish. The mycelium diameter (**A**) and images of the mycelium (**B-G**) for each fungus – *B. cinerea* (**A and B**), *C. acutatum* (**A and C**), *D. corticola* (**A and D**), *F. culmorum* (**A and E**), *P. cactorum* (**A and F**) and *P. cinnamomi* (**A and G**) – were both measured and captured. The mycelium diameter was calculated as the average of two perpendicular measurements. The mycelium diameter data are presented as the mean of three independent experiments ± SD. Variance analysis was conducted using t-tests for pairwise comparisons, with significance compared to the respective control for each fungus. The mycelium images provided are representative of the outcomes from the three experiments.

Annex 3



This image continues in the next page.



This image continues in the next page.

Figure 39 – Mutant strains *erg6*, *erg2*, *erg5*, *erg4*, *bck1*, as well as *mkk1/mkk2*, exhibited higher resistance, while *erg3* and *yca1* mutant strains displayed higher sensitivity to ethanolic extracts of *Curcuma longa* (CE) and *Myristica fragrans* (NME) compared to their respective wild-type (WT) strains. *Saccharomyces cerevisiae* cells were cultured in YPD at 30 °C and 200 rpm until reaching an OD₆₀₀ within the range of 0.4-0.6 and treatments were applied: CE (**A, C, E, G, I, K, M and O**) or NME (**B, D, F, H, J, L, N and P**) to mutants *erg6* (**A and B**), *erg2* (**C and D**), *erg3* (**E and F**), *erg5* (**G and H**), *erg4* (**I and J**), *bck1* (**K and L**), *mkk1/mkk2* (**M and N**), and *yca1* (**O and P**) mutant strains, in addition to their respective WT, BY4741 and W303-1A. The treatments consisted of 1.6% v/v solvent extract (ethanol; control) or CE or NME extracts at concentrations of 250, 500 and 1000 µg/mL. Aliquots were harvested along time, serially diluted up to a factor of 10⁴ and 40 µL drops were plated and incubated for 48 hours at 30 °C. Cell viability percentages were calculated by dividing the average CFUs by the average at 0 minutes. Data are presented as the mean of three independent experiments ± standard deviation (SD). Variance analysis was conducted using *t*-tests for each pair of comparisons, with notation as follows: ns (not significant), *0.01 < *p* ≤ 0.05, **0.001 < *p* ≤ 0.01, ***0.0001 < *p* ≤ 0.001 and *****p* ≤ 0.0001. Significance comparisons were made between pairs: WT untreated *vs.* mutant untreated, mutant untreated *vs.* mutant treated and WT treated *vs.* mutant treated at all three concentrations.

Annex 4

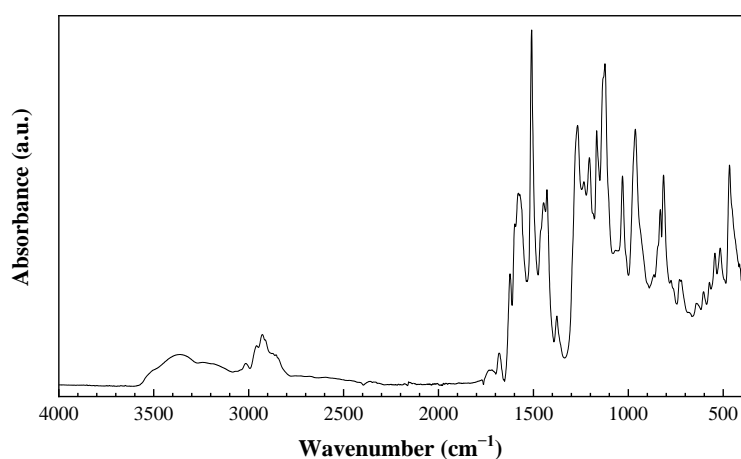


Figure 40 – Infrared spectrum analysis of *Curcuma longa* (CE) extract. After the CE extract was filtrated and freeze-dried, the infrared vibrational spectrum of the freeze-dried extract was measured using a Nicolet iS50 FTIR spectrometer with an ATR system. The measurement range was 400–4000 cm^{-1} , with a resolution of 1 cm^{-1} and the resulting spectrum was obtained by combining 64 scans.

Table 7 – Key infrared spectrum bands of *Curcuma longa* (CE) extract and their corresponding designations.

Wavenumber (cm^{-1})	Designation
3362	O–H stretching
2928	–CH ₂ groups stretching
1680	C=O stretching
1623	overlapping stretching of alkenes (C=C) and carbonyl (C=O)
1578	COO ⁻ antisymmetric stretching
1509	C=O stretching; CC–C and CC=O in-plane bending; aromatic CC–H in-plane bending and vCC stretching aromatic of keto and enol configurations.
1429	C=C aromatic stretching
1376	methyl groups bending
1267	v(C–O) phenolic bending
1205	CH ₃ symmetric deformation
1167	C=O stretching
1123	C–H bending
1030	C–O vibrations
963	C–H wag absorption (alkenyl)
832	C–H
814	out-of-plane ring bending
730	– (CH ₂) _n – in-phase rocking

Annex 5

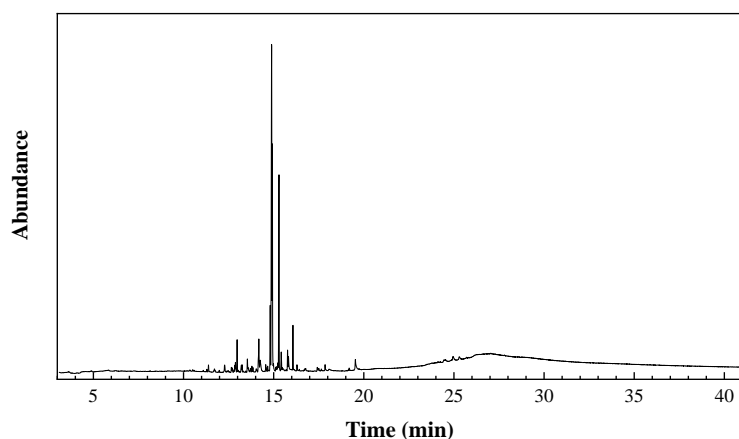


Figure 41 – GC-MS chromatogram of *Curcuma longa* (CE) extract. For GC–MS analysis the freeze-dried extract was dissolved in methanol (HPLC-grade) to yield a 5 mg mL⁻¹ solution. This solution was then filtered again. The chromatography conditions were as follows: injection volume = 1 µL; injector temperature = 280 °C (in splitless mode); initial oven temperature = 60 °C for 2 min, followed by a ramp of 10 °C min⁻¹ to a final temperature of 300 °C for 15 min. Then, with a column with a length of 30 m, diameter of 0.250 mm and film thickness of 0.25 µm was used for compound separation. The mass spectrometer conditions were as follows: electron impact source temperature = 230 °C; quadrupole temperature = 150 °C; and ionization energy = 70 eV. Identification of components was based on the comparison of their mass spectra and retention time with authentic compounds and utilizing the NIST11 database.

Table 8 – Chemical compounds detected in *Curcuma longa* (CE) extract by GC-MS.

RT (min)	Area (%)	Chemical species	Qual
10.5118	0.1164	Ethanone, 1-(3-methoxyphenyl)-	45
11.0935	0.1303	Phenol, 2-methoxy-4-(2-propenyl)- (or eugenol)	90
11.3902	0.4714	3,5,7-trimethyl-2E,4E,6E,8E-decatetraene	43
11.7167	0.2603	Isobenzofuran	43
11.7463	0.1743	Benzoic acid, 3,5-dimethyl-, (3,5-dimethylphenyl)methyl ester	55
11.9837	0.1657	2-Methylbicyclo[4.3.0]nona-2,9-diene dimer	35
12.2805	1.0108	Phenol, 2-methoxy-4-(1-propenyl)-	83
12.4170	0.1431	Oxime-, methoxy-phenyl-	38
12.4823	0.2227	Hydrazinecarboxamide, 2-(1-phenylethylidene)-	50
12.6604	0.3421	γ-curcumene	93
12.7019	0.3560	Benzene, 1-(1,5-dimethyl-4-hexenyl)-4-methyl-	99
12.8503	0.4319	Zingiberene	90
12.8859	0.8048	3,5-dimethoxy-2-methylnaphthalene	86
12.9749	1.9900	1-phenyl-2-(p-tolyl)-propane	72
13.0521	0.1909	1H-Benzocycloheptene, 2,4a,5,6,7,8-hexahydro-3,5,5,9-tetramethyl-, (R)-	38
13.2124	0.6186	β-Sesquiphellandrene	98
13.2479	0.4825	Dispiro[2.6.2.5]undecane, 10-methylen-	50
13.5447	1.4773	<i>Trans</i> -isoelemicin	90

13.5981	0.4081	3-Acetyl-2-methyl-4-phenylfuran	50
13.7169	0.4141	Acetic acid 2-acetylamino-phenyl ester	58
13.7999	0.4219	(E)-1-ethylidene-4,5,8-trimethyl-1,2,3,4-tetrahydronaphthalene	90
13.8474	0.3407	3,4-Dimethoxyphenylacetone	68
14.0374	0.4407	3,4-Dimethylbenzyl isothiocyanate	42
14.1798	3.4372	Benzene, 1-ethyl-4-(2-methylpropyl)-	74
14.8089	4.4816	Benzene, 1,2,4-trimethyl-	43
14.8920	28.9413	β -Tumerone	96
14.9336	15.3193	α -Tumerone	90
15.1295	0.3430	2,3,3a,8a-Tetrahydro-2,4-dihydroxy-6-methoxy-furo[2,3-b]benzofuran	83
15.1710	0.4089	3(5)-(4'-Methylphenyl)- 4-amino-5(3)-ethylaminopyrazole	83
15.2363	0.7148	Pyridine, 4-[(3-methoxyphenyl)methyl]-	58
15.2956	13.2673	α -Tumerone	91
15.4262	1.6288	Tetradecanoic acid, methyl ester	96
15.4856	0.3040	1,3-Cyclohexanedione, 2,2,5,5-tetramethyl-	43
15.5330	0.4373	3,7,7-Trimethyl-1-(3-oxo-but-1-enyl)-2-oxa-bicyclo[3.2.0]hept-3-en-6-one	38
15.7764	1.4119	1-Deuterioformyl-2-methoxybenzene	72
15.8239	1.8154	Tetradecanoic acid	99
16.0732	2.9617	(+)- α -Atlantone	68
16.2987	0.6141	1-Isopropenyl-3,3-dimethyl-5-(3-methyl-1-oxo-2-butenyl)cyclopentane	27
16.4233	0.1388	2-Methylthio-3,4-dihydronaphtho[2,1-c]thiophene	53
16.6964	0.0922	2H-1-Benzopyran, 3,5,6,8a-tetrahydro-2,5,5,8a-tetramethyl-, cis-	44
16.7438	0.1690	7(1H)-Quinolinone, octahydro-4a-(2-propenyl)-, trans-(+.-)-	35
17.4680	0.1231	Methyl 3,5-bis(ethylamino)benzoate	30
17.5095	0.2790	Hexadecanoic acid, methyl ester	96
17.8538	0.6914	n-Hexadecanoic acid	99
19.5394	1.7381	9-Octadecenoic acid (Z)-	99
19.7412	0.3431	1H-Indole-3-carboxylic acid, 5-hydroxy-	44
24.1214	0.5540	Gibberellin A3	43
24.2401	0.1306	6 Methyl-2 phenylindole	38
24.9524	1.0139	Hexahydropyridine, 1-methyl-4-[4,5-dihydroxyphenyl]-	46

RT = Retention Time; Qual = Quality of resemblance

Annex 6

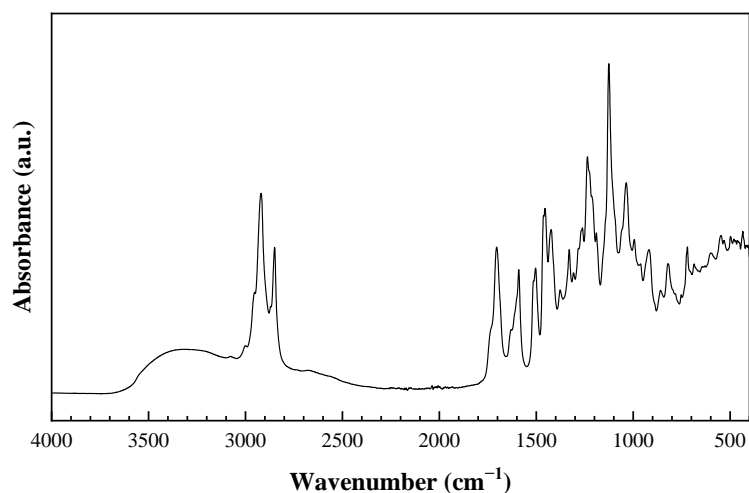


Figure 42 – ATR-FTIR spectrum of *Myristica fragrans* (NME) extract. After the NME extract was filtrated and freeze-dried, the infrared vibrational spectrum of the freeze-dried extract was measured using a Nicolet iS50 FTIR spectrometer with an ATR system. The measurement range was 400–4000 cm^{-1} , with a resolution of 1 cm^{-1} and the resulting spectrum was obtained by combining 64 scans.

Table 9 – Pricipal bands in *Myristica fragrans* (NME) extract infrared spectrum and their designations.

Wavenumber (cm^{-1})	Designation
2954	O–H stretching of most carboxylic acids
2915-2919	asymmetric C–H stretching of methyl and methylene groups
2848-2850	symmetric C–H stretching of methyl and methylene groups
1698-1704	carbonyl double bonds (C=O stretching)
1590	COO– stretching of the carboxyl group
1503	aromatic ring stretching
1455-1464	C–H bending
1423-1428	C=C aromatic stretching
1376	bending of methyl groups
1330	C–O stretching vibration of methoxy group (-OCH ₃)
1262-1285	unidentified ring mode
1236	C–O stretching; C–O–C vibrations
1212	CH ₃ symmetric deformation
1190	O–H bending
1125-1126	ring C–H bending; C–O–C
1036-1093	C–C stretching in the aliphatic chain
919-938	O–H out-of-plane bending
814-820	out-of-plane ring bending
720-726	–(CH ₂) _n – in-phase rocking

Annex 7

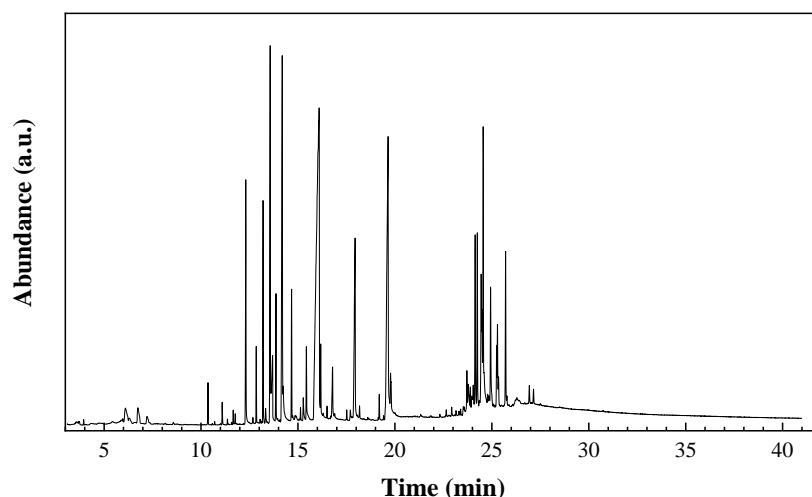


Figure 43 – Chromatogram of *Myristica fragrans* (NME) extract. For GC–MS analysis the freeze-dried extract was dissolved in methanol (HPLC-grade) to yield a 5 mg mL⁻¹ solution. This solution was then filtered again. The chromatography conditions were as follows: injection volume = 1 µL; injector temperature = 280 °C (in splitless mode); initial oven temperature = 60 °C for 2 min, followed by a ramp of 10 °C min⁻¹ to a final temperature of 300 °C for 15 min. Then, with a column with a length of 30 m, diameter of 0.250 mm and film thickness of 0.25 µm was used for compound separation. The mass spectrometer conditions were as follows: electron impact source temperature = 230 °C; quadrupole temperature = 150 °C; and ionization energy = 70 eV. Identification of components was based on the comparison of their mass spectra and retention time with authentic compounds and utilizing the NIST11 database.

Table 10 – Chemical compounds identified by GC–MS in *Myristica fragrans* (NME) extract

RT (min)	Area (%)	Chemical Species	Qual
6.1021	0.3411	α -Terpinolene	97
6.7431	0.6730	γ -Terpinene	96
10.3577	0.4669	Benzene, 1-methoxy-4-pentyl- (or <i>p</i> -pentylanisole)	83
12.3104	3.3712	<i>trans</i> -Isoeugenol	97
12.8506	0.8069	<i>trans</i> -methyl isoeugenol	98
13.2067	2.6466	1,3-Benzodioxole, 4-methoxy-6-(2-propenyl)-	98
13.5687	5.2184	Benzene, 1,2,3-trimethoxy-5-(2-propenyl)- (or elemicin)	98
13.6874	1.8965	Dodecanoic acid (or lauric acid)	99
13.8655	1.6491	3,4-Dimethoxyphenylacetone (or veratryl acetone)	96
14.1860	6.9547	Phenol, 2,6-dimethoxy-4-(2-propenyl)- (or methoxyeugenol)	98
14.2394	1.0242	3-(2-Methoxy-5-methylphenyl)propionic acid	58
14.6727	1.5085	<i>trans</i> -Isoelemicin	98
15.4324	1.1836	Ethyl 2,2,5-trimethyl-3,4-nonadienoate	64
16.0912	21.3603	Tetradecanoic acid (or myristic acid)	99
16.1803	1.0401	Dodecanoic acid, ethyl ester (or ethyl laurate)	97
16.7857	0.9704	6b,7,8,9,10,10a-Hexahydrobenz[a]acenaphthylen-9-one	72
17.9490	4.7691	n-Hexadecanoic acid	99

19.6465	10.0477	9-Octadecenoic acid (Z)- (or oleic acid)	99
19.7770	1.3103	Octadecanoic acid (or stearic acid)	99
23.7181	0.7030	5-Keto-7-methyl-1,2,3,4,5,6,7,8-octahydro-2-quinolone	64
23.7834	0.8237	Phthalide, 4,6-dimethoxy-	50
23.8961	0.4049	9-Carbomethoxy-11-methoxy-6-hydroxy-5-oxoxantho[3,2-g]tetralin	64
23.9733	0.4450	2-(5-Hydroxy-1,6-dimethyl-4,11-dioxo-4,11-dihydro-1H-isochromano(7,6-f)indazol-8-yl)acetic acid methyl ester	55
24.0445	0.5452	N-(4-phenyl-1,2,5-thiadiazol-3-yl)-5-imino-4-phenyl-1,2,3-dithiazole 2-Oxide	90
24.2523	2.4660	Naphthalene, 1,4-dihydro-1-(diphenylmethylene)-5-hydroxy-4-oxo-	90
24.4541	2.1928	Methyl 3,5,7-trimethoxy-1-methylanthraquinone-2-carboxylate	90
24.4897	1.3533	19-Norpregna-1,3,5(10),17(20)-tetraene-20-carboxylic acid, 3-hydroxy-, methyl ester	95
24.5550	5.2001	1,4,6-Trimethyl-2-azafluorene	64
24.8399	0.4043	6 α -methyl-5 α -cholestane-3 β ,6 β -diol	83
24.9408	2.1806	methyl (5R)-2-(methoxycarbonyl)-3-(dimethoxymalonyl)-5,9-dimethyldec-8-enoate	90
25.2494	0.8257	11 β -Hydroxybenzo-18,20]pregna-4,20-dien-3-one	78
25.2909	1.1488	Voaluteine, 20-hydroxy-, (20S)- (or montanine (C22 alkaloid), or tabernaemontana)	92
25.3503	0.4605	Selinane	86
25.7124	1.9767	19-hydroxy-gelsevirine	94

RT = Retention Time; Qual = Quality of resemblance